

# STATIC AND DYNAMIC STUDY OF CABLE-STAYED BRIDGES

THESIS SUBMITTED IN FULFILMENT OF THE REQUIREMENTS  
FOR THE AWARD OF THE DEGREE OF DOCTOR OF PHILOSOPHY  
IN EARTHQUAKE ENGINEERING OF THE UNIVERSITY OF ROORKEE

*By*

MEGHRAJ SETHIA

B.E. (Civil), M.E. (Struct.) (Hons); M.I.E. (India)



SCHOOL OF RESEARCH AND TRAINING IN  
EARTHQUAKE ENGINEERING  
UNIVERSITY OF ROORKEE  
ROORKEE, U.P., INDIA

C E R T I F I C A T E

Certified that the thesis entitled "STATIC AND DYNAMIC STUDY OF CABLE-STAYED BRIDGES" which is being submitted by Mr. M.R. Sethia in fulfilment of the requirements for the award of the Degree of Doctor of Philosophy in Earthquake Engineering of the University of Roorkee, is a record of the student's own work carried out by him under our supervision and guidance. The matter embodied in this thesis has not been submitted for the award of any other degree.

This is to further certify that he has worked full time for a period of 37 months from July 1975 to July 1978 for preparing this thesis.

University of Roorkee, Roorkee  
Certified that the attached Thesis/  
Dissertation has been accepted for the  
award of Degree of Doctor of  
Philosophy / Master of Engineering  
..... Ed Enay ..... vide notification  
No. Ex/... 136/69/1 (Degree) dated 10.9.77

*Premkrishna*

PREM KRISHNA  
PROFESSOR AND HEAD  
STRUCTURAL ENGINEERING SECTION  
DEPARTMENT OF CIVIL ENGINEERING  
UNIVERSITY OF ROORKEE  
ROORKEE

Assistant Registrar (Exam)

*Anand S. Arya*  
ANAND S. ARYA  
PROFESSOR AND HEAD  
SCHOOL OF RESEARCH AND TRAINING  
IN EARTHQUAKE ENGINEERING  
UNIVERSITY OF ROORKEE  
ROORKEE

## A B S T R A C T

Cable-stayed bridges are structural systems in which inclined cables emanate from one or more points of supporting towers and hold large span stiffening girders of the bridge deck at intermediate locations between the main supports. Modern cable-stayed bridges are found to fulfil the engineering requirement of optimum structural use of materials involved in their construction for a span range of 90-370 m. These bridges possess a good aesthetic appeal.

A wide acceptance of the concept of the cable-stayed bridge has faced organisational as well as technological problems in the past. The present study aims at advancing the understanding about the analysis procedure and the static and dynamic behaviour of such bridges through investigation of the influence of certain important parameters and experimental verification of the analytical results. The specific objectives of the present investigation are:

- (a) To determine the effects of parameters like nonlinear axial-flexural interaction, prestressing of the cables, and soil-structure interaction on the behaviour of the bridge under symmetric vertical loads.

(ii)

- (b) To investigate the behaviour of the bridge under eccentric vertical as well as lateral loads with and without soil-structure interaction effects.
- (c) To work out the influence of geometrical parameters of the bridge, like side to main span ratio, tower height to main span ratio etc., on its lateral load behaviour.
- (d) To study the free vibration mode shapes in the principal directions of the bridge and to compute the dynamic response to a specified base motion.
- (e) To verify some of the analytical results by comparison with experimental results of a small size laboratory structure.

Radiating type bridge structures having six cables on each side of the tower legs with (a) a main span and two side spans (referred to as a 3-span system) and (b) with anchor piers added at mid points of the side spans (referred to as a 5-span system) have been chosen for the present investigations. Parametric lateral load studies have been made on the three span structure having three equivalent cables, in place of six.

Appropriate two dimensional and three dimensional mathematical models have been developed to take into account the actual conditions of transfer of forces between

(iii),

the superstructure and the substructure. In the three dimensional models, the lateral stiffness of the transverse girders has been replaced by equivalent diagonal members.

The stiffness matrix method has been used for static analysis and for obtaining deflection influence coefficients. For free vibration analysis, the inverse iteration technique coupled with approximation to the Rayleigh Quotient has been used to find the fundamental period and associated modeshape. The higher periods and modes have been obtained by Wilkinson's deflation technique. As an illustration of seismic response calculations, maximum probable response of a bridge has been evaluated for a specified ground motion spectrum in the traffic direction.

Experimental studies under static and dynamic loading conditions have been made on a small size laboratory model of aluminium alloy. The laboratory structure has been scaled down from a major bridge proposed in India, using a scale factor of  $1/200$ . The analytical results of this laboratory structure have been obtained after taking due care to represent the actual conditions of rotational and torsional fixity available at the base of the substructure and to represent actual tensile stiffness of aluminium wires used as cables. A comparison of analytical and experimental values of the laboratory structure has been made.

The main conclusions arrived at from the study are the following:

The three span system is appreciably more flexible than the five span system. The effect of axial-flexural interaction is to increase the overall flexibility of the system. The increase is seen to be within 10% for the five span system, but the increase in the axial forces in main girder elements is seen to be significant.

The mutual sharing of eccentric vertical loads by the main girders is moderate as seen from the study of the bridge under vertical loads applied to one of the main girders. The forces and deformations in the unloaded side lie generally between 10 to 25% of those on the loaded side. Other effects of eccentric loading are the horizontal bending and twisting of the deck near the centre of main span which must be considered in the design.

Under the action of lateral forces, the deck tends to act as a horizontal girder with cables carrying only negligible axial forces. Axial forces and moments in the main girder elements are significantly effected by the ratio of the side span to centre span. The ratio of tower height to centre span has significant effect on twisting and horizontal bending of the main girders and axial forces, shears and moments in the tower and the substructure. The ratio of cable stiffness to girder torsional stiffness effects

horizontal bending and twisting of tower legs. The effects of increasing the width of deck is to decrease the horizontal bending of the deck.

The effect of soil-structure interaction, even when soil is soft, is seen to be negligible on the superstructure forces but the substructure forces are significantly increased.

Most of the lower modes of free vibration are characterised by the deflections of the deck in the vertical plane. Experimentally, it does not appear possible to induce a pure mode in the superstructure due to cable vibrations.

Comparison of analytical and experimental results is generally good which proves the adequacy of the analyses adopted.

A C K N O W L E D G E M E N T

The author expresses, with deep gratitude, his sincere thanks to his supervisors, Dr. A.S. Arya, Professor and Head, School of Research and Training in Earthquake Engineering and Dr. Prem Krishna, Professor and Head, Structural Engineering Section, Department of Civil Engineering, University of Roorkee, Roorkee, for their expert guidance and constant encouragement throughout the course of this study.

The author thanks Prof. S.C. Goyal, Dr. S. Divakaran and Dr. S.P. Gupta of University of Jodhpur, Jodhpur for encouraging him to take up his Ph.D. studies.

The author expresses his sincere thanks to Mr. A.D. Pandey, Lecturer in Earthquake Engineering for allowing the use of his dynamic analysis computer subroutines in the computations. The author thanks Dr. P. Nandakumaran, Reader and Mr. A.D. Pandey, Lecturer in Earthquake Engineering, University of Roorkee, Roorkee, for technical discussions he had with them at various stages of the work which proved useful.

Thanks are due to Mr. H.C. Dhiman, Mr. Laxmi Chand, Mr. Vijay Kumar and other staff of the workshop and laboratories of Earthquake and Civil Engineering Departments of the University of Roorkee for their help in model



fabrication and experimental work. Thanks are also due to Mr. Deen Dayal, Mr. S.C. Sharma and Mr. Gopinath for their help in bringing out the thesis in the present form.

The author is indebted to his respected mother who sacrificed all her comforts at an old age and to his wife, Padma, who took every care to keep the author free from the worries of his family. The author thanks his other family members for their constant encouragement during this study.

The funds for this study were provided by the Council of Scientific and Industrial Research (CSIR), India. Financial assistance to the author was provided partly by CSIR and partly by the University of Jodhpur, Jodhpur where the author is employed. The financial assistance is gratefully acknowledged.

## C O N T E N T S

Article No.	H E A D I N G	Page No.
	Abstract	(i)
	Acknowledgement	(vi)
	Contents	(viii)
	List of Tables	(xii)
	List of Figures	(xvi)
	List of Photographs	(xx)
	Notations	(xxi)
CHAPTER 1 - INTRODUCTION		
1.1	Basic Concepts	1
1.2	Structural Characteristics	1
1.3	Component Configuration	3
1.4	Methods of Analysis	14
1.5	Identification of Problems Associa- ted with Cable-Stayed Bridges	15
1.6	Objectives of the Study	19
1.7	Scope of work	20
1.8	Outline of Thesis	23
CHAPTER 2 - THE STATE OF THE ART		
2.1	Brief History of Development	25
2.2	Superiority Over Suspension Bridges	27
2.3	Economic Evaluation	28
2.4	Aesthetical Evaluation	29
2.5	Preliminary Design	29
2.6	Mathematical Idealization for Analysis	30
2.7	Influence Lines and Parametric Charts	30
2.8	Mathematical Simulation	32
2.9	Methods of Analysis	35
2.10	Nonlinearity	40

Article No.	H E A D I N G	Page No.
2.11	Soil-Structure Interaction	44
2.12	Experimental Studies	51
2.13	Wind Effects and Dynamics Response	52
2.14	Summary	53
CHAPTER 3 - ANALYSIS FOR STATIC LOADING		
3.1	Introduction	57
3.2	Representation of the Structure	57
3.3	Stiffness Method of Analysis	60
3.4	Member Stiffness Matrices	65
3.5	Rotation Transformation Matrices	74
3.6	Structural Discontinuity	74
3.7	Elastic Supports	79
3.8	Use of Symmetry/Antisymmetry	79
3.9	Effect of Cable Prestress	82
3.10	Bending Moment-Axial Force Interaction	82
3.11	Outline of Space Frame Computer Analysis	88
3.12	Outline of Plane Frame Computer Analysis	91
CHAPTER 4 - DYNAMIC ANALYSIS		
4.1	Introduction	96
4.2	Representation of the Structure	96
4.3	Free Vibration Analysis	97
4.4	Response Analysis	104
CHAPTER 5 - EXPERIMENTAL STUDIES		
5.1	Introduction	109
5.2	Aim of Study	109
5.3	Selection of Type of Bridge	110

Article No.	H E A D I N G	Page No.
5.4	Choice of Scale	112
5.5	Selection of Material and Preliminary Tests	112
5.6	Design of Model Bridge	114
5.7	Design Calculations	117
5.8	Description of Model Bridge	119
5.9	Model Fabrication	122
5.10	Support Details	132
5.11	Cable Anchorage Details	133
5.12	Preloading and Instrumentation of Cable Wires	139
5.13	Model Erection	141
5.14	Test Records	141
5.15	Test Details	143
5.16	Ancilliary Tests	147
CHAPTER 6 - STATIC PLANE FRAME INVESTI- GATIONS		
6.1	Introduction	152
6.2	Details of Structures S1 to S7	152
6.3	Loading	158
6.4	Loadings L1 to L4	158
6.5	Elastic Constants	159
6.6	Tabulation of Results	159
6.7	Interpretation of Results	165
6.8	Discussion of Results	171
6.9	Experimental Verification of Results	176
6.10	Summary	176
CHAPTER 7 - STATIC SPACE FRAME INVESTIGATIONS		
7.1	Introduction	180
7.2	Details of Structures S8 to S12	180
7.3	Loading L5 to L10	186

Article No.	H E A D I N G	Page No.
7.4	Eccentric Vertical Load Analysis	188
7.5	Lateral Load Analysis	202
7.6	Experimental Verification of Results	216
7.7	Parametric Study Under Lateral Forces	217
7.8	Summary	242
CHAPTER 8 - DYNAMIC INVESTIGATIONS		
8.1	Introduction	244
8.2	Structures for Dynamic Analysis	244
8.3	Vibrations in Vertical Plane	248
8.4	Vibrations in Transverse Direction of the Bridge	257
8.5	Discussion of Overall Behaviour of 5-span System	260
8.6	Experimental Verification of Results	262
8.7	Summary	265
CHAPTER 9 - SUMMARY AND CONCLUSIONS		
9.1	Studies Carried out	267
9.2	Significant Results	268
9.3	Conslusions	273
9.4	Scope for Further Research	274
	REFERENCES	277
	APPENDIX - A	298
	Calculations of Rotational Stiffness at the Base of Substructure Wells	
	APPENDIX - B	300
	Representation of Deck Plate Stiffness by Equivalent Truss Member	
	APPENDIX - C	303
	Representation of Deck Plate Stiffness of 6-cable System in Equivalent 3-Cable System	

## LIST OF TABLES

Table No.	C O N T E N T	Page No.
3.1	Stiffness matrix in member axes for fully restrained member in space	68
3.2	Stiffness matrix in member axes for truss member in space	71
3.3	Stiffness matrix in member axes for a member JK with J end hinged about $Z_M^-$ axis and restrained in other directions in space	72
3.4	Stiffness matrix in member axes for fully restrained member JK in a plane	73
3.5	Stiffness matrix in member axes for truss member JK in a plane	73
3.6	Stiffness matrix in member axes for a member JK with J end hinged about $Z_M^-$ axis and restrained in other directions in a plane	74
3.7	Stiffness matrix for symmetrical loading for fully restrained member JK in space cut transversely by line of symmetry of frame	83
3.8	Stiffness matrix for symmetrical loading for fully restrained member JK in a plane cut transversely by line of symmetry of frame	84
3.9	Stiffness matrix for antisymmetrical loading for fully restrained member in space cut transversely by line of symmetry of frame	85
3.10	Stiffness matrix for antisymmetrical loading for fully restrained member in a plane cut transversely by line of symmetry	84
3.11	Stiffness matrix under axial-flexural interaction for fully restrained member in a plane frame	89
3.12	Stiffness matrix under axial-flexural interaction for a member with first end hinged about Z-axis and restrained in other directions in a plane frame	89

Table No.	C O N T E N T	Page No.
3.13	Stability functions for various end conditions of a member	90
5.1	Comparison of component section properties of the prototype and the model	118
5.2	Significant dimensions of model bridge	121
5.3	Scheme of loading of bridge model for static tests	145
5.4	Results of ancilliary tests	150
6.1	Details of external restraints for S1 to S7	154
6.2	Geometrical properties of elements of structures S1 to S6	157
6.3	Elastic constants	160
6.4	Displacements in structures S1 to S6 under loading L1	161
6.5	Cable forces in structures S1 to S6 under loading L1	162
6.6	Axial forces in girder, tower, pier and well elements of S1 to S6 under L1	163
6.7	Moments in girder, tower and well elements of S1 to S6 under L1	164
6.8	Ratios of maximum deck deflections to main span for S1 to S6 under L1	175
6.9	Comparison of analytical and experimental results	177
7.1	Details of external restraints for S8 to S12	182
7.2	Geometrical properties of elements of structures S8 to S11	184
7.3	Loading L5 on S8 to S11 (Eccentric vertical loading)	187
7.4	Loading L6 on S8 to S11 (Lateral loading due to uniform wind pressure, varying with height)	187
7.5	Deformations at salient locations of S8 to S11 under eccentric vertical loads (L5)	188

Table No.	C O N T E N T	Page No.
7.6	Cable forces in S8 to S11 under eccentric vertical loads (L5)	189
7.7	Axial forces in girder, tower, pier and well elements of S8 to S11 under eccentric vertical loads (L5)	190
7.8	Twisting moments in girder, tower, pier and well elements of S8 to S11 under eccentric vertical loads (L5)	191
7.9	Bending moments (M-Z) in girder, tower, pier and well elements about axes parallel to transverse axis of S8 to S11 under eccentric vertical loads (L5)	192
7.10	Bending moments in tower, pier and well elements about axes parallel to longitudinal axis of S8 to S11 under eccentric vertical loads (L5)	193
7.11	Summary of maximum values of forces in S8 to S11 under eccentric vertical loads (L5)	194
7.12	Deformations at salient locations of S8 to S11 under lateral forces (L6)	203
7.13	Cable forces in S8 to S11 under lateral forces (L6)	204
7.14	Axial forces in girder, tower, pier and well elements of S8 to S11 under lateral forces (L6)	205
7.15	Twisting moments in girder, tower, pier and well elements of S8 to S11 under lateral forces (L6)	206
7.16	Bending moments (M-Y) in girder, tower, pier and well elements of S8 to S11 under lateral forces (L6)	207
7.17	Bending moments (M-Z) in girder, tower, pier and well elements of S8 to S11 about axes parallel to transverse axis of bridge under lateral forces (L6)	208
7.18	Summary of maximum values of forces in S8 to S11 under lateral forces (L6)	209



---

Table No.	C O N T E N T	Page No.
7.19	Comparison of analytical and experimental values of maximum deflections in S12 under L7 to L10	216
7.20	Comparison of lateral deformations of 6-cable system and equivalent 3 cable system	219
7.21	Geometrical properties of members of S13	221
7.22	Lateral forces (L11) applied to S13, S20 to S23	222
7.23	Lateral forces (L12) applied to S14	222
7.24	Lateral forces (L13) applied to S15	223
7.25	Lateral forces (L14) applied to S16	223
7.26	Lateral forces (L15) applied to S17	224
7.27	Lateral forces (L16) applied to S18	224
7.28	Lateral forces (L17) applied to S19	225
8.1	Nodal coordinates and weights lumped at different nodes of S24	246
8.2	Degrees of freedom considered and lumping of weights for dynamic analysis of S25	249
8.3	Spectral accelerations due to horizontal ground motion for 10% damping	256
8.4	Comparison of analytical and experimental values of natural frequencies in longitudinal, vertical and lateral directions	262

(xvi)  
LIST OF FIGURES

Figure No.	T I T L E	Page No.
1.1	A typical three span cable-stayed bridge	2
1.2	Cable configurations in longitudinal direction	4
1.3	Radial cable arrangements in space	8
1.4	Supporting towers	11
1.5	Deck superstructure	12
2.1	Representation of side and base resistance of well by Arya et al (38)	46
2.2	Representation of soil resistance by Ahmad (1)	46
3.1	Member stiffnesses in member axes for fully restrained member in space	67
3.2	Torsional constants	69
3.3	Use of symmetry and antisymmetry in a planar structure	81
3.4	Representation of cable pretension by equivalent joint loads on released structure	86
3.5	General deformation of a member	86
5.1	General view of proposed Second Hooghly Bridge, India	111
5.2	Cross-section of end well (No.1 & 4)	123
5.3	Cross-section of end pier (No.1 & 4)	124
5.4	End view of model bridge at tower location	125
5.5	Cross-section of mid-well (No.2 & 3)	126
5.6	Cross-section of mid-pier (No.2 & 3)	127
5.7	Cross-sections of tower top and bottom	128

Figure No.	T I T L E	Page No.
5.8	Portal cross-sections and tower portal connection	129
5.9	Deck cross-section details	130
5.10	Main girder splice cross-section	131
5.11	Deck plate splice	131
5.12	Hinge connection at end pier	134
5.13	Link connection at tower	134
5.14	Link connection at end pier	135
5.15	Anchor block at top of tower	136
5.16	Cable forces at tower top	140
5.17	Micrometer tensioning cum anchor device	140
5.18	Scheme of instrumentation and loading of bridge model	142
5.19	Test arrangement to determine tensile stiffness of aluminium wires	149
6.1	Mathematical models of structures S1 to S7	153
6.2	Distribution of deformations and forces (liner) in 5-span system (S1) under live loads (L1)	166
6.3	Distribution of deformations and forces (linear) in 3-span system (S3) under live loads (L1)	169
6.4	Nodal configurations of S2 and S4 under cable pretension and dead weight	174
7.1	Mathematical model of structures S8 to S12	181
7.2	Mathematical model of structures S13 to S23	196

Figure No.	T I T L E	Page No.
7.3	Distribution of deformations and forces (linear) in 3-span system (S10) under eccentric vertical loads (L5)	199
7.4	Deformations and forces in S8 under L6	210
7.5	Deformations and forces in S10 under L6	213
7.6	Mathematical model of structures S13 to S23	218
7.7	Variation of cable forces with $\alpha$ , $\beta$ under uniform wind load	226
7.8	Variation of cable forces with $\psi$ , $\eta$ under uniform wind load	227
7.9	Variation of axial forces in main girder elements with $\alpha$ , $\beta$ under uniform wind load	228
7.10	Variation of axial forces in main girder elements with $\psi$ , $\eta$ under uniform wind load	229
7.11	Variation of vertical shears in main girder elements under uniform wind load	230
7.12	Variation of horizontal shears in main girder elements under uniform wind load	231
7.13	Variation of twisting moments in main girder elements under uniform wind load	232
7.14	Variation of moments about vertical axis in girder elements under uniform wind load	233
7.15	Variation of moments about horizontal axis in girder elements under uniform wind load	234
7.16	Variation of axial forces in tower legs under uniform wind load	235

Figure No.	T I T L E	Page No.
7.17	Variation of shears F-Y (member axes) in tower legs, portals, piers and wells under uniform wind load	236
7.18	Variation of shears F-Z (member axes) in tower legs, portals, piers and wells under uniform wind load	237
7.19	Variation of twisting moments in tower legs and portals under uniform wind load	238
7.20	Variation of moments M-Y (member axes) in tower legs and portals under uniform wind load	239
7.21	Variation of moments M-Z (member axes) in tower legs and portals under uniform wind loads	240
8.1	Mathematical models of structures used for dynamic analysis	245
8.2	Free vibration modes I to III of structure S24	251
8.3	Free vibration modes IV to VI of structure S24	252
8.4	SRSS values of displacements and axial forces for structure S24	254
8.5	SRSS values of shears and moments for structure S24	255
8.6	Torsional/flexural modes I to III of structure S25	258
8.7	Torsional/flexural modes IV to VI of structure S25	259
8.8	Typical acceleration records of free vibration in vertical direction	264
A1	Sections at the base of concrete wells	299
B1	Representation of deck plate stiffness by equivalent truss member.	299

(xx)

LIST OF PHOTOGRAPHS

Photo No.	T I T L E	Page No.
P1	General view of model bridge with oscillator mounting for shaking in longitudinal direction	120
P2	Deck-pier connection through hinge	137
P3	Deck-pier connection through link	137
P4	Deck-tower connection through link	137
P5	The hinge and the link	138
P6	Cable anchor blocks at the tower top	138
P7	Micrometer tensioning cum gripping device	138
P8	Symmetric vertical loads on the bridge deck	144
P9	5-point lateral loading of the bridge deck	144
P10	(i) Loading of the bridge deck through clutch to induce lateral free vibrations	146
	(ii) Oscillator mounting for shaking in lateral direction	
P11	Strain recording for direct tension test on coupon from aluminium alloy sheet	146

## N O T A T I O N S

The notation symbols are defined here in alphabetical order. They are defined in the text also wherever they first occur

$A, A_X$	Cross-sectional area of a member
$A_M$	Force vector at the two ends of a member in member axes
$[A]$	Modified dynamic matrix
$C^r$	Mode participation factor in $r^{\text{th}}$ mode corresponding to ground motion represented by $S_a^r$
$C_{rh}, C_{rv}$	Mode participation factor for horizontal and vertical ground motion respectively
$C_u$	Coefficient of elastic uniform compression of soil
$C_X, C_Y, C_Z$	Direction cosines of member axes with respect to structure-axes
$C_\emptyset$	Coefficient of elastic nonuniform compression of soil
$[c]$	Damping matrix
$D_M$	Deformation vector at the two ends of a member in member axes
$D_S$	Deformation vector at the two ends of a member in structure axes
$E$	Modulus of elasticity
$E_{eq.}$	Equivalent modulus of elasticity
$\{ F_m^r \}$	Vector of member forces in $r^{\text{th}}$ mode
$\{ F(t) \}$	Time dependent force vector
$G$	Modulus of rigidity
$I_X$	Torsional constant of a member cross-section

$I_Y(Z)$	Principal moment of inertia of the cross-section of a member with respect to $Y_M(Z_M)$ axis
JK	A member with its two ends J and K
$K_V$	Vertical stiffness of soil
$K_\phi$	Rotational spring constant
$[K]$	Matrix of stiffness influence coefficients
$[K_n]$	Member stiffness matrix
L	Length of a member
$M_{JX}, M_{JY}, M_{JZ}$	Moments on end J of a member about $X_M, Y_M, Z_M$ directions
$M_{KX}, M_{KY}, M_{KZ}$	Moments on end K of a member about $X_M, Y_M, Z_M$ directions
$[M]$	Mass matrix
$m_i$	Mass associated with $i^{\text{th}}$ degree of freedom
n	Subscript used for model
n	Geometrical scale ratio, also order of a matrix
$n_H$	Stiffness factor of sand
$P_{JX}, P_{JY}, P_{JZ}$	Forces on end J of a member along directions $X_M, Y_M$ and $Z_M$
$P_{KX}, P_{KY}, P_{KZ}$	Forces on end K of a member along directions $X_M, Y_M$ and $Z_M$
P	Axial force in a member
$\{P\}$	Load vector
p	Subscript used for prototype
$p_r$	Natural frequency in $r^{\text{th}}$ mode
R	Rotation matrix



$R_P$	Rotation matrix of a member in a plane
$R_S$	Rotation matrix of a member in space
$R_T$	Rotation transformation matrix
$R_T'$	Transpose of matrix $R_T$
$R_{TP}$	Rotation transformation matrix of a plane frame member
$R_{TS}$	Rotation transformation matrix of a space frame member
$R_{\text{vert}}$	Rotation matrix of a vertical member in space
$S$	Shearing forces at the two ends of a member
$S_M$	Member stiffness matrix for member axes
$S_{MD}$	Member stiffness matrix for structure axes
$S_a^r$	Absolute acceleration spectrum corresponding to the frequency in $r^{\text{th}}$ mode
$U_{JX}, U_{JY}, U_{JZ}$	Translations of end J of a member JK along directions $X_M, Y_M$ and $Z_M$
$U_{KX}, U_{KY}, U_{KZ}$	Translations of end K of a member JK along directions $X_M, Y_M$ and $Z_M$
$X_M, Y_M, Z_M$	Member oriented set of orthogonal axes, referred to as member-axes in the text
$X_S, Y_S, Z_S$	Set of orthogonal axes used for the structure as a whole referred to as structure axes in the text
$\{X\}$	Dynamic displacement vector
$\{\dot{X}\}$	Velocity vector
$\{\ddot{X}\}$	Acceleration vector
$x_J, y_J, z_J$	Coordinates of end J of a member JK in structure axes
$x_K, y_K, z_K$	Coordinates of end K of a member JK in structure axes

$Y_i^r$	Dynamic displacement at node $i$ in $r^{\text{th}}$ mode
$\{Y\}$	Modeshape vector
$\delta^r$	Nodal deformations obtained in the $r^{\text{th}}$ mode
$\delta_m^r$	Deformations at the two ends of a member obtained from $\delta^r$
$\{\delta\}$	Static deformation vector
$\Delta$	Relative displacement of two ends in a direction perpendicular to the longitudinal axis of a plane frame member
$\epsilon$	A specified small quantity
$\sigma$	Unit tensile stress in cable
$\lambda_r^i$	$i^{\text{th}}$ iterate of eigen value for $r^{\text{th}}$ mode
$\mu$	Specific weight of cable
$\theta_{JX}, \theta_{JY}, \theta_{JZ}$	Rotations of end J of a member JK about $X_M, Y_M, Z_M$ directions
$\theta_{KX}, \theta_{KY}, \theta_{KZ}$	Rotations of end K of a member JK about directions $X_M, Y_M$ and $Z_M$
$\phi_2$ to $\phi_5$	Stability functions
$\phi_{ih}$	Horizontal modal displacement of $i^{\text{th}}$ node
$\phi_{iv}$	Vertical modal displacement of $i^{\text{th}}$ node
$\phi_i^r$	Normalized amplitude at node $i$ in $r^{\text{th}}$ mode

# C H A P T E R 1

## INTRODUCTION

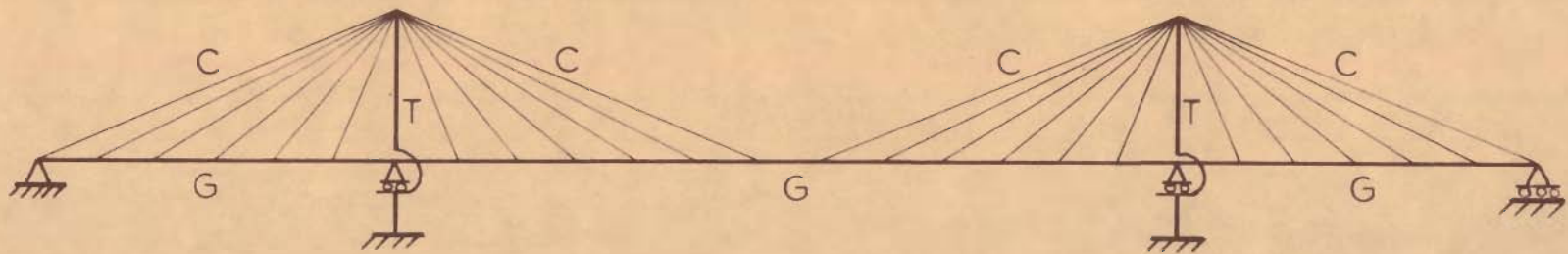
### 1.1 BASIC CONCEPTS

Modern cable-stayed bridges fulfil the engineering requirement, for a certain span range, of optimum structural use of the materials involved in their construction. Inclined cables, which emanate from one or more points on the supporting towers, are used to hold large span stiffening girders of the bridge deck at intermediate locations between the main supports. A typical three span cable-stayed bridge is represented in a plane in fig. 1.1.

Apart from the inclined cables in tension and supporting towers in compression, a cable-stayed bridge is a three dimensional system comprising of stiffening girders, transverse and longitudinal bracings and orthotropic type deck with high moment of inertia. The strong orthotropic type deck permits the use of shallower girders resulting in economy in steel. The girder depth can be further reduced by distributing the points of attachment of the cables as much as possible along the stiffening girder.

### 1.2 STRUCTURAL CHARACTERISTICS

In practice, a cambered profile of the deck is obtained by tensioning the cables to a level such that



T \_ Tower  
G \_ Stiffening Girder  
C \_ Cable

FIG.1.1 \_A TYPICAL THREE SPAN CABLE - STAYED BRIDGE

they do not become slack at any stage of subsequent loading. The longitudinal girders are stressed primarily due to prestressing forces of the cables. The dead loads and a major portion of the anticipated live loads on the main girders act to nullify the bending effects of prestressing forces. The inclined cables transmit axial forces to the stiffening girders and the girders are subjected to nonlinear bending moment-axial force interaction. The cables provide a stable geometrical configuration to the bridge for any positioning of the live loads. In this form of bridge the contribution of the structure acting as a space system is particularly drawn under lateral and eccentric vertical loading.

### 1.3 COMPONENT CONFIGURATION

Cable-stayed bridges with two spans, three spans or multi-spans have been successfully built in the recent past. Salient details of the components of such bridges are given in the following paragraphs.

#### 1.3.1. Cable Configuration in the Longitudinal Direction

Based on the sense of proportions of clear spans and tower heights one can choose from four basic and a number of combinations of cable arrangements in the longitudinal direction of the bridge. Fig. 1.2 shows the basic arrangements and a few possible combinations. The definitions and comparative merits and demerits of the basic

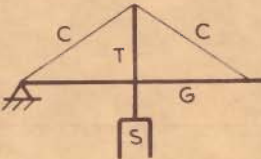
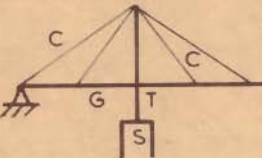
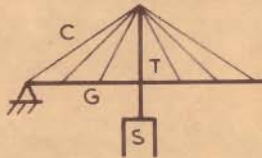
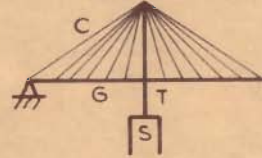
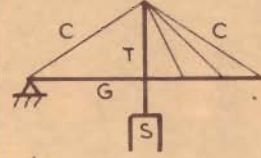
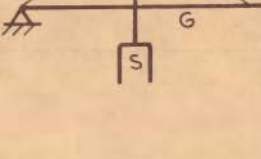
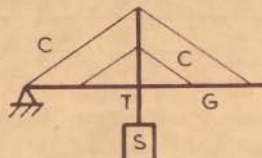
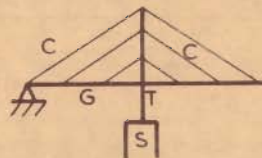
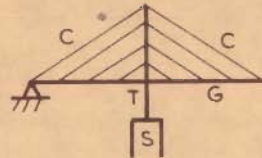
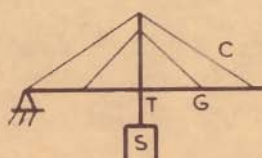
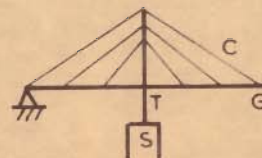
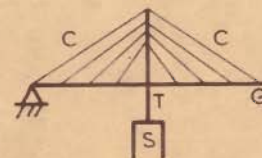
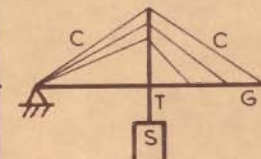
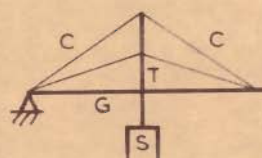
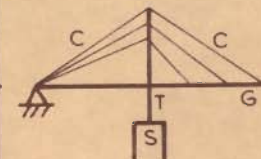
LONGITUDINAL STAY CONFIGURATION	SINGLE STAY	DOUBLE STAY	TRIPLE STAY	MULTIPLE STAY	COMBINED STAY	
RADIATING						
HARP						
FAN						
STAR			<p>C - CABLE - STAY  T - TOWER  G - GIRDER  S - SUBSTRUCTURE</p>			

FIG. 1.2 \_CABLE CONFIGURATIONS IN LONGITUDINAL DIRECTION

arrangements are given below.

(i) Radial or Converging Configuration

(2, 3, 9-12, 14, 16, 17, 20-23, 26, 28, 33-35, 41, 51, 56, 64, 65, 68, 72, 82, 87, 93, 96, 101, 2, 12, 13, 27, 36, 43-47, 53, 54, 67, 73, 75, 79, 89, 96, 97, 99, 201, 2, 13-16, 18, 20) The cables emerging from several points of the deck converge at the top of the tower. The arrangement makes the optimum utilization of cable steel due to maximum possible inclination of cables with the deck. The cables, thus, carry the maximum component of the dead and live load forces. The axial force in the main girder components of the deck is minimum (180). The radial arrangement with large number of cables, however, requires complicated supporting saddles at the tower tops and full height of the tower has to be designed for heavy axial forces.

(ii) Harp or Parallel Configuration

(15, 18, 19, 27, 29, 48, 49, 61-63, 68, 81, 86, 87, 114, 19, 31, 91, 98) In this arrangement the cables run parallel, maintaining equal spacing along the tower height and the deck. The arrangement offers a better aesthetical appeal, when compared to the radial one, due to minimum visual intersection of cables when viewed from an oblique angle. However, it causes greater bending moment in the tower and axial forces in the main girder components. The top cables can either be fixed to the towers or placed on moving saddles. For the lower cables it becomes necessary to study whether it is feasible to obtain fixed supports

at the tower legs or they must be made movable in a horizontal direction. The movable cable supports present problems of mathematical idealization.

The harp arrangement is less stiff than the radial arrangement but good stiffness can be obtained if each back stay is anchored to an individual pier (18, 27, 191). The axial forces in the main girder components can be reduced by increasing the height of the tower. Cable-steel requirement in this arrangement is slightly higher.

(iii) Fan Configurations (24, 25, 31, 32, 43, 80, 85, 87, 141, 66, 74, 212): Non-parallel cables emanate from the tower with equal but small spacings along the height and connect with equal spacings along the length of the deck. The arrangement, which is a combination of the radiating and the harp arrangements, is used when all the cables can not be accommodated at the top of the tower. The merits and demerits of both radiating and harp arrangements are encountered to a lesser degree in this arrangement.

(iv) Star Configuration (4-6, 40, 97-100, 186): The cables emerge from the tower at different heights and converge on each side of the tower at one point on the deck. The two small cables function as a single large cable which gives a unique aesthetic appearance to the structure. The arrangement is limited in its application to small spans as it contradicts the



principle that the points of attachment of the cables should be distributed as much as possible along the main girder.

Apart from the four basic longitudinal arrangements of cables, a variety of combinations (8, 13, 30, 44, 57, 114, 15, 33, 65, 69) have been successfully tried.

### 1.3.2 Cable Arrangement in Space

One may choose to place the cable stays in a single plane; a plane of symmetry (fig. 1.3a) or an asymmetric plane (fig 1.3b), or two planes; either vertical (fig 1.3c) or oblique (fig. 1.3d). Any arrangement described in section 1.3.1 may be chosen. Cables in three vertical planes have also been tried.

The single plane symmetric cable arrangement (4-6, 33-35, 97-100 etc.), which is economical and aesthetically appealing, provides lane separation, unobstructed view of the landscape to the user and needs relatively smaller pier widths. However, relatively large concentrated cable forces are transferred to the main girder of the superstructure. High torsional rigidity of the main girder, through box section, is required to take the asymmetrical vehicular and wind or earthquake loading.

Asymmetrical single plane cables have been used for pedestrian bridges (2, 127) with the plane of cables at the edge of the walkway. The system is suitable only for small loadings.

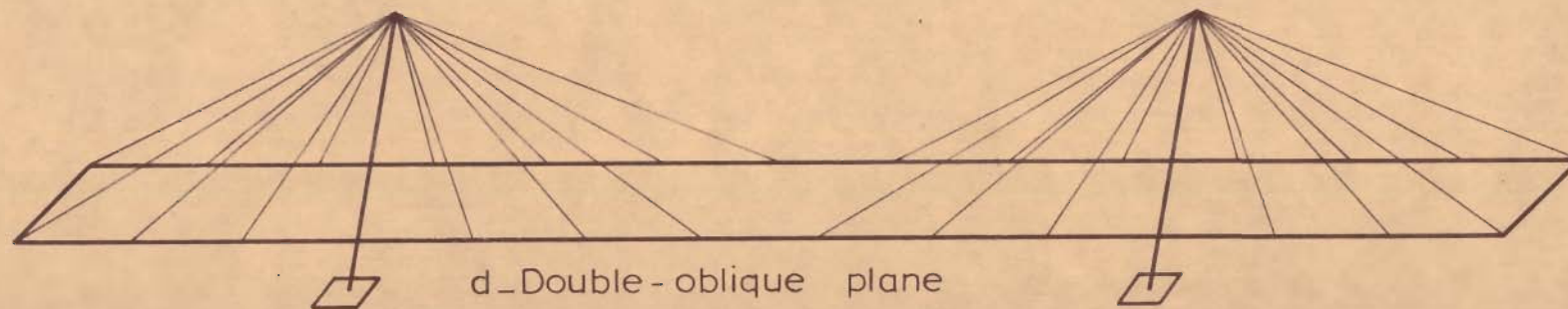
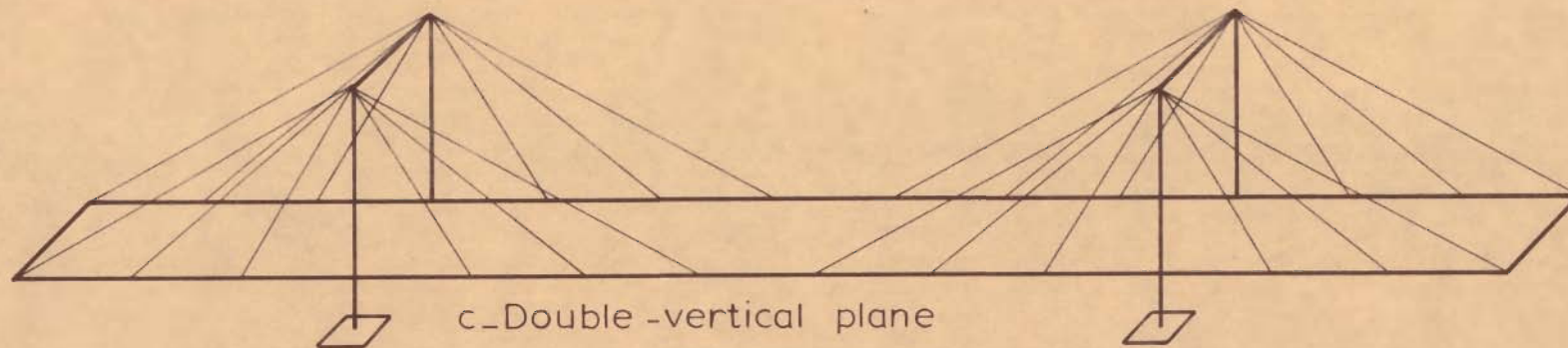
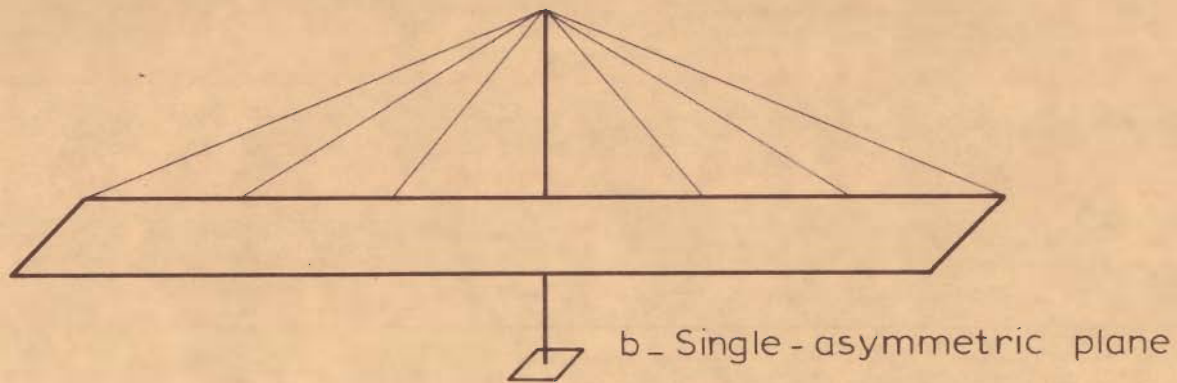
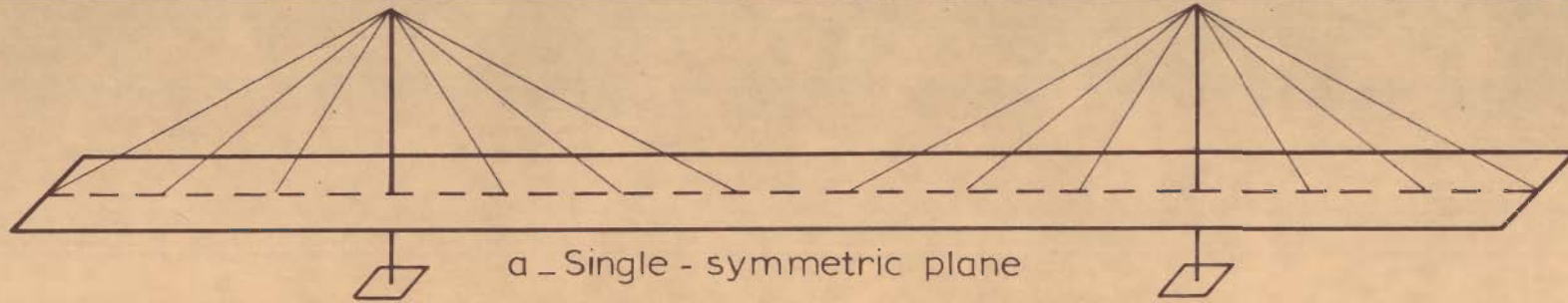


FIG.1.3 \_RADIAL CABLE ARRANGEMENTS IN SPACE

In the double-plane vertical cable arrangement (10, 28, 72, 112, 45, 53, 89, 214, 20 etc.) the anchors may be either on the outside of the deck structure or built inside the main girders. The former arrangement has the advantage of unobstructed deck surface but additional reinforcement is required to transmit eccentric cable loadings into the main girders. The pier, which supports the towers, has to be wider. In the latter arrangement the overall width of the deck has to be increased for the full length of the bridge to safely accommodate the anchorage fittings. The cost of superstructure is, thus, increased.

The double plane oblique cable arrangement (12, 20, 44, 102, 33, 54, 97, 215, 16 etc.) is suitable for long spans with very high A-shaped towers which are laterally stiff due to triangle and frame action. The arrangement prevents dangerous torsional movements of the deck due to wind oscillations. The term 'plane' is to be interpreted loosely in this case. Stays connected at more than one level on the tower (harp or fan arrangement), or any vertical and horizontal curvature in the roadway, geometrically forms a warped surface in space.

### 1.3.3. Supporting Towers

Towers are also referred to as pylons. Factors that decide the shape of a supporting tower are the arrangement of cables, bridge site conditions, desired

ratio of tower height to span length, clearance required, aesthetics and economics. Towers are normally cellular sections fabricated of steel or constructed in reinforced concrete. Various shapes of towers are shown in fig.1.4.

The tower may be fixed or hinged at the foundation or it may be fixed to the superstructure. Magnitude of the vertical loads and distribution of cable forces along the tower height are the factors which should be considered. A fixed base, though induces large moments at the base, increases the overall rigidity of the structure. A pinned bearing at the base of the tower, which may be preferred for structural reasons, needs external supports to the tower until the cables are connected.

#### 1.3.4. Deck Superstructure

There are two basic types of main girders; the stiffening truss and the solid web girder. The deck is usually of orthotropic steel construction having various cross-section types of the longitudinal ribs as well as the cross-girders. A latticed type of main girder is obsolete in the current designs as it requires more fabrication, is relatively more difficult to maintain, is more susceptible to corrosion and less appealing. Various types of bridge deck cross-sections with solid web main girders are shown in fig. 1.5. Plate girders have very low torsional rigidity. Depending on the type of loading and number of lanes a specific cross-section of the deck may be chosen. The orthotropic arrangement with trapezoidal

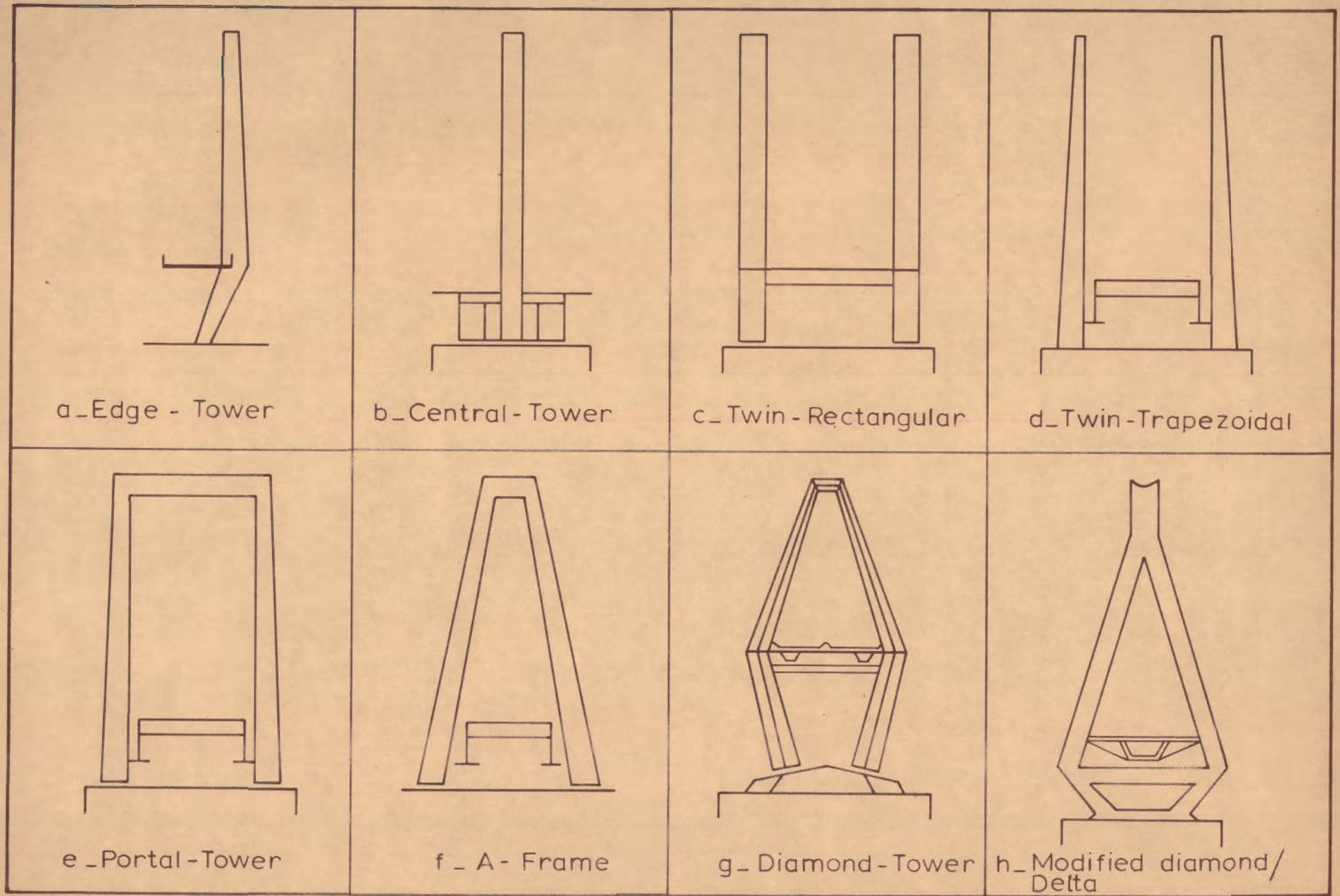


FIG.1.4 \_ SUPPORTIG TOWERS

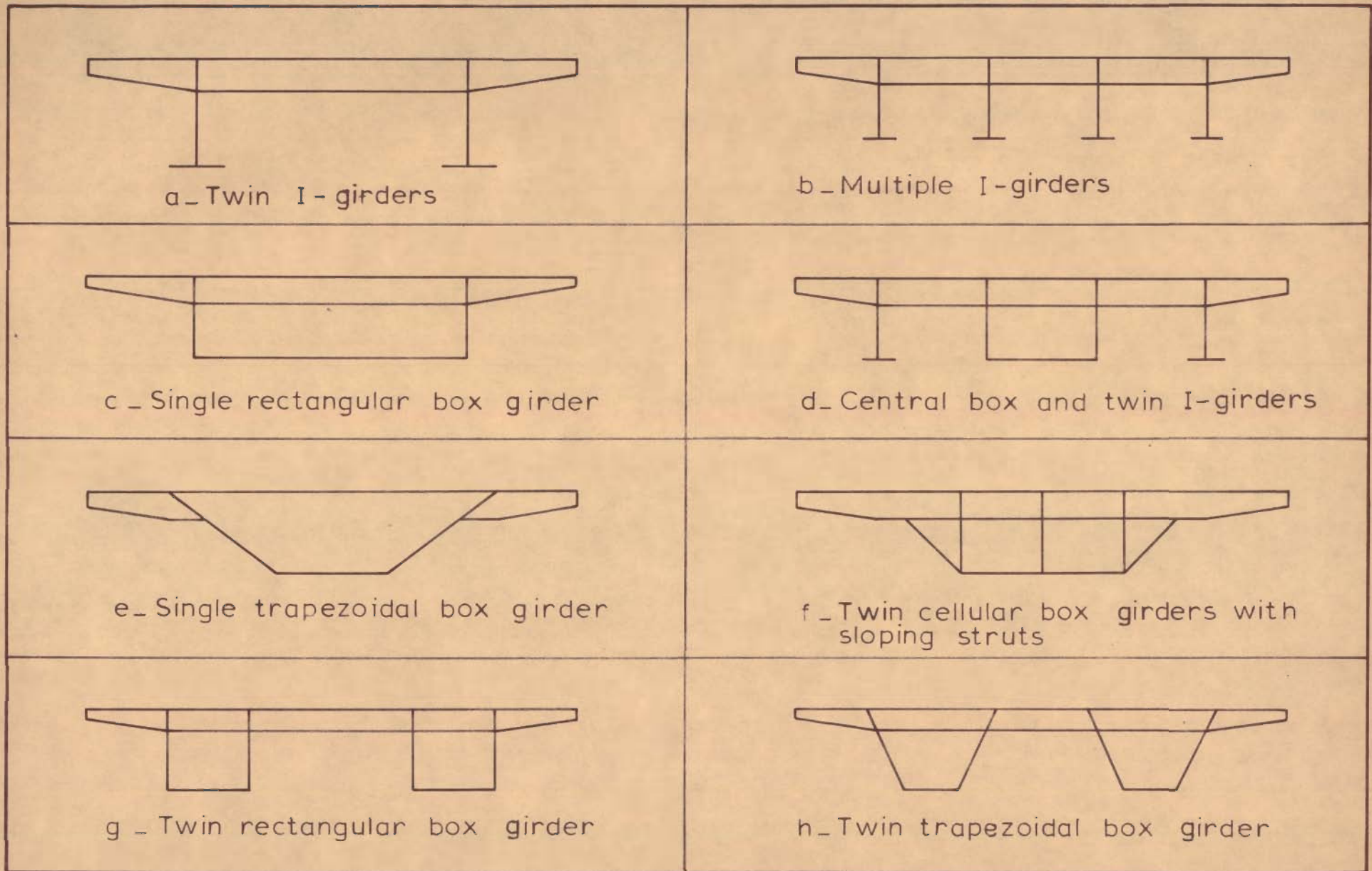


FIG. 1.5 \_DECK SUPERSTRUCTURE

configuration and cantilever extensions provides a better aerodynamic stability.

#### 1.3.5. Cables

A cable is a flexible tension member consisting of one or more groups of wires, strands or ropes. A wire is a single continuous length drawn from a cold bar. A strand, with the exception of parallel wire strand, is an arrangement of wires helically placed about a centre wire to produce a symmetrical section. A rope is an assembly of number of strands helically wound around a core that is composed of a strand or another rope.

Structural strand is generally preferred to a rope for cable-stayed bridges because of its greater breaking strength for equal size, higher modulus of elasticity and more corrosion resistance for a given class of zinc coating. However, the strands have a lesser curvature capability. Locked-coil-strands are also used in which the wires in some layers are specially shaped to lock together around the core.

#### 1.3.6. Cable Connections

Special end fittings attached to the cable ends have to ensure full transfer of loads. Standard fittings can be used with due consideration to the procedure of erection. Access for initial tensioning and subsequent adjustments and inspection, protection against weather

and accidental damages are the main requirements of an efficient cable-connection design.

A cable may be terminated at the tower connection or may be permitted to pass through as a continuous member. In the latter case the cable is supported on a grooved fitting, referred to as saddle, which may be either rigidly connected to the tower or supported on expansion bearings to permit longitudinal movements. The overall rigidity of the structure is enhanced by the fixed saddles. A movable saddle reduces bending moments on the tower when the base of the tower is fixed. In case of large number of cables on a tower, the saddle for the top cable may be fixed and all or a few of the lower saddles may be permitted to move.

#### 1.4. METHODS OF ANALYSIS

Approximate analysis (183) can be carried out by considering the stiffening girder as a continuous beam on elastic supports. Standard two dimensional plane frame and three dimensional space frame methods of exact analyses can be used with proper modifications to account for nonlinearity present in cable-stayed bridges.

Smith (183, 184) used a linear mixed method of analysis by formulating a matrix of unknown displacements and forces. Troitsky and Lazar (208) used a flexibility technique. Lazar, Troitsky and Douglass (122) proposed a load balancing analysis to partially reduce the live



load effects by applying prestressing forces. Stiffness method of nonlinear analysis was used by Lazar (121) as well as Podolny and Fleming (157, 160). Transfer matrix method was used by Tang (192, 193) to accommodate non-linearity by using fictitious loads. Arya and Thakkar (36) used a modified transfer matrix method for calculating seismic response of a cable-stayed bridge including soil-structure interaction. Kajita and Cheung (107) used a linear finite element method to consider torsion in the deck of three dimensional bridge structure. The method was extended to perform dynamic analysis also. Morris (148) presented a method for linear and nonlinear dynamic analysis of three dimensional cable stiffened structures stressed in the elastic range. Tang (194) used energy approach to calculate the overall buckling load of the structure.

#### 1.5 IDENTIFICATION OF PROBLEMS ASSOCIATED WITH CABLE-STAYED BRIDGES

Although the first modern cable-stayed bridge came in existence in 1955 and a number of such bridges were subsequently constructed in Germany, a wide acceptance of the concept of stayed bridge type faces both organisational and technological problems listed in the following paragraphs. An unreserved application of the concept, at the present and in the times to come, depends on how quickly and effectively these problems are tackled.

(a) Bridge specifications of most of the countries do not include provisions for cable-stayed bridges and the designers have to adapt their design to satisfy the existing specifications, wherever possible, and be prepared to explain their design, analysis and construction details, not covered by the specifications, to the approving authority. This prompts the designers to restrict their choice to conventional types. Lack of data on the cost of construction, which is normally derived from the past experience, leads the contractors to overbid to hedge against unforeseen problems.

(b) The available technical data, in terms of influence lines and parametric charts, which helps in the preliminary design of a bridge structure is insufficient.

(c) The erection sequence and procedure may govern the design of some of the components of the bridge structure. An analysis of forces and deformations in different stages of erection of the bridge is very important.

(d) The effect of nonlinearity due to large deformations should be investigated .

A parallel programme of doctoral research is in progress at the University of Roorkee to study the effect of various parameters on the behaviour of cable-stayed bridges under vertical live loads, distribution of forces and deformations in the stages of erection and the non-linear effect of large deformations.

(e) A cable-stayed bridge is a statically indeterminate system to a very high degree which is somewhat difficult to analyse with reasonable degree of accuracy. Computer programs must be developed to include all the effective parameters to ensure greatest precision possible in the prediction of forces and deformations.

(f) A suitable mathematical idealization of the bridge structure, which gives results as close to the actual behaviour of the structure as possible, must be made. Assumptions made in the idealization must be clearly identified and the validity of the idealization should be supported by experimental evidences.

(g) Stayed type bridges are considered to exhibit inherent flexibility compared to conventional girder and truss types. The live load deflection of the Severin Bridge at Cologne is  $1/225$  of the span - 3.5 times more flexible than that allowed by the AASHTO specifications (162). Studies are required to eliminate this disparity in the design of the stayed bridge type which must be due to the nonlinear beam-column action of girders and towers and nonlinear behaviour of the cables. The magnitude of prestress in the cables must also effect the nonlinear behaviour of the structure. The substructure which is normally assumed to rest on rigid soil mass, is subjected to soil-structure interaction that must result in increased flexibility of the bridge superstructure.

A realistic mathematical model of the bridge structure should, therefore, include both the superstructure and the substructure, with appropriately represented connections between the two. The analysis should be capable of incorporating nonlinearity due to beam column action, nonlinearity of cables, presence of prestress in cables and; thus; in all other components of the bridge; and rotations and translations of the substructure due to soil-structure interaction.

(h) When the cables are located in vertical planes, they fail to impart stiffness to the bridge in the lateral direction. A study of the behaviour of the bridge under lateral static loads is, therefore, important. This can be done only through an appropriate three dimensional mathematical model. A study of effects of geometrical parameters on the lateral load behaviour of the bridge can provide a guide line to the designers.

(i) It is important to know the fundamental and a few higher modes of free vibrations of the bridge structure and to know the response of the structure to dynamic wind and earthquake forces in all the three principal directions of the bridge, viz.; vertical, longitudinal and lateral directions; through suitable lumped mass mathematical model of the structure.

(j) The problem of computer storage space for large size two dimensional and three dimensional mathematical

idealizations can be solved partly but effectively by taking symmetry of the structure into account and by dividing the loading into a symmetric and an antisymmetric loading.

#### 1.6 OBJECTIVES OF THE STUDY

The present study, which is related to 5-span and 3-span systems of radiating type cable-stayed bridges, aims to advance the understanding about their static and dynamic behaviour through investigation of the influence of certain important parameters, to have an experimental verification of the mathematical analyses developed and to increase the capability in regard to analysis of such bridges. More specifically these aims can be listed as follows:

(a) To study the effect of following parameters on the vertical load behaviour of cable-stayed bridges:

- (i) the nonlinear axial-flexural interaction
- (ii) prestressing of the cables
- (iii) soil-structure interaction.

(b) To study the behaviour under eccentric vertical and lateral loads and the effect of soil-structure interaction.

(c) To study the effect of following geometrical parameters on the lateral load behaviour:

- (i) ratio of side span and centre span,
- (ii) ratio of tower height and centre span,
- (iii) ratio of cable stiffness to girder torsional stiffness,

(iv) change in deck width.

(d) To study free vibration characteristics in the three principal directions and to obtain dynamic response to a specified base motion.

(e) To verify some of the analytical results by comparison to experimental results of a laboratory structure.

## 1.7 SCOPE OF WORK

### 1.7.1. Structure Considered

Considering the structural superiority of the radiating type over other types of cable-stayed bridges and influenced by the proposed Second Hooghly Bridge, India, which is of radiating type and for which technical data was available for ready reference, radiating type bridge structures were chosen for the proposed study. A radiating type bridge structure of major dimensions equal to those of proposed second Hooghly Bridge but reduced number of equivalent cables has been chosen so as to make the structure proposed for analysis to suit the available computer facilities. The structure for plane frame studies has six cables of varying size on each side of the tower leg. The structure for lateral load studies has six cables each on both sides of each of the tower legs.

The cables have been further reduced to three equivalent cables for parametric lateral load studies. The structure for two dimensional and three dimensional dynamic studies has six cables on each side of the tower leg.

#### 1.7.2. Mathematical Models

Appropriate mathematical models have been developed to undertake the proposed studies. The superstructure has been considered connected to the substructure through hinge at one end and links at other end and intermediate supports to provide free longitudinal movement of the deck. The cables have been considered to act as truss members.

The continuous deck plate between the two main girders of the three dimensional mathematical model for lateral load analysis has been replaced by an equivalent diagonal brace permitted to take axial forces only.

Lumping of masses has been done for the dynamic analysis. Mass of a member between any two nodes has been equally lumped at the two nodes.

#### 1.7.3. Methods of Analysis and Computer Programs

The stiffness matrix method of analysis has been used. Stability functions, for both compression and tension, have been introduced in the member stiffness matrix to carry out iterative nonlinear beam-column analysis. Stability coefficients for conditions

(i) both ends fixed and (ii) one end fixed-other end hinged, of the member have been used.

The effect of soil-structure interaction has been studied by assuming translational and/or rotational soil springs at appropriate nodes of the structure.

A plane frame computer program has been developed which can carry out linear as well as nonlinear iterative beam-column analysis, two step analysis of prestressed bridge structure and incorporate soil springs at appropriate nodes in a single run. Variation in the value of modulus of elasticity of different components of the structure can be considered. A structural hinge can be analysed.

A space frame program has been developed which can analyse structure cut at its lines of symmetry for loadings divided into symmetric and antisymmetric loadings. Structural hinges and the effect of soil-structure interaction can be studied. Effect of eccentric vertical and lateral loads and the effect of geometrical parameters on lateral load behaviour of cable-stayed bridges has been studied.

Rayleigh type method of analysis has been used to find fundamental frequency and Wilkinson's deflation technique has been used to get few higher modes of the vibrations. A spectral acceleration v/s time period curve has been considered for dynamic response analysis by mode superposition technique.



#### 1.7.4. Experimental Study

A three span radiating type cable-stayed bridge model of aluminium alloy, with six cables on each side of a tower leg, was designed and fabricated to conduct static vertical and lateral load tests and dynamic free vibration and steady state vibration tests to check the validity of the assumptions of analytical methods and to verify adequacy of the proposed mathematical models. Ancilliary tests were carried out to determine modulus of elasticity of sheets, actual stiffness of the riveted construction, rotational stiffness of supports at base, modulus of elasticity of aluminium wires and their structural stiffness in tension.

#### 1.8 OUTLINE OF THESIS

Chapter two deals with the present state of the art. Formulations for static studies based on plane frame and space frame analyses are given in chapter three. The material relevent to dynamic analysis is contained in Chapter four and the features of experimental studies are highlighted in Chapter five. Description of mathematical models used and the results and discussions of plane frame investigations are given in Chapter 6 while those for the space frame investigations are contained in Chapter 7. The results of dynamic investigations are presented and discussed in Chapter eight. The comparison of analytical and

experimental results has been made at appropriate locations in the relevant chapters. Conclusions and scope for further research are presented in Chapter nine of the thesis. Calculations for rotational stiffnesses at the base of the substructure and representation of deck-plate stiffness by equivalent truss member are given in appendices.

## C H A P T E R 2

### THE STATE OF THE ART

#### 2.1. BRIEF HISTORY OF DEVELOPMENT

The history of development of cable-stayed bridges can be traced from the primitive bridges of ancient times to the modern cable-stayed bridges.

The idea of supporting a beam by inclined rope or chains hanging from mast (tower) was applied to sailing ships (120). Materials like vines and bamboos were used in the primitive bridges (139) which were stayed by sloping vines attached to trees on banks.

The bridges designed by Clive (59), Redpath and Brown (70), Faustus (79), Hatley (126), Loscher (135), Motley (149), Poyet and Navier (151) and Lefevre (211) incorporated the main features and basic principles of metal suspension bridges stiffened by stays. Materials like timber, mild steel chains and wires, and wrought iron bars were used for sloping stays. A number of these early bridges failed, probably because of the use of inferior and insufficient materials for sloping stays and use of imperfect techniques of erection, which led to partial abandonment of this type of bridge. Due to improper tightening of the sloping stays of these early bridges, the stays performed their proper function only after substantial deformation of the whole structure had

occurred under the action of loads. This aspect led to the opinion that cable-stayed bridges are exceptionally flexible and unsafe. Navier, a famous French engineer of his time commented adversely on the performance of these bridges (162, 209) and advocated the superiority of suspension bridges over cable-stayed bridges.

The idea of "stay" cables was then used to reduce the deflections of suspension bridges and to stiffen the ~~floor~~ floor of the bridge against build-up of undulations induced by the action of wind. Arnodin (66, 124), Dischinger (67), Gisclard (92), Leinekugel le Cocq (125), Roebling (188), Ordish (211) and others extensively applied the idea and designed even rail road suspension bridges. These designers had not been able to calculate the forces in inclined cables correctly and the influence of hyperstatic behaviour and the sag of stay cables was underestimated. The bridges of the mixed suspension-stay system did not find wide application mainly because of their aesthetical imperfection.

Nearly fifteen thousand bridges in West Germany were destroyed in World War II. Reconstruction of these bridges in post-war period was greatly influenced by the short supply of steel. Emphasis had to be shifted to minimum weight design. More reliable methods of analysis could now be used with the advent and fast development of digital computers. The importance and performance of tensioned high strength cables was realised. Methods of

erection were improved due to mechanisation. The development and successful use of orthotropic plate deck system combined with the concept of cable-stayed design produced bridges that were, in some cases, 40% lighter (162) than their pre-war counterparts with the added advantage of speedy construction. A leading role in this development was played by Dischinger (67) who published the results of his studies in 1949. Stromsund Bridge (219) in Sweden, considered to be the first modern cable-stayed bridge, was designed by Dischinger and completed in 1955. The Rhine Bridge in Dusseldorf, though designed by Leonhardt (129) in 1952, was erected in 1958.

The successful completion of two modern cable-stayed bridges, which were very stiff under traffic loads, aesthetically appealing, economical, simpler and quicker to erect, started the new era of wide and successful application of the stayed beam concept. Approximately sixty cable-stayed bridges have been built, or are being planned, since 1955, including the one across River Hooghly in India. A fuller review of the development of cable-stayed bridges can be found in recent publications on this subject (80, 110, 58, 59, 61, 200, 23).

## 2.2 SUPERIORITY OVER SUSPENSION BRIDGES

The superiority of cable-stayed bridges over modern suspension bridges is clearly indicated with respect to deflections, overall stiffness cable-steel requirements,

deck performance, anchorages, overall economy and methods of erection from comparative studies of Leonhardt (129,30) on the design of a combined highway and railroad bridge with a main span of 1300 m. The position improves if high clearance under the bridge is required for navigation and if the cable anchorages of the suspension bridge require deep foundations.

### 2.3 ECONOMIC EVALUATION

For a span range of 90-300 m (162, 209) the cable-stayed bridge system, with only one box as the main girder support, provides an economical and an aesthetical solution. Intermediate supports at the location of cable connections of the flanking spans may be very economical with a relatively small cost of additional supports. Use of variable panel lengths to reduce the action of local loading may lead to substantial economy in the metal of main girders. Open design competitions in Germany have conclusively indicated the economic superiority of cable-stayed bridges in that country for span range of 150-370 m. Homberg (105) and Leonhardt (129) have found the cable-stayed bridge more economical than, suspension bridge for spans between 500 m and 800 m.

Utmost economy in material at an adequate carrying capacity is the general trend in the design of modern steel bridges and this seems to be achieved to a high degree in the cable-stayed bridge system though, no simple formula can be applied to evaluate the conditions in which the economy of a system can be guaranteed.

## 2.4 AESTHETICAL EVALUATION

The reasons for the popularity of the cable-stayed bridge system during the last two decades, in addition to a deeper understanding of the technical features, are its elegant form and capability to blend with the landscape. Cable-stayed bridges are pleasing in outline, clean in their anatomical conception and free from ornamentation.

Free standing towers of a single plane system give a pleasing appearance as there is no intersection of the lines of cables in elevation and the user has an unobstructed view from one side of the bridge.

A two plane radial system may not provide the most attractive solution due to unsightly intersections in the lines of cables. A harp system is an attractive alternative.

With structural simplicity and harmonious proportions of towers the bridge attracts vision from many points of the terrain. The aesthetical height of the tower may be determined by the clear height of deck above water at the centre, depth of deck structure and the arrangement and inclination of cables. Tower surfaces may be given pleasing appearance by an appropriate choice of form and by economical construction of sections using metal for structural purpose only.

## 2.5 PRELIMINARY DESIGN

In the preliminary stage of design; based on vertical and horizontal clearances, foundation problems,

terrain conditions and environmental factors of the site; several types of bridge structures may be investigated to decide the merits of a specific type. Span proportions, cable-stay configuration, height of pylons and their conditions of anchorage, type of girder and deck, types of cables and their connections, design loads and forces which the proposed structure has to withstand are the primary decisions made in the preliminary design of a cable-stayed bridge.

## 2.6. MATHEMATICAL IDEALIZATION FOR ANALYSIS

A suitable mathematical idealization, based on clearly identified assumptions, of the structure conceived from the preliminary design has to be made to analyse it for the design loads by an approximate or an exact method of analysis. Connections of cables, girders and towers are idealised to determine the stiffness or flexibility of each component of the bridge.

## 2.7. INFLUENCE LINES AND PARAMETRIC CHARTS

Homberg (104) presented analytical results in the form of influence lines, for cable forces, and tower and girder moments, of three span bridge systems proposed for the bidding of the North Bridge at Dusseldorf and the Rhine Bridge at Speyer. Influence lines for radiating and harp systems with varying conditions of support have been drawn. O'connor (152) produced influence lines, for



bending (deck) moments and cable forces, for comparison of the performance of three span radiating and harp configurations. Sawhney (170) produced influence lines for axial forces in cables and tower, for two span radiating type systems. Influence lines for varying ratio of tower height to total span were also drawn.

Podolny (157) studied the influence of the following parameters on moments in girder and pylon, and tension in the cables:

- (a) ratio of moment of inertia of pylon to girder,
- (b) stiffness ratio of outside cable to girder,
- (c) stiffness ratio of inside cable to outside cable.

The influence of the above parameters was also studied on the nonlinear behaviour of cables due to change in cable sag with the change in tension in the cable.

The use of influence lines and parametric charts is evident in the preliminary design of a cable-stayed bridge. Span proportions, stay geometry, type and height of pylons, type of girder, type of cable and its connection to the pylon and the girder, anchorage conditions at the base of the tower and mode of transfer of forces between the superstructure and the substructure can be decided with greater confidence at the preliminary stage if enough data is available to the designer in the form of influence lines and parametric charts. In short, the available literature (104, 57, 70) covers influence lines, under vertical

loads, for two span and three span radiating and harp configurations.

The available information can not however, be considered sufficient to cover various possibilities of cable configurations, conditions of cable supports at the pylon, support conditions at the base of the tower and mode of transfer of forces between the superstructure and the substructure. Information regarding the behaviour of cable-stayed bridges under eccentric vertical loads and lateral loads is not available.

## 2.8 MATHEMATICAL SIMULATION

### 2.8.1. General

When the idealized mathematical model of a structure or the solution procedure used for its analysis fails to represent its actual behaviour, mathematical simulation technique can be used. The simulation can be achieved by adding fictitious members, or nodes, or both, in the mathematical model or by altering the stiffness of some of its components.

Protte and Tross (164) used the technique of simulation in the flexibility analysis (74, 111, 72) of cable-stayed bridges. Simulation was effected by introducing additional truss members or by reducing bending or axial stiffness of certain parts of the structure. The hinged support of the tower, for instance, was simulated by

choosing a very flexible spring connection to a fixed support. This type of simulation was achieved to analyse the actual behaviour of a structure from the available computer programs which could handle only fixed supports. However, with the present state of knowledge of analysis and computer programming, the hinged support can be directly incorporated into the analysis.

### 2.8.2 Use of Simulation Technique

The simulation technique can be used in the following cases also:

(a) To permit free relative longitudinal movements at the junction of deck and tower, an extra member with a small length free to rotate at one end about an axis parallel to the transverse axis of the bridge can be used at the junction of the deck and the tower.

(b) In a three dimensional skeletal bridge structure, the parallel girder elements and the tower legs are located away from the axis of symmetry while the substructure elements are located on the axis of symmetry. Rigid links can be used to connect parallel girder elements and the tower legs to the corresponding substructure elements. The rigid links provide means of transfer of forces between superstructure and substructure and can simulate the actual behaviour of the structure.

(c) The lateral stiffness of the stressed skin of the deck can not be considered directly in a skeletal

structure. The stiffness can be simulated by using a diagonal truss member of equivalent stiffness which connects the parallel girder elements of a panel.

### 2.8.3. Stiffness of Equivalent Diagonal Truss Member

Based on experimental investigations, several empirical formulae are available for representing the equivalent stiffness of the deck plate in the lateral direction which represents the lateral stiffness of the masonry or concrete infills of frames. Holmes (103) suggested that the infill can be replaced by an equivalent diagonal strut of the same thickness whose width is one-third the diagonal length of the frame. The recommendation is based on the assumption that the bond between the frame and the infill is not broken. Benjamin (54), Mallick (138), Polyakov (163) and Smith (181, 82) have also worked in this field.

The experimental finding of Holmes (103) for square infills can be applied to rectangular infills with proper modification in the stiffness of the diagonal strut.

### 2.8.4. Numerical Instability

The problem of numerical instability is generally encountered in the computer solutions of simulated structures with members of high rigidity occurring away from boundaries. The problem can be tackled by using better computational techniques, use of higher precision in calculations and by choosing proper values of stiffnesses

of the rigid links (discussed in 2.8.2b) to give a numerically stable and a reliable solution.

## 2.9 METHODS OF ANALYSIS

Approximate as well as exact methods of analyses have been used for static and dynamic loading conditions.

### 2.9.1. Approximate Methods

These methods are essentially linear and involve several simplifying assumptions.

(a) Beam on elastic supports: Approximate analysis can be carried out by considering the stiffening girder as a continuous beam on elastic supports. Smith (183) outlined a procedure to determine the equivalent spring constants for any specific cable-stayed bridge system. The method can be applied either in conjunction with available tables for continuous beams on elastic supports or by carrying out a complete analysis. In the latter case, the solution of the system of equations written on the basis of continuity of slopes and displacements at joints may be obtained.

(b) Mixed force-displacement method: Smith (183-84) used the method to examine the linear behaviour of single plane and double plane (in space) cable-stayed girder bridges. Analysis, based on the physical behaviour of the structure, has been done by isolating and considering separately the rotation and shortening of the tower and stretching of cables. These actions have been represented by a set of

simultaneous equations which were developed by initially assuming the girder to behave as though supported by rigid cables and a rigid tower. Modifications in the influence coefficients, through superposition of effects, were made to account for rotation, stretching and shortening. The method has been further extended to allow for bending of the cantilever towers and shortening of the deck.

(c) Flexibility method: Troitsky and Lazar (205) used bending moments at fixed and flexible supports of a cable-stayed bridge as redundants to obtain a well conditioned, banded flexibility matrix. The technique was used for analysis of a bridge for dead and live loads as well as for post tensioning forces.

(d) Dynamic analysis : Arya et al (39) have used an approximate method of preliminary seismic analysis to get the fundamental time period of a cable-stayed bridge in the longitudinal direction by disregarding the flexibility of the superstructure and lumping the mass of the deck at the top of the lone end pier which provides fixed bearing to the superstructure. Connections through links have been assumed between the superstructure and the substructure at other points which permit free longitudinal movement of the deck. Today, the problems can be solved more efficiently and accurately by standard two dimensional plane frame and three dimensional space frame programs, with appropriate modifications, on larger and faster computers systems.

### 2.9.2. Exact Linear and Nonlinear Methods

Transfer matrix method, load balancing method, finite element method, stiffness approach and the energy approach have been used for exact linear and nonlinear analysis for static as well as dynamic loadings. The results from exact methods of analysis are subject to varying degree of accuracy due to computational errors depending on the method of analysis being used.

(a) Transfer matrix method : General theory of the transfer matrix method was introduced in 1956 by Folk (74-77). The method is ideally suited to systems consisting of a number of elements linked together, end to end, in the form of a chain (111, 23, 55, 92). In this approach only successive matrix multiplications are necessary to fit the elements together. Tang (192) presented detailed analysis of two dimensional problems of cable-stayed bridges, with different types of cable saddles, by using the transfer matrix method. Nonlinear effects were considered in the form of imaginary external loads in the calculations. Deformations due to shear, torsion and warping were neglected. Arya and Thakkar (36) used transfer equations wherein deformations due to shear and bending and the effect of rotary inertia were included. The seismic response of a cable stayed bridge, considering soil-structure interaction was computed.

(b) Load balancing method : Load balancing concept was developed by Lin (132) for concrete structures with prestressed cables embedded in the body of the member. The concept has been extended by Lazar et al (122) to cables acting outside of the balanced structural elements to determine the magnitude of post-tensioning forces to be applied to the cables of the bridge. Partial balancing of external loads and, thereby, reduction in maximum bending moment or the maximum displacement was achieved, through post-tensioning of cables, by increasing the forces in members which are less stressed.

(c) Finite element method: The method was used for linear static and dynamic analyses of cable-stayed bridges by Kajita and Cheung (107). For static analysis, the bridge deck was divided into a number of shell elements and the whole structure was treated as a three dimensional system. Variation in saddle types and the connections between the tower and the deck were studied. For dynamic analysis, the bridge deck was considered as a shell and cables were assumed to behave as springs.

(d) Stiffness approach: The stiffness method of analysis has been widely used for linear as well as nonlinear analysis of the bridge under static and dynamic loadings.

Podolny and Fleming (157, 60) conducted linear studies on radiating and harp configurations in a single plane cable arrangement. The girder was rigidly supported vertically at the pylon but independent of it. Transfer of



moments between girder and pylon was not allowed. An iterative procedure was used to account for cable nonlinearity. The effect of the amount of initial tension in cables, as measured by sag ratio, and the type of live load distribution on the structure was studied.

Baron and Lien (46, 47) presented a three dimensional static and dynamic analyses of the proposed Southern Bay Crossing Cable-Stayed Bridge in San Francisco.

Nonlinear analysis for planar frames for large displacements, bending moment-axial force interaction and shortening of the member due to bowing has been studied extensively in the past decade (60, 140, 42, 68). Saafan (168) has developed a physical concept which allows nonlinear analysis by successive iterations of linear subroutines. Lazar (121) presented a procedure of two dimensional linear and nonlinear stiffness analysis of cable-stayed bridges under joint loads. Nonlinearity due to large displacements, bending moment-axial force interaction and catenary action of cables was considered under full dead and live loads. A wider application of the algorithm of Saafan to the nonlinear problems of cable-stayed bridges is not known to be reported.

Morris (148) presented a method for the linear and nonlinear dynamic analyses of three dimensional cable stiffened structures stressed within the elastic range. The method was applied to a typical cable-stayed bridge with harp configuration of cables in a single plane.

(e) Energy approach: Energy method was used by Tang (194) to calculate the overall buckling load of cable-stayed bridges considering the whole structure as one entirety in a plane. Local stability was not considered. An approximate method was suggested for the preliminary estimation of the lowest critical load.

A comparison of the relative merits and demerits of various methods of analysis is not available. The stiffness approach of linear and nonlinear analyses of skeletal form of cable-stayed bridges can be considered to be a versatile method. Sasfan's (168) physical concept of nonlinear analysis by successive iterations of linear sub-routines can be incorporated in the linear computer programs of stiffness analysis with comparatively less additional programming effort.

## 2.10. NONLINEARITY

### 2.10.1 Catenary Action

Change in sag of cable with change in its axial tension (catenary action) is one of the causes of nonlinearity in cable-stayed bridges. Non-linearity due to catenary action can be incorporated into the analysis by the use of the concept of equivalent modulus of elasticity of the cable material. Gimsing (91), Goschy (94) and Tung and Kudder (210) have studied the problem of equivalent modulus of elasticity to account for the action of cable force acting along the inclined chord by assuming a straight member with

its modulus of elasticity depending on the magnitude of the tension force in cable. The approach used by these investigators results in the solution provided by Earnst (73) who developed the following formula for equivalent modulus of elasticity ( $E_{eq}$ )

$$E_{eq} = \frac{E}{1 + \frac{(\mu l)^2}{12 \sigma^3} \cdot E} \quad \dots (2.1)$$

where,

$E$  = modulus of elasticity of cable material,

$\mu$  = specific weight of cable, weight per unit volume,

$\sigma$  = unit tensile stress in cable.

Podolny (157) has shown that a significant indicator of the stiffness of a cable-stayed bridge is the initial stiffness of the cables. The initial sag ratio of the cable is a measure of its stiffness. The nonlinear action has been found to be confined to the dead load or erection stages. Under full dead load the sag ratio decreases to a degree of tautness such that the response of the structure may be considered to be linear during the application of live load. This conclusion is in agreement with that of Seim et al (177, 78). The conclusion is important as it permits the construction of influence lines if nonlinearity due to other reasons can also be ignored.

### 2.10.2 Large Displacements

Analysis can be carried out by successive iterations of linear subroutines (168). In the first step of analysis a vector of displacements based on initial geometry of the system and external loads is determined. In the second step, an additional displacement vector due to the difference between the joint loads and the resultants of internal reactions at each joint is obtained. In performing the second step, the stiffness matrix of the system is assembled on the basis of the deformed geometry determined in step 1. Each subsequent step  $i$  uses data determined in step  $(i - 1)$ . The iteration continues until the last displacement vector obtained is a negligible fraction of the total displacement.

### 2.10.3. Bending Moment-Axial Force Interaction

Method of successive iterations of linear subroutines (168) can again be used. Member stiffnesses with zero axial force in each member are used in the first step of analysis. The axial forces determined in step  $i$  are used to modify the member stiffnesses to be used in step  $(i + 1)$ . The iterations are continued till the axial force in each member obtained in step  $i$  is the same as that obtained in step  $(i-1)$  within the limit of specified tolerance.

Sondh (185) has observed significant nonlinear effects caused due to bending moment-axial force interaction in radiating and harp configurations of cable stayed bridges. The influence of variation of various geometrical parameters

on the bending moment-axial force interaction has also been studied.

Lazar (121) has studied the combined effect of nonlinearity due to catenary action of cables, large displacements and bending moment-axial force interaction. The maximum effect of nonlinearity has been found to be 8.3% in the cable forces and 8.06% in bending moments at interior supports of a three span cable-stayed bridge with harp configuration.

The study of Podolny (157) gives conclusive direction that the effects of catenary action can be ignored for the analysis of live loads whereas, the effects must be considered during the analysis of erection stages. An independent study of nonlinear effects due to large displacements is not available in the literature to date while the study of Sondh as well as that of Lazar can not be considered to be conclusive. The nonlinear effects may be negligible or may be quite significant depending on the disposition of stiffnesses in an individual bridge structure. Further studies in this direction are necessary to form firm and separate opinions about the nonlinear effects due to large displacements and bending moment-axial force interaction.

The live loads are carried by cable-stayed bridges in a stressed state under the action of dead loads. Post-tensioning of cables is generally done to set the geometry of the structure which results in redistribution of forces

in its elements. The nonlinear analysis of such bridges should be carried out for fully stressed state under full dead and live loads because it is not possible to determine the stresses and displacements by superposition of influence lines.

## 2.11 SOIL-STRUCTURE INTERACTION

The soil present at the base and at the sides of the bridge substructure resists the forces transmitted by the superstructure to the substructure. The resisting soil undergoes deformations which depend on the properties of the soil and the distribution of soil pressure. The deformations undergone at the base of the substructure change the pattern of distribution of forces in the superstructure elements. This problem of soil-structure interaction can be incorporated into the analysis by taking into account the estimated stiffness of the soil at appropriate nodes of the structure.

(i) Arya et al (38) accounted for soil-structure interaction in the seismic investigations of Second Hooghly Bridge, India. The elastic resistance of soil, below scour level, on the sides of well foundations was represented by translational side springs. The base resistance was simulated by a rotational spring at the base. The portion of the well below scour level was considered as rigid body that could tilt without translation about the point of rotation at the base.

The stiffness of side springs (sandy soil) were calculated (fig. 2.1a and b) from the following formulae:

$$\begin{aligned} K_1 &= \frac{1}{6} n_h (\Delta_h)^2 \\ K_i &= (i - 1) n_h (\Delta_h)^2 \quad \dots (2.2) \\ K_n &= \frac{3n-4}{6} n_h (\Delta_h)^2 \end{aligned}$$

where;

- $K_{1,2, \dots, i, \dots, n}$  = stiffness of side spring in  $t/m^2$ ,
- $n_h$  = stiffness factor of sand in  $t/m^3$ ,
- $n$  = total number of nodes between scour level and the base of the well where side springs are lumped,
- $\Delta_h$  = spacing of soil springs in metres.

At the base (clay), the rotational stiffness due to base pressure is given by:

$$K_\theta = \frac{1}{12} K_v \cdot D^3 \quad \dots (2.3)$$

where;

- $D$  = dimension of well in metres in the direction of the bridge in which rotation is considered,

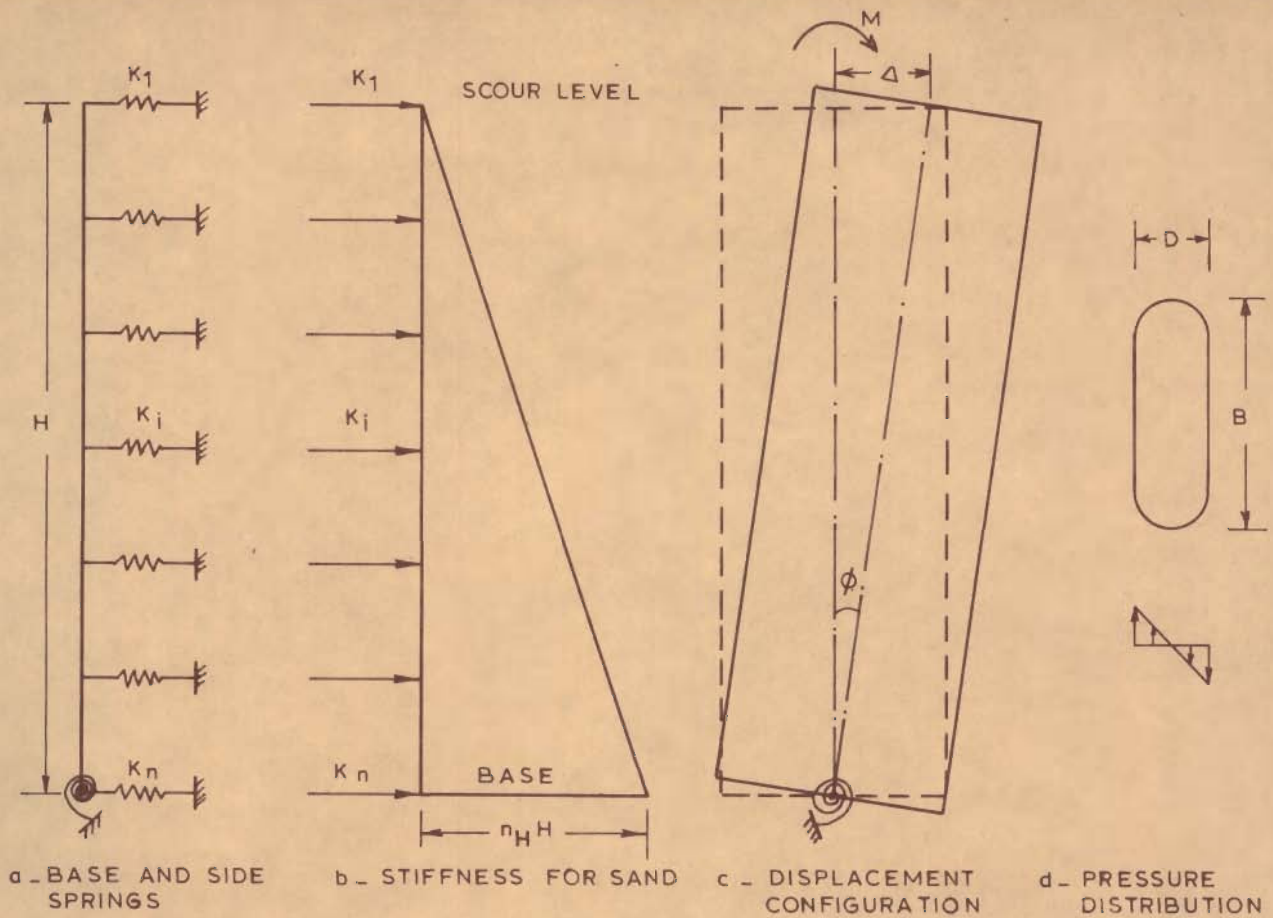


FIG. 2.1 REPRESENTATION OF SIDE AND BASE RESISTANCE OF WELL BY ARYA ET. AL. (38)

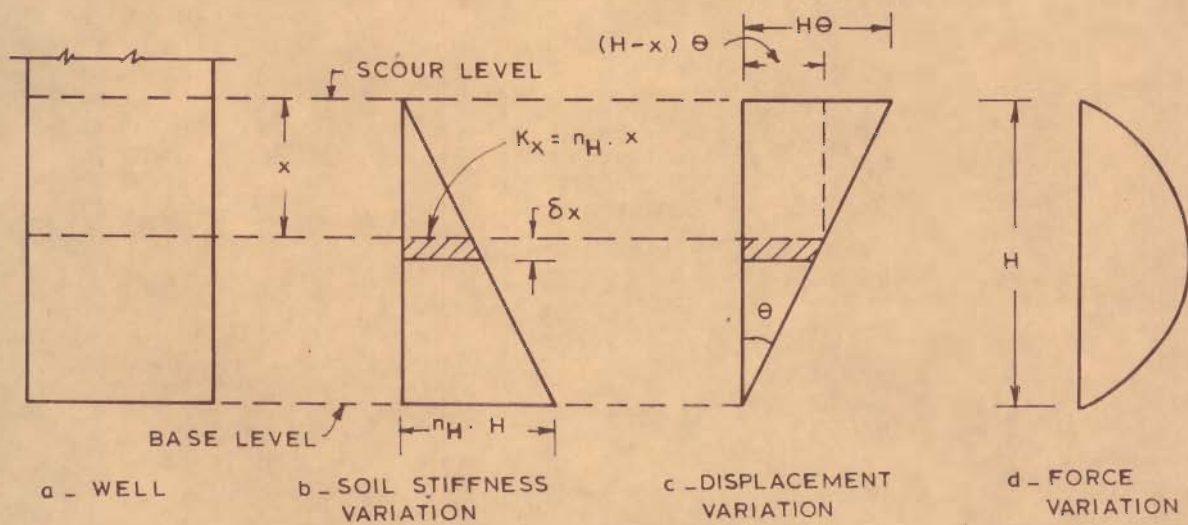


FIG. 2.2 REPRESENTATION OF SIDE RESISTANCE OF WELL BY AHMAD (1)



$K_v$  = vertical stiffness of soil in  $t/m^2$ .

$K_\theta$  = rotational spring constant at base in  
 $t-m/rad$ .

Values of  $n_h$  and  $K_v$  as suggested by Terzaghi (195) were used.

(ii) Ahmad (1) studied the influence of horizontal subgrade reaction ( $n_h$ ) on dynamic behaviour of a symmetric, two span, radiating cable-stayed bridge. The foundation well was assumed to rotate, without translation at the base, as a rigid body. The effect of elastic properties of the soil at the sides as well as at the base of the foundation was considered to calculate the total reactive moment (M) transmitted by the soil to the foundation as follows:

(a) Soil at the sides: According to Terzaghi (195), the intensity of side-soil stiffness ( $K_x$ ) at any depth (x) is a linear function of the modulus of subgrade reaction ( $n_h$ ) and the depth as shown in fig. 2.2b. Thus;

$$K_x = n_h \cdot x \quad \dots (2.4)$$

With the assumption that the well is a rigid body allowed to rotate without translation at the base, the movement of soil has to be maximum at the scour level and zero at the base as shown in fig. 2.2c.

By combining the effects explained in fig. 2.2b and c, the variation of force along the depth of the well

is represented in fig. 2.2d. The resultant horizontal force on the vertical face of the well can be assumed to act at  $H/2$  from the base of the well. The total horizontal force per unit width represented by fig. 2.2d can be expressed as:

$$F = \int_0^H (n_h \cdot x) (H - x) \cdot \theta \cdot dx$$

or

$$F = n_h \cdot \frac{H^3}{6} \cdot \theta \quad \dots (2.5)$$

The reactive moment,  $(M_1)$  caused by this force at the base of the well is given by:

$$M_1 = F \cdot \frac{H}{2} = \frac{1}{12} n_h \cdot H^4 \cdot \theta$$

Thus, the rotational stiffness  $(K_{\theta 1})$  at the base is given by:

$$K_{\theta 1} = \frac{M_1}{\theta} = \frac{1}{12} n_h \cdot H^4 \quad \dots (2.6)$$

(b) Soil at the base: Reactive moment  $(M_2)$  transmitted by soil to the foundation, according to Barkan (45) is given by:

$$M_2 = C_{\phi} \cdot I \cdot \phi \quad \dots (2.7)$$

where;

$C_{\phi}$  = coefficient of elastic nonuniform compression of soil,

$I$  = moment of inertia of the base area of well, in contact with soil, about the axis of rotation of the well.

$\phi$  = angle with which the foundation is tilted.

The rotational stiffness due to vertical reaction at the base ( $K_{\theta 2}$ ) can be written as:

$$K_{\theta 2} = \frac{M_2}{\phi} = C_{\phi} \cdot I \quad \dots(2.8)$$

The horizontal and vertical moduli of subgrade reaction are considered to have the same value at the base of the well foundation which may be at a substantial depth below ground level. According to Barkan (45),

$$C_{\phi} = 2 C_u \quad \dots(2.9)$$

where;

$$C_u = \text{coefficient of uniform elastic compression} \\ = n_h \cdot H$$

Eq. 2.8 can, thus, be written as:

$$K_{\phi 2} = 2 n_h \cdot H \cdot I \quad \dots(2.10)$$

The total rotational stiffness at the base of the foundation ( $K_{\theta}$ ) is given by:

$$K_{\theta} = K_{\theta 1} + K_{\theta 2}$$

$$\text{or } K_{\theta} = 2 n_h \cdot H \left( I + \frac{H^3}{24} \right) \quad \dots(2.11)$$

(iii) The soil stiffnesses calculated by Arya et al (38) are based on the recommendations of Terzaghi (195). The calculations of translational stiffness of side soil and rotational stiffness at the base are independent of the width (B) of well foundation (fig. 2.1d). The soil stiffnesses calculated by Ahmad (1) are based on the recommendations of Barkan (45). The calculation of translational stiffness of side soil is independent of the width of well while the rotational stiffness at the base takes into account the width of well also. An overall rotational stiffness at the base of the foundation has been lumped which includes the effect of translational side-soil stiffness in the form of rotational stiffness at the base and the rotational stiffness due to vertical soil reaction at the base.

Terzaghi's (195) recommendations, in which the width of footing is ignored in calculating the side-soil stiffness, are meant primarily for piles having small width compared to their depth. The recommendation is supported by the experimental findings that the diameter of the pressure bulb of the soil increases proportionately with the width of footing at ultimate load, thus, resulting in no change in the stiffness of the resisting soil due to a change in the width of contact. Well foundations at working loads may not undergo large displacements and the side soil stiffness may be more than that computed on the basis of unit width. In the absence of any data for well foundations, the

conservative approach used by Ahmad (1) and Arya et al (38), to calculate side-soil stiffness, can be considered logical.

The rotational stiffness of the base due to vertical soil reaction computed on the basis of unit width results in very flexible soil spring. The approach of Barkan (45) which takes into account the moment of inertia of the actual base of the foundation can be considered more logical.

The foundation well can be assumed to undergo only rigid body movements because of high cross-sectional rigidity. Working loads are not expected to mobilize huge frictional forces at the base of the well. Assumption of translational fixity at the base can, therefore, be justified.

## 2.12 EXPERIMENTAL STUDIES

(i) Use of models as an aid to bridge design and analysis was pioneered by Baker (42), Beggs (52), Fairbairn (58), Eney (71), Gottshalk (95), Pippard (156) and others. First steel model of a suspension bridge was tested in U.S.A. in 1930 (53, 187). A wide and successful application of model analysis has been made in the design of many cable-stayed bridges (50, 57, 80, 190). Troitsky and Lazar (203, 4, 6-8) have carried out detailed model studies to cover aspects of model design and analysis, influence lines, nonlinear behaviour of the bridge and post tensioning of cables. Seismic investigations have been carried out on perspex models of cable-stayed bridges by Arya et al (37) and Krishna et al (117).

(ii) Experimental studies on a properly designed and scaled model are important to verify the physical behaviour of the proposed structure. The analytical and test results of the experimental structure can be compared to check the validity of the analytical tools employed in calculating the design forces and deformations.

### 2.13 WIND EFFECTS AND DYNAMIC RESPONSE

(i) The study of aerodynamic aspects can be separated from the structural aspects by wind tunnel tests, which are gaining importance (116), to assess the aerodynamics of cable-stayed bridges. Important developments in wind tunnel techniques for bridge testing were made by Scruton (176). An extensive wind tunnel program was carried out to examine proposed sections for Severn River Crossing. Full model and sectional model tests were conducted and it was established that the results using the sectional approach provided a satisfactory picture of the bridges aerodynamic behaviour. The conditions of dynamic similarity between model and full scale bridge have been discussed by Farquharson (78) and Frazer and Scruton (84, 176). The aerodynamically shaped design of Leonhardt (128) for Tagus Bridge was tested by Scruton in 1959. The test proved that aerodynamic stability can be obtained by simple means with very slender structures. Humber Bridge (7) in England, Severn Bridge (89, 90) in Denmark and Bosphorus Bridge (217) in Turkey were designed along the same principle and using

flat hollow box.

(ii) Cable stayed bridges may be sensitive to static wind effects and the effect of ground motion due to an earthquake. Three dimensional static analysis for wind forces and dynamic analysis for earthquake forces is not known to be reported. A proper skeletal representation of the components of the structure for its frame analysis is important to simulate the actual behaviour.

(iii) It is relatively more difficult to provide and maintain a resonant oscillation with attendant large amplitudes in a multi-cable stayed structure. The cables tend to disturb the formation of the first and second mode of oscillation by interfering with smaller wave lengths of higher order. Thus, the inherent system damping of the cable stayed structure produces relatively smaller amplitudes compared with the suspension system. A-frame towers provide increased resistance to torsional oscillations of the roadway deck.

#### 2.14 SUMMARY

The review of literature presented in this chapter can be summarised as follows:

(i) The first modern cable-stayed bridge was erected in 1955. About sixty cable-stayed bridges have since been built or are being planned.

(ii) Structural and economic superiority of a cable-stayed bridge over suspension bridge has been indicated from studies of Leonhardt on a main span of 1300 m.

(iii) Economic superiority of cable-stayed bridges has been established in Europe for span range of 90-370 m.

(iv) Cable stayed bridges present better aesthetic appeal.

(v) Available information in the form of influence lines or parameteric charts is not sufficient to cover various possibilities of cable configurations, cable-supports at pylons, support conditions at the base of the tower, mode of transfer of forces between superstructure and substructure.

(vi) Information in the form of influence lines or parametric charts is not known to be available regarding the behaviour under eccentric vertical and lateral loads.

(vii) Technique of mathematical simulation is an important aid to the analysis to represent actual physical behaviour.

(viii) Lateral stiffness of the deck of a cable-stayed bridge can be represented by replacing the infill between parallel girder members by an equivalent diagonal strut of appropriate stiffness.

(ix) Approximate methods of analysis are useful in the preliminary design of bridge structure.



(x) For the skeletal representation of a cable-stayed bridge, the stiffness approach of linear and non-linear analysis can be considered to be a versatile method.

(xi) Non linear analysis can be performed by successive iterations of linear subroutines. The procedure can be incorporated in linear computer program with comparatively lesser additional programming effort.

(xii) Nonlinearity due to catenary action can be accounted for in the analysis by using the concept of equivalent modulus of elasticity.

(xiii) Nonlinearity due to catenary action can be ignored in the live load analysis but should be considered in the erection stage analysis.

(xiv) Separate studies on nonlinearity due to large displacements are not known to be reported.

(xv) Separate studies on nonlinearity due to bending moment-axial force interaction are not conclusive. The nonlinear effects may be negligible or significant depending on the overall stiffness of the bridge structure.

(xvi) Nonlinear analysis should be carried out for fully stressed state under full dead and live loads.

(xvii) Studies on soil resistance offered to well foundations are not known to be reported. In the absence of data, the side soil stiffness may be computed on the basis of unit width of contact while the rotational stiffness at

the base may be computed on the basis of full area of contact.

(xviii) The foundation well can be assumed to undergo rigid body rotations with translational fixity at the base.

(xix) Three dimensional static analysis for wind forces and dynamic analysis for earthquake forces is not known to be reported.

(xx) Experimental studies on a properly designed and scaled model are important.

## C H A P T E R 3

### ANALYSIS FOR STATIC LOADING

#### 3.1 INTRODUCTION

Stiffness method of structural analysis and Gaussian elimination technique of solution have been briefly described. Assumptions involved in representing the bridge as a space system and as a planar system have been outlined. Various types of member stiffness matrices have been presented. Static space frame and plane frame computer analyses used in the present investigation have been described.

#### 3.2 REPRESENTATION OF THE STRUCTURE

As stated earlier, the main components of a cable-stayed bridge are the following:

(i) the deck consisting of a reinforced concrete slab supported by cross girders and longitudinal stiffening girders,

(ii) the towers providing support to the deck at piers,

(iii) the cables tied at the top of the towers and at points of the deck for supporting the deck,

(iv) the piers and,

(v) the foundation caissons.

The bridge structure can be represented, with reasonable assumptions, as a skeletal structure having a high

kinematic indeterminacy.

### 3.2.1 Representation as Space System

For studying the behaviour under lateral horizontal and eccentric vertical forces, the bridge is represented by a rigid jointed three dimensional skeletal structure, halved at its transverse axis of symmetry. Axial, flexural and torsional deformations of members are included in the analysis as found appropriate for the nature of a member. The stressed skin of the deck between parallel stiffening girder elements is replaced by transverse and diagonal braces of appropriate stiffness. The following simplifying assumptions are made:

(a) The cables possess only axial stiffness and are completely flexible so far as bending stiffness is concerned. Thus, the skeletal representing the cables would possess only area and no moment of inertia.

(b) Cables can take axial compressive forces also. Since the superimposed compressive forces are found to be less than the initial pretension of the cables, the cables would not slacken.

(c) The nodes are chosen at the points of intersection and free nodes of the members and the points of supports.

(d) The loads on the structure are concentrated actions at the nodes.

(e) In actual practice, the superstructure is connected to the substructure through hinge at one end and links at tower support locations and another end support. The space structure, used for analysis, is halved at transverse axis of symmetry. The halved structure represents a bridge hinged at both ends and provided with links at tower support locations. Thus, in the longitudinal direction, rotational deformations are permitted at all the locations of supports while rolling is permitted at locations of links. The hinged end and the links permit only elastic deformations in transverse direction of the bridge.

(f) For studying the effect of soil-structure interaction the foundation caissons are treated as (i) fixed at the bottom, (ii) supported on springs of varying stiffnesses representing the soil stiffnesses against translation and rotation.

### 3.2.2 Representation as Planar System

For studying the bridge structure under symmetric vertical loads and horizontal actions acting along the longitudinal axis of the bridge. The skeletal representation can be simplified and the structure can be idealized as a planar system. In addition to assumptions made above for space representation, it is assumed that, by virtue of symmetry of the structure about the longitudinal axis, half the bridge may be considered in analysis under symmetric loading. Symmetry of deformations will exist. Therefore,

all the members, loads and actions lie in a single plane and the deck elements will not offer any torsional resistance.

### 3.3 STIFFNESS METHOD OF ANALYSIS

This approach of analysis, which is one of the most powerful methods available to the structural analyst, has been used to solve both the space and the planar frames. The important steps involved in the method used in conjunction with an automatic digital computer are described in the following paragraphs.

#### 3.3.1 Assembly of Structure Data

Number of members, joints and degrees of freedom; geometric and elastic properties of member sections; nodes incident at two ends of each member, coordinates of the nodes and conditions of restraints at the supports of the structure are coded in a convenient manner.

#### 3.3.2 Generation of Joint Stiffness Matrix

The joint stiffness matrix of the structure is generated by summing up the contributions from individual member stiffness matrices. These are discussed later in this section.

#### 3.3.3 Generation of Load Vectors

The joint loads acting on the structure are handled directly while distributed loads on the members are converted

to equivalent joint loads. The equivalent joint loads are then added to the actual joint loads and the load vector assembled.

### 3.3.4 Solution for Joint Displacements; Gauss' Elimination Technique

The joint stiffness matrix of the structure and its nodal forces and deformations are related by the following linear system of simultaneous equations presented in the matrix form

$$\begin{bmatrix} k_{11} & k_{12} & \text{-----} & k_{1n} \\ k_{21} & k_{22} & \text{-----} & k_{2n} \\ \text{-----} & \text{-----} & \text{-----} & \text{-----} \\ k_{n1} & k_{n2} & \text{-----} & k_{nn} \end{bmatrix} \begin{Bmatrix} \delta_1 \\ \delta_2 \\ \text{---} \\ \delta_n \end{Bmatrix} = \begin{Bmatrix} P_1 \\ P_2 \\ \text{---} \\ P_n \end{Bmatrix} \quad \dots(3.1)$$

or  $[k]_{n,n} \cdot \{\delta\}_n = \{P\}_n$

where,  $[k]_{n,n}$  = Matrix of stiffness influence coefficients

$\{\delta\}_n$  = Deformation vector

$\{P\}_n$  = Force vector

$n$  = Number of degrees of freedom.

Gauss' elimination (pivotal condensation) technique has been used to solve equations 3.1. The method is based on triangularization of the stiffness coefficient matrix by virtue of the elementary property of the determinants that

The determinant of a matrix is not changed when a multiple of one row (or column) is added to another row (or column). The unknown deformations  $\{\delta\}$  are, then, evaluated by back substitution starting from the last equation.

The solution of equations 3.1 follows these steps:

(a) Eliminate the coefficients of  $\delta_1$  in the second and subsequent equations by selecting  $k_{11}$  as pivot and

(i) add the multiple  $-k_{21}/k_{11}$  of the first row to the second row,

(ii) add the multiple  $-k_{31}/k_{11}$  of the first row to the third row,

(iii) continue the procedure until the nth row.

The system will be reduced to the following form at the end of this step

$$\begin{bmatrix} k_{11} & k_{12} & \text{-----} & k_{1n} \\ 0 & k'_{22} & \text{-----} & k'_{2n} \\ \text{-----} & & & \\ 0 & k'_{n2} & \text{-----} & k'_{nn} \end{bmatrix} \begin{Bmatrix} \delta_1 \\ \delta_2 \\ \text{---} \\ \delta_n \end{Bmatrix} = \begin{Bmatrix} P_1 \\ P_2' \\ \text{---} \\ P_n' \end{Bmatrix} \quad \dots(3.2)$$

(b) Eliminate the coefficient of  $\delta_2$  in third and subsequent equations of equations 3.2 by selecting  $k'_{22}$  as pivot and

(i) add the multiple  $-k'_{32}/k'_{22}$  of the second row to the third row.



(ii) add the multiple  $-k'_{42}/k'_{22}$  of the second row to the fourth row.

(iii) continue the procedure until the nth row.

The system will be reduced to the following form at the end of this steps

$$\begin{bmatrix}
 k_{11} & k_{12} & k_{13} & \dots & k_{1n} \\
 0 & {}^1k_{22} & {}^1k_{23} & \dots & {}^1k_{2n} \\
 0 & 0 & {}^2k_{33} & \dots & {}^2k_{3n} \\
 \dots & \dots & \dots & \dots & \dots \\
 0 & 0 & {}^2k_{n3} & \dots & {}^2k_{nn}
 \end{bmatrix}
 \begin{Bmatrix}
 \delta_1 \\
 \delta_2 \\
 \delta_3 \\
 \dots \\
 \delta_n
 \end{Bmatrix}
 =
 \begin{Bmatrix}
 P_1 \\
 P'_2 \\
 P''_3 \\
 \dots \\
 P''_n
 \end{Bmatrix}
 \dots(3.3)$$

(c) Repeat the above steps in succession in the remaining rows with  ${}^2k_{33}$ ,  ${}^3k_{44}$  -----  ${}^{n-1}k_{nn}$  as pivots. Finally the system will be triangularized in the form

$$[U] \{ \delta \} = \{ Q \} \text{ in which } u_{ij} = 0 \text{ for } i > j \dots(3.4)$$

(d) Determine  $\delta_n$  from the last equation as

$$\delta_n = \frac{{}^{n-1}P_n}{{}^{n-1}k_{nn}} \dots(3.5)$$

and by back substitution, all other unknowns can be evaluated.

Steps (a) to (d) can be summarised by two equations;

$$k_{ij} = k_{ij} - \frac{k_{mj}}{k_{mm}} k_{im} \quad \dots(3.6)$$

$$\delta_i = \frac{1}{k_{ii}} (k_{i,n+1} - \sum_{r=i+1}^n k_{ir} \delta_r)$$

for  $m = 1, 2, \dots, n-1$

$i = K+1, \dots, n$

$j = K, \dots, n+1$

here,  $k_{i, n+1} = P_i$  represents the load vector

### 3.3.5 Limitations of Gauss' Elimination Technique:

(a) The term  $k_{ii}$  in the stiffness matrix must be nonzero since it is a divisor at each stage of operation. An original stiffness matrix with nonzero elements does not guarantee that the pivots at each stage will be nonzero.

(b) Sequential selection of pivots, without testing whether a particular one is the best possible, may cause loss of accuracy in the results.

A test to determine whether  $k_{ii}$  is zero at any stage and, if so, interchanges of rows of the stiffness and force matrices by keeping a proper track of the operations can solve the problem. Selecting the largest in the absolute value of the elements in any column (called partial pivoting strategy) or by selecting the largest element of the whole matrix (called the complete pivoting strategy) of the

remaining equations, the accuracy of the results can be improved. These operations are possible at the cost of computation time and may, normally, not be required for the structural problems of well conditioned structure stiffness matrices.

### 3.3.6 Member Forces and Reactions

From the joint deformations, obtained by solving linear simultaneous equations, support reactions and member end actions are computed in the final phase of analysis and printouts of joint deformations, member end forces and support reactions are taken in suitable format. The equilibrium of forces at each joint is ascertained.

## 3.4 MEMBER STIFFNESS MATRICES (88,109,34,221)

The stiffness coefficients for a member restrained at its ends are the actions exerted on the member by the restraints when unit displacements, induced one at a time, are imposed at the member ends. Member stiffness matrices developed in conjunction with a set of member oriented orthogonal system of axes have twofold use in the analysis:

(a) Stiffness contributions of the member at the nodes, which connect it to the structure, are obtained by suitable transformations into the 'structure axes'.

(b) Final actions at the ends of the member, in member axes, are calculated after the joint displacements have been found.

The member stiffness matrices presented in this section hold good for prismatic members with the assumption that the shear centre and the centroid of the member coincide so that there is no interaction between the twisting and bending of the member. The shearing deformations are neglected.

### 3.4.1 Fully Restrained Member in Space

For the most general case of a restrained member of a space structure, coefficients for twelve possible types of displacements of its two ends are represented in fig. 3.1. In each case, the various restraint actions (member stiffnesses), required to hold the member in equilibrium, are shown as vectors. An arrow with single head represents a force vector and an arrow with double head represents a moment vector. The member stiffness matrix thus obtained is given in table 3.1. Here the deformations are taken in the order of translations along  $X_M$ ,  $Y_M$  and  $Z_M$  axes and rotations about the same axes respectively. The various notations used are,

$L$  = Length of the member

$A_x$  = Area of cross-section of the member

$I_Y$  = Principal moment of inertia of the cross-section  
of the member with respect to  $Y_M$  axis

$I_Z$  = Principal moment of inertia of the cross-section  
of the member with respect to  $Z_M$  axis

$I_X$  = Torsional constant for the cross-section (fig.  
3.2).

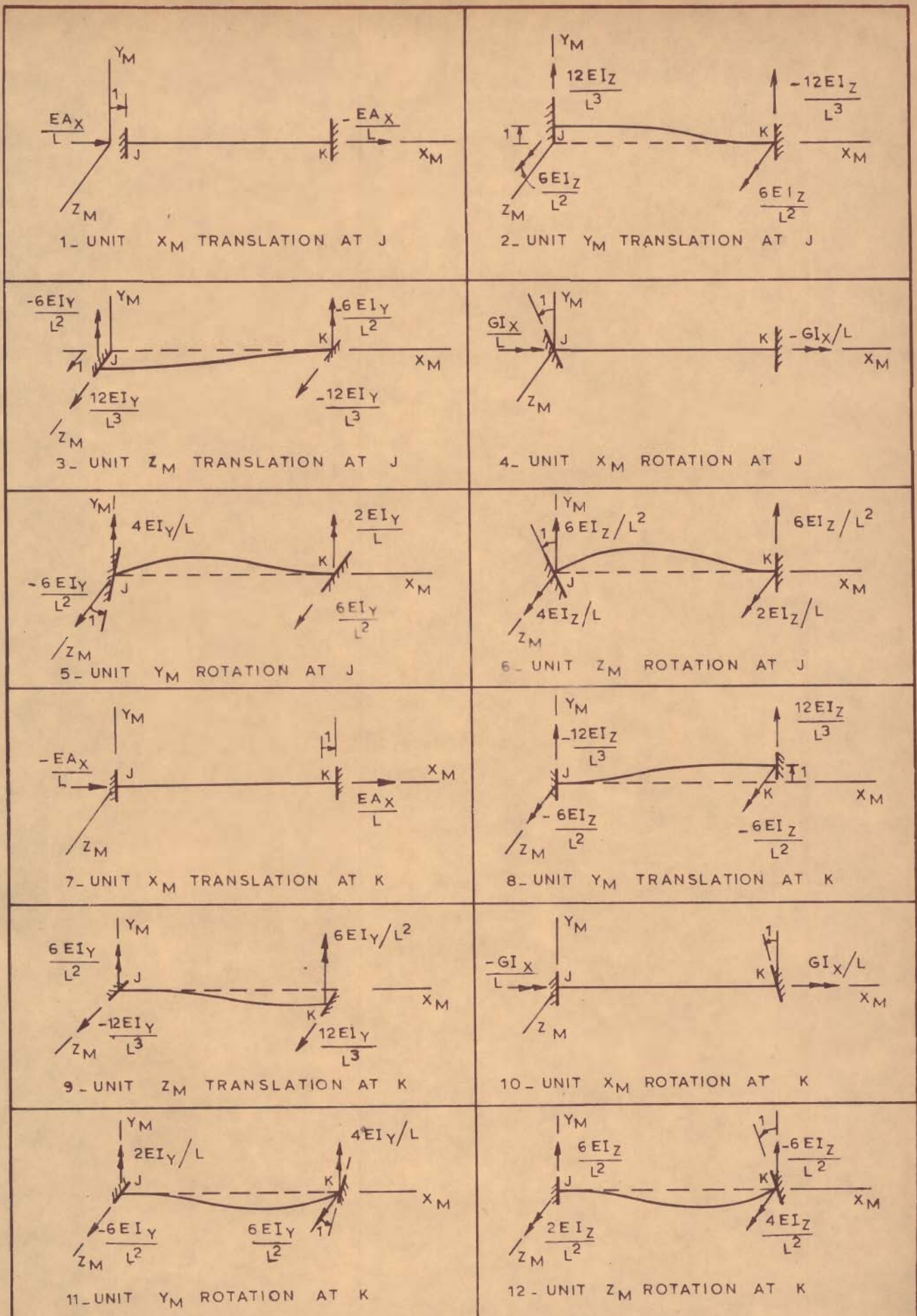


FIG. 3.1 \_ MEMBER STIFFNESSES IN MEMBER AXES FOR FULLY RESTRAINED MEMBER IN SPACE

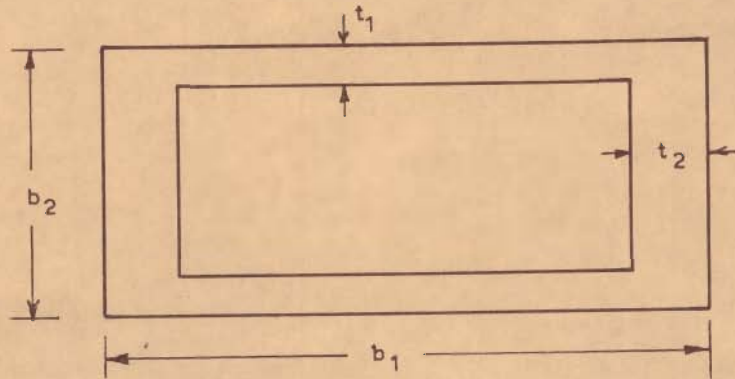
TABLE 3.1 STIFFNESS MATRIX IN MEMBER AXES FOR FULLY RESTRAINED MEMBER IN SPACE

	$U_{JX}$	$U_{JY}$	$U_{JZ}$	$\theta_{JX}$	$\theta_{JY}$	$\theta_{JZ}$	$U_{KX}$	$U_{KY}$	$U_{KZ}$	$\theta_{KX}$	$\theta_{KY}$	$\theta_{KZ}$
$P_{JX}$	$M_1$	0	0	0	0	0	$-M_1$	0	0	0	0	0
$P_{JY}$	0	$M_2$	0	0	0	$M_3$	0	$-M_2$	0	0	0	$M_3$
$P_{JZ}$	0	0	$M_4$	0	$-M_5$	0	0	0	$-M_4$	0	$-M_5$	0
$M_{JX}$	0	0	0	$M_6$	0	0	0	0	0	$-M_6$	0	0
$M_{JY}$	0	0	$-M_5$	0	$M_7$	0	0	0	$M_5$	0	$\frac{M_7}{2}$	0
$M_{JZ}$	0	$M_3$	0	0	0	$M_8$	0	$-M_3$	0	0	0	$\frac{M_8}{2}$
$P_{KX}$	$-M_1$	0	0	0	0	0	$M_1$	0	0	0	0	0
$P_{KY}$	0	$-M_2$	0	0	0	$-M_3$	0	$M_2$	0	0	0	$-M_3$
$P_{KZ}$	0	0	$-M_4$	0	$M_5$	0	0	0	$M_4$	0	$M_5$	0
$M_{KX}$	0	0	0	$-M_6$	0	0	0	0	0	$M_6$	0	0
$M_{KY}$	0	0	$-M_5$	0	$\frac{M_7}{2}$	0	0	0	$M_5$	0	$M_7$	0
$M_{KZ}$	0	$M_3$	0	0	0	$\frac{M_8}{2}$	0	$-M_3$	0	0	0	$M_8$

$$M_1 = \frac{EA_X}{L}, \quad M_2 = \frac{12EI_Z}{L^3}, \quad M_3 = \frac{6EI_Z}{L^2}$$

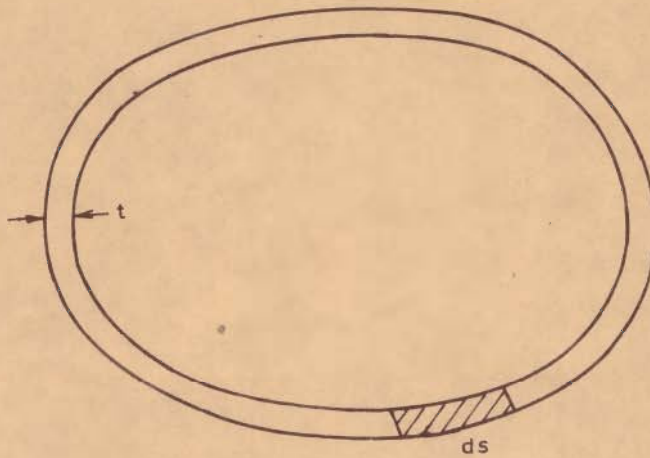
$$M_4 = \frac{12EI_Y}{L^3}, \quad M_5 = \frac{6EI_Y}{L^2}, \quad M_6 = \frac{GI_X}{L}$$

$$M_7 = \frac{4EI_Y}{L}, \quad M_8 = \frac{4EI_Z}{L}$$



$$I_{xx} = \frac{2 t_1 t_2 (b_1 - t_2)^2 (b_2 - t_1)^2}{b_1 t_2 + b_2 t_1 - t_2^2 - t_1^2}$$

a\_ HOLLOW RECTANGULAR CROSS - SECTION



$$I_{xx} = \int \frac{4 a^2}{t} ds$$

a - AREA ENCLOSED BY A LINE THROUGH THE CENTRE OF THE THICKNESS

INTEGRATION IS CARRIED OUT OVER THE CIRCUMFERENCE

b\_ CLOSED HOLLOW CROSS - SECTION (GENERAL)

FIG. 3.2\_ TORSIONAL CONSTANTS

### 3.4.2 Truss Member in Space

The general stiffness matrix given in table 3.1 can be simplified for cases of members where the end conditions are specified. For instance, for a simple truss member with no rotational restraint at the end or the cables having no flexural rigidity, only axial forces will exist in the member. The significant joint displacements will be nodal translations. The member stiffness matrix of such a member coordinates is given in table 3.2 for twelve possible displacements at its ends.

### 3.4.3 Partially Restrained Member in Space

If the end J of the member JK shown in fig. 3.1 was hinged about the  $Z_M$  axis, the effect of the free rotation about  $Z_M$  axis could be considered as such and the coefficients in cases 2, 6, 8 and 12 will get modified. The resulting stiffness matrix would be as shown in table 3.3. Use of such a matrix would reduce the number of unknowns and hence the computation time.

### 3.4.4 Fully Restrained Member in a Plane

The stiffness coefficients for six possible types of co-planar displacements at two ends of a fully restrained member are given in table 3.4. The deformations have been considered in the order of translations along  $X_M$  and  $Y_M$  axes and rotation about  $Z_M$  axis for ends J and K respectively.



TABLE 3.2 STIFFNESS MATRIX IN MEMBER AXES FOR TRUSS MEMBER  
IN SPACE

	$U_{JX}$	$U_{JY}$	$U_{JZ}$	$\theta_{JX}$	$\theta_{JY}$	$\theta_{JZ}$	$U_{KX}$	$U_{KY}$	$U_{KZ}$	$U\theta_{KX}$	$\theta_{KY}$	$\theta_{KZ}$
$P_{JX}$	$\frac{EA_X}{L}$	0	0	0	0	0	$-\frac{EA_X}{L}$	0	0	0	0	0
$P_{JY}$	0	0	0	0	0	0	0	0	0	0	0	0
$P_{JZ}$	0	0	0	0	0	0	0	0	0	0	0	0
$M_{JX}$	0	0	0	0	0	0	0	0	0	0	0	0
$M_{JY}$	0	0	0	0	0	0	0	0	0	0	0	0
$M_{JZ}$	0	0	0	0	0	0	0	0	0	0	0	0
$P_{KX}$	$-\frac{EA_X}{L}$	0	0	0	0	0	$\frac{EA_X}{L}$	0	0	0	0	0
$P_{KY}$	0	0	0	0	0	0	0	0	0	0	0	0
$P_{KZ}$	0	0	0	0	0	0	0	0	0	0	0	0
$M_{KX}$	0	0	0	0	0	0	0	0	0	0	0	0
$M_{KY}$	0	0	0	0	0	0	0	0	0	0	0	0
$M_{KZ}$	0	0	0	0	0	0	0	0	0	0	0	0

TABLE 3.3 STIFFNESS MATRIX IN MEMBER AXES FOR  
A MEMBER JK WITH J END HINGED  
ABOUT  $Z_M$ - AXIS AND RESTRAINED IN  
OTHER DIRECTIONS IN SPACE

	$U_{JX}$	$U_{JY}$	$U_{JZ}$	$\theta_{JX}$	$\theta_{JY}$	$\theta_{JZ}$	$U_{KX}$	$U_{KY}$	$U_{KZ}$	$\theta_{KX}$	$\theta_{KY}$	$\theta_{KZ}$
$P_{JX}$	$N_1$	0	0	0	0	0	$-N_1$	0	0	0	0	0
$P_{JY}$	0	$N_2$	0	0	0	0	0	$-N_2$	0	0	0	$N_3$
$P_{JZ}$	0	0	$N_4$	0	$-N_5$	0	0	0	$-N_4$	0	$-N_5$	0
$M_{JX}$	0	0	0	$N_6$	0	0	0	0	0	$-N_6$	0	0
$M_{JY}$	0	0	$-N_5$	0	$N_7$	0	0	0	$N_5$	0	$\frac{N_7}{2}$	0
$M_{JZ}$	0	0	0	0	0	0	0	0	0	0	0	0
$P_{KX}$	$-N_1$	0	0	0	0	0	$N_1$	0	0	0	0	0
$P_{KY}$	0	$-N_2$	0	0	0	0	0	$N_2$	0	0	0	$-N_3$
$P_{KZ}$	0	0	$-N_4$	0	$N_5$	0	0	0	$N_4$	0	$N_5$	0
$M_{KX}$	0	0	0	$-N_6$	0	0	0	0	0	$N_6$	0	0
$M_{KY}$	0	0	$-N_5$	0	$\frac{N_7}{2}$	0	0	0	$N_5$	0	$N_7$	0
$M_{KZ}$	0	$N_3$	0	0	0	0	0	$-N_3$	0	0	0	$N_8$

$$N_1 = \frac{EA_X}{L}, \quad N_2 = \frac{3EI_Z}{L^3}, \quad N_3 = \frac{3EI_Z}{L^2}$$

$$N_4 = \frac{12EI_Y}{L^3}, \quad N_5 = \frac{6EI_Y}{L^2}, \quad N_6 = \frac{GI_X}{L}$$

$$N_7 = \frac{4EI_Y}{L}, \quad N_8 = \frac{3EI_Z}{L}$$

TABLE 3.4 STIFFNESS MATRIX IN MEMBER AXES FOR FULLY RESTRAINED MEMBER JK IN A PLANE

	$U_{JX}$	$U_{JY}$	$\theta_{JZ}$	$U_{KX}$	$U_{KY}$	$\theta_{KZ}$
$P_{JX}$	$\frac{EA_X}{L}$	0	0	$-\frac{EA_X}{L}$	0	0
$P_{JY}$	0	$\frac{12EI_Z}{L^3}$	$\frac{6EI_Z}{L^2}$	0	$-\frac{12EI_Z}{L^3}$	$\frac{6EI_Z}{L^2}$
$M_{JZ}$	0	$\frac{6EI_Z}{L^2}$	$\frac{4EI_Z}{L}$	0	$-\frac{6EI_Z}{L^2}$	$\frac{2EI_Z}{L}$
$P_{KX}$	$-\frac{EA_X}{L}$	0	0	$\frac{EA_X}{L}$	0	0
$P_{KY}$	0	$-\frac{12EI_Z}{L^3}$	$-\frac{6EI_Z}{L^2}$	0	$\frac{12EI_Z}{L^3}$	$-\frac{6EI_Z}{L^2}$
$M_{KZ}$	0	$\frac{6EI_Z}{L^2}$	$\frac{2EI_Z}{L}$	0	$-\frac{6EI_Z}{L^2}$	$\frac{4EI_Z}{L}$

### 3.4.5 Truss Member in a Plane

The stiffnesses for six possible types of coplanar displacements at the two ends of a 'truss' member are given in table 3.5.

TABLE 3.5 STIFFNESS MATRIX IN MEMBER AXES FOR TRUSS MEMBER JK IN A PLANE

	$U_{JX}$	$U_{JY}$	$\theta_{JZ}$	$U_{KX}$	$U_{KY}$	$\theta_{KZ}$
$P_{JX}$	$\frac{EA_X}{L}$	0	0	$-\frac{EA_X}{L}$	0	0
$P_{JY}$	0	0	0	0	0	0
$M_{JZ}$	0	0	0	0	0	0
$P_{KX}$	$-\frac{EA_X}{L}$	0	0	$\frac{EA_X}{L}$	0	0
$P_{KY}$	0	0	0	0	0	0
$M_{KZ}$	0	0	0	0	0	0

### 3.4.6 Partially Restrained Member in a Plane

The stiffnesses for six possible types of coplanar displacements at the two ends of a member with J end hinged about  $Z_M$ -axis and restrained in other directions are given in table 3.6.

TABLE 3.6 STIFFNESS MATRIX IN MEMBER AXES FOR A MEMBER JK WITH J END HINGED ABOUT  $Z_M$ -AXIS AND RESTRAINED IN OTHER DIRECTIONS IN A PLANE

	$U_{JX}$	$U_{JY}$	$\theta_{JZ}$	$U_{KX}$	$U_{KY}$	$\theta_{KZ}$
$P_{JX}$	$\frac{EA_X}{L}$	0	0	$\frac{-EA_X}{L}$	0	0
$P_{JY}$	0	$\frac{3EI_Z}{L^3}$	0	0	$\frac{-3EI_Z}{L^3}$	$\frac{3EI_Z}{L^2}$
$P_{JZ}$	0	0	0	0	0	0
$P_{KX}$	$\frac{-EA_X}{L}$	0	0	$\frac{EA_X}{L}$	0	0
$P_{KY}$	0	$\frac{-3EI_Z}{L^3}$	0	0	$\frac{3EI_Z}{L^3}$	$\frac{-3EI_Z}{L^2}$
$M_{KZ}$	0	$\frac{3EI_Z}{L^2}$	0	0	$\frac{-3EI_Z}{L^2}$	$\frac{3EI_Z}{L}$

### 3.5 ROTATION TRANSFORMATION MATRICES

Rotation Transformation matrix  $R_T$  is required to transform the member stiffness matrix from member axes

to structure axes.  $R_T$  can be obtained from a rotation matrix (R) expressed in terms of direction cosines of the member.

### 3.5.1 Space Frame Member

The rotation transformation matrix for a space frame member is given by:

$$R_T = R_{TS} = \begin{bmatrix} R & 0 & 0 & 0 \\ 0 & R & 0 & 0 \\ 0 & 0 & R & 0 \\ 0 & 0 & 0 & R \end{bmatrix} \dots(3.7)$$

The form of rotation matrix R depends upon the orientation of the member axes. For a member having principal axes of its cross-section lying in horizontal and vertical planes, the member axes are defined as follows:

$X_M$  is the axis of the member,

$Y_M$  is the axis located in a vertical plane passing through  $X_M$  and  $Y_S$  axes,

$Z_M$  is the axis located in a horizontal plane lying in  $X_S - Z_S$  plane.

$X_S$ ,  $Y_S$  and  $Z_S$  refer to the axes of the structure.

For the member axes specified in the manner described above and for inclined cable members which are circular in the cross-section, the rotation matrix (R) is

given by:

$$R = R_S = \begin{bmatrix} C_X & C_Y & C_Z \\ \frac{-C_X C_Y}{\sqrt{C_X^2 + C_Z^2}} & \sqrt{C_X^2 + C_Z^2} & \frac{-C_Y C_Z}{\sqrt{C_X^2 + C_Z^2}} \\ \frac{-C_Z}{\sqrt{C_X^2 + C_Z^2}} & 0 & \frac{C_X}{\sqrt{C_X^2 + C_Z^2}} \end{bmatrix} \dots(3.8)$$

where,

$$C_X = \frac{x_K - x_J}{L}, \quad C_Y = \frac{y_K - y_J}{L}, \quad C_Z = \frac{z_K - z_J}{L} \quad \dots(3.9)$$

and,

$$L = \sqrt{(x_K - x_J)^2 + (y_K - y_J)^2 + (z_K - z_J)^2} \quad \dots(3.10)$$

$x_J, y_J, z_J, x_K, y_K$  and  $z_K$  refer to the coordinates of the two ends of a member in space.

From the specifications of the member axes described above in this section, the position of  $Z_M$  is not fixed uniquely for a vertical member in space. This difficulty can be overcome by specifying  $Z_M$  axis along the  $Z_S$  axis for a vertical member. The rotation matrix (R) is, then given by

$$R = R_{\text{vert}} = \begin{bmatrix} 0 & C_Y & 0 \\ -C_Y & 0 & 0 \\ 0 & 0 & 1 \end{bmatrix} \quad \dots(3.11)$$

where  $C_Y$  has already been defined.

For members that are nearly vertical, a quantity  $Q = \sqrt{C_X^2 + C_Z^2}$  is calculated and if  $Q$  is found to be less than a specified quantity (0.001 used here), the member is considered vertical.

### 3.5.2 Plane Frame Member

The rotation transformation matrix for a plane frame member is given by:

$$R_T = R_{TP} = \begin{bmatrix} R & 0 \\ 0 & R \end{bmatrix} \quad \dots(3.12)$$

where,

$$R = R_P = \begin{bmatrix} C_X & C_Y & 0 \\ -C_Y & C_X & 0 \\ 0 & 0 & 1 \end{bmatrix} \quad \dots(3.13)$$

$$C_X = \frac{x_K - x_J}{L}, \quad C_Y = \frac{y_K - y_J}{L} \quad \dots(3.14)$$

$$L = \sqrt{(x_K - x_J)^2 + (y_K - y_J)^2} \quad \dots(3.15)$$

$x_J$ ,  $y_J$ ,  $x_K$  and  $y_K$  refer to the coordinates of the two ends of a member in a plane.

### 3.5.3 Use of Rotation Transformation Matrices

(i) Member stiffness matrix for structure axes ( $S_{MD}$ ) is obtained from the member stiffness matrix for

member axes ( $S_M$ ) by,

$$S_{MD} = R_T' S_M R_T \quad \dots(3.16)$$

where  $R_T'$  is the transpose of rotation transformation matrix  $R_T$ .

(ii) Joint deformations at the two ends of a member in member axes ( $D_M$ ) are obtained from the joint deformations at the two ends of a member in structure axes ( $D_S$ ) by

$$D_M = R_T D_S \quad \dots(3.17)$$

The joint deformations  $D_M$  are further used to calculate forces at the ends of a member in member axes by:

$$A_M = S_M D_M \quad \dots(3.18)$$

### 3.6 STRUCTURAL DISCONTINUITY

To account for the action of a hinge at one or more internal joints of the structure, a rotational discontinuity has to be introduced at such joints. The particular member, meeting at the joint and which is considered free to rotate about that joint, is considered to have a hinged support at this joint and a rigid connection to the other members at the other end. The analysis of structures consisting of members with hinged end conditions at joints other than supports requires the use of proper stiffness matrices for the members. The stiffness matrices relevant to the



present study are already given in 3.4.3 and 3.4.6.

Members meeting at an internal hinge would rotate independently of each other. The final computer results provide the rotation corresponding to the end of the member in which the hinge is not located. The rotation of the end of the member in which the hinge is located can be calculated using the hinged member deformations.

### 3.7 ELASTIC SUPPORTS

The soil present underneath and at the sides of the foundation caissons is assumed to remain linearly elastic under the action of applied load and is represented by uncoupled translational and rotational elastic springs. The structural components of the foundation are then subjected to the reactive forces of the elastic springs which are proportional to their corresponding deformations. The stiffness of the structure at the joints where the springs are coupled, will increase by the amount of these stiffnesses and can be directly added to the overall joint stiffness matrix at appropriate joints of the structure. The movements of the elastic supports are entirely controlled by their reactions and are found using the computed reaction components.

### 3.8 USE OF SYMMETRY/ANTISYMMETRY

A general unsymmetrical loading on a symmetrical structure can be divided into symmetrical and antisymmetrical

loadings according to the principle of superposition. The methods of analysis can, thus, be applied to two different substructures of smaller size with two different loadings to give the results of analysis of a larger structure with unsymmetrical loading. Fig 3.3 explains the substructures separated out from a main planar structure at axis of symmetry with boundary conditions imposed at cut points. For structures with large number of degrees of freedom, the method is economical and needs less computer storage space without any additional analytical or programming effort.

A further economy in the computation time and computer storage space can be achieved by making suitable changes in the stiffness influence coefficients of the members that are cut in transverse direction by the line of symmetry. The relationship between the deformations at the two ends J and K of such a member for symmetrical and antisymmetrical loadings of the structure are expressed as:

Symmetrical Loading:

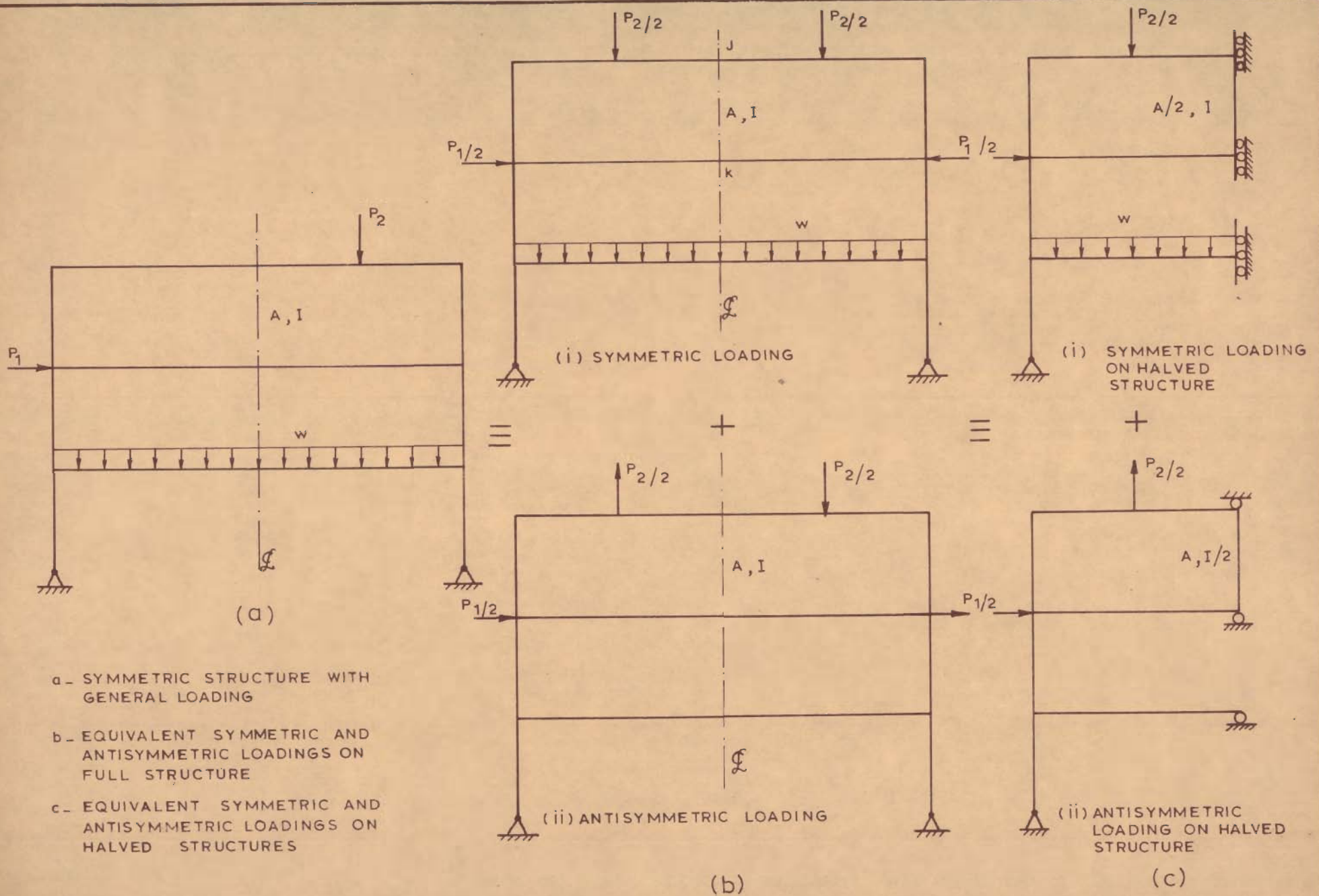
a) Member in Space Frame

$$U_{JX} = -U_{KX}, U_{JY} = U_{KY}, U_{JZ} = U_{KZ} \quad \dots(3.19)$$

$$\theta_{JX} = \theta_{KX}, \theta_{JY} = -\theta_{KY}, \theta_{JZ} = -\theta_{KZ}$$

b) Member in Plane Frame

$$U_{JX} = -U_{KX}, U_{JY} = U_{KY}, \theta_{JZ} = -\theta_{KZ} \quad \dots(3.20)$$



- a - SYMMETRIC STRUCTURE WITH GENERAL LOADING
- b - EQUIVALENT SYMMETRIC AND ANTISYMMETRIC LOADINGS ON FULL STRUCTURE
- c - EQUIVALENT SYMMETRIC AND ANTISYMMETRIC LOADINGS ON HALVED STRUCTURES

FIG. 3.3 \_ USE OF SYMMETRY & ANTISYMMETRY IN A PLANAR STRUCTURE

Antisymmetrical Loading:

a) Member in Space Frame

$$\begin{aligned} U_{JX} &= U_{KX}, U_{JY} = -U_{KY}, U_{JZ} = -U_{KZ}, \\ \theta_{JX} &= -\theta_{KX}, \theta_{JY} = \theta_{KY}, \theta_{JZ} = \theta_{KZ} \end{aligned} \quad \dots(3.21)$$

b) Member in Plane Frame

$$U_{JX} = U_{KX}, U_{JY} = -U_{KY}, \theta_{JZ} = \theta_{KZ} \quad \dots(3.22)$$

where  $U_{JX}$ ,  $U_{JY}$ ,  $U_{JZ}$ ,  $U_{KX}$ ,  $U_{KY}$ ,  $U_{KZ}$  are the displacements in  $X_M$ ,  $Y_M$  and  $Z_M$  directions of member axes at the ends of the member JK and  $\theta_{JX}$ ,  $\theta_{JY}$ ,  $\theta_{JZ}$ ,  $\theta_{KX}$ ,  $\theta_{KY}$ ,  $\theta_{KZ}$  are the rotations about the axes respectively.

Using equations 3.19 to 3.22, the modified form of stiffness influence coefficients at the two ends of a member in space, and in plane, is given in table 3.7 to 3.10 for symmetrical and antisymmetrical loads respectively.

### 3.9 EFFECT OF CABLE PRESTRESS

The effect of cable prestress can be incorporated into the analysis by including the prestressing force as equivalent joint loads on the released structure as shown in fig. 3.4.

### 3.10 BENDING MOMENT - AXIAL FORCE INTERACTION

In the linear elastic method of analysis, it is assumed that the changes in actual shape and dimensions

TABLE 3.7 STIFFNESS MATRIX FOR SYMMETRICAL LOADING FOR FULLY RESTRAINED MEMBER JK IN SPACE CUT TRANSVERSELY BY LINE OF SYMMETRY OF FRAME

	$U_{JX}$	$U_{JY}$	$U_{JZ}$	$\theta_{JX}$	$\theta_{JY}$	$\theta_{JZ}$	$U_{KX}$	$U_{KY}$	$U_{KZ}$	$\theta_{KX}$	$\theta_{KY}$	$\theta_{KZ}$
$P_{JX}$	$\frac{2EA_X}{L}$	0	0	0	0	0	0	0	0	0	0	0
$P_{JY}$	0	0	0	0	0	0	0	0	0	0	0	0
$P_{JZ}$	0	0	0	0	0	0	0	0	0	0	0	0
$M_{JX}$	0	0	0	0	0	0	0	0	0	0	0	0
$M_{JY}$	0	0	0	0	$\frac{2EI_Y}{L}$	0	0	0	0	0	0	0
$M_{JZ}$	0	0	0	0	0	$\frac{2EI_Z}{L}$	0	0	0	0	0	0
$P_{KX}$	0	0	0	0	0	0	$\frac{2EA_X}{L}$	0	0	0	0	0
$P_{KY}$	0	0	0	0	0	0	0	0	0	0	0	0
$P_{KZ}$	0	0	0	0	0	0	0	0	0	0	0	0
$M_{KX}$	0	0	0	0	0	0	0	0	0	0	0	0
$M_{KY}$	0	0	0	0	0	0	0	0	0	0	$\frac{2EI_Y}{L}$	0
$M_{KZ}$	0	0	0	0	0	0	0	0	0	0	0	$\frac{2EI_Z}{L}$

TABLE 3.8 STIFFNESS MATRIX FOR SYMMETRICAL LOADING FOR FULLY RESTRAINED MEMBER JK IN A PLANE CUT TRANSVERSELY BY LINE OF SYMMETRY OF FRAME

	$U_{JX}$	$U_{JY}$	$\theta_{JZ}$	$U_{KX}$	$U_{KY}$	$\theta_{KZ}$
$P_{JX}$	$\frac{2EA_X}{L}$	0	0	0	0	0
$P_{JY}$	0	0	0	0	0	0
$M_{JZ}$	0	0	$\frac{2EI_Z}{L}$	0	0	0
$P_{KX}$	0	0	0	$\frac{2EA_X}{L}$	0	0
$P_{KY}$	0	0	0	0	0	0
$M_{KZ}$	0	0	0	0	0	$\frac{2EI_Z}{L}$

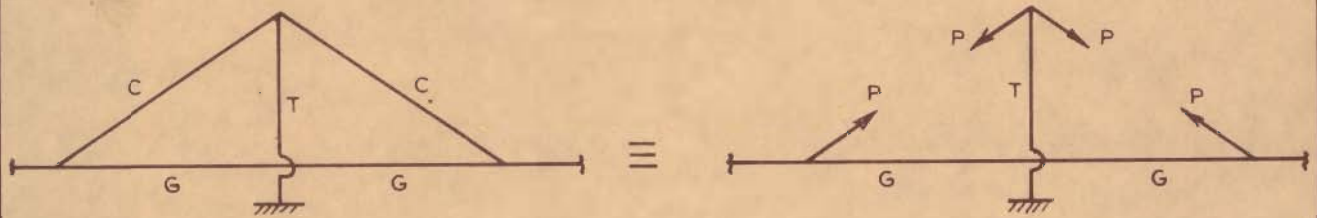
TABLE 3.10 STIFFNESS MATRIX FOR ANTISYMMETRICAL LOADING FOR FULLY RESTRAINED MEMBER IN A PLANE CUT TRANSVERSELY BY LINE OF SYMMETRY OF FRAME

	$U_{JX}$	$U_{JY}$	$\theta_{JZ}$	$U_{KX}$	$U_{KY}$	$\theta_{KZ}$
$P_{JX}$	0	0	0	0	0	0
$P_{JY}$	0	$\frac{24EI_Z}{L^3}$	$\frac{12EI_Z}{L^2}$	0	0	0
$M_{JZ}$	0	$\frac{12EI_Z}{L^2}$	$\frac{6EI_Z}{L}$	0	0	0
$P_{KX}$	0	0	0	0	0	0
$P_{KY}$	0	0	0	0	$\frac{24EI_Z}{L^3}$	$\frac{-12EI_Z}{L^2}$
$M_{KZ}$	0	0	0	0	$\frac{-12EI_Z}{L^2}$	$\frac{6EI_Z}{L}$

TABLE 3.9 STIFFNESS MATRIX FOR ANTISYMMETRICAL LOADING FOR FULLY RESTRAINED MEMBER IN SPACE CUT TRANSVERSELY BY LINE OF SYMMETRY OF FRAME

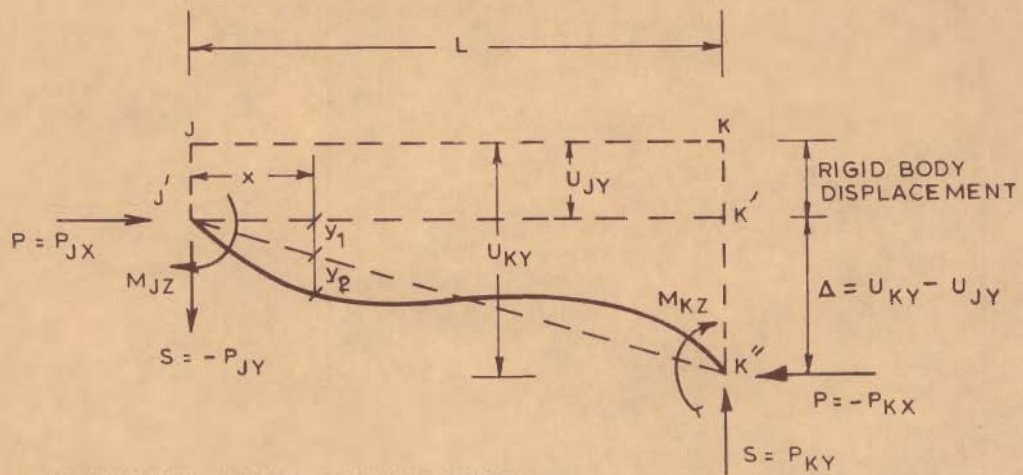
	$U_{JX}$	$U_{JY}$	$U_{JZ}$	$\theta_{JX}$	$\theta_{JY}$	$\theta_{JZ}$	$U_{KX}$	$U_{KY}$	$U_{KZ}$	$\theta_{KX}$	$\theta_{KY}$	$\theta_{KZ}$
$P_{JX}$	0	0	0	0	0	0	0	0	0	0	0	0
$P_{JY}$	0	$L_1$	0	0	0	$L_2$	0	0	0	0	0	0
$P_{JZ}$	0	0	$L_3$	0	$-L_4$	0	0	0	0	0	0	0
$M_{JX}$	0	0	0	$L_5$	0	0	0	0	0	0	0	0
$M_{JY}$	0	0	$-L_4$	0	$L_6$	0	0	0	0	0	0	0
$M_{JZ}$	0	$L_2$	0	0	0	$L_7$	0	0	0	0	0	0
$P_{KX}$	0	0	0	0	0	0	0	0	0	0	0	0
$P_{KY}$	0	0	0	0	0	0	0	$L_1$	0	0	0	$-L_2$
$P_{KZ}$	0	0	0	0	0	0	0	0	$L_3$	0	$L_4$	0
$M_{KX}$	0	0	0	0	0	0	0	0	0	$L_5$	0	0
$M_{KY}$	0	0	0	0	0	0	0	0	$L_4$	0	$L_6$	0
$M_{KZ}$	0	0	0	0	0	0	0	$-L_2$	0	0	0	$L_7$

$$\begin{aligned}
 L_1 &= \frac{24EI_Z}{L^3}, & L_2 &= \frac{12EI_Z}{L^2} \\
 L_3 &= \frac{24EI_Y}{L^3}, & L_4 &= \frac{12EI_Y}{L^2} \\
 L_5 &= \frac{2GI_X}{L}, & L_6 &= \frac{6EI_Y}{L} \\
 L_7 &= \frac{6EI_Z}{L}
 \end{aligned}$$



T - TOWER , G - GIRDER ,  
C - CABLE WITH PRETENSION P

FIG. 3.4 - REPRESENTATION OF CABLE PRETENSION BY EQUIVALENT JOINT LOADS ON RELEASED STRUCTURE



$y_1$  IS DUE TO JOINT TRANSLATION  
 $y_2$  IS DUE TO MEMBER CURVATURE

FIG. 3.5 - GENERAL DEFORMATION OF A MEMBER



of the structure, resulting from the working loads, are immaterial. For any angular deformation  $\theta$  at the end of a member, it is assumed that,  $\cos \theta = 1$ ;  $\sin \theta = \tan \theta = \theta$ . The effect of axial loads in the members is neglected when deriving the equilibrium equations for a structure. Thus, for a general member, such as shown in fig. 3.5, it is assumed that for the equilibrium of the member:

$$M_{JZ} + M_{KZ} = S.L \quad \dots (3.23)$$

With reference to fig. 3.5, it is evident that when either the deformation  $\Delta$  or the axial force  $P$  or both  $P$  and  $\Delta$  are large, equation 3.23, used in linear elastic method, becomes inaccurate and should be altered to read:

$$M_{JZ} + M_{KZ} + P.\Delta = S.L$$

or  $S = \frac{1}{L} (M_{JZ} + M_{KZ} + P.\Delta) \quad \dots (3.24)$

The effect of  $P$  on the equilibrium of the structure ( $P - \Delta$  effect) is one of the causes of nonlinearity in the structure.

A difficulty is experienced in the nonlinear structural analysis due to the member axial forces being unknown. An iterative method is, therefore, used to overcome this difficulty. A linear analysis is initially performed by assuming the axial forces to be zero, to estimate the first approximation of joint displacements and resulting member forces. These axial member forces are then used to

construct an improved stiffness matrix of the structure through improved member stiffness coefficients after accounting for the axial-flexural interaction. A reanalysis of the structure is now done under the same set of externally applied loads. An improved approximation of the set of axial member forces is, thus, obtained at the end of each cycle of analysis. The iterations are continued until the difference between the axial loads of members used to calculate improved stiffness matrices and those obtained at the end of the same cycle is within a specified tolerance.

The improvement in the stiffness matrices of a planar member, to account for P- $\Delta$  effect, can be achieved by introducing suitable stability functions in the stiffness matrices presented in tables 3.4 and 3.6. The corresponding improved stiffness matrices are given in tables 3.11 and 3.12 respectively. In these tables,  $\phi_2$ ,  $\phi_3$ , etc. are called stability functions whose values depend on the slenderness ratio of the member and ratio of the axial load applied to the critical buckling load of the member. These have been derived in detail by Majid (137) and Sondh (185). The formulae for the calculation of these stability functions are given in table 3.13

### 3.11 OUTLINE OF SPACE-FRAME COMPUTER ANALYSIS

A space-frame computer program, which can handle members with different end conditions as discussed earlier, has been developed for lateral and eccentric vertical load

TABLE 3.11 STIFFNESS MATRIX UNDER AXIAL-FLEXURAL INTER-ACTION FOR FULLY RESTRAINED MEMBER IN A PLANE FRAME

	$U_{JX}$	$U_{JY}$	$\theta_{JZ}$	$U_{KX}$	$U_{KY}$	$\theta_{KZ}$
$P_{JX}$	$\frac{EA_X}{L}$	0	0	$\frac{-EA_X}{L}$	0	0
$P_{JY}$	0	$\frac{12EI_Z}{L^3} \phi_5$	$\frac{6EI_Z}{L^2} \phi_2$	0	$\frac{-12EI_Z}{L^3} \phi_5$	$\frac{6EI_Z}{L^2} \phi_2$
$M_{JZ}$	0	$\frac{6EI_Z}{L^2} \phi_2$	$\frac{4EI_Z}{L} \phi_3$	0	$\frac{-6EI_Z}{L^2} \phi_2$	$\frac{2EI_Z}{L} \phi_4$
$P_{KX}$	$\frac{-EA_X}{L}$	0	0	$\frac{EA_X}{L}$	0	0
$P_{KY}$	0	$\frac{-12EI_Z}{L^3} \phi_5$	$\frac{-6EI_Z}{L^2} \phi_2$	0	$\frac{12EI_Z}{L^3} \phi_5$	$\frac{-6EI_Z}{L^2} \phi_2$
$M_{KZ}$	0	$\frac{6EI_Z}{L^2} \phi_2$	$\frac{2EI_Z}{L} \phi_4$	0	$\frac{-6EI_Z}{L^2} \phi_2$	$\frac{4EI_Z}{L} \phi_3$

TABLE 3.12 STIFFNESS MATRIX UNDER AXIAL-FLEXURAL INTER-ACTION FOR A MEMBER WITH FIRST END HINGED ABOUT Z-AXIS AND RESTRAINED IN OTHER DIRECTIONS IN A PLANE FRAME

	$U_{JX}$	$U_{JY}$	$\theta_{JZ}$	$U_{KX}$	$U_{KY}$	$\theta_{KZ}$
$P_{JX}$	$\frac{EA_X}{L}$	0	0	$\frac{-EA_X}{L}$	0	0
$P_{JY}$	0	$\frac{3EI_Z}{L^3} \phi_5$	0	0	$\frac{-3EI_Z}{L^3} \phi_5$	$\frac{3EI_Z}{L^2} \phi_2$
$M_{JZ}$	0	0	0	0	0	0
$P_{KX}$	$\frac{-EA_X}{L}$	0	0	$\frac{EA_X}{L}$	0	0
$P_{KY}$	0	$\frac{-3EI_Z}{L^3} \phi_5$	0	0	$\frac{3EI_Z}{L^3} \phi_5$	$\frac{-3EI_Z}{L^2} \phi_2$
$M_{KZ}$	0	$\frac{3EI_Z}{L^2} \phi_2$	0	0	$\frac{-3EI_Z}{L^2} \phi_2$	$\frac{3EI_Z}{L} \phi_3$

TABLE 3.13 STABILITY FUNCTIONS FOR VARIOUS END CONDITIONS OF A MEMBER

A. BOTH ENDS RESTRAINED

Stability Function	Compressive Force	Eulerian Force	Zero force	Tensile Force
$\phi_2$	$\frac{(kL)^2(1-\cos kL)}{6 \phi_C}$		1	$\frac{(kL)^2(\cosh kL - 1)}{6 \phi_T}$
$\phi_3$	$\frac{kL(\sin kL - kL \cos kL)}{4 \phi_C}$		1	$\frac{kL(kL \cosh kL - \sinh kL)}{4 \phi_T}$
$\phi_4$	$\frac{kL(kL - \sin kL)}{2 \phi_C}$		1	$\frac{kL(\sinh kL - kL)}{2 \phi_T}$
$\phi_5$	$\frac{(kL)^3 \sin kL}{12 \phi_C}$		1	$\frac{(kL)^3 \sinh kL}{12 \phi_T}$

$$\phi_C = 2 - 2 \cos kL - kL \sin kL$$

$$\phi_T = 2 - 2 \cosh kL + kL \sinh kL$$

$$k = \sqrt{\frac{P}{EI_Z}}$$

L - Length of member,  $I_Z$  - Moment of inertia about Z axis,  
 E - Modulus of elasticity of the material, P - Axial load on the member

B. ONE END HINGED ABOUT Z-AXIS, OTHER END RESTRAINED

$\phi_2$	$\frac{(kL)^2(1-\cos kL)(2\sin kL - kL - kL \cos kL)}{3 \phi_{CC}}$		1	$\frac{(kL)^2(\cosh kL - 1)(2\sinh kL - kL - kL \cosh kL)}{3 \phi_{TT}}$
$\phi_3$	$\frac{(kL)^2(1-\cos kL)(2\sin kL - kL - kL \cos kL)}{3 \phi_{CC}}$		1	$\frac{(kL)^2(\cosh kL - 1)(2\sinh kL - kL - kL \cosh kL)}{3 \phi_{TT}}$
$\phi_4$	0		0	0
$\phi_5$	$\frac{(kL)^3 \cos kL(2 - 2\cos kL - kL \sin kL)}{3 \phi_{CC}}$		1	$\frac{-(kL)^3 \cosh kL(2 - 2\cosh kL + kL \sinh kL)}{3 \phi_{TT}}$

$$\phi_{CC} = \phi_C(\sin kL - kL \cos kL)$$

$$\phi_{TT} = \phi_T(\sinh kL - kL \cosh kL)$$

analysis of the proposed cable-stayed bridges. The program has the following features:

(a) Use of symmetry of the structure to reduce the size of the problem by modifying stiffness matrices of the symmetrically loaded members. Antisymmetrical loadings are also similarly treated to reduce the size of the structure to almost half.

(b) Provision for considering structural discontinuity by modifying stiffness matrix of the concerned member for different end conditions.

(c) Consideration of elastic supports by inclusion of elastic spring stiffnesses at appropriate locations in the overall joint stiffness matrix of the structure.

Linear displacement analysis for nodal concentrated forces of general nature is carried out by the program to obtain;

- (i) Nodal deformations.
- (ii) Member end actions in member axes.
- (iii) Support reactions.

There is a provision to check the nodal equilibrium of the resulting forces.

### 3.12 OUTLINE OF PLANE-FRAME COMPUTER ANALYSIS

A plane-frame computer program, which can handle beam and truss types of structural elements, has been

suitably developed for study of nonlinear axial-flexural interaction and effect of prestress of cables on the behaviour of cable-stayed bridges. The program has the following features:

- i) Use of symmetry of the structure to reduce the size of the problem.
- ii) Provision for structural discontinuity at inner points of the frame.
- iii) Use of elastic supports.

The following studies are possible with the plane-frame program.

- a) Linear displacement analysis to obtain:
  - i) Nodal deformations.
  - ii) Member end forces in member axes.
  - iii) Support reactions.
  - iv) Nodal equilibrium check on resulting member forces in structure axes.
- b) Iterative axial-flexural interaction analysis by using modified stiffness of the members. The important steps of this procedure are:
  - i) Axial forces in members, determined by elastic analysis, are used to calculate the stability functions which, in turn, are used to modify the stiffness matrix of each member.

ii) Stability functions are calculated for members fixed at both ends; fixed at one end and hinged at other end, as necessary.

iii) Analysis is carried out with the use of modified structure stiffness to obtain nodal deformations, member end forces in member axes, support reactions and nodal equilibrium check.

iv) Convergence Criterion:

When absolute value of

$$\left( \frac{\text{axial force in current cycle}}{\text{axial force in preceding cycle}} - 1 \right)$$

is less than, or equal to, .0001 in every member of the structure, the convergence is assumed to have been achieved.

v) Analysis is carried out for a specified number of iterations, or, till the convergence is achieved, whichever is earlier.

c) The study of the effect of prestress of cables on the behaviour of cable-stayed bridges is carried out in the following two steps:

Step 1

i) Iterative axial-flexural analysis of a structure is carried out with cables replaced by forces resulting from cable pretension at appropriate nodes.

ii) Nodal deformations, member end forces, support reactions and nodal equilibrium check are obtained after each cycle of analysis.

## Step 2

i) Cables with specified prestress are added to the deformed configuration of the structure resulting from step 1. The number of nodes in the new structure has not changed while the number of members in the new structure has increased.

ii) Elastic analysis is carried out for external forces acting on the new structure. Nodal deformations, member end forces, support reactions and nodal equilibrium check are obtained.

iii) Axial forces in all the members due to the external forces and due to the prestressing forces of the cables are added and the sum of the two axial forces in a member is used for calculating the stabilisyt functions which are used in the subsequent iterations.

iv) Nonlinear axial-flexural interaction analysis is carried out, for the structure with cables, for the convergence criterion specified.

v) Final member forces and support reactions are obtained by superposition of the member forces and support reactions of the final cycles of the two steps of analysis. This operation is performed manually, if needed.



Limitation: In practice, the prestretching of the cables is done in stages and there are adjustments in the cable tensions and forces in other members of the bridge at every stage. The proposed procedure does not cover the analysis of prestressing in stages. For the purpose of estimating the axial forces in members, which would interact with the flexural deformations, the final prestressed state is considered as if reached simultaneously in all cables.

d) Loading:

Nodal concentrated forces of general nature and uniformly distributed loads acting perpendicular to the longitudinal axis of the member can be applied on the structure.

## C H A P T E R 4

### DYNAMIC ANALYSIS

#### 4.1 INTRODUCTION

Cable-stayed bridges are considered to be flexible structures with long natural periods. Moving loads, wind gust and movement of supports during a probable earthquake cause dynamic forces in such structures. The dynamic effects of these forces are more pronounced when they induce frequencies of vibrations matching with any one of the natural frequencies of the structure. Since the natural frequencies depend upon mass and stiffness distribution, for a proper dynamic analysis the appropriate disposition of masses and stiffnesses of the structural elements is of primary importance.

Dynamic response analysis consists of the determination of time variant deflections from which stresses are computed by using principles of static structural analysis. The scope of this presentation is limited to free vibration analysis and dynamic response analysis, within the elastic range.

#### 4.2 REPRESENTATION OF THE STRUCTURE

A cable-stayed bridge structure can be idealised, with reasonable accuracy, as a discrete multidegree of freedom system with finite number of lumped masses connected by close-coupled elastic springs. The number of degrees

of freedom of the system is equal to the number of independent coordinates necessary to define the configuration of the system completely. In the most general case of a three dimensional motion, six coordinates are required to define the position of each mass of a three dimensional skeletal structure. A two dimensional skeletal structure involves three degrees of freedom per mass.

Member stiffness matrices and rotation transformation matrices presented in section 3.4 and 3.5 are used to calculate stiffnesses of elastic springs connecting the masses. The assumptions for skeletal three dimensional and two dimensional analyses enumerated in section 3.2 are applicable to dynamic analyses also.

#### 4.3 FREE VIBRATION ANALYSIS

When a multidegree of freedom system is set into a mode of vibration such that all masses of the system attain maximum amplitudes of that mode simultaneously and, also, all masses pass through the equilibrium position simultaneously, the system is said to vibrate in a natural (or principal or normal) mode of harmonic vibration. When all the masses of the system vibrate in phase, the mode is the fundamental or the lowest mode of vibration and the frequency associated with this mode is lowest in magnitude. When all the adjacent masses vibrate out of phase with each other, the mode is the highest and the frequency associated with this mode is the highest. The fundamental

and a few higher frequencies and modes of a multidegree of freedom system are of primary significance and can be determined, with reasonable accuracy, by the method described in the following paragraphs.

#### 4.3.1 Lowest Frequency- Modeshape Determination

The equation of motion of a multidegree of freedom system can be written as(55, 118),

$$[M]_n \{\ddot{X}\}_n + [C]_n \{\dot{X}\}_n + [K]_n \{X\}_n = \{F(t)\}_n \quad \dots(4.1)$$

where,

$[M]$  = mass matrix,

$[C]$  = damping matrix,

$[K]$  = stiffness matrix,

$\{X\}$  = displacement vector,

$\{\dot{X}\}$  = velocity vector,

$\{\ddot{X}\}$  = acceleration vector and,

$\{F(t)\}$  = force vector

$n$  = order of matrices and vectors.

Considering undamped free vibration, Eq. 4.1 reduces to,

$$[M]_n \{\ddot{X}\}_n + [K]_n \{X\}_n = 0 \quad \dots (4.2)$$

If we assume  $X = x \sin pt$ , Eq. 4.2 is converted to

$$K_n x_n = p^2 \cdot M_n x_n \quad \dots (4.3)$$

Equation 4.3 is in the form of a standard eigenvalue problem,  $AX = \lambda B X$ . Power iteration techniques (83, 171), coupled with any particular root or vector eliminating (deflation) procedure (222), applied to Eq. 4.3 will yield the highest and the subsequent eigenvalues in the descending order. However, to obtain the lowest and a few more eigenvalues in the ascending order, Eq. 4.3 can be expressed in the form

$$K^{-1}_n M_n x_n = \frac{1}{p^2} x_n \quad \dots (4.4)$$

Equation 4.4 retains the analogy of the standard eigenvalue problem,  $AX = \lambda X$ , and yields lowest and higher eigenvalues in required number by repeated application of power iteration and deflation techniques. A considerable reduction in computational effort can be achieved by adopting algorithms which take advantage of symmetry of the matrix for eigenvalue determination. The product  $K^{-1} M$  of eq. 4.4 is able to maintain symmetry conditionally if  $m_1 = m_2 = \dots = m_n$ , where  $m_1, m_2, \dots, m_n$  are the diagonal elements of  $[M]$  of order  $n$ . In general, this condition may never be achieved and the symmetry can be enforced by resorting to the following transformation:

$$[M^{1/2}]_n [K^{-1}]_n [M^{1/2}]_n [M^{1/2}]_n \{X\}_n = \frac{1}{p^2} [M^{1/2}]_n \{X\}_n \quad \dots (4.5)$$

Substituting,

$$A_n \quad (\text{the modified dynamic matrix}) \\ = [M^{1/2}]_n [K^{-1}]_n [M^{1/2}]_n$$

$$Y = [M^{1/2}] \{X\}$$

= mode shape vector of the modified dynamic matrix and,

$$\lambda = \frac{1}{p^2} = \text{eigen value of the system,}$$

we get,

$$[A]_n \{Y\}_n = \lambda \{Y\}_n \quad \dots(4.6)$$

The eigenvector of the original system (Eq. 4.4) may be calculated by,

$$\{x\} = [M^{-1/2}] \{y\} \quad \dots(4.6a)$$

Equation 4.6 can be solved by number of available techniques among which Rayleigh quotient and iteration type of techniques are more popular. The approximation to the Rayleigh Quotient is achieved in the following manner to get the lowest eigen value and its associated eigenvector. Premultiply both sides of Eq. 4.6 by  $\{Y^T\}$ .

$$\{Y^T\}_n [A]_n \{Y\}_n = \lambda \{Y^T\}_n \{Y\}_n$$

$$\text{or } \lambda = \frac{\{Y^T\}_n [A]_n \{Y\}_n}{\{Y^T\}_n \{Y\}_n} \quad \dots(4.7)$$

The termination criterion of the iterative solution of eq. 4.7 is

$$\frac{\lambda_r^i - \lambda_r^{i-1}}{\lambda_r^i} \leq \epsilon \quad \dots (4.8)$$

where,

$$\lambda_r^i = \text{ith iterate for rth eigenvalue}$$

$$\lambda_r^{i-1} = (i-1)^{\text{th}} \text{ iterate for rth eigenvalue,}$$

$$\epsilon = \text{a specified small quantity,} \\ \text{say 0.001}$$

Another limitation on the iterative procedure can be imposed by specifying the maximum number of iterations.

At the end of the iterative procedure for one particular eigenvalue ( $\lambda_r$ ), which is the lowest every time, it is deemed that

$$\{X_r\} = \{X_r^i\} \quad \dots (4.9)$$

where,

$$\{X_r\} = \text{final modeshape vector of rth mode}$$

$$\{X_r^i\} = \text{modeshape vector of ith iteration for the} \\ \text{rth mode.}$$

#### 4.3.2 Deflation Technique

Deflation technique, due to Wilkinson (222), to evaluate higher eigenvalues and associated eigenvectors, has been adopted for the present study. The deflation technique can be summarised as:

$$A_{r+1} = A_r - \lambda_r X_r X_r^T \quad \dots (4.10)$$

where,

- $A_r$  = matrix for the evaluation of  $r$ th root,  
 $A_{r+1}$  = matrix (to be used) for the evaluation of  
 $(r + 1)^{th}$  root,  
 $\lambda_r$  =  $r^{th}$  eigenvalue of the system,  
 $X_r$  =  $r^{th}$  eigenvector of the system.

The deflated matrix  $A_{(r+1)}$  of eq. 4.10 can be used to obtain the next lowest root  $\lambda_{(r+1)}$  following the lowest root  $\lambda_r$  obtained in the  $r^{th}$  step of determination of lowest roots by power iteration technique described in the preceding paragraphs. The validity of eq. 4.10 can be proved as follows:

In its standard form, the eigenvalue equation for the root  $\lambda_{(r+1)}$  can be written as,

$$A_{(r+1)} X_{(r+1)} = \lambda_{(r+1)} X_{(r+1)} \quad \dots (4.11)$$

using eq. 4.10, one can write,

$$(A_r - \lambda_r X_r X_r^T) X_{(r+1)} = \lambda_{(r+1)} X_{(r+1)}$$

$$\text{or } A_r X_{(r+1)} - \lambda_r X_r X_r^T X_{(r+1)} = \lambda_{(r+1)} X_{(r+1)} \quad \dots (4.12)$$

two cases, which can be considered, are:

(i)  $X_{r+1} \approx X_r$ ; eq. 4.12 can be written as;

$$A_r X_r - \lambda_r X_r X_r^T X_r = \lambda_{(r+1)} X_r$$



From the property of orthogonality,  $X_r^T X_r = 1$

$$A_r X_r = (\lambda_{r+1} + \lambda_r) X_r$$

This is true only when  $\lambda_{r+1} = 0$ . Thus, the deflated matrix of eq. 4.10 will not contain the eigenvalue  $\lambda_r$  and the eigenvector  $X_r$ .

(ii)  $X_{r+1} \neq X_r$ ; eq. 4.12 can be written as;

$$A_r X_{(r+1)} - \lambda_r X_r X_r^T X_{(r+1)} = \lambda_{(r+1)} X_{(r+1)}$$

From the property of orthogonality,  $X_r^T X_{(r+1)} = 0$

Thus, the deflated matrix of eq. 4.10 can be written as;

$$A_{(r+1)} X_{(r+1)} = \lambda_{(r+1)} X_{(r+1)}$$

which is the standard form of the eigen value equation for the root  $\lambda_{(r+1)}$ . The deflated matrix of eq. 4.10 will thus eliminate all the roots which have been determined and can be used to determine the subsequent lowest root.

#### 4.3.3 Limitations

The eigen solution technique and the deflation technique, described above, are subject to the following limitations:

(i) The flexibility matrix (A) is obtained from the numerical inversion of the stiffness matrix (K). The inversion can be performed only with finite precision afforded by digital computation and ordering of the matrix.

Thus KA or AK will satisfy conditions of inversion only within certain degree of accuracy.

(ii) The accuracy check imposed on eigenvalues is not sufficient to ensure a similar accuracy of the corresponding eigenvectors. Thus, though computationally the convergence of roots is cubic in nature, the corresponding eigenvectors are calculated with lesser accuracy.

(iii) The accuracy with which the natural period and the mode shape of any mode is computed is dependant on the accuracy with which all preceding modal parameters are evaluated.

Inspite of the limitations, mentioned above, the combination of methods, as indicated above, is popular for its speed of convergence and simplicity of implementation.

#### 4.4 RESPONSE ANALYSIS

Depending on the availability of the dynamic data, the response analysis of a structure can be performed in several ways. When accelerograms for probable ground motion at the base of the structure are used, timewise response analysis can be resorted to by employing either mode superposition techniques or the method of explicit integration. When response spectra for displacements or accelerations are used, the maximum probable response can be computed by superimposing modal contributions by means of appropriate techniques to find all quantities of interest such as accelerations, displacements and inertia forces at various

points of the structure or the resultant forces in the members themselves. The methods used in the present study are described in the following paragraphs.

#### 4.4.1 Modal Response

Natural frequencies and corresponding mode shapes of the plane frame structure, determined by considering two degree of freedom (rotary inertia ignored) per node, have been used along with the acceleration response spectrum of the expected ground motion to compute the modal response.

$$Y_i^r = \frac{1}{p_r^2} S_a^r C^r \phi_i^r \quad \dots(4.13)$$

where

$Y_i^r$  = absolute dynamic displacement at node  $i$  in  $r^{\text{th}}$  mode,

$p_r$  = natural frequency in  $r^{\text{th}}$  mode

$S_a^r$  = absolute acceleration spectrum ordinate corresponding to the time period of  $r^{\text{th}}$  mode (usually denoted by  $S_{ah}$  for horizontal and  $S_{av}$  for vertical ground motion)

$C^r$  = mode participation factor in  $r^{\text{th}}$  mode corresponding to ground motion represented i.e. horizontal or vertical.

$\phi_i^r$  = normalised amplitude at node  $i$  in  $r^{\text{th}}$  mode.

The mode participation factor  $C^r$  will have different values for horizontal and vertical ground motions as given below:

$$C_{rh} = \frac{\sum m_i \phi_{ih}}{\sum m_i (\phi_{ih}^2 + \phi_{iv}^2)} \quad \dots(4.14)$$

and

$$C_{rv} = \frac{\sum m_i \phi_{iv}}{\sum m_i (\phi_{ih}^2 + \phi_{iv}^2)} \quad \dots(4.15)$$

where,

$C_{rh}$  = mode participation factor for horizontal ground motion

$C_{rv}$  = mode participation factor for vertical ground motion,

$m_i$  = mass associated with  $i^{\text{th}}$  degree of freedom,

$\phi_{ih}$  = horizontal modal displacement of  $i^{\text{th}}$  node

$\phi_{iv}$  = vertical modal displacement of  $i^{\text{th}}$  node

The force vector for  $r^{\text{th}}$  mode ( $F_i^r$ ) corresponding to the displacements obtained from Eq. 4.13 can be determined as;

$$F_i^r = m_i S_a^r C^r \phi_i^r \quad \dots(4.16)$$

The vector obtained from Eq. 4.16, when applied as static nodal forces, will result in a deformed configuration of the plane frame structure (with three degrees of

freedom at each node) given by,

$$\{F\} = [K]\{\delta^r\} \quad \dots(4.17)$$

where,

$[K]$  = stiffness matrix of structure

$\{\delta^r\}$  = overall deformation vector of  $r^{\text{th}}$  mode.

Thus, from Eq. 4.16 and 4.17,

$$\{\delta^r\} = [K]^{-1}[M]\{\phi^r\} S_a^r C^r \quad \dots(4.18)$$

Deformation vector obtained from Eq. 4.18 includes translations and rotations at various nodes. Individual member forces are, now, determined by using the deformations at the two ends of a member.

$$\{F_m^r\} = [K_m]\{\delta_m^r\} \quad \dots(4.19)$$

where,

$\{F_m^r\}$  = member forces in the  $r^{\text{th}}$  mode

$[K_m]$  = member stiffness matrix

$\{\delta_m^r\}$  = deformation vector at the two ends of a member, obtained from  $\{\delta^r\}$ .

#### 4.4.2 Superposition of Modal Responses

Total spectral response of the bridge structure can be computed by (a) absolute sum method which gives an upper bound solution, (b) SRSS (squareroot of sum of squares)

method, (c) RMS (squareroot of mean value of squares) method which is considered as a probability approach, (d) weighted combination of modal responses as followed by Russian and Yugoslavian codes and (e) average of (a) and (c). In the absence of data about relative superiority of the methods for bridge problems, SRSS method has been used in the present investigation.

## C H A P T E R 5

### EXPERIMENTAL STUDIES

#### 5.1 INTRODUCTION

Experimental studies carried out on a ratiating type, small size, cable-stayed bridge, hereafter referred as model, are described in this chapter. For purposes of analysis, the small size experimental bridge has been used as a prototype, but for arriving at realistic proportions and sizes of members a linear scale ratio was used to relate the experimental bridge to a large bridge of 457.2m main span that was physically conceived. Static vertical and lateral load tests and dynamic free vibration and steady state tests have been conducted.

#### 5.2 AIM OF STUDY

The primary aim of the experimental study carried out was to verify experimentally the validity of the assumptions made in analysis and to ascertain the reliability of the mathematical formulation of the structural problems involved. Experiments under static and dynamic loading conditions were planned to accomplish the following specific objectives.

(a) To compare analytical and experimental results for the following static loading cases:

- i) symmetric vertical loads
- ii) eccentric vertical loads
- iii) lateral loads.

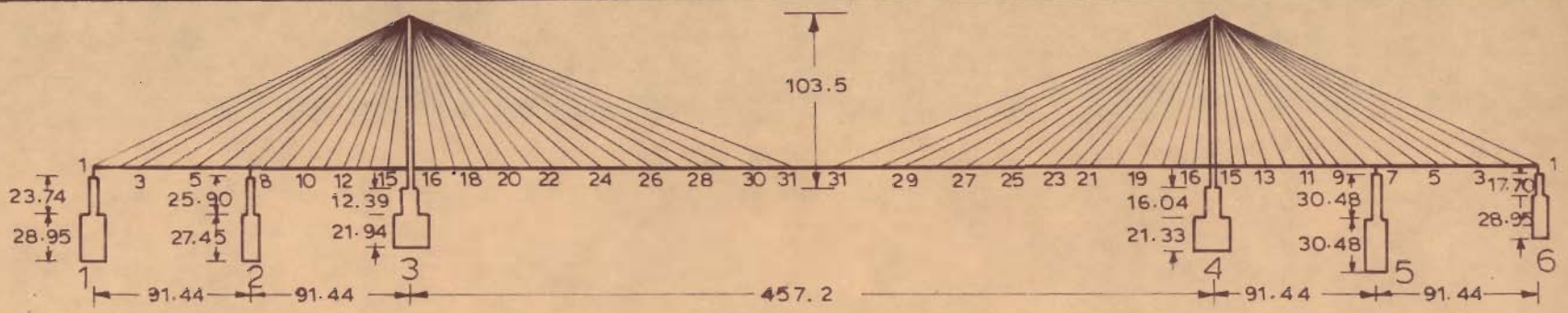
(b) To determine predominant vibration modes in vertical, longitudinal and lateral directions and to compare these with the analytical results.

(c) To gain an insight into the physical behaviour of this type of bridge under static and dynamic loading conditions.

### 5.3 SELECTION OF TYPE OF BRIDGE

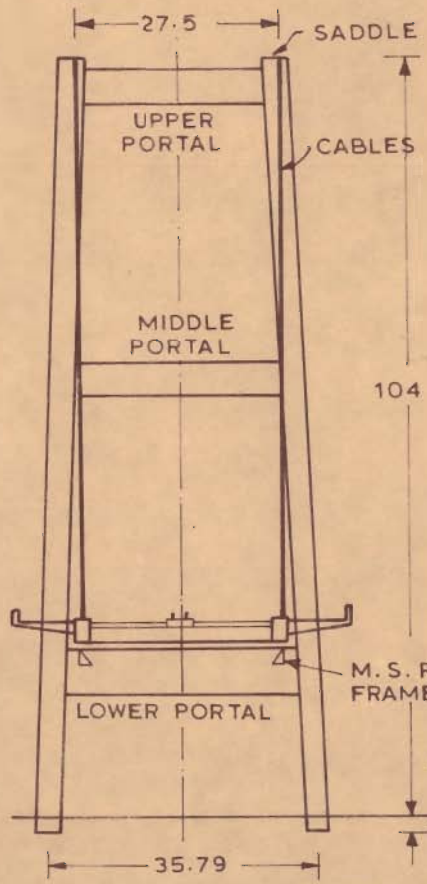
The choice of the bridge type was influenced by the proposed Second Hooghly Bridge to be built by Calcutta Port Authority, India. Salient details of the bridge are shown in fig. 5.1. The bridge is of radiating cable-stayed type with a total span of 822.96m. The towers of the bridge consist of two tapering, slightly inclined legs joined by three box portals; one below deck level, one below saddle level and a third midway between the two. The deck section comprises of two longitudinal rectangular steel boxes with cross-girders spanning between them. A reinforced concrete roadway slab is supported on rolled steel joist section stringers spanning between the cross-girders. The bridge is considered to be restrained in horizontal and vertical directions at one end and held only in vertical directions at the other five support points (fig. 5.1). Links, which permit longitudinal movements to accommodate temperature changes as well as rotation of deck in the vertical plane, are provided at these five points of support. The deck is supported from the tower tops by steel strands



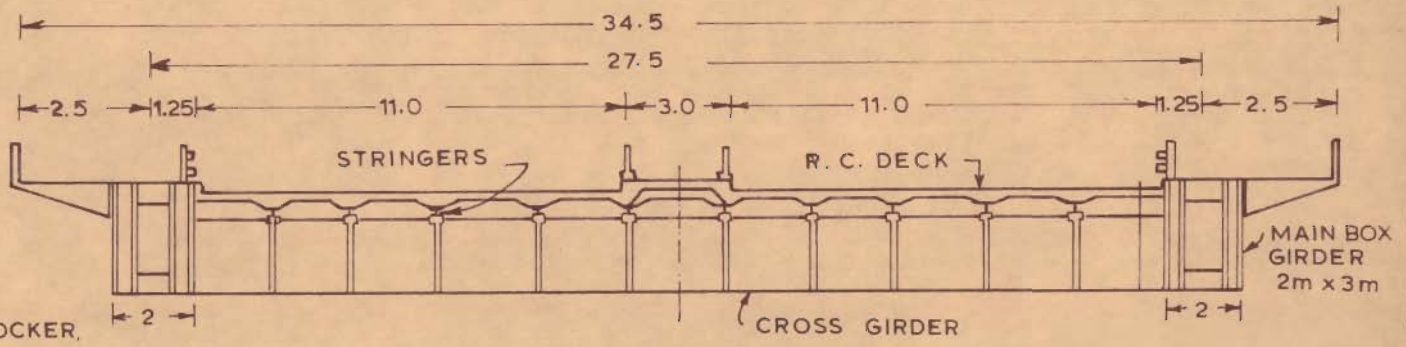


a - LONGITUDINAL VIEW

DIMENSIONS IN m



b - ELEVATION AT TOWER



c - CROSS SECTION OF DECK

FIG. 5.1 - GENERAL VIEW OF PROPOSED SECOND HOOGHLY BRIDGE INDIA

which are connected to the main boxes by means of cast steel sockets. There are thirty one strands at each tower leg. The substructure consists of six piers and six monoliths/wells.

Executable drawings of the proposed Second Hooghly Bridge were available for reference. It was, therefore, decided to more or less scale out a radiating type cable-stayed bridge structure for experimentation.

#### 5.4 CHOICE OF SCALE

Keeping in view the availability of the shake table, facilities of testing equipments available, cost of model and the time required in its fabrication and erection, a scale factor of 200 was chosen. This scale factor was used primarily to fix up the overall dimensions of the model and to provide general guidance to determine the overall cross-sectional dimensions of the components. The shape of the cross-sections was altered, as necessary, to suit the requirements of workability. Exact geometrical proportioning was neither achieved nor intended.

#### 5.5 SELECTION OF MATERIAL AND PRELIMINARY TESTS

Dynamic tests (37) were performed prior to this work on a perspex model of the above described Bridge. For these tests, perspex had been chosen as model material due to its low modulus of elasticity, ease of fabrication and easy availability. Smoothly finished joints of various

components were made by using chloroform. The cables were represented by wires of spring steel and their cast steel sockets were represented by grips made of brass. Use of more than one material in the model was necessary due to the limitation of perspex to represent steel cables and cast steel sockets. The hinge action of the prototype support was represented by clamping the deck to the pier by steel wires, and the link was represented by a vertical steel pin inserted in conical pivots. The arrangement did not represent the exact support conditions of the prototype bridge.

Perspex is known to develop crystallization within the material after some time (not exactly known). The crystallization changes the modulus of elasticity of the material and renders the behaviour of the structure uncertain. Keeping in view the time gap of more than four years between the date of fabrication of the above model and the dates of proposed tests by the author and the observations of the preceding paragraph, the perspex model, though available, was not used for the proposed tests.

In order to eliminate the time dependent problems connected with perspex it was decided to use an aluminium alloy which was commercially available in the form of sheets of varying thickness as well as in the form of wires and rods which could be used for cables and cable grips respectively. Riveted construction was used in the model to

simulate the actual bridge construction. The process of making riveted connections between thin sheets, and also, the particularly difficult connections at some joints were developed early in the experimental program to avoid any uncertainty or delay during actual fabrication. Araldite was used to paste the surfaces together just before riveting to avoid local out of phase vibrations of surfaces between two rivets during dynamic tests. Excepting for the use of steel screws to join thick plates and the connecting hinge and links at piers and towers which were of mild steel, the fabrication of the model bridge was from the aluminium alloy chosen. Preliminary direct tension tests on specimens from sheets and wires of aluminium were performed to ensure elastic behaviour of the material within the range of working loads.

#### 5.6 DESIGN OF MODEL BRIDGE

The cross-sections of the components of the bridge were designed such that the stiffness ratio ( $K_p/K_m$ ) remained constant for every component of the bridge. The subscripts  $p$  and  $m$  stand for prototype and model respectively. To achieve the aim in the design, the substructure was proportioned geometrically to give certain  $K_p/K_m$  and the stiffness ratio of the other components of the bridge was then adopted to be the same as that of the substructure.

For any elastic member, the flexural stiffness of the member is proportional to  $EI/L^3$  and its axial stiffness

is proportional to  $EA/L$ , where;

$E$  = modulus of elasticity,

$I$  = moment of inertia,

$L$  = significant length, and

$A$  = area of cross-section of the member.

The stiffness ratio of the substructure is given by:

$$\frac{K_{p1}}{K_{m1}} = \frac{E_{p1} I_p}{E_m I_m} \cdot \frac{L_m^3}{L_p^3} = n \frac{E_{p1}}{E_m} \quad \dots(5.1)$$

where;  $n = L_p/L_m = 200$ , is the scale ratio adopted;  $E_{p1}$  is the modulus of elasticity of concrete used in the prototype substructure (assumed =  $1507 \text{ Kg/mm}^2$ ),  $E_m$  is the modulus of elasticity of aluminium alloy used in model substructure ( $10000 \text{ Kg/mm}^2$ ). Thus;

$$\frac{K_{p1}}{K_{m1}} = 200 \times \frac{1507}{10000} = 30.14 \quad \dots(5.1a)$$

The stiffness ratio for the deck, towers and portals is represented by:

$$\frac{K_{p2}}{K_{m2}} = \frac{1}{n^3} \frac{E_{p2}}{E_m} \cdot \frac{I_{p2}}{I_{m1}}$$

where;

$E_{p2}$  = modulus of elasticity of steel in prototype deck, tower or portal (assumed =  $21100 \text{ kg/mm}^2$ ),

$I_{p2}$  = moment of inertia of member in prototype deck,  
tower or portal,

$E_m$  = modulus of elasticity of the material of  
model (10,000 Kg/mm<sup>2</sup>),

$I_{m1}$  = moment of inertia of a member in model.

For the stiffness ratio of deck, tower or portal to  
be equal to the stiffness ratio of the substructure, we  
have;

$$\frac{1}{n^3} \cdot \frac{E_{p2}}{E_m} \cdot \frac{I_{p2}}{I_{m1}} = n \cdot \frac{E_{p1}}{E_m} \quad \dots(5.2)$$

The moment of inertia of the model member (deck,  
tower or portal) is, thus calculated from the formula;

$$I_{m1} = \frac{1}{n^4} \cdot \frac{E_{p2}}{E_{p1}} \cdot I_{p2} \quad \dots(5.3)$$

$$\text{or } I_{m1} = \frac{1}{200^4} \times \frac{21100}{1507} \times I_{p2} = 0.875 \times 10^{-8} I_{p2} \quad \dots(5.3a)$$

The depth of the section in the model deck and the  
cross-sections of the tower legs and portals were so adjusted  
as to achieve the desired stiffness ratio.

The stiffness ratio for cables is represented by:

$$\frac{K_{p3}}{K_{m3}} = \frac{E_{p3} A_{p3} L_m}{E_{m2} A_{m2} L_p}$$

where;

$E_{p3}$  = modulus of elasticity of cable steel in prototype  
(assumed = 16500 kg/mm<sup>2</sup>),

$A_{p3}$  = area of cross-section of cable in prototype,

$L_p$  = length of prototype cable,

$E_{m2}$  = modulus of elasticity of cable wire of the model (assumed 10000 kg/mm<sup>2</sup> for the purpose of calculations),

$A_{m2}$  = area of cross-section of the cable wire of the model,

$L_m$  = length of model cable wire.

For the stiffness ratio of cables to be equal to the stiffness ratio of the substructure, we have;

$$\frac{E_{p3} A_{p3} L_m}{E_{m2} A_{m2} L_p} = n \frac{E_{p1}}{E_m} \quad \dots(5.4)$$

The area of cross-section of the model cable is, thus, calculated from the formula:

$$A_{m2} = \frac{1}{n^2} \cdot \frac{E_m}{E_{p1}} \cdot \frac{E_{p3}}{E_{m2}} A_{p3} \quad \dots(5.5)$$

$$\begin{aligned} \text{or } A_{m2} &= \frac{1}{200} \times \frac{10000}{1507} \times \frac{16500}{10000} A_{p3} \\ &= 2.737 \times 10^{-4} A_{p3} \quad \dots(5.5a) \end{aligned}$$

## 5.7 DESIGN CALCULATIONS

Table 5.1 gives a comparison of the section properties of the components of the prototype and the model bridge. The following points need special mention in respect

TABLE 5.1 COMPARISON OF COMPONENT SECTION PROPERTIES OF THE PROTOTYPE AND THE MODEL

Component	P R O T O T Y P E				Q	M O D E L			
	A (m <sup>2</sup> )	I <sub>X-X</sub> (m <sup>4</sup> )	I <sub>Y-Y</sub> (m <sup>4</sup> )	I <sub>Z-Z</sub> (m <sup>4</sup> )		A (mm <sup>2</sup> )	I <sub>X-X</sub> (mm <sup>4</sup> )	I <sub>Y-Y</sub> (mm <sup>4</sup> )	I <sub>Z-Z</sub> (mm <sup>4</sup> )
Individual box girder with partial deck	0.264 To 0.495	0.264 To 0.608	0.257 To 0.380	0.369 To 0.819	145.5	2360.4	12276.6	4178.9	
Two box girders with complete deck	-	-	-	-	444.8	-	-	12179.4	
Tower	0.475 To 0.689	1.189 To 2.173	1.181 To 1.774	0.818 To 1.605	276.0 To 303.0	14742.3 To 34723.7	40052.3 To 47369.3	36070.3 To 80017.3	
Top portal,	0.199	0.301	0.154	0.584	162.0	5847.7	9905.0	10454.1	
Middle portal									
Bottom portal	0.236	0.435	0.190	1.176	177.0	9497.4	11191.3	16982.7	
Cross-girder (each)	0.073	0.000018	0.00225	0.063	40.0	203.8	213.3	83.3	
Cables	0.0106 <sup>+</sup> To 0.0310	-	-	-	7.07 To 12.57	-	-	-	
End pier	3.059 <sup>++</sup>	0.984 <sup>++</sup>	181.181 <sup>++</sup>	6.058 <sup>++</sup>	1420.0	333654.6	3406833.3	109323.3	
End well	12.087 <sup>++</sup>	588.896 <sup>++</sup>	603.818 <sup>++</sup>	311.951 <sup>++</sup>	4170.0	8727603.7	10608187.0	4204988.7	
Middle pier	13.733 <sup>++</sup>	304.430 <sup>++</sup>	2915.864 <sup>++</sup>	105.302 <sup>++</sup>	4613.0	1897486.4	48754096.0	984006.0	
Middle well	32.311 <sup>++</sup>	3721.333 <sup>++</sup>	4284.787 <sup>++</sup>	1564.012 <sup>++</sup>	7530.0	42139116.0	69153725.0	16611185.0	

+ Values obtained by lumping, ++ Equivalent values in terms of steel.



to table 5.1.

(i) Actual values of areas and inertias were calculated for concrete piers and wells of the prototype and were converted to equivalent values in terms of steel.

(ii) Actual values of area and inertias were calculated for all length segments of the longitudinal girders with partial concrete deck and average values were found by taking weighted mean.

(iii) The prototype deck is a composite structure of steel main girders and concrete deck. Equivalent values in terms of steel were used in the calculations.

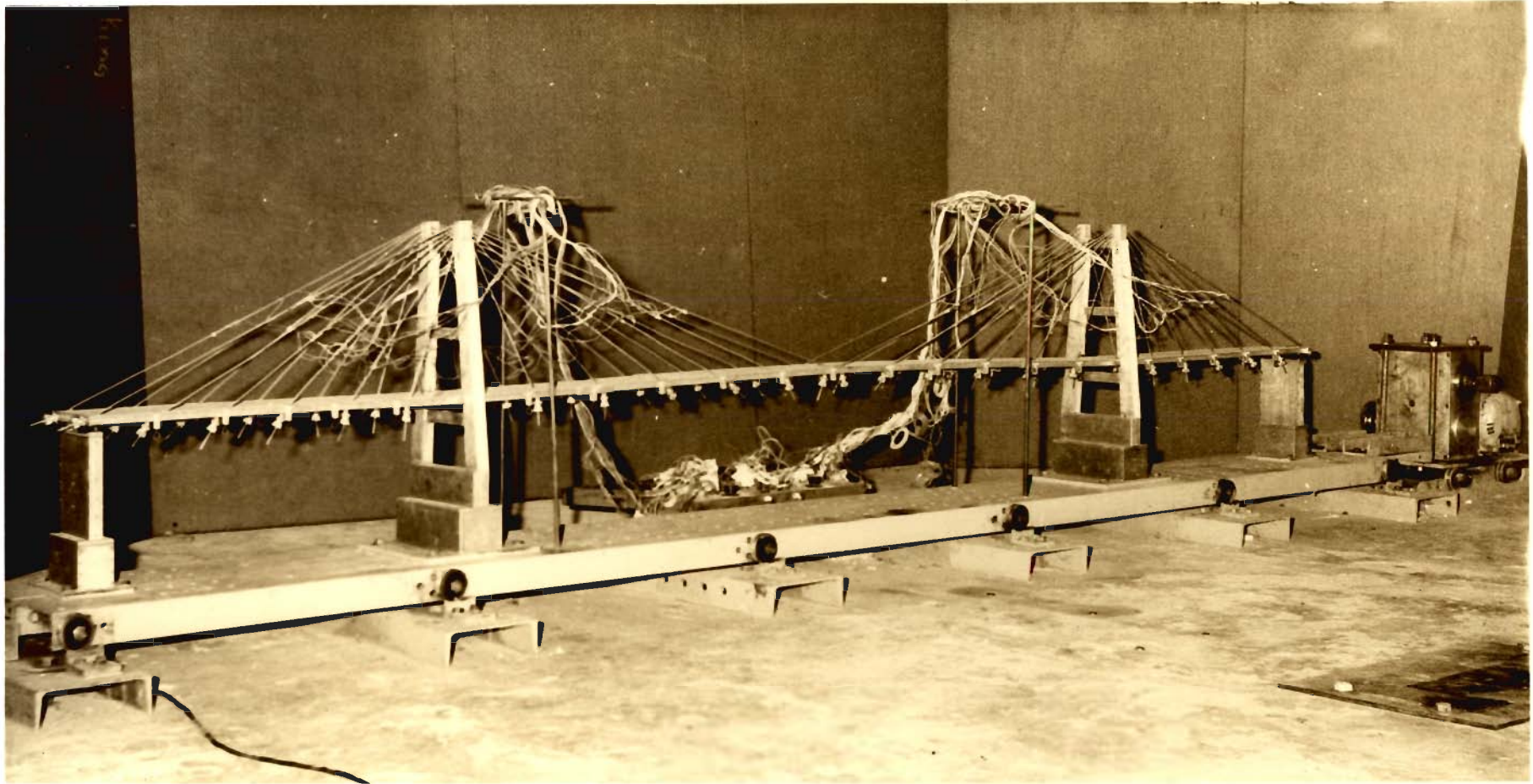
(iv) Number of cables at a tower leg in the prototype was reduced from 31 to 12 by lumping of the areas. The cable areas in the model were then calculated.

## 5.8 DESCRIPTION OF MODEL BRIDGE

General view of the model bridge is shown in photo P1 and significant dimensions of the model bridge are given in table 5.2. These are precisely 1/200 of Second Hooghly Bridge. Important technical features of Second Hooghly Bridge, hereafter referred as prototype, are represented in the model bridge also. The intermediate supports in the end span (fig. 5.1) of the prototype have been abandoned<sup>+</sup>

---

<sup>+</sup> The intermediate piers in the end spans of proposed Second Hooghly Bridge (prototype) were designed as aids in the erection of the bridge. These piers have been dropped in the subsequent revised design of the bridge. Changes in the cross-section details of the components of the bridge, if any, have not been used in the design calculations of the bridge model.



P 1: GENERAL VIEW OF LABORATORY BRIDGE STRUCTURE WITH OSCILLATOR MOUNTING FOR SHAKING IN LONGITUDINAL DIRECTION

in the model bridge leaving the deck on four supports only. The tapering steel towers of prototype are represented by

TABLE 5.2 SIGNIFICANT DIMENSIONS OF MODEL BRIDGE

---

Total length	(mm)	4114.8
Central span between the towers	(mm)	2286.0
End spans (total two) each	(mm)	914.4
Height of towers	(mm)	520.0
Total width of deck	(mm)	172.5
C/C distance of main box girders	(mm)	137.5
Spacing of cross-girders	(mm)	75.0
Size of box girders	(mm x mm )	10 x 18

---

similar construction of aluminium alloy. Composite construction of concrete deck and steel boxes is represented by aluminium alloy plate deck and stiffening boxes of the same material. Thirty one steel cables at each tower leg of prototype are represented by twelve wire cables of aluminium alloy at each tower leg. Aluminium grips fitted with a micrometer tensioning arrangement have been used to hold the deck against tensioned cables. Concrete substructure of prototype is represented by a corresponding substructure of aluminium alloy.

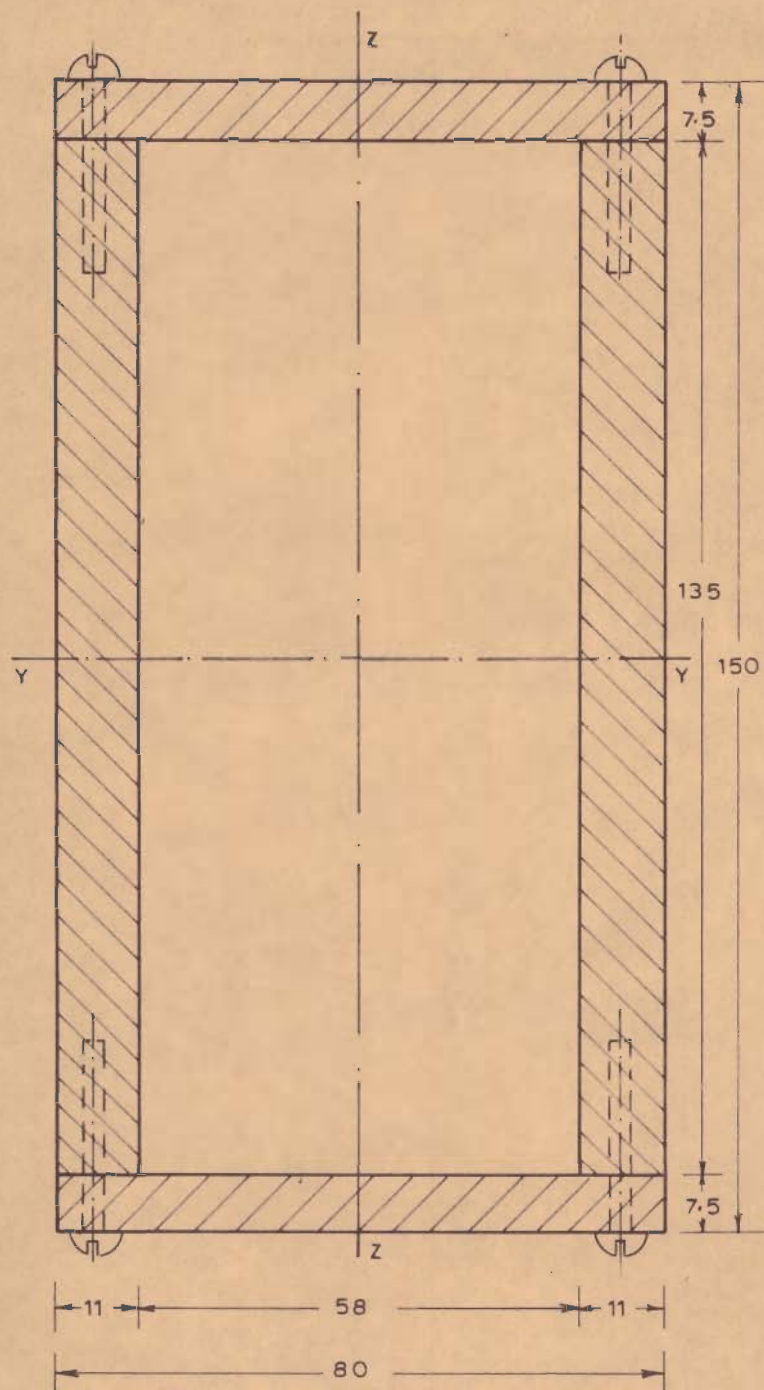
## 5.9 MODEL FABRICATION

The detailed drawings of the components of the model bridge are given in fig. 5.2 to 5.11. Aluminium plates of thicknesses varying from 1.5 mm to 11 mm were used for the fabrication of various components of the model. Aluminium rivets of 3mm x 6mm (long) size were used for jointing thin plates of 1.5mm thickness. Steel screws of sizes varying from 3mm x 6mm to 6mm x 38mm were used for connecting thicker plates. Aluminium wires of 3, 3.5 and 4mm diameters were used as cables. The micrometer tensioning-cum-gripping device was made from 25mm dia. rods of aluminium. The special size of the anchor block fitted at the top of each tower leg was an aluminium casting. The hinge and the links connecting the deck and the piers/towers were made from mild steel.

Riveting was done immediately after applying araldite between the surfaces to produce requisite pressure on the surfaces needed to ensure a thin and strong adhesive layer between them.

Special features of fabrication of the individual components of the model, if any, in addition to those detailed out in the relevant figures, are described in the following paragraphs.

Figures 5.2 and 5.3 show the details of cross-sections of the end wells and the end piers respectively. An assembly of tower legs, portals, middle piers and wells is

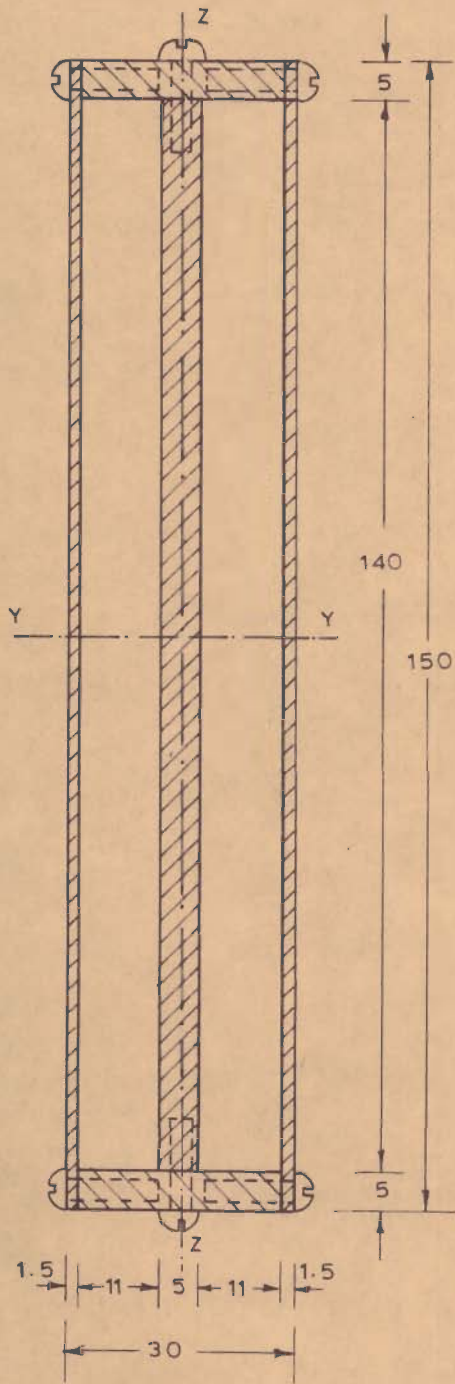


- DIMENSIONS IN mm
- HEIGHT OF WELL = 90 mm
- SCREWS 4 mm x 25 mm
- FOUR SCREWS ON EACH JOINT ALONG HEIGHT
- CONNECTED TO SHAKE TABLE BY 6 Nos SCREWS WITH SPRING WASHERS
- CONNECTED TO 10 mm THICK PLATE (BETWEEN WELL AND PIER) BY 10 Nos SCREWS 4 mm x 25 mm

AREA	4170	mm <sup>2</sup>
INERTIA - X	8727603.7	mm <sup>4</sup>
INERTIA - Y	10608187.0	mm <sup>4</sup>
INERTIA - Z	4204988.7	mm <sup>4</sup>

SCALE 1:1

FIG. 5.2 \_ CROSS-SECTION OF END WELL (No. 1 & 4)



- DIMENSIONS IN mm
- HEIGHT OF PIER = 208 mm
- 6Nos SCREWS 3mm x 12mm ON EACH JOINT ALONG HEIGHT
- CONNECTED TO WELL BY 10 mm THICK PLATE WITH 3mm x 25mm SCREWS IN CENTRAL 5mm PLATE 4 Nos
- 2.5mm THICK COVER PLATE AT TOP CONNECTED TO 5 mm PLATE BY 6 Nos SCREWS 3mm x 12mm

AREA	1420	mm <sup>2</sup>
* INERTIA - X	333654.6	mm <sup>4</sup>
INERTIA - Y	3406833.3	mm <sup>4</sup>
INERTIA - Z	109323.3	mm <sup>4</sup>

\* CENTRAL WEB IGNORED

SCALE - 1:1

FIG. 5.3 \_CROSS-SECTION OF END PIER(No. 1 & 4)

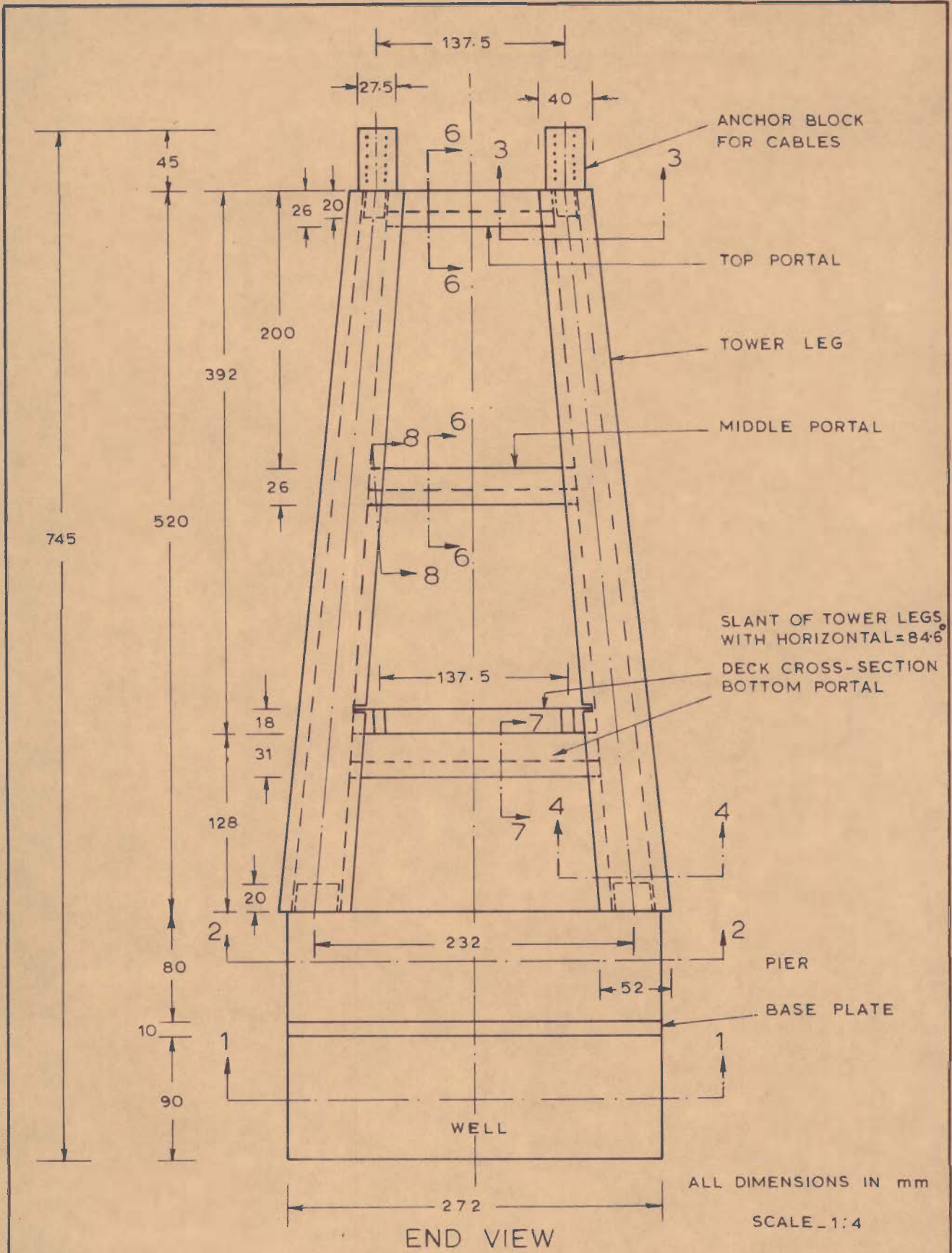
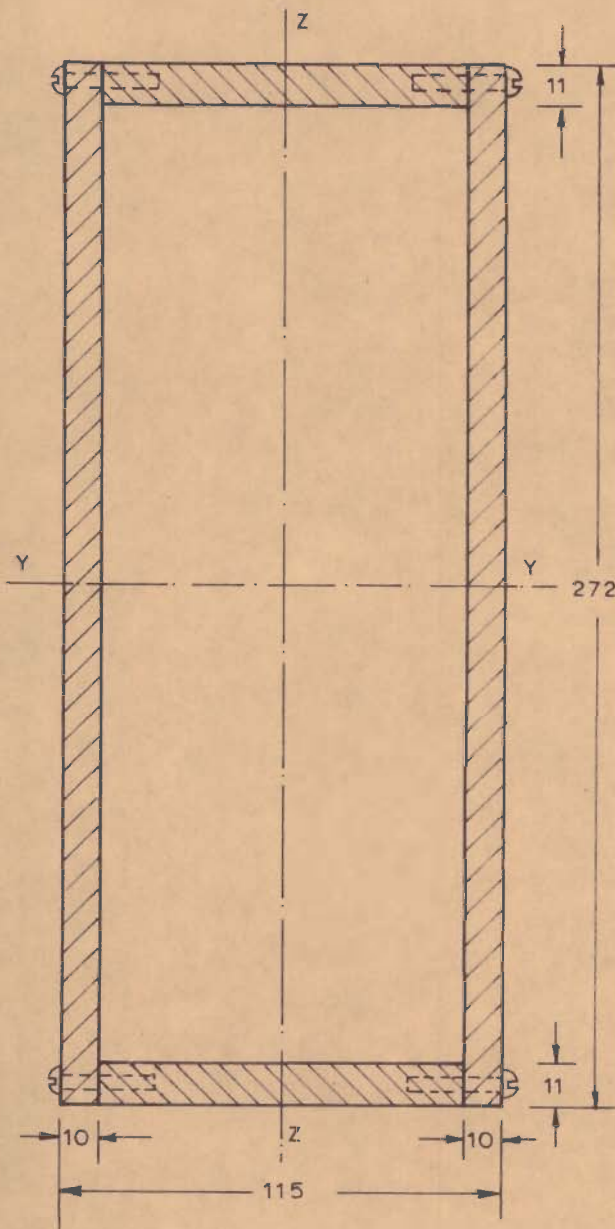


FIG. 5.4 - END VIEW OF MODEL BRIDGE AT TOWER LOCATION  
(SECTIONS 1-1 TO 8-8 SHOWN IN FIG. 5.5 TO 5.8)



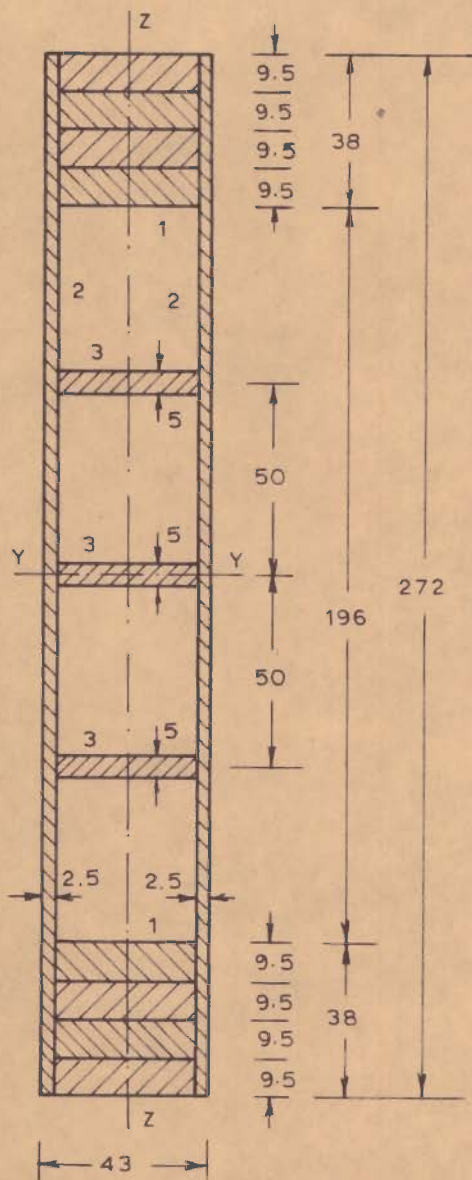
- ALL DIMENSIONS IN mm
- HEIGHT OF WELL = 90 mm
- 4 Nos. SCREWS 4mm x 25 mm ON EACH JOINT ALONG HEIGHT
- CONNECTED TO SHAKE TABLE BY 8 Nos SCREWS 4.5mm x 37mm WITH SPRING WASHERS
- CONNECTED TO 10 mm THICK PLATE (BETWEEN WELL AND PIER) BY 14 Nos SCREWS 4 mm x 25 mm

AREA	7530	mm <sup>2</sup>
INERTIA - X	42139116	mm <sup>4</sup>
INERTIA - Y	69153725	mm <sup>4</sup>
INERTIA - Z	16611185	mm <sup>4</sup>

SCALE - 1:2

FIG. 5.5 - CROSS-SECTION OF MID WELL (No. 2 & 3)  
(SECTION 1-1 OF FIG. 5.4)





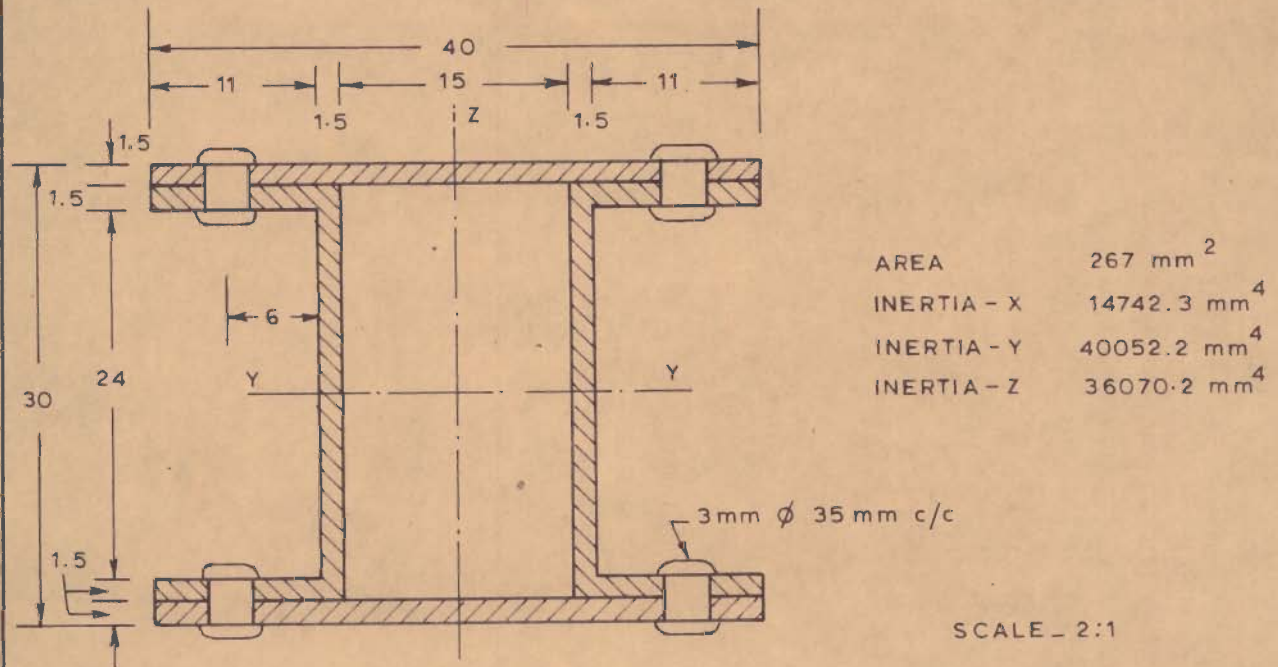
- DIMENSIONS IN mm
- HEIGHT OF PIER = 80 mm
- FOUR PLATES, 9.5 mm THICK, RIVETED AT SIX POINTS TO MAKE PART 1
- PART 3 CONNECTED TO PART 2 BY THREE SCREWS, 3 mm X 12 mm ALONG HT.
- PART 2 CONNECTED TO PART 1 BY TWO COLUMNS OF SCREWS, 4 mm X 18 mm, (THREE IN EACH COLUMN) ON EACH SIDE
- CONNECTED TO WELL BY 10 mm THICK PLATE SCREWED TO PART 1, FIVE SCREWS 4 mm X 25 mm
- 2.5 mm THICK COVER PLATE AT TOP OF PIER CONNECTED TO PART 3 BY 3 mm X 12 mm SCREW ONE ON EACH PART 3

AREA	4818.0	mm <sup>2</sup>
* INERTIA - X	1897486.4	mm <sup>4</sup>
INERTIA - Y	49217399.0	mm <sup>4</sup>
INERTIA - Z	1005299.7	mm <sup>4</sup>

\* MIDDLE WEBS IGNORED

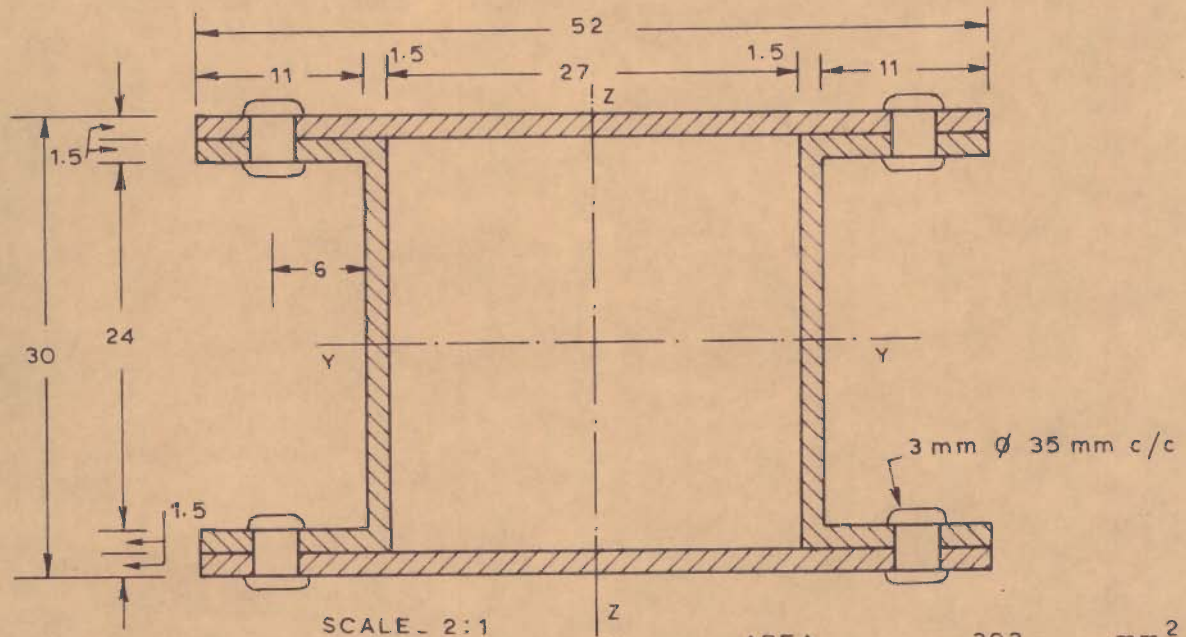
SCALE\_ 1:2

FIG. 5.6 - CROSS - SECTION OF MID-PIER (No. 2 & 3)  
(SECTION 2-2 OF FIG. 5.4)



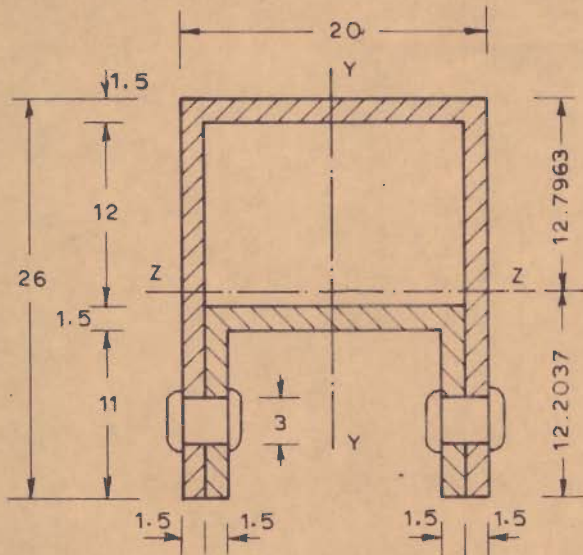
a\_ TOWER TOP CROSS-SECTION  
(SECTION 3-3 OF FIG. 5.4)

ALL DIMENSIONS IN mm



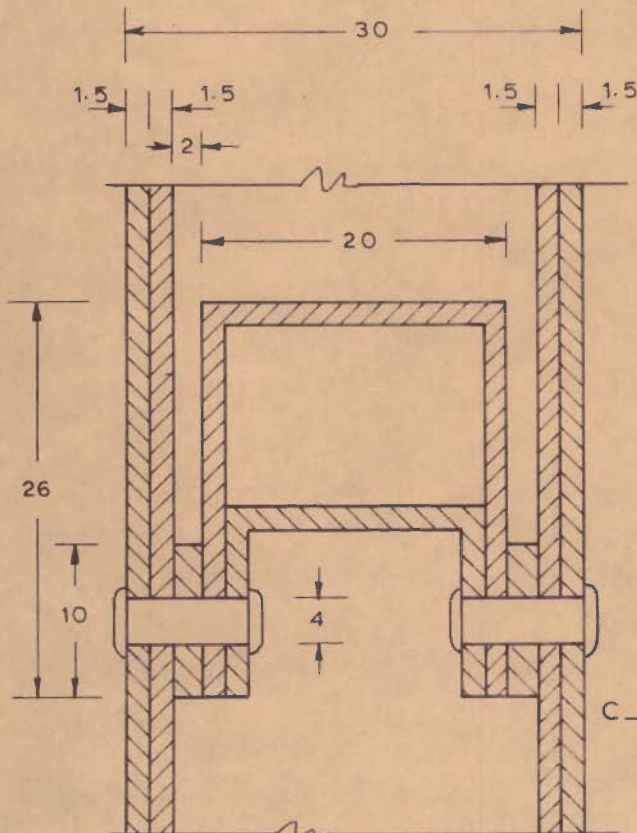
b\_ TOWER BOTTOM CROSS-SECTION  
(SECTION 4-4 OF FIG. 5.4)

FIG. 5.7 \_ CROSS-SECTIONS OF TOWER TOP AND BOTTOM



a\_ TOP AND MIDDLE PORTAL  
(SECTION 6-6 OF FIG. 5.4)

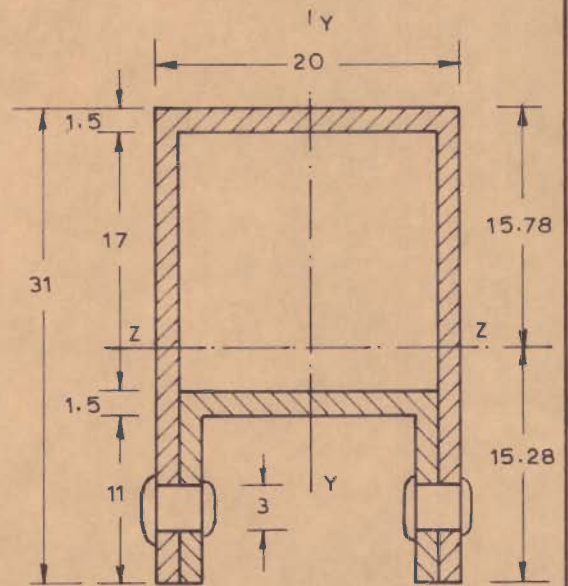
ALL DIMENSIONS IN mm  
SCALE\_ 2:1



c\_ TOWER LEG-PORTAL  
CONNECTION  
(SECTION 8-8 OF FIG. 5.4)

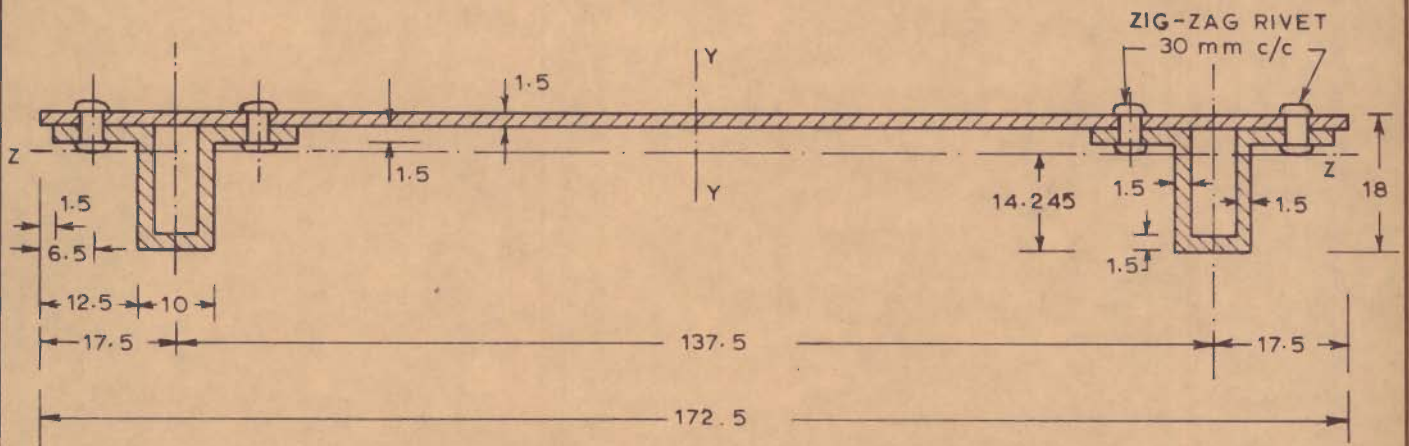
	TOP PORTAL	BOTTOM PORTAL	UNIT
AREA	162	177	mm <sup>2</sup>
* INERTIA - X	5847.7	9497.4	mm <sup>4</sup>
INERTIA - Y	9905.0	11191.2	mm <sup>4</sup>
INERTIA - Z	10454.1	16982.6	mm <sup>4</sup>

\* ONLY ENCLOSED BOX CONSIDERED

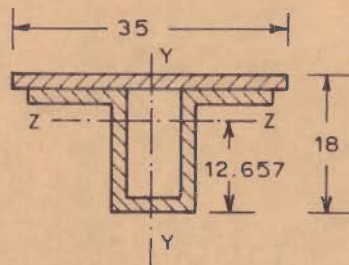


b\_ BOTTOM PORTAL  
(SECTION 7-7 OF FIG. 5.4)

FIG. 5.8 \_ PORTAL CROSS SECTIONS AND  
TOWER- PORTAL CONNECTION



a\_FULL DECK CROSS- SECTION



SCALE - 1:1

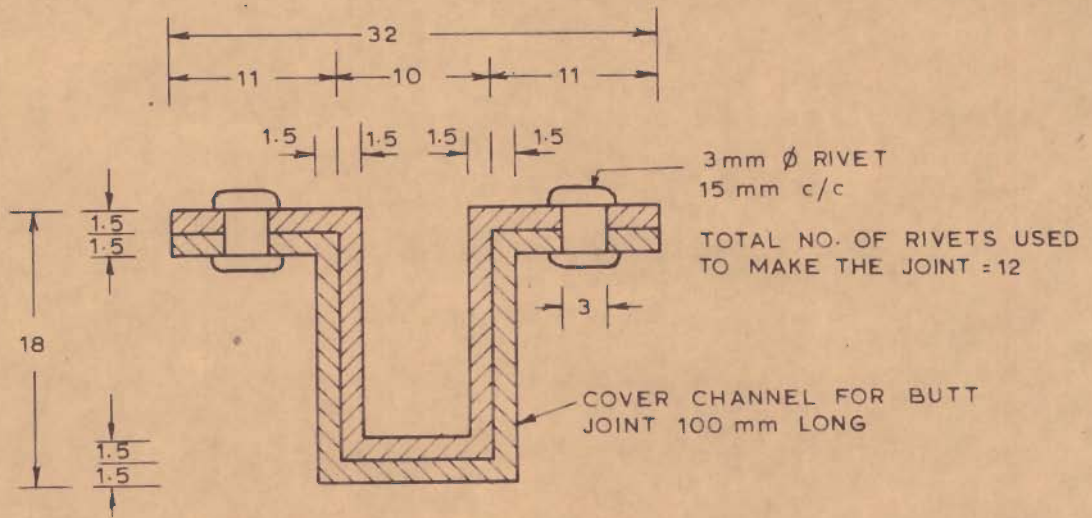
b\_MAIN GIRDER WITH DECK

SECTION PROPERTIES		
	(a)	(b)
AREA	444.7	145.5 mm <sup>2</sup>
+ INERTIA - X	-	2360.4 mm <sup>4</sup>
INERTIA - Y	-	10276.6 mm <sup>4</sup>
INERTIA - Z	12179.4	4178.9 mm <sup>4</sup>

+ ONLY ENCLOSED BOX CONSIDERED

RIVETS 3 mm x 6 mm

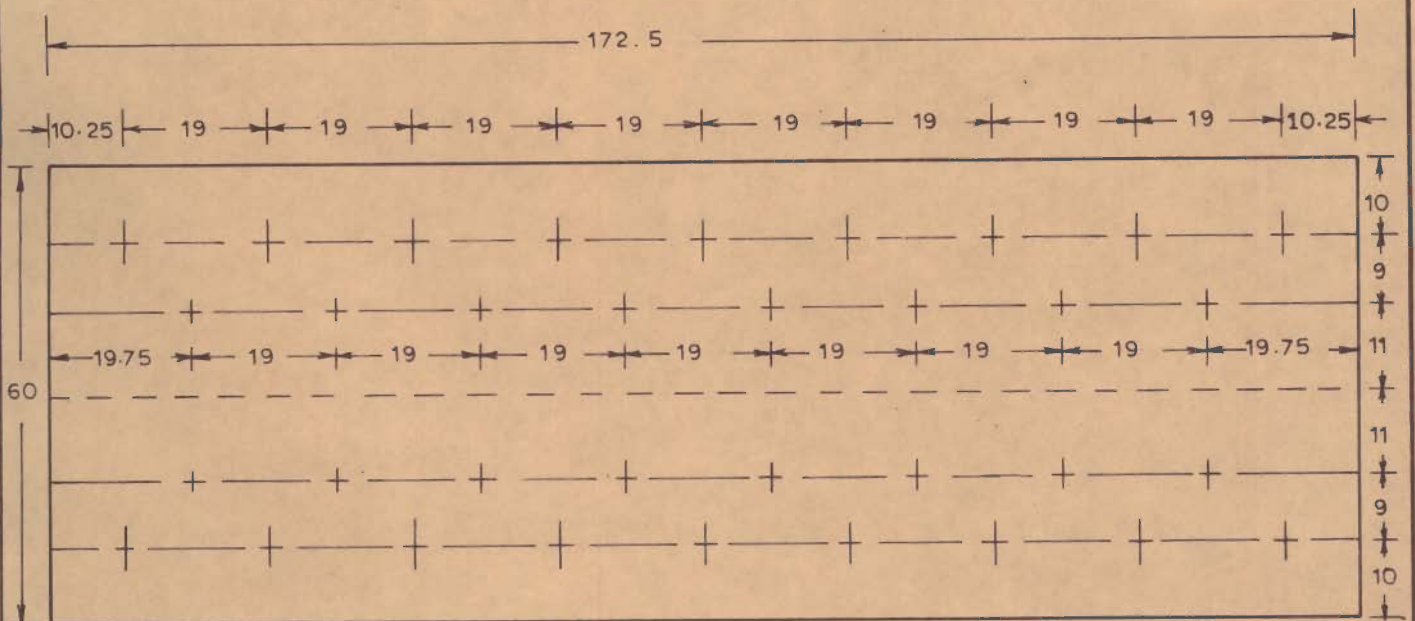
FIG. 5.9 \_DECK CROSS- SECTION DETAILS



DIMENSIONS IN mm

SCALE 2:1

FIG. 5.10 MAIN GIRDER SPLICE CROSS-SECTION



PLAN

ALL DIMENSIONS IN mm

+ LOCATION OF RIVET  
3 mm Ø

FIG. 5.11 DECK PLATE SPLICE

SCALE 1:1

shown (fig. 5.4) in the end view of the model bridge at tower location. Figures 5.5 and 5.6 show details of cross-sections of the middle wells and middle piers respectively. The slanting and tapering tower legs <sup>were</sup> fabricated by jointing two channels of uniform cross-section with two tapering plates to form boxes with cross-sections (fig. 5.7) varying with the height of the tower. The peculiar cross-section of the portals (fig. 5.8) was chosen to facilitate the jointing of the ends of the portals with the tower legs by riveting. The cross-section of the deck with main box girders is shown in fig. 5.9. The total length of the girder (4114.8mm) was obtained by jointing three pieces of equal length. Single cover butt riveting with three rivets, spaced 15mm, on each side of the joint (fig. 5.10) was done. The deck was a 1.5 mm thick plate 172.5 mm wide and 4114.8 mm long. The length of the deck was obtained by jointing three pieces of plate with single cover, double riveted, zig-zag butt joint (fig. 5.11). The joints in the deck plate and the joints in the box girders were kept sufficiently staggered (250 mm) to avoid concentration of structural weakness on a section.

#### 5.10 SUPPORT DETAILS

To restrain the movements of the deck with respect to the supporting pier in the horizontal and vertical planes and to allow free rotation at one end of the model bridge, a hinge connection, similar in action to the hinge of the actual bridge, was provided. The detailed drawings of the mild steel

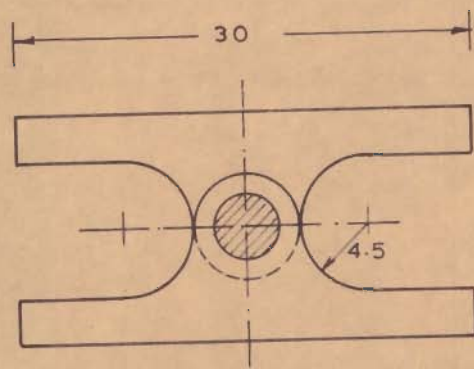
hinge are shown in fig. 5.12. The other three points of deck supports in the model bridge were provided with mild steel links to permit horizontal translation and free rotation of the deck with respect to the supporting portals/pier. The relative movements in the vertical plane were restrained. The details of link connection between deck and the tower portals are shown in fig. 5.13 and the link connection at one end pier of the bridge is described in fig. 5.14. Photos P2 to P4 show the positioning of hinge and the links at appropriate locations of the model bridge. Photo P5 shows the detached hinge and the link.

## 5.11 CABLE ANCHORAGE DETAILS

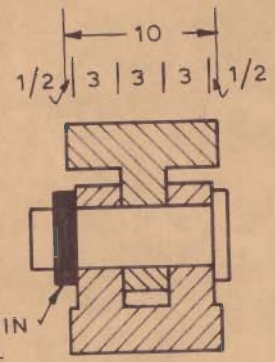
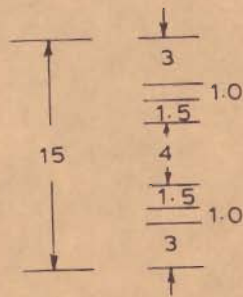
### 5.11.1 Anchor Block

Detailed drawings of the anchor block are shown in fig. 5.15. The anchor block was fitted to tower leg by inserting its solid projecting web into the hollow leg cross-section and by screwing the two together. Araldite was used at the joint. The holes for wires of end span were drilled on one side of the centre line of the anchor block and those for the mid span were drilled on another side. Each cable was anchored to the block by two screws providing a grip to the cable end. Photo P6 illustrates the positioning of the anchor block.

Under symmetric loads, the twisting caused due to tension in eccentrically connected wires at the anchor block



a - ELEVATION SEEN ACROSS THE AXIS OF BRIDGE



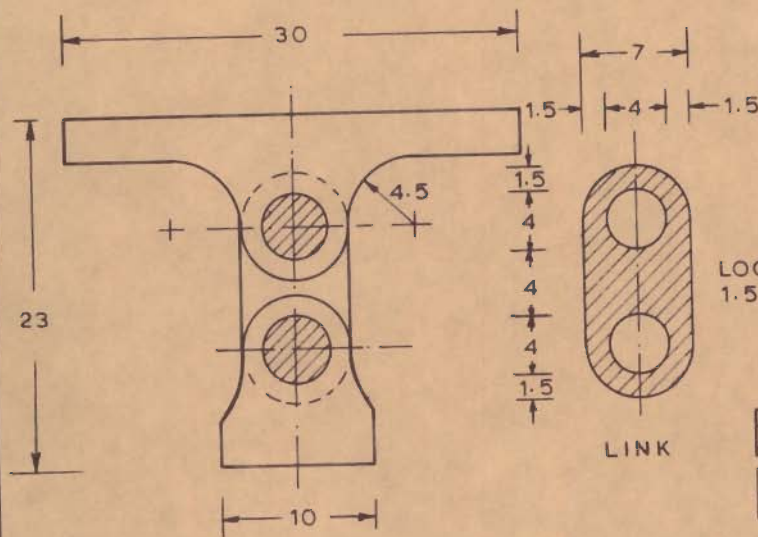
b - ELEVATION SEEN ALONG THE AXIS OF BRIDGE

DIMENSIONS IN mm

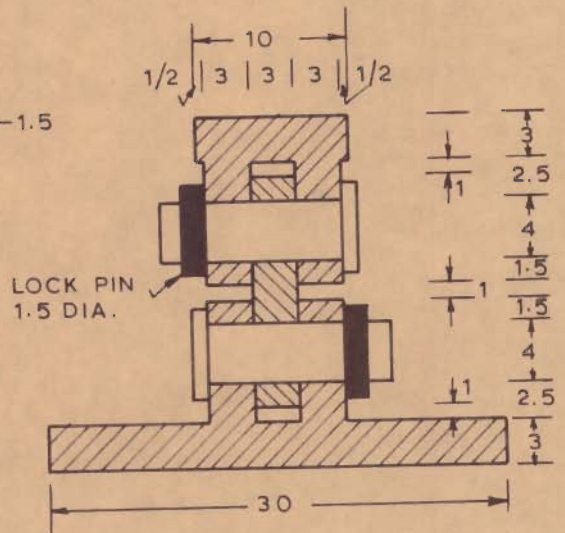
SCALE - 2:1

HOLES FOR CONNECTION TO BRIDGE COMPONENTS NOT SHOWN

FIG. 5.12 - HINGE CONNECTION AT END PIER



a - ELEVATION SEEN ACROSS THE AXIS OF BRIDGE



b - ELEVATION SEEN ALONG THE AXIS OF BRIDGE

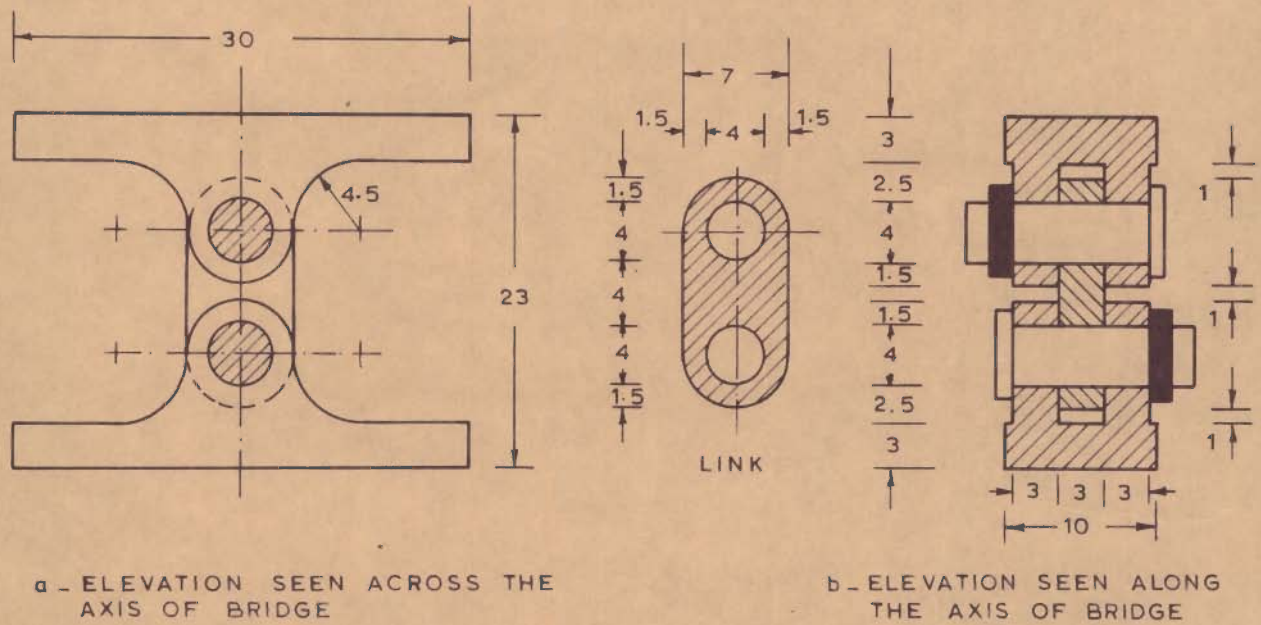
DIMENSIONS IN mm

SCALE - 2:1

HOLES FOR CONNECTION TO BRIDGE COMPONENTS NOT SHOWN

FIG. 5.13 - LINK CONNECTION AT TOWER





HOLES FOR CONNECTION TO BRIDGE COMPONENTS NOT SHOWN  
ALL DIMENSIONS IN mm  
SCALE - 2:1\*

FIG. 5.14 - LINK CONNECTION AT END PIER

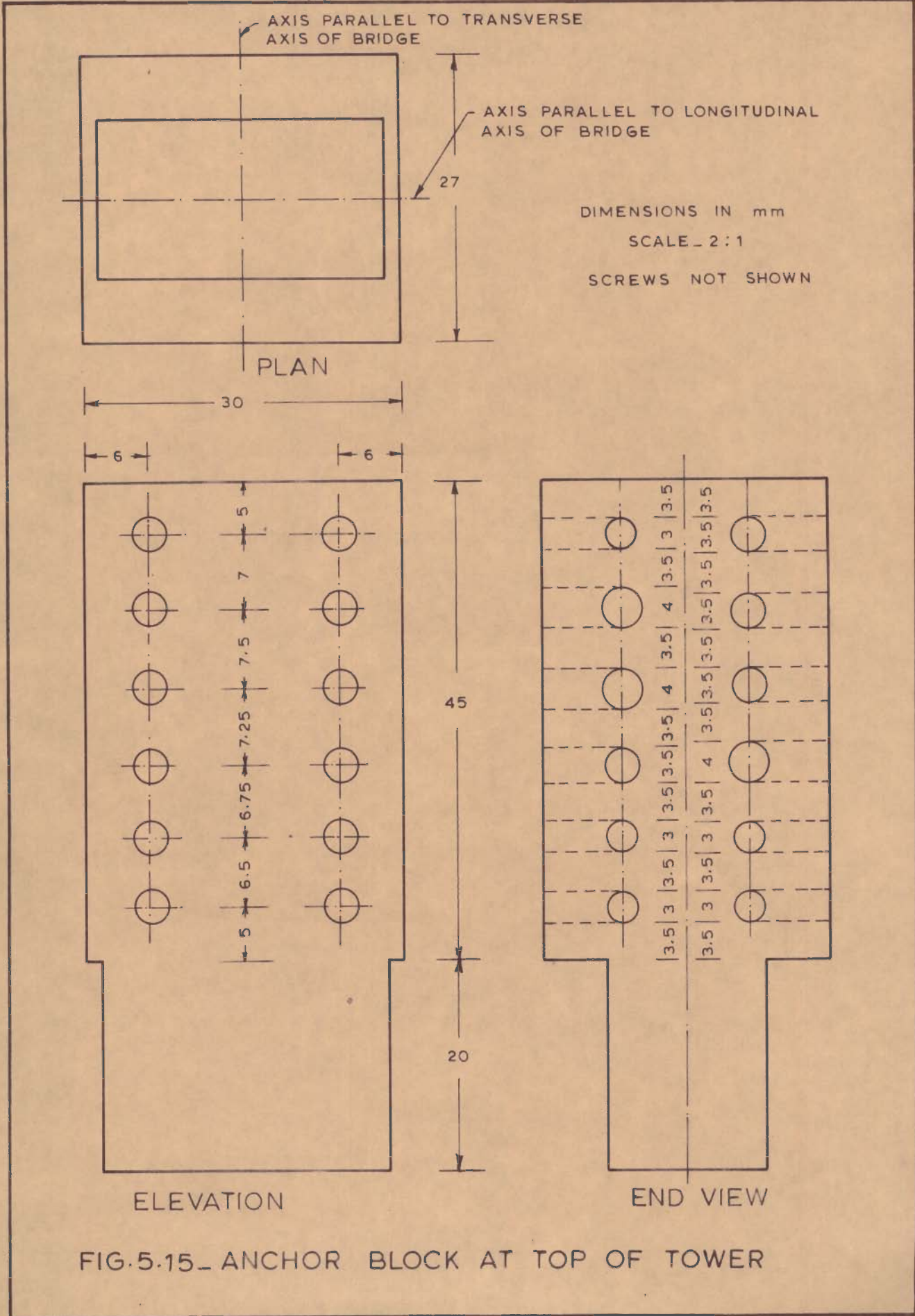
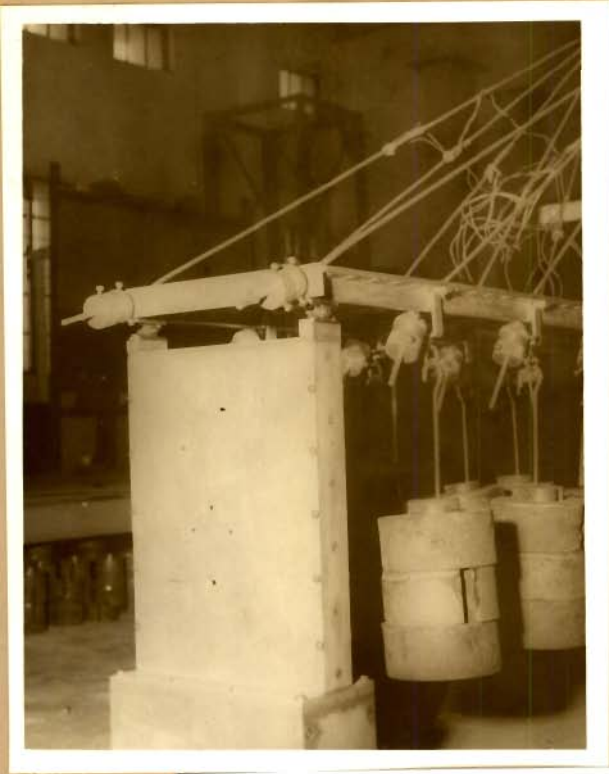
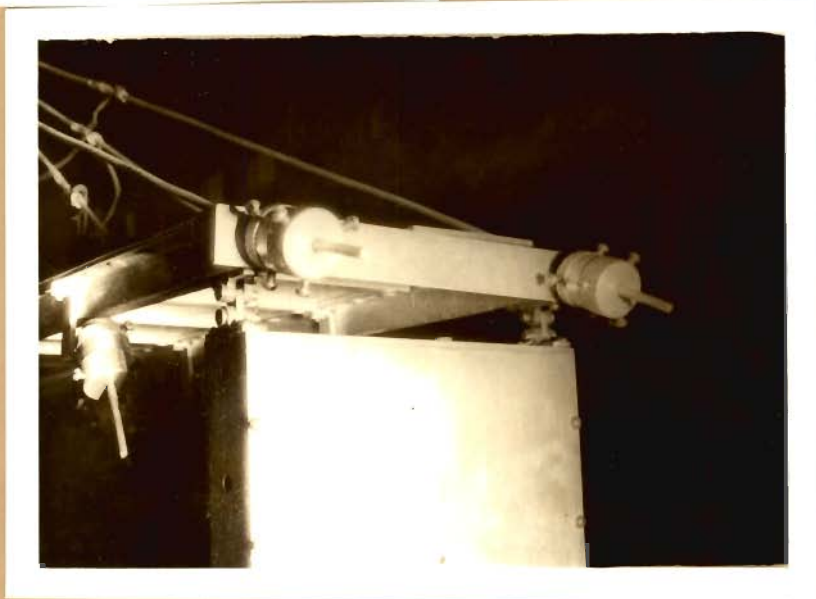


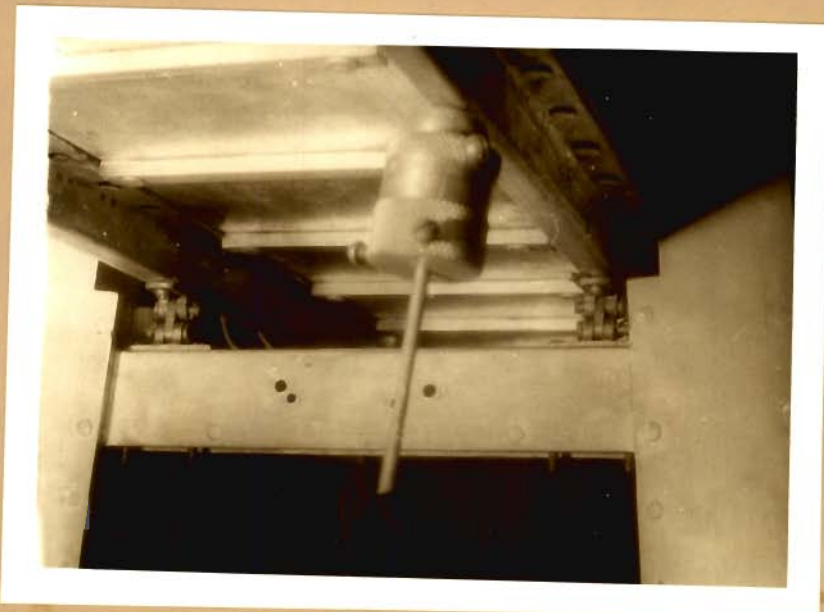
FIG.5.15\_ ANCHOR BLOCK AT TOP OF TOWER



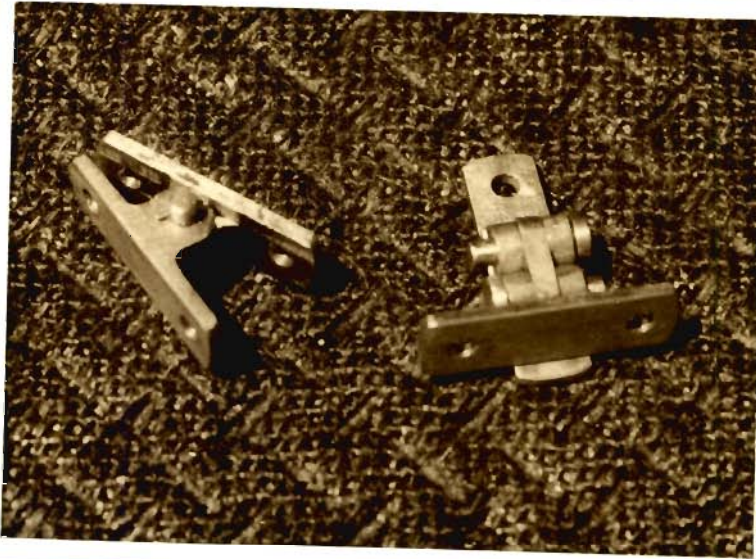
P 2: DECK-PIER CONNECTION THROUGH HINGE



P 3: DECK-PIER CONNECTION THROUGH LINK



P 4: DECK-TOWER CONNECTION THROUGH LINK



P 5: THE HINGE AND THE LINK



P 6: CABLE ANCHORAGE BLOCKS AT THE TOWER TOP



P 7: MICROMETER TENSIONING CUM GRIPPING DEVICE

was counteracted by the twisting caused at the anchor block of the other leg of the tower (fig. 5.16). Eccentric anchoring of the cables was considered necessary to limit the height of the anchor block. This constructional feature induced a deviation in the physical behaviour, under non-symmetric loads, of the experimental bridge and its mathematical formulation in which a concentric cable connection was assumed at the top of the tower.

#### 5.11.2 Micrometer Tensioning-cum-Gripping Device

The micrometer tensioning-cum-gripping device was developed to serve the dual purpose of holding the deck against the tension of the cable and to increase or release the tension of any cable. The movement of the joint in the direction of the cable can be roughly known by the micrometer which can move into the grip. The gripping was done by three screws meeting at  $120^{\circ}$  on the cable. The tensioning device was mainly used for adjusting the cable tensions to obtain an arbitrary cambered deck profile. No measurements were made on the micrometer in the present test programme. The details of the device are given in fig. 5.17 and Photo P 7.

#### 5.12 PRELOADING AND INSTRUMENTATION OF CABLE WIRES

Aluminium wires in pieces of required lengths were kept stressed to a level of about  $4 \text{ Kg/mm}^2$  for a period of  $24 \pm 2$  hours to overcome the creep effects, if any. Strain

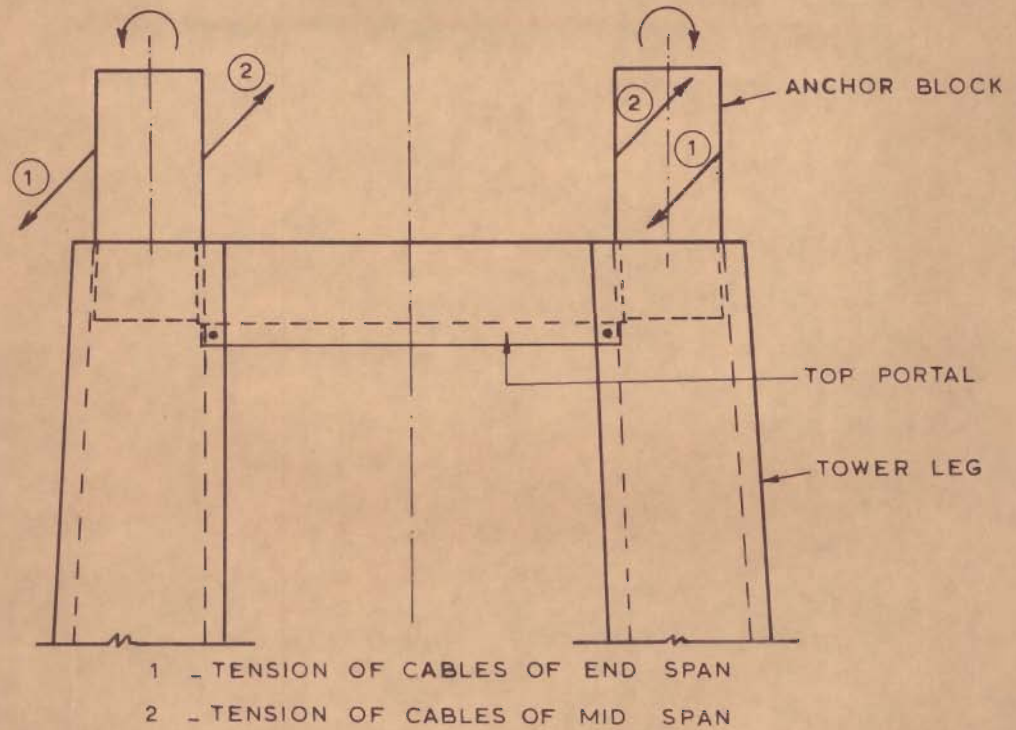


FIG.5.16 \_ CABLE FORCES AT TOWER TOP

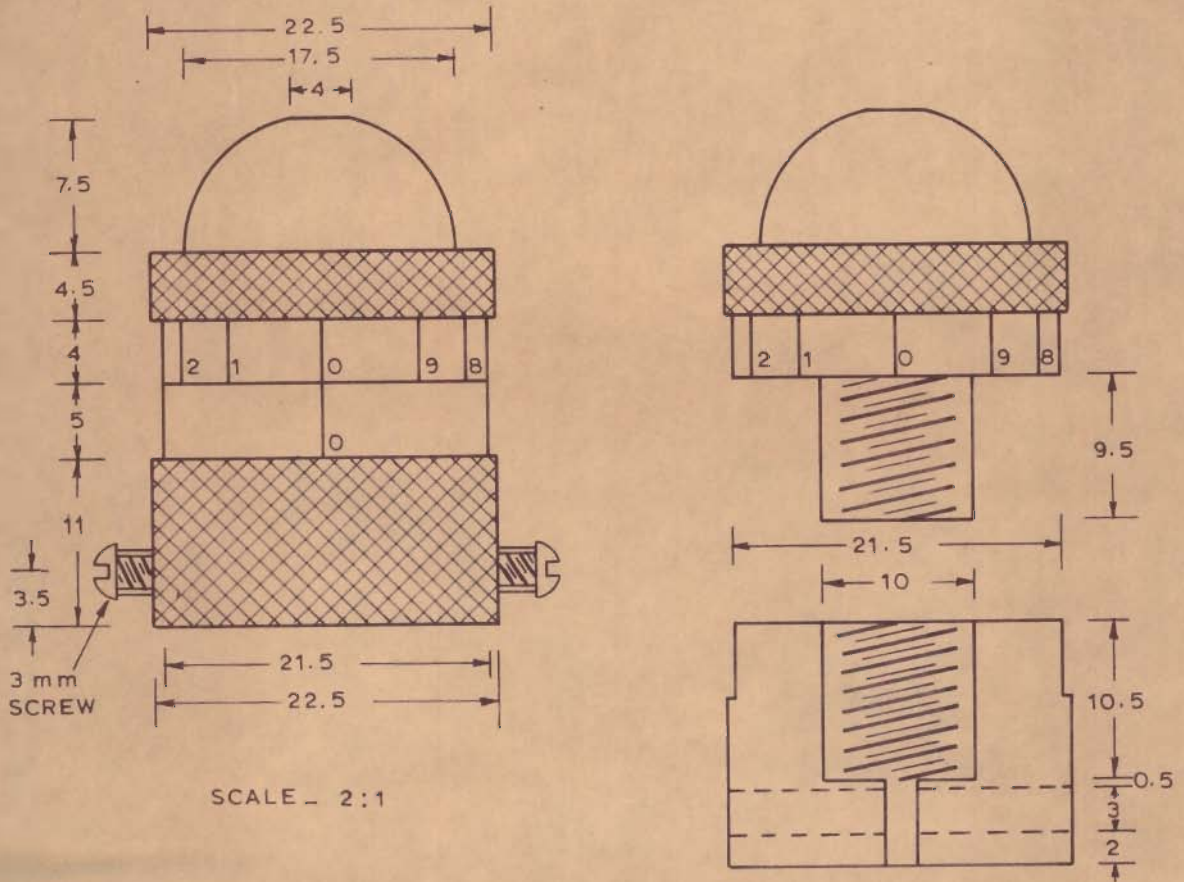


FIG.5.17 \_ MICROMETER TENSIONING CUM ANCHOR DEVICE

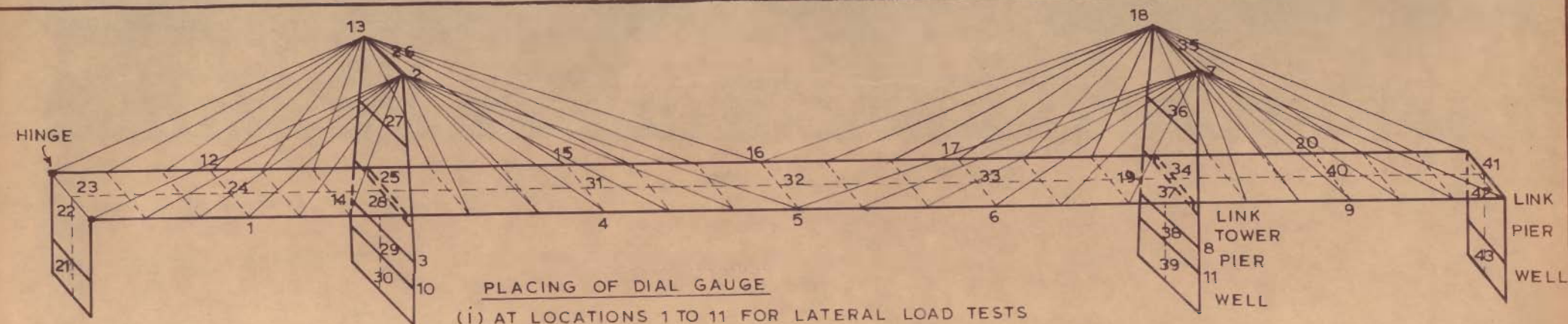
gauges were then pasted near the centre of the wires to record static cable forces. The instrumented wires were used as cables in the model bridge.

### 5.13 MODEL ERECTION

The assemblies of piers and wells were mounted on the shake table. The towers, fitted with portals and anchor heads, were installed on the middle piers. The deck was placed on the substructure system and connected to it through a hinge at one end and links at other locations. The deck was adjusted to an arbitrary cambered profile by providing a temporary prop at the centre of the main span and the cables were installed. The cables were gripped at the tower heads first and then at the girder locations. Micrometer tensioning device was used for adjustments in the cable tensions. The central prop was then removed and a final cambered profile for the deck was obtained (Photo P1).

### 5.14 TEST RECORDS (FIG. 5.18a)

Static deflections at various locations of the deck, towers, piers and wells were measured with dial gauges. Deflections of towers, piers and wells in the longitudinal direction of the bridge and vertical deflections of the deck were measured for symmetric and eccentric vertical loadings. Lateral deflections were measured for lateral loadings. Strain gauge records were taken to get static cable forces.

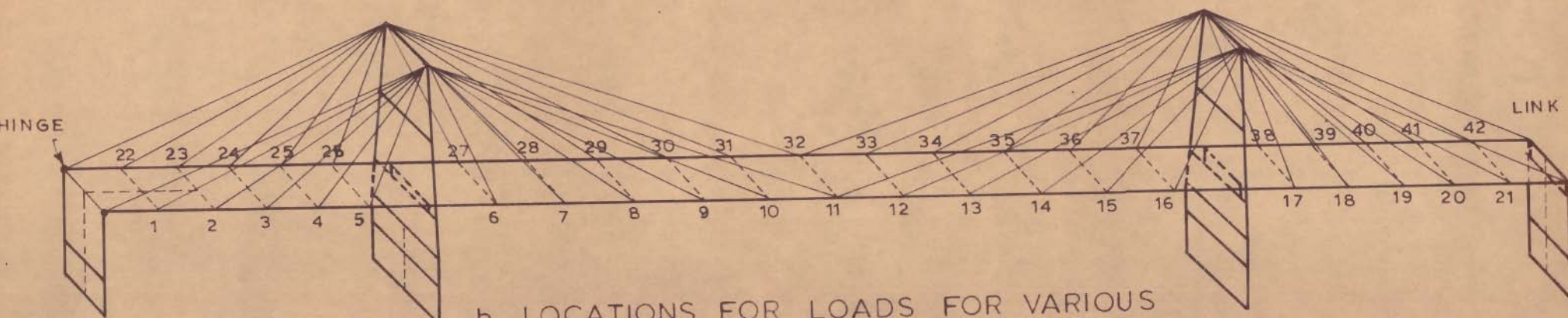


PLACING OF DIAL GAUGE  
 (i) AT LOCATIONS 1 TO 11 FOR LATERAL LOAD TESTS  
 (ii) AT LOCATIONS 1 TO 9 AND 12 TO 20 FOR VERTICAL LOAD TEST

PLACING OF ACCELEROMETERS  
 AT LOCATIONS 21 TO 43 FOR FREE VIBRATION AND STEADY STATE VIBRATION TESTS

SUDDEN RELEASE OF LOAD TO INDUCE FREE VIBRATIONS  
 (i) AT LOCATION 5 FOR LATERAL DIRECTION  
 (ii) AT LOCATION 32 FOR VERTICAL DIRECTION  
 (iii) AT LOCATION 41 FOR LONGITUDINAL DIRECTION

a - SCHEME OF INSTRUMENTATION



b - LOCATIONS FOR LOADS FOR VARIOUS LOADING CONDITIONS

FIG. 5.18 - SCHEME OF INSTRUMENTATION AND LOADING OF BRIDGE MODEL



Accelerations in vertical, longitudinal and lateral directions of the bridge were recorded at different locations of deck, towers, piers and wells.

## 5.15 TEST DETAILS

### 5.15.1 Static Tests

The following static load tests were carried out:

(a) Tests under symmetric vertical loads through both stiffening girders (Photo P8), loadings 11 to 16 of table 5.3.

(b) Tests under eccentric vertical loads through one stiffening girder, loadings 21 to 26 of table 5.3.

(c) Tests under lateral forces (Photo P9), loadings 31 to 36 of table 5.3.

Records for the following conditions of loading of the bridge were obtained:

(i) End span with hinge at the end loaded (Loadings 11, 21 and 31 of table 5.3).

(ii) End span with hinge at the end and centre span loaded (loadings 12, 22 and 32 of table 5.3).

(iii) Centre span loaded (loadings 13, 23 and 33 of table 5.3).

(iv) Centre span and end span with link at the end loaded (loadings 14, 24 and 34 of table 5.3).



P 8: SYMMETRIC VERTICAL LOADS ON THE BRIDGE DECK



P9: 5-POINT LATERAL LOADING OF THE BRIDGE DECK

(v) End span with link at the end loaded (loadings 15, 25 and 35 of table 5.3).

(vi) Full span loaded (loadings 16, 26 and 36 of table 5.3).

TABLE 5.3 SCHEME OF LOADING OF BRIDGE-MODEL FOR STATIC TESTS

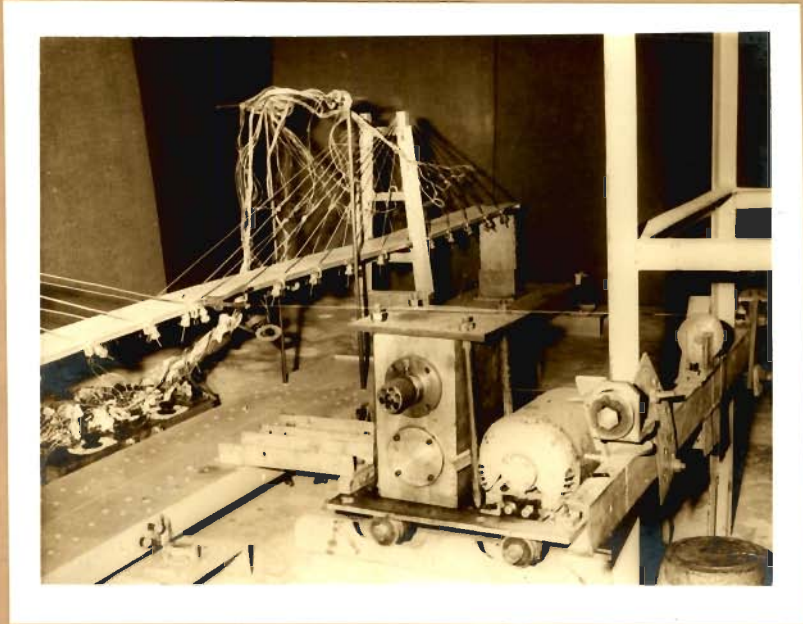
TYPE OF STATIC LOADING	LOADS ON END SPAN WITH HINGE	LOADS ON END SPAN WITH HINGE AND CENTRE SPAN	LOADS ON CENTRE SPAN	LOADS ON CENTRE SPAN AND END SPAN WITH LINK	LOADS ON END SPAN WITH LINK	LOADS ON FULL SPAN
LOADING NO.	11	12	13	14	15	16
SYMMETRIC VERTICAL	AT NODES 1 TO 5 AND 22 TO 26	AT NODES 1 TO 16 AND 22 TO 37	AT NODES 6 TO 16 AND 27 TO 37	AT NODES 6 TO 21 AND 27 TO 42	AT NODES 17 TO 21 AND 38 TO 42	AT NODES 1 TO 42
LOADING NO.	21	22	23	24	25	26
ECCENTRIC VERTICAL	AT NODES 1 TO 5	AT NODES 1 TO 16	AT NODES 6 TO 16	AT NODES 6 TO 21	AT NODES 17 TO 23	AT NODES 1 TO 21
LOADING NO	31	32	33	34	35	36
LATERAL	AT NODE 3	AT NODES 3, 8, 11 AND 14	AT NODES 8, 11 AND 14	AT NODES 8, 11, 14 AND 19	AT NODE 19	AT NODES 3, 8, 11, 14 AND 19

(Node numbers Referred to fig. 5.18)

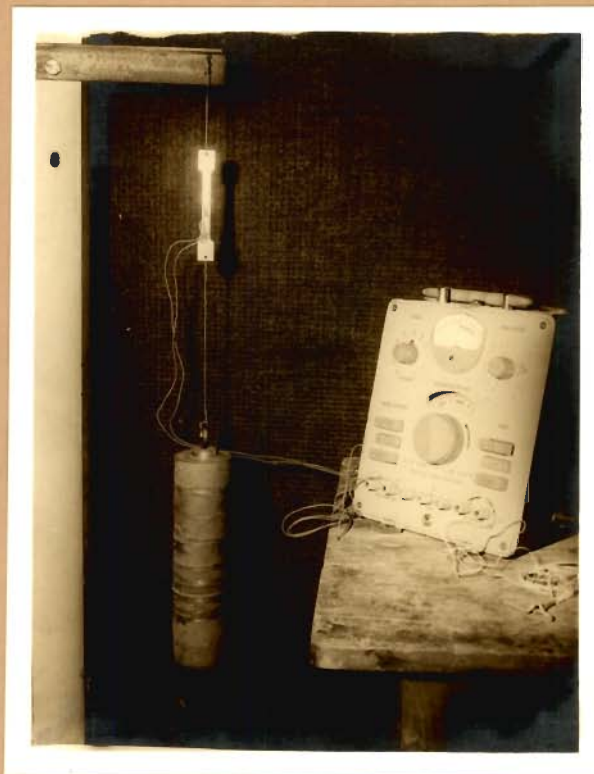
### 5.15.2 Dynamic Tests

The following dynamic tests were carried out

(a) Free vibration tests in the vertical, longitudinal and lateral (Photo P 10) directions of the bridge.



P10: (i) LOADING OF THE BRIDGE THROUGH CLUTCH TO INDUCE LATERAL FREE VIBRATIONS  
(ii) OSCILLATOR MOUNTING FOR SHAKING IN LATERAL DIRECTION



P11: STRAIN RECORDING FOR DIRECT TENSION TEST ON COUPON FROM ALUMINIUM ALLOY SHEET

(b) Steady state vibration test in the lateral direction of the bridge (Photo P 10).

The steady state tests in longitudinal and lateral directions of the bridge could not be carried out due to limitations of testing facilities.

#### 5.16 ANCILLIARY TESTS

Direct tension tests were conducted on coupons cut from aluminium alloy sheets (Photo P 11) as well as on wires. Electrical resistance strain gauges were used to measure tensile strains and the modulus of elasticity of the material was calculated from the stress-strain diagram. Tensile strains of wires were measured from two strain gauges, pasted as closely as possible on diametrically opposite faces of the wire and connected in series to overcome the effect of initial curvature in the wire on the recorded tensile strain.

The wires were not perfectly straight and suffered from out-of-straightness, locally, at one or more locations along the lengths. These curvatures could not be fully straightened even after preloading. As will be described, this crookedness did alter the overall axial stiffness of the wires in varying measures. To eliminate the effect of curvature of wires on the computed vertical deflections of the deck, the actual tensile stiffness of each individual wire used in the model was found by loading the length of wire

actually used in the model and recording the total extension of the wire. The details of this testing arrangement are shown in fig. 5.19. From the load deflection plots of all the wires, average value of equivalent modulus of elasticity ( $E_{eq}$ ) for a particular diameter of wire was determined. This value  $E_{eq}$  was used in the analysis of the model structure. .

Fixity at the base of the substructure was achieved by screwing the substructure wells to the shake table. Tests were conducted to ascertain the actual rotational stiffness at the base of the supports. Loads in the longitudinal and lateral directions were applied at the top of (i) the substructure assembly at the end and (ii) assembly of tower, pier and well at the middle supports of the deck. Deflection at top in the direction of application of the force was measured and this was compared with the analytical deflection of fixed base supports. Extra experimental deflection was considered to be caused due to the rotation of support at its base. Torsional stiffness of the substructure assembly at the hinged end was also experimentally evaluated.

To find the stiffness of riveted deck construction, the deck without cables was tested as a three span slab subjected to symmetrical vertical loads applied at the stiffening girders. The measured vertical deflections of the deck were compared with the analytical results.

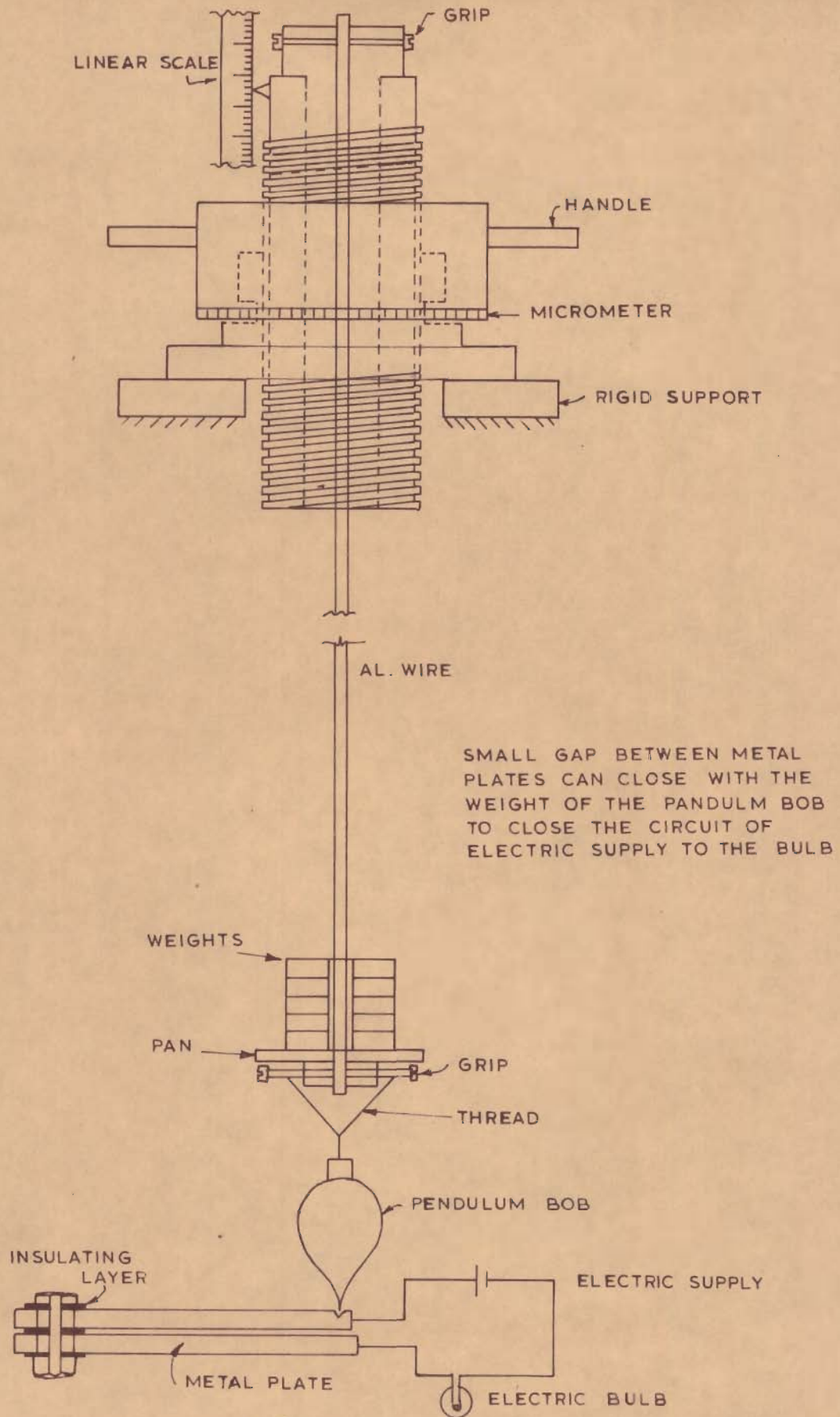


FIG. 5.19 \_ TEST ARRANGEMENT TO DETERMINE TENSILE STIFFNESS OF ALUMINIUM WIRES

The results of ancilliary tests are presented in table 5.4.

TABLE 5.4 RESULTS OF ANCILLIARY TESTS

---

(a) Modulus of Elasticity (E)	
(i) Aluminium alloy plates, obtained from coupon tests	10000 kg/mm <sup>2</sup>
(ii) Aluminium alloy wires, Obtained from strain gauge records	6971 kg/mm <sup>2</sup>
(b) Equivalent Modulus of Elasticity of Wires (Eq. )	
Obtained from load-deflection records of actual length of wires	
(i) 3 mm dia. (7.07 mm <sup>2</sup> )	2869 kg/mm <sup>2</sup>
(ii) 3.5 mm dia (9.68 mm <sup>2</sup> )	3673 kg/mm <sup>2</sup>
(iii) 4.0 mm dia. (12.57 mm <sup>2</sup> )	3061 kg/mm <sup>2</sup>
(c) Stiffness of Riveted Construction Symme- tric vertical loads of 1 kg applied at nodes of deck with cables removed and ana- lytical and experimental results compared.	
Deflection at centre of main span	
(i) analytical	14.2096 mm
(ii) experimental	13.68 mm
(d) Rotational Stiffnesses (kg-mm/rad.)	
(i) torsional stiffness, substructure at end	1014441.7



(ii) Rotational stiffness about transverse axis of bridge

Substructure at end	910160.0
Substructure below tower	3288600.0

(iii) Rotational stiffness about longitudinal axis of bridge

Substructure at end	3220280.0
Substructure below tower	30087400.0

---

It is observed from table 5.4 that the modulus of elasticity of cable wires and their equivalent moduli of elasticity. ( $E_{eq.}$ ) are quite different. Average value of  $E_{eq.}$  for a particular diameter of wire could be obtained from the straight portions of the load-deflection records which were exhibited after small curved portions in the initial stages of loading. Values of  $E_{eq.}$  were used in the computations for analytical verifications. The riveted construction of the model components can be assumed to attain full stiffness and the experimentally evaluated springs must be considered in the analysis to obtain the results which can be compared with the experimental results.

## C H A P T E R 6

### STATIC PLANE FRAME INVESTIGATIONS

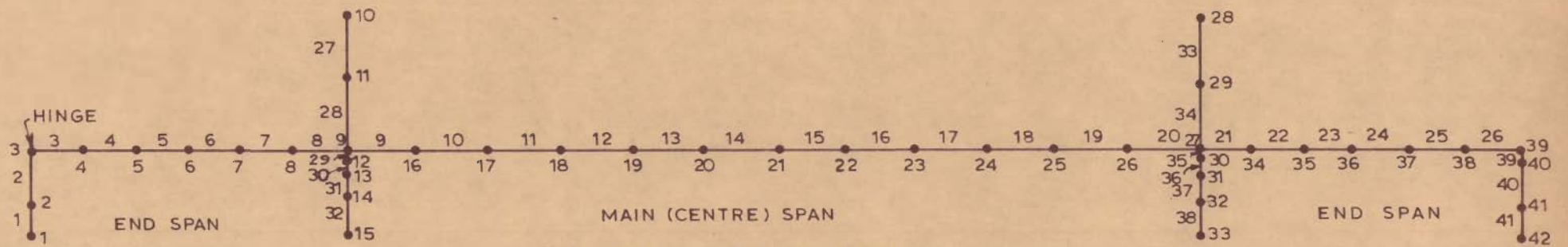
#### 6.1 INTRODUCTION

Idealized planar mathematical models of structures chosen for analytical studies and various loadings applied on them have been described herein. Conditions of external restraints and geometrical properties of components of mathematical models have been tabulated. Salient results obtained from analytical and experimental studies have been presented, interpreted and discussed.

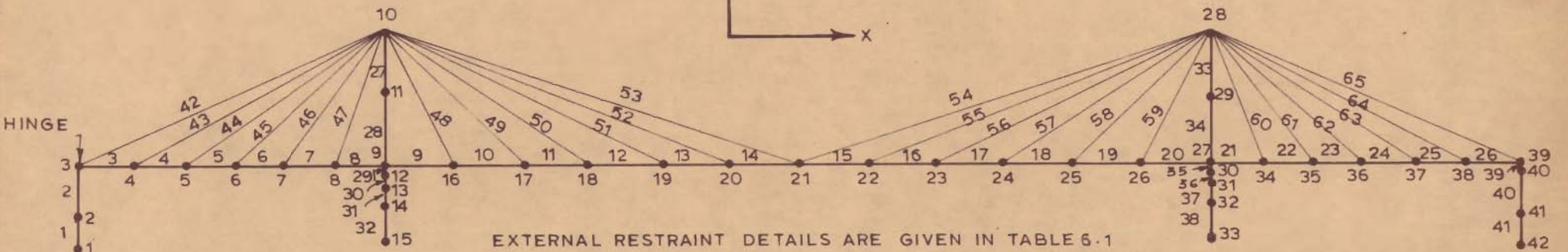
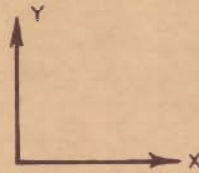
#### 6.2 DETAILS OF STRUCTURES S1 TO S7

Idealized mathematical model shown in fig. 6.1 has been used for (a) carrying out linear analysis, (b) determination of extent of bending moment-axial force interaction and (c) studying the effect of initial prestressing on the nonlinearity due to axial-flexural interaction. The structures considered are described below and the conditions of external restraints of these structures are given in table 6.1.

(a) Structure S1: A- 5 span system (fig. 6.1a) having substructure fixed at the base. It has a main span of 457.2 m, four side spans of 91.44 m each and a tower height of 85.22m from the level of deck. The deck is taken as straight horizontal without camber.



(b) S2-a, S4-a, S7-a



EXTERNAL RESTRAINT DETAILS ARE GIVEN IN TABLE 6.1

(a) S1 TO S7

FIG.6.1 - MATHEMATICAL MODELS OF STRUCTURES S1 TO S7

TABLE 6.1 DETAILS OF EXTERNAL RESTRAINTS FOR S1 TO S7

STRUCTURE DESIGNATION AND DESCRIPTION	RESTRAINED+ NODE No.	STIFFNESS DUE TO EXTERNAL RESTRAINT		
		TRANSLATIONAL ALONG		ROTATIONAL ABOUT AXIS
		AXIS OF X	Y	OF Z
S1 (fig. 6.1a)	1	RIGID SUPPORT		
S2 (fig. 6.1a,b)	6	ZERO	RIGID	ZERO
5-Span system with sub-structure fixed at the base	15	RIGID SUPPORTS		
	33			
	36	ZERO	RIGID	ZERO
	42	RIGID SUPPORT		
S3 (fig. 6.1a)	1	$10^{11}$	$10^{11}$	$6.08 \times 10^7$
5-span system with sub-structure supported on elastic springs at the base	6	0	$10^{11}$	0
	15	$10^{11}$	$10^{11}$	$1.94 \times 10^8$
	33			
	36	0	$10^{11}$	0
t-m UNITS	42	$10^{11}$	$10^{11}$	$6.08 \times 10^7$
S4 (fig. 6.1a)	1			
S5 (fig. 6.1a,b)	15			
3-span system with sub-structure fixed at the base	33	RIGID SUPPORTS		
	42			
S6 (fig. 6.1a)	1	$10^{11}$	$10^{11}$	$6.08 \times 10^7$
3-span system with sub-structure supported on elastic springs at the base t-m UNITS	15	$10^{11}$	$10^{11}$	$1.94 \times 10^8$
	33			
	42	$10^{11}$	$10^{11}$	$6.08 \times 10^7$
S7 (fig. 6.1a,b)	1	$10^{11}$	$10^{11}$	$9.10 \times 10^5$
3-span system (model) with substructure supported on elastic springs at base Kg-mm UNITS	15			
	33	$10^{11}$	$10^{11}$	$3.29 \times 10^6$
	42	$10^{11}$	$10^{11}$	$9.10 \times 10^5$

+ See fig. 6.1

(b) Structure S2 : A 5-span structure (fig.6.1a) which is similar to S1 except that the initial geometrical configuration and the member force system is in equilibrium with cable prestress and dead loads - a factor not considered in S1. The prestressed state has been accounted for while carrying out nonlinear axial-flexural analysis of S2 for live loads.

(c) Structure S3: A structure similar to S1 but its substructure is supported on elastic springs at the base. The stiffnesses of these springs are given in table 6.1.

(d) Structure S4: A 3-span system (fig. 6.1a) having substructure fixed at the base. The structure has two side spans of 182.88 m each. Other features are same as described for S1 in (a).

(e) Structure S5: A 3-span system (fig. 6.1a) which is similar to S4 except in as far as prestressing considered as at (b).

(f) Structure S6: A 3-span system similar to S4 but its substructure is supported on elastic springs at the base. The stiffnesses of these springs are given in table 6.1.

(g) Structure S7: This structure represents the laboratory model made from an aluminium alloy with its main dimensions proportioned to a scale ratio of 1:200 from S4. For analysis purposes the bridge substructure is taken as

supported on elastic springs so as to account for the fact that complete fixity could not be obtained in the model. The spring stiffnesses, as experimentally determined, have been used (values in table 6.1).

Geometrical properties of elements of structures S1 to S6 are presented in table 6.2. The values of areas and inertias given in table 6.2 represent members in a vertical plane passing through one of the main stiffening girders of the bridge. The vertical plane has not been considered on the longitudinal line of symmetry and the elements represent only half the overall stiffness of the bridge. This has been done to study the nonlinear axial-flexural interaction effects on members with actual forces. The loadings on the structures have been correspondingly modified to represent total loads on the structure. Geometrical properties of S7 have been picked up from the data given in chapter 5. From the assumptions and features of the idealized mathematical models S1 to S7 are restated here below:

(i) Independent rotation of members at node 3 (fig 6.1).

(ii) Use of links (elements 29, 35 and 39, fig. 6.1) for transfer of vertical forces between deck and tower/pier while allowing free longitudinal movement and rotation of the deck at junctions with tower/pier.

TABLE 6.2 GEOMETRICAL PROPERTIES OF ELEMENTS OF STRUCTURES S1 TO S6

Member No. <sup>+</sup>	Area (m <sup>2</sup> )	Inertia Z (m <sup>4</sup> )	Member No. <sup>+</sup>	Area (m <sup>2</sup> )	Inertia-Z (m <sup>4</sup> )
1	12.087	311.95	34	0.569	1.195
2	3.059	6.058	35	0.219	0.01
3	0.363	0.543	36	0.689	1.605
4	0.376	0.550	37	13.733	105.3
5	0.340	0.489	38	32.311	1564.0
6	0.392	0.576	39	0.219	0.01
7	0.356	0.499	40	3.059	6.058
8	0.379	0.553	41	12.087	311.95
9	0.359	0.520	42	0.022	0
10	0.305	0.426	43	0.021	0
11	0.290	0.405	44	0.016	0
12	0.265	0.370	45	0.031	0
13	0.264	0.369	46	0.014	0
14	0.264	0.369	47	0.011	0
15	0.264	0.369	48	0.012	0
16	0.264	0.369	49	0.014	0
17	0.265	0.370	50	0.017	0
18	0.290	0.405	51	0.023	0
19	0.305	0.426	52	0.027	0
20	0.359	0.520	53	0.014	0
21	0.379	0.553	54	0.014	0
22	0.356	0.499	55	0.027	0
23	0.392	0.576	56	0.023	0
24	0.340	0.489	57	0.017	0
25	0.376	0.550	58	0.014	0
26	0.363	0.543	59	0.012	0
27	0.475	0.818	60	0.011	0
28	0.569	1.195	61	0.014	0
29	0.219	0.01	62	0.031	0
30	0.689	1.605	63	0.016	0
31	13.733	105.3	64	0.021	0
32	32.311	1564.0	65	0.022	0
33	0.475	0.818			

<sup>+</sup>See fig 6.1

Note: Equivalent values in terms of superstructure steel are tabulated

(iii) Members representing cables can take both tension and compression.

### 6.3 LOADING

Loadings on S1 to S6, which are described hereafter, have the following features:

(a) Forces of pretension in the cables have been calculated on the basis of uniform cable prestress of  $4\text{t/cm}^2$  in all the cables.

(b) On the basis of calculation of actual dead weights of all the components of the bridge, a dead weight of  $21.3\text{ t/m}$  intensity has been assumed.

(c) A live load of  $5\text{t/m}^+$  intensity has been assumed to act on the bridge.

(d) Only half of the total loads acting on the bridge have been applied at appropriate nodes of S1 to S6.

### 6.4 LOADINGS L1 TO L4

(a) Loading L1 : A uniform live load of  $2.5\text{t/m}$  intensity applied at deck level for S1 to S6.

---

<sup>+</sup> This intensity of live load has been arrived at by considering a traffic hold up in three out of the six lanes of the carriageway in one direction and normal traffic on other three lanes in the reverse direction. IRC class A loading (108) on 50% of the total carriageway lanes induces a load intensity of  $4\text{ t/m}$ . One load train consists of one bus, two cars, one truck, two cars, one truck, one car, one truck, one car, one bus, one car following in succession. Overloading by 20% for buses and trucks was considered.



(b) Loading L2: Vertical loads of 5 kg each at nodes (fig. 6.1a) 4 to 8, 16 to 26 and 34 to 38 of S7.

(c) Loading L3: Vertical loads of 5 kg each at nodes 4 to 8 and 16 to 26 of S7.

(d) Loading L4: Vertical loads of 5 kg each at nodes 16 to 26 of S7.

## 6.5 ELASTIC CONSTANTS

Elastic constants used in the analysis of S1 to S7, and the space frame structures to be described hereafter, are given in table 6.3. The values of cable areas and geometrical properties of piers and wells given in table 6.2 are equivalent values of areas and inertias of these components as if they were made of steel with values of elastic constants same as that of the superstructure steel.

## 6.6 TABULATION OF RESULTS

Results of linear and nonlinear axial-flexural interaction analyses of structures S1 to S6 under loading L1 are presented in tables 6.4 to 6.7. For ease of comparison, while the actual values of deformations and forces in structure S1 under loading L1 are tabulated as such for the linear case, the values for other conditions are tabulated as ratios of the former. Shears have not been tabulated as they were found insignificant in the superstructure.

TABLE 6.3 ELASTIC CONSTANTS

Description	Modulus of Elasticity	Modulus of Rigidity	Unit
<u>S1 TO S6</u>			
(a) Superstructure steel	$2.11 \times 10^7$	$0.8373 \times 10^7$	t/m <sup>2</sup>
(b) Cable steel	$1.65 \times 10^7$	-	
(c) Substructure, concrete	$0.1507 \times 10^7$	-	
<u>S7</u>			
(a) Superstructure and substructure, aluminium alloy	10000	4000	
(b) Cable-aluminium alloy <sup>+</sup>			kg/mm <sup>2</sup>
(i) 3 mm $\emptyset$	2869	-	
(ii) 3.5 mm $\emptyset$	3673	-	
(iii) 4 mm $\emptyset$	3061	-	

<sup>+</sup>Experimentally evaluated stiffness in direct tension.

TABLE 6.4 - DISPLACEMENTS IN STRUCTURES S1 TO S6 UNDER LOADING L1

LOCATION	Node <sup>+</sup> No.	Axis <sup>+</sup> of deflection (linear case)	Actual value in S1 (linear case) (m)	VALUES AS RATIOS OF CORRESPONDING VALUE IN S1 (LINEAR CASE)											
				S1		S2		S3		S4		S5		S6	
				L	L	NL	L	L	L	NL	L				
End pier top	3	X	0.01246	1	0.474	0.426	1.336	1.119	1.896	5.830	1.486				
End span	5	Y	0.00435	1	0.874	1.265	0.972	27.7 <sup>x</sup>	24.21 <sup>x</sup>	53.66 <sup>x</sup>	28.1 <sup>x</sup>				
End span	7	Y	0.00482	1	0.830	1.079	1.076	14.8 <sup>x</sup>	15.52 <sup>x</sup>	30.29 <sup>x</sup>	15.1 <sup>x</sup>				
Tower top	10	X	0.10186	1	0.913	0.928	1.036	1.634	1.561	2.593	1.683				
Centre span	18	Y	0.25455	1	0.987	1.021	1.013	1.338	1.296	1.834	1.357				
Centre span	21	Y	0.51306	1	1.039	1.066	1.017	1.302	1.248	1.718	1.326				
Centre span	24	Y	0.25395	1	0.989	1.026	1.014	1.333	1.287	1.824	1.355				
Tower top	28	X	0.10123	1	0.916	0.996	1.038	1.622	1.542	2.600	1.678				
End span	35	Y	0.00489	1	0.838	1.063	1.070	14.4 <sup>x</sup>	14.92 <sup>x</sup>	29.43 <sup>x</sup>	14.7 <sup>x</sup>				
End span	37	Y	0.00303	1	0.634	1.104	1.102	38.7 <sup>x</sup>	2.043 <sup>x</sup>	52.70 <sup>x</sup>	39.6 <sup>x</sup>				
End pier top	39	X	0.01217	1	0.477	0.953	1.351	1.059	1.816	6.05	1.454				

<sup>+</sup> See fig. 6.1

<sup>x</sup> Values at points close to the supports removed in 3 span system

L = Linear, NL = Nonlinear

TABLE 6.5 - CABLE FORCES IN STRUCTURES S1 TO S6 UNDER LOADING L1

LOCATION	Memb <sup>+</sup> No.	Actual linear value in S1 (t)	VALUES AS MULTIPLE OF CORRESPONDING LINEAR VALUES IN S1										
			S1		S2		S3		S4		S5		S6
			L	L	NL	L	L	L	L	NL	L		
Top cable, end span	42	-173.3	1	0.971	0.994	0.994	1.749	1.545	2.203	1.754			
	43	-181.4	1	0.984	1.000	0.998	1.267	1.286	1.514	1.270			
	44	-147.6	1	0.988	1.001	1.003	0.790	0.896	0.739	0.790			
Location of in- termediate supp- ort of 5-spar systems	45	-309.3	1	0.989	1.032	1.006	0.486	0.509	0.239	0.485			
	46	-113.7	1	1.010	1.041	1.004	0.611	0.536	0.284	0.610			
Cable near tower	47	- 37.3	1	1.086	1.080	1.000	0.885	0.710	0.482	0.879			
Cable near tower	48	-69.4	1	1.107	1.125	1.001	1.001	1.120	1.327	1.004			
	49	-133.8	1	1.012	1.024	1.000	0.999	1.029	1.156	0.999			
	50	-158.4	1	0.944	0.959	1.006	1.006	0.986	1.071	1.006			
	51	-216.0	1	0.949	0.969	1.001	1.014	0.983	1.039	1.015			
	52	-243.3	1	0.982	0.993	1.001	1.003	0.989	0.984	1.004			
Top cable centre span	53	-98.1	1	0.978	0.974	0.995	0.929	0.937	0.765	0.924			

<sup>+</sup>See fig. 6.1a

L = Linear, NL = Nonlinear, -ve = Tension

TABLE 6.6 - AXIAL FORCES IN GIRDER, TOWER, PIER AND WELL ELEMENTS OF S1 TO S6 UNDER LOADING L1

LOCATION	Memb. <sup>+</sup> No.	Actual <sup>x</sup> linear value in S1 (t)	VALUES AS MULTIPLE OF CORRESPONDING LINEAR VALUE IN S1										
			S1		S2		S3		S4		S5		S6
			L	L	NL	L	L	L	NL	L			
Pier, well at the end	1,2	-45.9	1	0.93	0.987	0.989	2.595	2.508	2.942	2.608			
Deck element at end pier	3	-95.3	1	-0.344	1.637	0.148	0.081	2.501	-3.449	0.905			
	4	63.0	1	2.995	4.99	2.286	3.062	0.500	9.112	4.559			
	5	184.0	1	1.676	2.373	1.442	1.568	0.429	3.610	2.080			
	6	410.3	1	1.299	1.635	1.201	0.971	0.481	1.753	1.201			
	7	476.4	1	1.041	1.283	1.174	0.921	0.408	1.286	1.119			
Deck element near tower	8	489.0	1	1.254	1.540	1.170	0.920	0.508	1.538	1.112			
-do-	9	435.3	1	1.753	1.771	1.140	1.018	0.631	1.739	1.167			
	10	407.0	1	1.796	1.814	1.149	1.019	0.602	1.771	1.178			
	11	317.8	1	2.012	2.032	1.191	1.025	0.487	1.948	1.228			
	12	190.8	1	2.709	2.730	1.318	1.038	0.163	2.538	1.376			
	13	2.3	1	145.4	145.5	27.26	3.04	-66.44	126.05	30.9			
Element at centre of main span	14	-219.8	1	-0.511	-0.502	0.726	0.981	1.692	-0.342	0.691			
Tower legs above deck	27,28	1081.6	1	0.970	0.991	1.001	0.919	0.907	0.911	0.919			
Link between tower and deck	29	148.1	1	1.162	1.133	0.999	1.039	1.105	1.213	1.039			
Tower leg below deck, pier, well	30-32	1229.7	1	0.995	1.009	1.001	0.933	0.930	0.947	0.934			

-163-

<sup>+</sup>See fig. 6.1      <sup>x</sup>-ve = tension,  
L = Linear, NL = Nonlinear

TABLE 6.7 - MOMENTS IN GIRDER, TOWER AND WELL ELEMENTS OF S1 TO S6 UNDER LOADING L1

LOCATION	Node <sup>+</sup> No.	Actual linear value in S1 (t-m)	VALUE AS MULTIPLE OF CORRESPONDING LINEAR VALUE IN S1										
			S1		S2		S3		S4		S5		S6
			L	L	NL	L	L	L	NL	L			
Base of end well	1	13687.3	1	0.474	0.001	0.675	1.119	1.899	0.058	0.75			
Node in deck near end well	4	135.4	1	1.115	1.539	0.985	5.14	3.023	11.02	5.19			
Node in deck	5	88.2	1	1.291	1.720	0.997	5.56	5.791	17.36	5.61			
-do-	6	214.2	1	1.171	1.559	1.026	2.66	4.426	5.198	2.68			
-do-	7	108.9	1	1.182	1.431	1.049	1.356	0.535	0.706	1.332			
Node in deck near Tower	8	64.0	1	1.303	1.082	0.916	4.15	3.654	4.561	4.09			
Base of tower	13	1545.0	1	0.276	0.081	1.206	0.885	0.138	0.188	1.171			
Base of well below tower	15	3582.6	1	0.151	0.013	1.293	0.560	0	0.009	0.669			
Node in deck near tower	16	146.5	1	1.497	1.510	0.986	0.969	1.301	1.491	0.954			
Node in deck	17	41.2	1	0.706	0.832	1.066	1.112	0.292	0.452	1.182			
-do-	18	58.6	1	1.858	1.975	1.053	1.154	1.141	1.464	1.208			
-do-	19	98.5	1	1.582	1.427	1.017	0.918	1.066	0.856	0.940			
-do-	20	248.7	1	1.183	1.301	1.020	1.325	1.352	2.138	1.347			
Centre of main span	21	752.2	1	1.137	1.111	1.019	1.217	1.176	1.446	1.240			

<sup>+</sup> See fig. 6.1

L = Linear, NL = Nonlinear

## 6.7 INTERPRETATION OF RESULTS

### 6.7.1 5-Span Systems (S1 to S3)

(a) Structure S1 : Distribution of deformations and forces in 5 span system (S1) under live loads (L1) in the linear case is shown in fig. 6.2. The following specific observations are made from the figure.

(i) Maximum vertical deflection occurs at the centre of main span and its ratio to the main span is  $1/891$ .

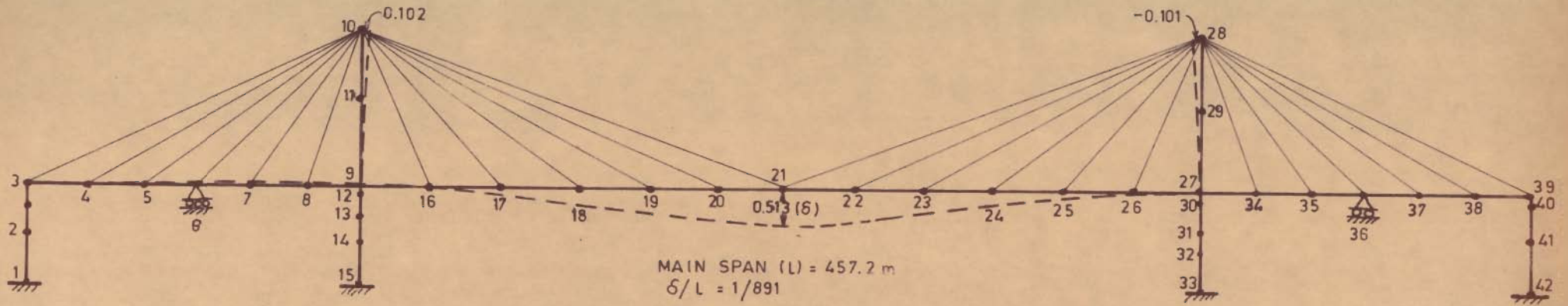
(ii) Maximum longitudinal deflection at the top of tower is about 20% of the maximum deck deflection.

(iii) Supports at the ends are subjected to small tensile forces.

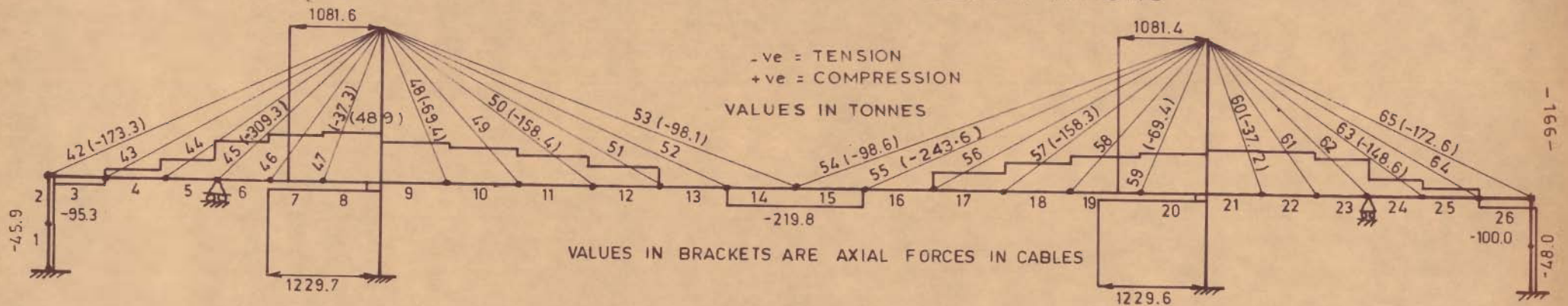
(iv) Maximum axial compression in a deck element occurs near tower and is about 40% of the maximum axial compression in a tower leg which occurs at its foot.

(v) Maximum sagging moment in the deck element occurs at the centre of main span which is about 80% of the maximum hogging moment occurring at the location of tower.

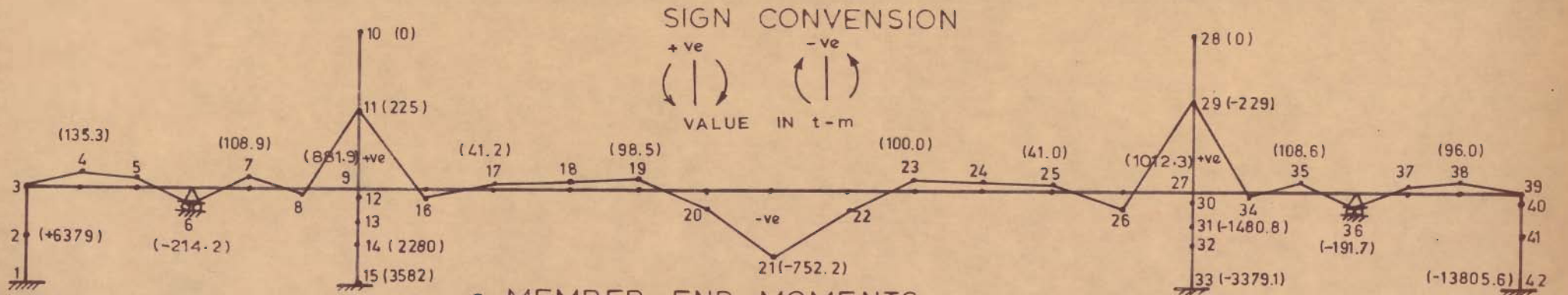
(b) Structure S2: This structure is different from S1 only to the extent of its nodal configuration which represents a prestressed configuration of S1 under the action of cable pretension and dead loads. The general pattern of deformations and forces in the elements of S2 is similar to those of S1. The following is the deviation



a - LONGITUDINAL AND VERTICAL DEFORMATIONS



b - AXIAL FORCES



c - MEMBER END MOMENTS

FIG. 6.2 - DISTRIBUTION OF DEFORMATIONS AND FORCES LINEAR IN 5-SPAN SYSTEM (S1) UNDER LIVE LOADS (L1)



of the results of linear analysis of S2 from that of S1.

Maximum vertical deflection of the deck is about 4% more while the longitudinal displacement at the top of the tower is about 10% less. The change in cable forces is, in general, less than 5%. Maximum axial compression in the deck occurs near the tower in the main span. This is about 75% higher than its corresponding value in S1. The axial forces in tower, pier and well elements change by less than 10%. The moment at the centre of the span increases by about 14%. The moment at the base of the end well has reduced to about 47% while that at the base of well below tower is reduced to about 15%.

The extent of axial-flexural interaction for S2 takes into account the presence of axial forces in the elements due to its prestressed state. The maximum vertical deflection at the centre of deck is increased by about 3% and the maximum longitudinal displacement at the top of the tower is increased by about 9%. Cable forces change by less than 5%. Axial compression in the deck element near tower (end span) increases by about 23%. The moment at the centre of main span is reduced by about 3%. The moments at the base of the substructure are reduced by negligible value.

(c) Structure S3: This structure is different from S1 only to the extent that its substructure is supported on elastic springs. The stiffnesses of these elastic springs (table 6.1) represent the stiffnesses of soil at the base

and the side of the substructure (calculations in appendix A1) activated due to soil-structure interaction. The general pattern of deformations and forces in the elements of S3 is similar to those of S1 with the following deviations in the values of linear analysis.

Increase in the value of maximum deformations is less than 5%. Cable forces are changed by less than 1%. Maximum axial force in the deck increases by about 17% while the axial force in tower, pier and well elements changes by less than 2%. The change in the deck moments is within 5%. The moment at the base of the end well is reduced to 67.5 % and the moment at the base of the well below tower is increased by about 30%.

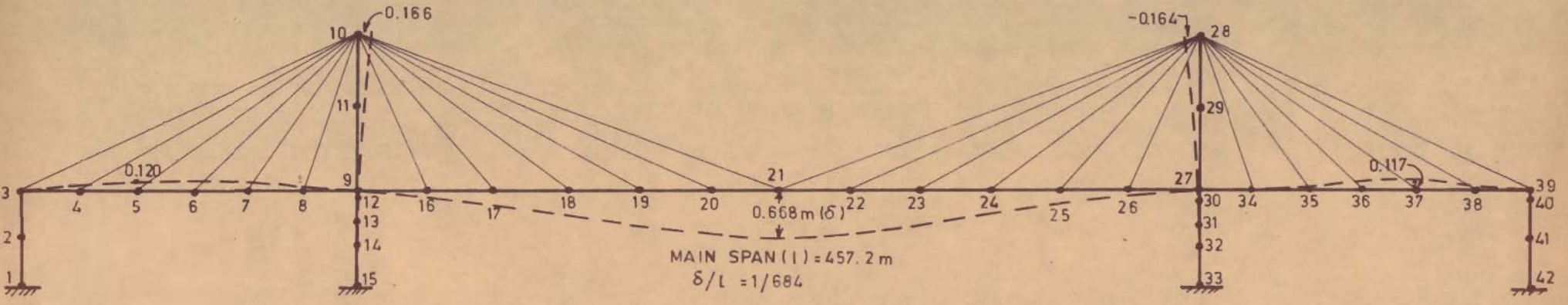
#### 6.7.2. 3-Span Systems (S4 to S6)

(a) Structure S4: Distribution of deformations and forces in 3-span system (S4) under live loads (L1) in the linear case is shown in fig. 6.3. The following specific observations are made from the figure.

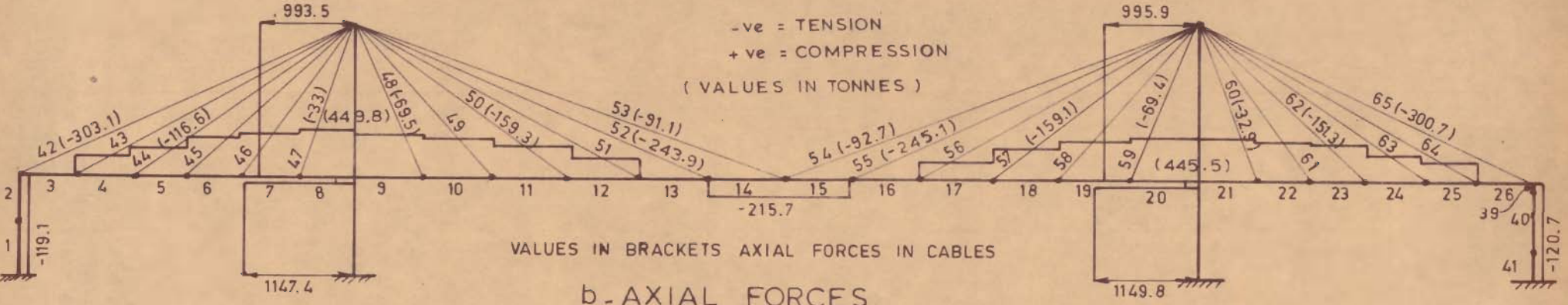
(i) Ratio of maximum vertical deflection at the centre of main span to the span length is  $1/684$ .

(ii) Maximum longitudinal deflection at the top of the tower is about 25% of the maximum deck deflection.

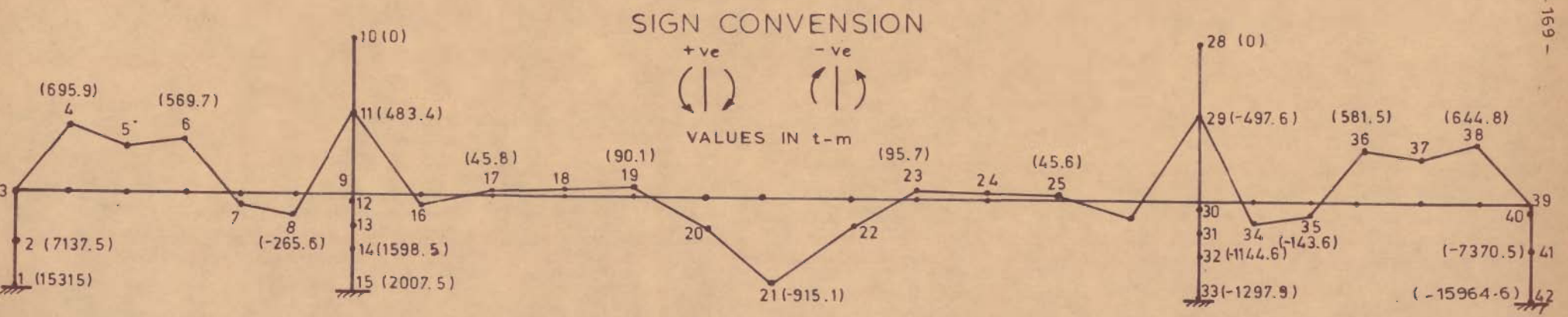
(iii) Maximum axial compression in a deck element occurs near tower and is about 40% of the maximum axial compression in a tower leg which occurs at its foot.



a-LONGITUDINAL AND VERTICAL DEFORMATIONS



b-AXIAL FORCES



c-MEMBER-END-MOMENTS

FIG. 6.3 DISTRIBUTION OF DEFORMATIONS AND FORCES LINEAR IN 3-SPAN SYSTEM (S3) UNDER LIVE LOAD (L1)

(iv) Maximum sagging moment in the deck element occurs at the centre of main span which is about 4% more than the maximum hogging moment at the location of tower.

(b) Structure S5: This 3-span system has similar features as described for S2. The general pattern of deformations and forces in the elements of S5 is similar to those of S4. The following are the deviations in the linear results of S4 and S5.

Maximum values of vertical deck deflection and longitudinal tower deflection are reduced by about 5%. Maximum axial force in the deck element is reduced by about 45% while the cable forces change by less than 10% in general. Moment at the centre of main span is reduced by 4%. The moment at the base of end well is increased by about 70% while that at the base of well below tower is reduced to zero.

The effect of axial flexural interaction on S5 with respect to its linear analysis is to increase the deflection of deck by 38%. Increase in the deflection of tower is 7%. Maximum cable force in the top cable of end span increases by about 43%. Axial force in the deck element near tower increases by about 200% while the moment at the centre of main span increases by about 23%. Moments at the base of the substructure are reduced to almost a negligible value while the axial forces in these elements are not much changed. Non linear effects on S5 are, in general, very high.

(c) Structure S6: Substructure of this 3-span system is supported on elastic springs which are similar to those described for S3. The deviations in the linear results of S6 compared to those of S4 are as follows.

The maximum vertical deflection of the deck increases by about 2% and the tower deflection increases by about 4%. The cable forces vary within 1%. Axial force in the deck near tower is increased by 22% while the moment at the centre of main span is increased by about 2%. The axial forces in tower, pier and well elements are not altered. The moment at the base of the end well is reduced to about 67% while the moment at the base of well below tower is increased by about 20%.

## 6.8 DISCUSSION OF RESULTS

The 5-span and 3-span systems chosen for the present investigation represent a bridge structure with main span of 457.2 m. Linear and nonlinear behaviour of both 5-span and 3-span systems are compared. A constant prestress in the cables of the two systems has been assumed.

### 6.8.1 Conditions of Symmetry.

Structures S1 to S7, analysed in the present investigation, represent the full structure on the longitudinal axis of the bridge. The deck is hinged to the substructure element at one end and connected to the substructure

with a link, which is free to rotate as well as provide rolling at the other end. The structures are, thus, not symmetric about the centre of the main span.

It is observed from the magnitudes of displacements and forces tabulated in table 6.4 and shown in figures 6.2 and 6.3 that the values at two nodes or members lying symmetrically with respect to the transverse axis of the bridge differ by less than 10%. As the difference is not large, tables 6.5 to 6.7 present values for only half the structure. This observation may be considered to hold true on results of space frame analysis also. Taking advantage of this observation, space frame investigations presented and discussed in the subsequent chapter have been carried out on half the structure only.

#### 6.8.2 Comparison of Results of S1 and S4.

(i) Maximum value of nonlinear vertical deflection of the deck in S4 is about 31% higher and the maximum deflection of the tower is about 64% higher than the corresponding value in S1. Thus the 3-span systems are quite flexible as compared with the 5 span system.

(ii) In S1, the cables connected to externally restrained intermediate nodes of the end spans draw the heaviest forces while in S4, the top cables of the end spans draw the heaviest forces. The pattern of distribution of cable forces in the main spans of both S1 and S4 is almost the same and the magnitudes of forces are not much

different.

(iii) Axial forces and moments in other elements of both S1 and S4 have comparable magnitudes.

### 6.8.3 Comparison of Results of S2 and S5

Nodal configurations of S2 and S5 obtained by analysing S2-a and S5-a respectively under cable prestress and dead weights are shown in fig. 6.4. It can be observed from the figure that S2 is a more stable configuration for resisting live loads as compared to S5. The effects of axial flexural interaction are high on S5 whereas the prestressed configuration of S2 helps in reducing the nonlinear effects.

With suitable modifications in cable pretensions and cable areas, the deck of 3-span system (S5) can also be stressed to a cambered profile which should be more stable and less prone to the nonlinear axial-flexural interaction effects. Structure S4, thus, may not be considered as a practical structure and therefore, high nonlinear effects observed in S4 do not carry significant implications. However, the general observations made from the study of S2 and S5 under similar forces are indicative of the general behaviour of the two systems. Importance of achieving appropriate pretensioning forces in the cables to avoid undesirable nonlinear effects is also reflected from this study.

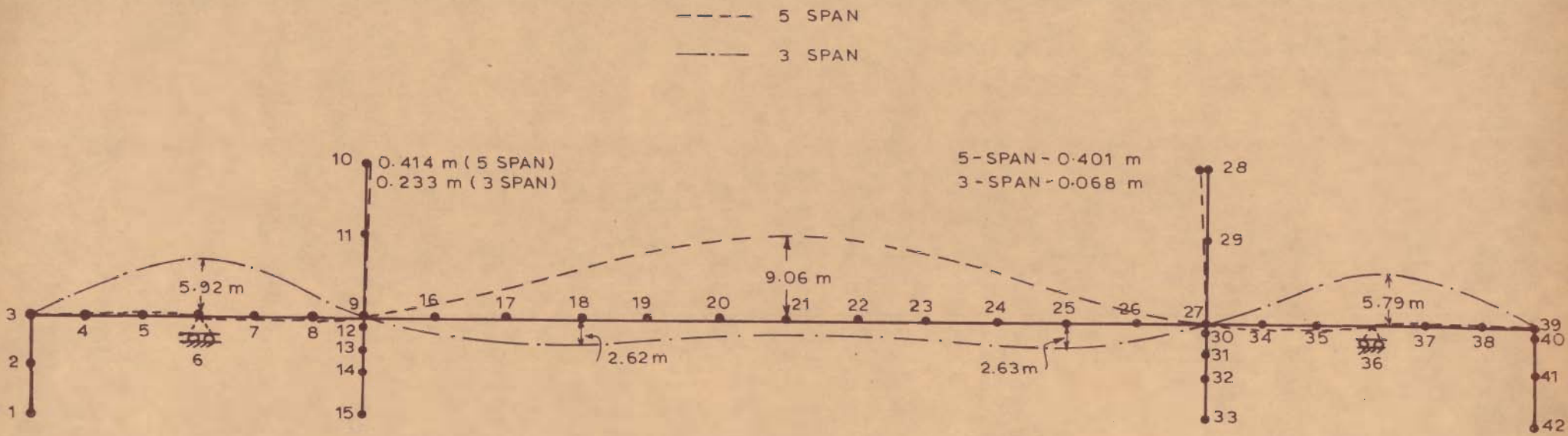


FIG. 6.4 \_ NODAL CONFIGURATIONS OF S2 AND S4 UNDER CABLE PRETENSION AND DEAD WEIGHT



#### 6.8.4 Comparison of Overall Stiffnesses

The ratios of maximum deck deflections to the main span ( $\delta/l$ ) as found from linear and nonlinear analyses of S1 to S6 under live loads L1 are given in table 6.8.

TABLE 6.8 RATIOS OF MAXIMUM DECK DEFLECTIONS TO MAIN SPAN FOR S1 TO S6 UNDER L1

Structure	$\delta/l$	
	Linear	Nonlinear
S1 (5-span, straight deck, fixed base)	1/891	
S2 (5-span, stressed deck, fixed base)	1/857	1/836
S3 (5-span, straight deck, elastic base)	1/876	
S4 (3-span, straight deck, fixed base)	1/684	
S5 (3-span, stressed deck, fixed base)	1/714	1/519
S6 (3-span, straight deck, elastic base)	1/671	

From the values of  $\delta/l$ , it can be observed that the effects of nonlinearity are high in 3-span system. From the linear results it is observed that the overall stiffness of the 5-span system is more when the effect of prestress is not considered while for 3-span system, it is more when the effect of prestress in consideration. On comparison of results of S1 with S3 and S4 with S6

it is observed that the overall stiffness gets reduced by about 2%.

#### 6.9 EXPERIMENTAL VERIFICATION OF RESULTS

A comparison of linear and nonlinear analytical and experimental results of model bridge (S7) is given in table 6.9. It is observed that the experimental values are in between the values of linear and nonlinear analysis. The values are close to the nonlinear analytical values for comparatively heavy loading L2 while they are close to the linear analytical values for lighter loadings L3 and L4.

Similar trend in the deformation pattern of the laboratory bridge model was observed under different types of loadings described in chapter 5. However, all the experimental results could not analytically be verified because of the limitation of computational time hence not reported.

#### 6.10 SUMMARY

Linear as well as 'nonlinear axial-flexural interaction' behaviour of various 5-span and 3-span variations of a cable-stayed bridge under live loads has been studied in this chapter. The observations and discussions of results can be summarised as follows:

(i) Pattern of distribution of forces in cables of the end spans changes with the introduction of external

TABLE 6.9 COMPARISON OF ANALYTICAL AND EXPERIMENTAL RESULTS

Loading on Model Bridge (S7)			Deformations (mm)		% variation from analytical value
			Analytical	Experimental	
Loads on full deck (L2)	Linear	A	1.909	2.37	24.14
		B	0.3097	0.503	52.4
	Non linear	A	2.97		20.2
		B	0.5123		1.8
Loads in one end span and centre span (L3)	Linear	A	2.3422	2.7825	18.8
		B	0.6352	0.5975	5.9
	Non linear	A	3.1247		10.9
		B	0.8784		32.0
Loads in centre span (L4)	Linear	A	2.7983	3.13	11.8
		B	0.6187	0.655	5.9
	Non linear	A	3.3337		6.1
		B	0.8755		25.2

A = Maximum vertical deflection of deck.

B = Maximum horizontal deflection of tower in longitudinal direction.

restraints at intermediate nodes of the end span but this does not significantly change the distribution of cable forces in main span.

(ii) Maximum axial compression in the deck elements occurs near tower, which is about 40% of the maximum axial compression in tower leg and the substructure below it, in both 5-span and 3-span systems. Nonlinear axial-flexural interaction increases the axial forces in deck elements by

20% to 60% or more while keeping the maximum axial compression in tower leg and the sub-structure below it more or less constant.

(iii) Some elements of deck near end supports and at the centre of main span, which are found to be in tension from the linear analysis, come in compression when axial-flexural interaction is considered.

(iv) Incidentally, moments at the base of the sub-structure elements, which are found to be quite high in the linear analysis are reduced to almost negligible magnitudes when axial-flexural interaction is considered.

(v) From the pattern of overall deformations of the structure, it may be concluded that the 3-span system, in general, is more flexible than the 5-span system. The effect of axial-flexural interaction on overall stiffness of 5-span system can be assumed to be less than 10%. The effect of soil structure interaction on the overall stiffness is found to be about 2% in both 5-span and 3-span systems for a case of loose sand. For stiffer sands the effects can be expected to be even lesser.

(vi) Appreciable change in the magnitude of forces and deformations is seen to occur between the geometrical configurations of a bridge with straight and cambered decks.

(vii) Cambered configuration obtained by cable pre-tensions together with dead loads has shown a reduction in the nonlinear effects by about 2%.

(viii) The comparison of analytical and experimental values of the laboratory bridge model is reasonably good.

(ix) The bridge structure can be considered symmetrical about the axis through centre of the main span by assuming a variation within 10% due to different support conditions at two ends of the bridge deck.

## C H A P T E R 7

### STATIC SPACE FRAME INVESTIGATIONS

#### 7.1 INTRODUCTION

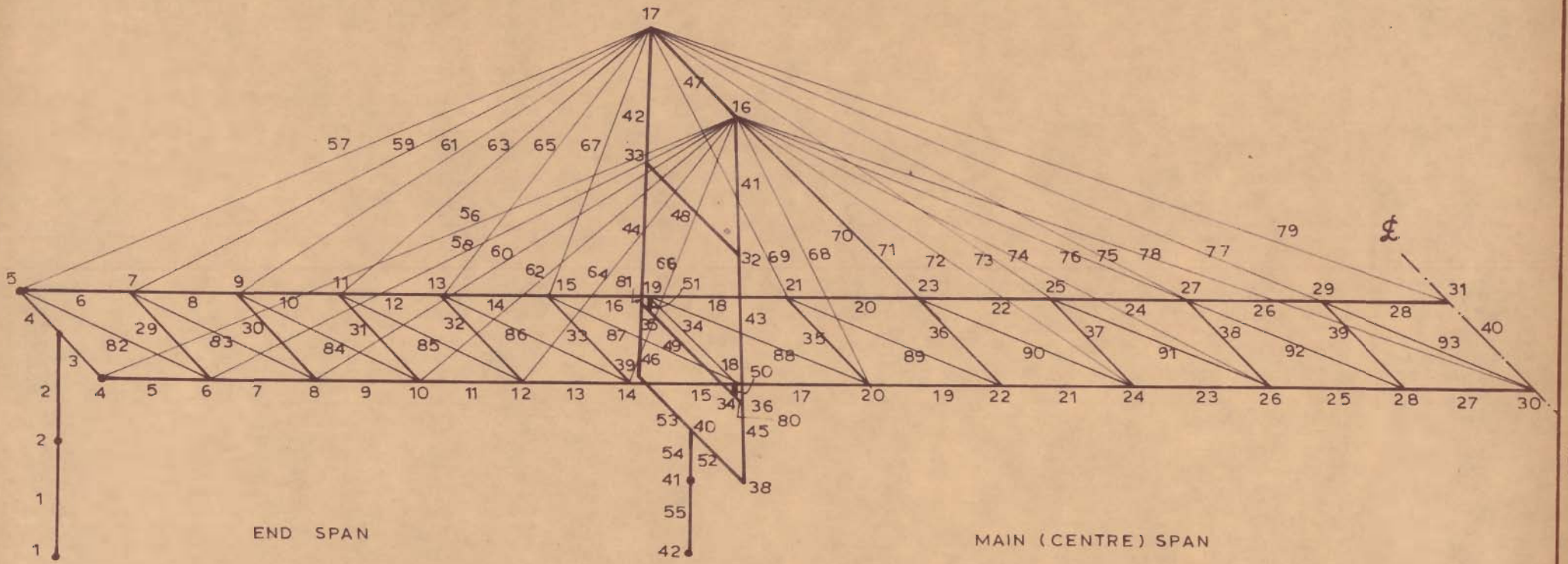
In this chapter, idealized mathematical model of the cable-stayed bridge as a space frame has been described and the conditions of external restraints as well as geometrical properties of the various elements of the frame have been tabulated. Salient results obtained from analytical and experimental studies have been presented, interpreted and discussed.

#### 7.2 DETAILS OF STRUCTURES S8 TO S12

The idealized mathematical model of the bridge as shown in fig. 7.1 has been used for eccentric vertical and lateral load analysis. The structures considered are described below and their external restraint conditions are given in table 7.1

(a) Structure S8 : A five span radiating system with substructure fixed at the base. The structure has a main span of 457.2m, four side spans of 91.44m each, total tower height of 103.59 m projecting by 77.9m above the deck. The camber in the deck is  $1/25$  in end spans and  $1/50$  in the centre span.

(b) Structure S9: A structure similar to S8, but the substructure is supported on elastic springs.



EXTERNAL RESTRAINT DETAILS FOR S 8 TO S 12 ARE GIVEN IN TABLE 7.1

FIG. 7.1 MATHEMATICAL MODEL OF STRUCTURES S 8 TO S 12

TABLE 7.1- DETAILS OF EXTERNAL RESTRAINTS FOR S8 TO S12

STRUCTURE DESIGNATION AND DESCRIPTION	REST- RAINED <sup>+</sup> NODE No.	STIFFNESS DUE TO EXTERNAL RESTRAINT					
		TRANSLATIONAL, ALONG AXIS OF			ROTATIONAL, ABOUT AXIS OF		
		X	Y	Z	X	Y	Z
S8	1	RIGID			SUPPORT		
5-SPAN SYSTEM WITH SUBSTRUC- TURE FIXED AT THE BASE	10	ZERO	RIGID	RIGID	RIGID	ZERO	ZERO
	11						
	30	RIGID	ZERO	ZERO	ZERO	RIGID	RIGID
	31						
	42	RIGID			SUPPORT		
S9	1	$10^{11}$	$10^{11}$	$10^{11}$	$1.20 \times 10^8$	$10^{11}$	$6.08 \times 10^7$
5-SPAN SYSTEM WITH SUBSTRUC- TURE SUPPORTED ON ELASTIC SPR- INGS AT THE BA- SE t-m UNITS	10	0	$10^{11}$	$10^{11}$	$10^{11}$	0	0
	11						
	30	$10^{11}$	0	0	0	$10^{11}$	$10^{11}$
	31						
	42	$10^{11}$	$10^{11}$	$10^{11}$	$7.27 \times 10^8$	$10^{11}$	$1.94 \times 10^8$
S10	1	RIGID			SUPPORT		
3-SPAN SYSTEM WITH SUBSTRUC- TURE FIXED AT THE BASE	30	RIGID	ZERO	ZERO	ZERO	RIGID	RIGID
	31						
	42	RIGID			SUPPORT		
S11	1	$10^{11}$	$10^{11}$	$10^{11}$	$1.20 \times 10^8$	$10^{11}$	$6.08 \times 10^8$
3-SPAN SYSTEM WITH SUBSTRUC- TURE SUPPORTED ON ELASTIC SPR- INGS AT THE BASE t-m UNITS	30	$10^{11}$	0	0	0	$10^{11}$	$10^{11}$
	31						
	42	$10^{11}$	$10^{11}$	$10^{11}$	$7.27 \times 10^8$	$10^{11}$	$1.94 \times 10^5$
S12	1	$10^{11}$	$10^{11}$	$10^{11}$	$3.22 \times 10^6$	$10^{11}$	$9.10 \times 10^8$
3-SPAN SYSTEM (MODEL) WITH SUBSTRUCTURE SUPPORTED ON ELASTIC SPRINGS AT THE BASE Kg-mm UNITS	30	$10^{11}$	0	0	0	$10^{11}$	$10^{11}$
	31						
	42	$10^{11}$	$10^{11}$	$10^{11}$	$3.01 \times 10^7$	$10^{11}$	$3.29 \times 10^6$

+See fig. 7.1



(c) Structure S10 : A three span radiating system with substructure fixed at the base. The structure has two side spans of 182.88 m each. Other features are same as described in (a).

(d) Structure S11 : Similar to S10 but the substructure is supported on elastic springs at the base.

(e) Structure S12: This structure represents the laboratory model of aluminium alloy with main dimensions proportioned to a scale ratio of 1:200 from S10. The bridge substructure is assumed to be supported on elastic springs at the base. The value of the spring constants is evaluated experimentally.

Stiffness offered by external restraints for structures S8 to S12 are presented in table 7.1. The numerical value  $10^{11}$  is arbitrarily chosen to be relatively large as compared with component stiffnesses so as to represent 'fixed' condition. Geometrical properties of elements of S8 to S11 are given in table 7.2. The geometrical properties of S12 have been picked up from the data given in chapter 5. In continuation to assumptions outlined in section 3.2.1, the salient features of the idealized mathematical models, S8 to S12, are as follows:

(i) Only half the structure has been considered for analysis by separating it from the other half at its transverse axis of symmetry. Appropriate external restraints

TABLE 7.2 - GEOMETRICAL PROPERTIES OF ELEMENTS OF STRUCTURES S8 TO S11

Member <sup>+</sup> No.	Area m <sup>2</sup>	Inertia-X m <sup>4</sup>	Inertia-Y m <sup>4</sup>	Inertia-Z m <sup>4</sup>
1	2	3	4	5
1	12.09	588.90	603.82	311.95
2	3.06	0.984	181.18	6.06
3,4	152.95	49.22	9059.1	302.89
5,6	0.363	0.365	0.324	0.543
7,8	0.376	0.387	0.336	0.550
9,10	0.340	0.332	0.307	0.489
11,12	0.392	0.402	0.343	0.576
13,14	0.356	0.372	0.330	0.499
15,16	0.379	0.389	0.338	0.553
17,18	0.359	0.362	0.324	0.520
19,20	0.305	0.295	0.289	0.426
21,22	0.290	0.273	0.278	0.405
23, 24	0.265	0.237	0.258	0.370
25-28	0.264	0.235	0.257	0.369
29-33	0.292	0.703 x 10 <sup>-4</sup>	0.009	0.252
34-40	0.365	0.879 x 10 <sup>-4</sup>	0.011	0.315
41,42	0.475	1.189	1.181	0.818
43,44	0.569	1.655	1.432	1.195
45,46	0.689	2.173	1.774	1.605
47,48	0.199	0.301	0.154	0.584
49	0.236	0.435	0.189	1.176
50,51	0.219	0.024	0.254	0.010
52, 53	686.65	1.52 x 10 <sup>4</sup>	1.46x10 <sup>5</sup>	5.27x10 <sup>3</sup>
54	13.73	304.4	2915.9	105.3
55	32.31	3721.3	4284.8	1564.0
56,57	0.022	0	0	0
58,59	0.021	0	0	0
60,61	0.016	0	0	0
62, 63	0.031	0	0	0
64,65	0.014	0	0	0
66,67	0.011	0	0	0
68,69	0.012	0	0	0
70,71	0.014	0	0	0
72,73	0.017	0	0	0
74,75	0.023	0	0	0
76,77	0.027	0	0	0
78,79	0.014	0	0	0
80,81	0.236	0.435	0.189	1.176
82-87	0.354	0	0	0
88-93	0.327	0	0	0

+ See fig. 7.1

Note: Equivalent values in terms of superstructure steel are tabulated.

(table 7.1) have been imposed at the nodes incident at the axis of symmetry.

(iii) Rotations of members 5,6, 50 and 51 (fig.7.1) can freely occur at nodes 4,5, 34 and 35 respectively, independent of the rotations of other members meeting at these nodes.

(iii) Any of the fictitious members 3,4, 52 and 53 (fig 7.1), used to provide the means of transfer of forces between the super-structure and the substructure, has been assumed to be relatively rigid. This has been achieved by taking their stiffness fifty times greater than that of the stiffest member connected to them.

(iv) The stiffnesses of the fictitious truss members 82 to 93 (fig. 7.1), which represent the stiffness of the continuous deck plate between the two main girders, has been derived in accordance with the criterion described in appendix 'B'.

(v) The soil at the base and sides of the substructure elements 1 and 55 (fig. 7.1) of S9 and S11 is assumed to provide rotational stiffness at nodes 1 and 42. These nodes are assumed to be restrained against translations and twisting. The calculations for rotational stiffnesses are given in Appendix 'A'.

### 7.3 LOADINGS L5 to L10

The following loadings have been considered for computing the resulting deformations and forces in the structures:

(a) Loading L5: Eccentric vertical loads (table 7.3) applied at the deck nodes of S8 to S11. The loads are equivalent to an eccentric uniform load of 2.5 t/m intensity applied on the axis of one of the longitudinal girders.

(b) Loading L6: Lateral forces (table 7.4) representing a uniform wind pressure of  $320 \text{ kg/m}^2$  at the level of deck of S8 to S11. The wind pressures were varied with the height of tower. The calculations were based on Indian Road Congress specifications (108).

(c) Loading L7: Vertical weights placed on S12 consisting of 5 Kg each at nodes 4,6,8,10,12, 14, 20, 22, 24, 26 and 28 and 2.5 Kg at node 30 (see fig. 7.1).

(d) Loading L8: Vertical weights placed on S12 consisting of 5 Kg each at nodes 20,22,24, 26 and 28 and 2.5 Kg at node 30 (see fig. 7.1).

(e) Loading L9: Lateral forces of 5 Kg each applied to S12 at nodes 10 and 24 and 2.5 Kg at node 30 (fig. 7.1).

(f) Loading L10: Lateral forces of 5Kg and 2.5 Kg at nodes 24 and 30 respectively (fig. 7.1) applied on S12.

TABLE 7.3 - LOADING L5 ON S8 TO S11 (ECCENTRIC VERTICAL LOADING)

Node <sup>+</sup> no.	Vertical Force (t)	Node <sup>+</sup> no.	Vertical Force (t)	Node <sup>+</sup> No.	Vertical Force (t)
4	-38.10	14	-76.20	26	-95.25
6	-76.20	18	-85.73	28	-95.25
8	-76.20	20	-95.25	30	-47.62
10	-76.20	22	-95.25	-	-
12	-76.20	24	-95.25	-	-

<sup>+</sup>See fig. 7.1

TABLE 7.4- LOADING L6 ON S8 TO S11 (LATERAL LOADING DUE TO UNIFORM WIND PRESSURE, VARYING WITH HEIGHT)

Node <sup>+</sup> no.	Lateral Force (t)	Node <sup>+</sup> no.	Lateral Force (t)	Node <sup>+</sup> no.	Lateral Force (t)
2	15.95	17	34.22	32	60.77
4	45.09	18	65.56	33	60.77
6	58.28	20	72.85	36	31.14
8	58.28	22	72.85	37	31.14
10	58.28	24	72.85	38	20.87
12	58.28	26	72.85	39	20.87
14	58.28	28	72.85	41	17.58
16	34.22	30	36.42	-	-

<sup>+</sup>See fig. 7.1

## 7.4 ECCENTRIC VERTICAL LOAD ANALYSIS

### 7.4.1 Tabulation of Results

The results of analysis of S8 to S11 under loading L5 are presented in tables 7.5 to 7.11. Actual values of deformations at salient locations and axial forces and bending moments in important elements of S8 have been tabulated and comparative values for S9 to S11 as ratio to corresponding values of S8 have been presented.

TABLE 7.5- DEFORMATIONS AT SALIENT LOCATIONS OF S8 TO S11 UNDER ECCENTRIC VERTICAL LOADS (L5)

LOCATION	Node <sup>x</sup> No.	Actual <sup>x</sup> values in S8 (m)	Values expressed as ratios to corresponding values in S8			
			S8	S9	S10	S11
Vertical deflec- tions in end span of deck	8	.00089	1	0.75	106.7 <sup>+</sup>	107.0 <sup>+</sup>
	9	.00319	1	1.00	15.38 <sup>+</sup>	15.56 <sup>+</sup>
	12	.00548	1	1.01	11.47 <sup>+</sup>	11.52 <sup>+</sup>
	13	.00301	1	1.05	8.95 <sup>+</sup>	9.14
Horizontal deflec- tion at tower top	16	.09287	1	1.01	1.52	1.53
	17	.01311	1	1.06	2.72	2.80
Vertical deflec- tions in centre span of deck	24	-.27189	1	1.01	1.27	1.28
	25	-.01998	1	1.02	2.72	2.78
	30	-.55315	1	1.01	1.23	1.24
	31	-.06098	1	1.01	2.05	2.08

<sup>x</sup>See fig. 7.1

<sup>+</sup>Values at points close to the supports removed in 3-span system

TABLE 7.6 - CABLE FORCES IN S8 TO S11 UNDER ECCENTRIC VERTICAL LOADS (L5)

LOCATION	Memb. <sup>x</sup> No.	Actual <sup>+</sup> values in S8 (t)	Values as multiple of corresponding value in S8			
			S8	S9	S10	S11
Top cables, end span	56	-164.8	1	0.997	1.578	1.578
	57	-13.9	1	0.964	4.576	4.576
	58	-178.6	1	0.998	1.211	1.211
	59	- 10.6	1	0.981	2.745	2.755
	60	-149.5	1	0.999	0.841	0.841
Middle cables, end span	61	- 10.1	1	1.010	-0.015	-0.012
	62	-311.0	1	0.999	0.571	0.571
	63	- 32.8	1	1.009	-0.485	-0.485
	64	-117.9	1	0.999	0.657	0.656
	65	- 8.5	1	1.012	-0.529	-0.529
Cables near tower	66	- 44.1	1	1	0.880	0.875
	67	+ 0.3	1	1	3.333	3.667
	68	- 69.3	1	1	1	1.001
	69	- 0.4	1	1.25	-1	-1.50
	70	-138.0	1	0.999	0.997	0.997
Middle cables, centre span	71	- 0.2	1	- (1.5)	- (2.5)	- (2.5)
	72	-166.0	1	1	1.002	1.002
	73	- 1.4	1	1.071	1.786	1.786
	74	-225.0	1	1	1.005	1.005
	75	- 8.1	1	1	1.284	1.284
Top cables centre span	76	-245.9	1	0.998	0.989	0.988
	77	- 17.5	1	0.960	1.091	1.069
	78	- 96.3	1	0.993	0.923	0.918
	79	- 7.4	1	0.919	0.703	0.635

<sup>x</sup>See fig. 7.1

<sup>+</sup> -ve = Tension

TABLE 7.7 - AXIAL FORCES IN GIRDER, TOWER, PIER AND WELL ELEMENTS OF S8 TO S11 UNDER ECCENTRIC VERTICAL LOADS (L5)

LOCATION	Memb. <sup>x</sup> no.	Actual <sup>+</sup> values in S8 (t)	Values as multiple of corresponding value in S8			
			S8	S9	S10	S11
Well, Pier	1,2	- 41.7	1	0.935	2.844	2.794
End, members, end span	5	76.0	1	1.364	2.182	2.553
	6	32.5	1	1.446	0.298	1.911
	7	145.1	1	1.268	2.278	2.475
	8	132.1	1	1.020	0.465	0.686
	9	179.8	1	1.281	2.284	2.443
Central members, end span	10	229.9	1	0.965	0.395	0.522
	11	322.3	1	1.190	1.598	1.688
	12	215.0	1	1.022	0.500	0.636
	13	433.3	1	1.112	1.229	1.295
	14	179.3	1	1.100	0.751	0.913
E Members near tower	15	488.7	1	1.073	1.054	1.113
	16	135.8	1	1.235	1.166	1.379
	17	614.3	1	1.028	1.041	1.060
	18	99.7	1	1.213	1.315	1.436
	19	568.4	1	1.029	1.043	1.063
C	20	100.1	1	1.210	1.315	1.435
	21	488.6	1	1.035	1.052	1.076
	22	99.6	1	1.211	1.314	1.435
	23	350.4	1	1.049	1.072	1.105
K	24	98.0	1	1.212	1.310	1.432
	25	149.1	1	1.114	1.161	1.239
	26	90.2	1	1.232	1.315	1.448
Member at centre of main span	27	-79.4	1	0.780	0.669	0.519
	28	74.4	1	1.286	1.356	1.523
Tower legs	41	1016.2	1	0.999	0.920	0.920
	42	94.2	1	0.999	0.791	0.791
	43	977.8	1	0.998	0.917	0.917
	44	132.7	1	1.002	0.847	0.847
	45	1069.7	1	0.983	0.929	0.918
	46	171.6	1	1.089	0.906	0.964
	47	22.5	1	1.000	0.907	0.907
Portals	48	0.6	1	1.167	1.333	1.333
	49	6.5	1	0.661	0.862	0.831
Well, Pier below tower	54,55	1240.2	1	0.998	0.926	0.924

<sup>x</sup>See fig. 7.1

<sup>+</sup> -ve = Tension



TABLE 7.8 - TWISTING MOMENTS IN GIRDER, TOWER, PIER AND WELL ELEMENTS OF S8 TO S11 UNDER ECCENTRIC VERTICAL LOADS (L5)

LOCATION	Memb <sup>+</sup> No.	Actual values in S8 (t-m)	Values as multiple of corresponding value in S8			
			S8	S9	S10	S11
Well, Pier, end span	1,2	22.5	1	1.324	2.693	2.676
	5,6	5.9	1	0.847	15.831	15.797
D End span	7,8	0.4	1	2.000	188.250	187.750
	9,10	6.9	1	1.130	3.725	3.725
	11,12	9.3	1	0.968	7,290	7.300
	13,14	3.2	1	0.781	22.375	22.375
E Members near tower	15,16	11.8	1	0.831	5.559	5.381
	17,18	216.8	1	1.015	1.165	1.173
C Centre span	19,20	205.5	1	0.989	1.133	1.134
	21,22	198.8	1	1.004	1.142	1.143
	23,24	186.3	1	1.003	1.128	1.128
	25,26	175.4	1	1.003	1.106	1.107
K	27,28	88.2	1	1.003	1.090	1.090
Tower legs	41,42	342.9	1	1.006	1.343	1.338
	43,44	289.4	1	0.995	1.326	1.308
	45,46	238.4	1	0.953	1.477	1.377
Portals	47	129.9	1	1.011	1.346	1.348
	48	97.7	1	1.010	1.341	1.342
	49	25.2	1	0.972	1.079	1.087
Well, pier below tower	54,55	908.0	1	1.095	1.723	2.014

<sup>+</sup>See fig. 7.1

TABLE 7.9 - BENDING MOMENTS (M-Z) IN GIRDER, TOWER, PIER AND WELL ELEMENTS ABOUT AXES PARALLEL TO TRANSVERSE AXIS OF S8 TO S11 UNDER ECCENTRIC VERTICAL LOADS (L5)

LOCATION	Memb. + No.	Actual values in S8 (t-m)	Values as multiple of corresponding values in S8			
			S8	S9	S10	S11
1	2	3	4	5	6	7
Pier, well, end span	1	7569.8	1	0.602	1.003	0.586
	2	3527.9	1	0.602	1.003	0.586
D Central members	5	69.5	1	0.964	6.449	6.469
	6	90.6	1	0.979	3.864	3.881
	7	69.5	1	0.964	6.449	6.469
	8	90.6	1	0.979	3.864	3.881
	9	146.1	1	0.980	3.910	3.918
E end span	10	139.5	1	1.017	1.888	1.900
	11	146.1	1	0.980	3.910	3.918
	12	139.5	1	1.017	0.496	0.507
	13	120.6	1	1.013	1.837	1.816
	14	63.8	1	1.005	0.387	0.375
C Member near tower	15	893.0	1	1.000	0.960	0.964
	16	53.2	1	1.000	0.500	0.618
	17	928.4	1	0.997	0.993	0.988
	18	4.8	1	1.333	3.417	3.208
	19	99.7	1	0.980	0.935	0.921
K Members at centre of main span	20	8.7	1	1.138	1.460	1.552
	21	72.4	1	1.012	1.058	1.069
	22	27.2	1	1.015	1.210	1.224
	23	68.6	1	1.004	1.080	1.085
	24	48.8	1	0.963	0.961	0.936
	25	269.6	1	1.013	1.253	1.263
	26	48.7	1	0.963	1.587	1.643
	27	784.6	1	0.996	1.145	1.144
28	143.0	1	0.964	1.445	1.436	
Tower legs	41	482.7	1	1.001	0.943	0.944
	42	476.4	1	1.001	0.943	0.943
	43	337.8	1	0.972	0.956	0.957
	44	359.7	1	0.976	0.924	0.930
	45	126.3	1	0.956	6.349	5.479
	46	135.7	1	0.892	5.874	5.064

Table Contd---

+ See fig. 7.1

	1	2	3	4	5	6	7
Portals <sup>++</sup>		47	482.7	1	1.001	0.943	0.944
		48	593.6	1	1.010	0.981	0.982
		49	481.5	1	1.345	1.015	1.250
Pier, well below tower		54	327.5	1	1.335	5.645	5.029
		55	1159.0	1	0.571	3.649	4.441

<sup>++</sup> Moments about axes parallel to longitudinal axis of the bridge.

TABLE 7.10- BENDING MOMENTS IN TOWER, PIER AND WELL ELEMENTS ABOUT AXES PARALLEL TO LONGITUDINAL AXIS OF S8 TO S11 UNDER ECCENTRIC VERTICAL LOADS (L5)

LOCATION	Memb. <sup>+</sup> No.	Actual values in S8 t-m	Values as multiple of corresponding values in S8			
			S8	S9	S10	S11
Well, pier	1	4194.1	1	0.875	0.159	0.160
	2	1817.6	1	0.865	0.050	0.049
Tower legs	41	475.7	1	0.969	1.675	1.604
	42	144.0	1	1.010	1.472	1.347
	43	1103.9	1	0.978	1.647	1.587
	44	146.0	1	0.859	2.328	2.095
	45	1080.4	1	0.979	1.658	1.597
	46	322.8	1	1.529	0.673	1.735
Portals (Moments about vertical axis)	47	348.5	1	1.007	1.343	1.339
	48	56.2	1	1.004	1.633	1.562
	49	173.5	1	0.985	1.542	1.472
Well, pier below tower	54	16276.6	1	0.972	0.832	0.821
	55	16956.0	1	0.990	0.700	0.725

<sup>+</sup> See fig. 7.1

<sup>++</sup> Moments about parallel to longitudinal axis of the bridge.

TABLE 7.11 - SUMMARY OF MAXIMUM VALUES OF FORCES IN S8 TO S11 UNDER ECCENTRIC VERTICAL LOADS (L5)

DESCRIPTION	S8	S9	S10	S11
AXIAL FORCES (t)				
Cables	-311.0	-310.8	-260.0	-260.1
Deck	614.3	631.3	639.2	650.9
Tower leg	1069.7	1051.7	993.4	981.5
Portal	22.5	22.5	20.4	20.4
End pier/well	-41.7	-39.0	-118.6	-116.5
Pier/well below tower	1240.2	1237.5	1147.9	1145.9
TWISTING MOMENT (t-m)				
Deck	216.8	220.0	252.5	254.3
Tower leg	342.9	345.1	460.6	458.9
Portal	129.9	131.3	174.9	175.1
End pier/well	22.5	29.8	60.6	60.2
Pier/well below tower	908.0	994.3	1564.8	1829.0
M-Y <sup>+</sup> (t-m)				
Deck	68.7	65.1	84.1	78.0
Tower leg	1103.9	1080.8	1818.4	1751.9
Portal	348.5	350.8	468.2	466.5
End pier/well	4194.1	3670.6	666.6	670.1
Pier/well below tower	16956.0	16790.4	11874.2	12296.3
M-Z <sup>+</sup> (t-m)				
Deck	928.4	925.5	922.1	917.6
Tower leg <sup>++</sup>	482.7	483.3	801.9	692.0
Portal <sup>++</sup>	593.6	647.5	584.2	601.7
End pier/well	7569.8	4556.4	7592.2	4434.7
Pier/well below tower	1159.0	662.2	4229.2	5146.6

+ Refer to member axes defined in sec. 3.4

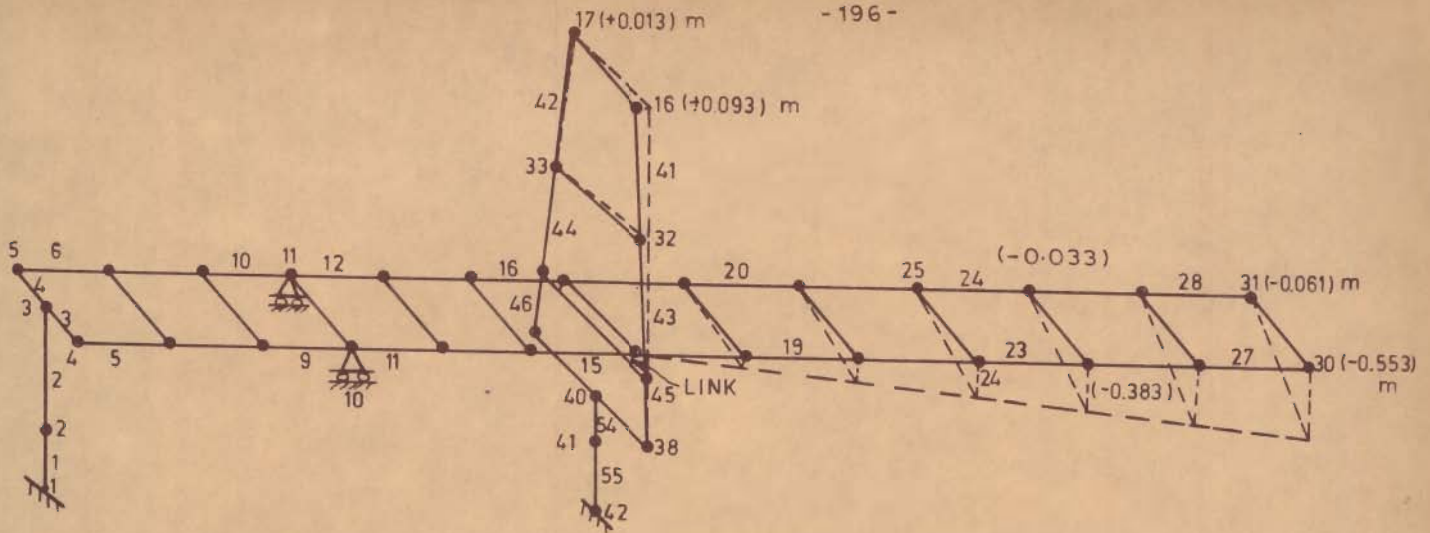
++ Location of maximum value has changed.

#### 7.4.2 Interpretation

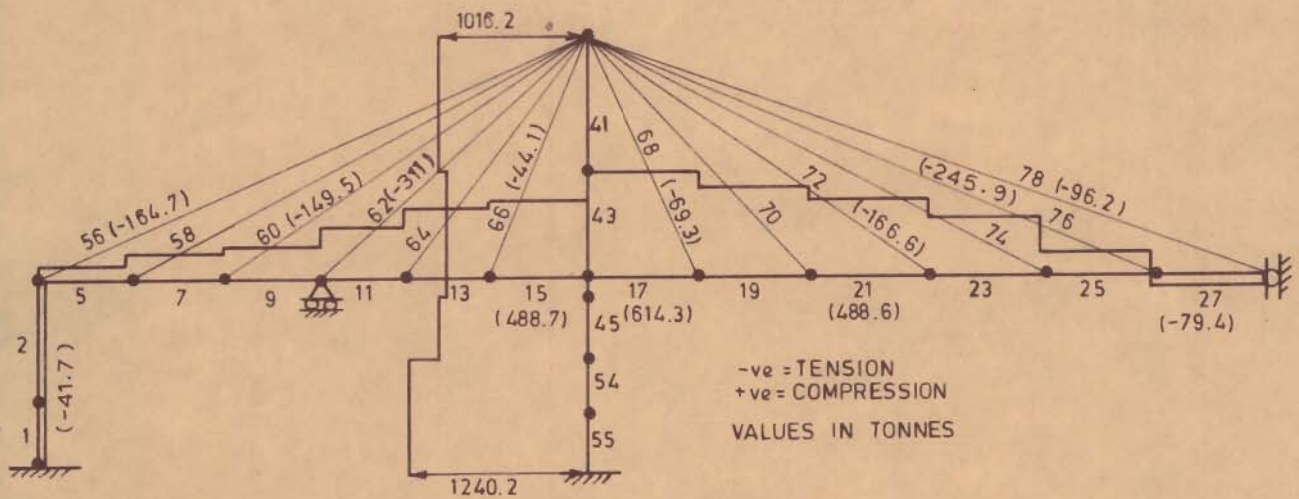
The loading L5 applied on idealised space frames S8 to S11 consists of an eccentric vertical loading of 2.5 t/m intensity on the axis of one of the two stiffening girders. The symmetric vertical loading L1 applied on planar structures S1 to S6 corresponds to a total load of intensity 5 t/m applied on the longitudinal axis of symmetry of the bridge. A comparison of the results of planar and space frame structures for the respective loading actions is attempted herein.

##### (a) 5-span Systems (S8)

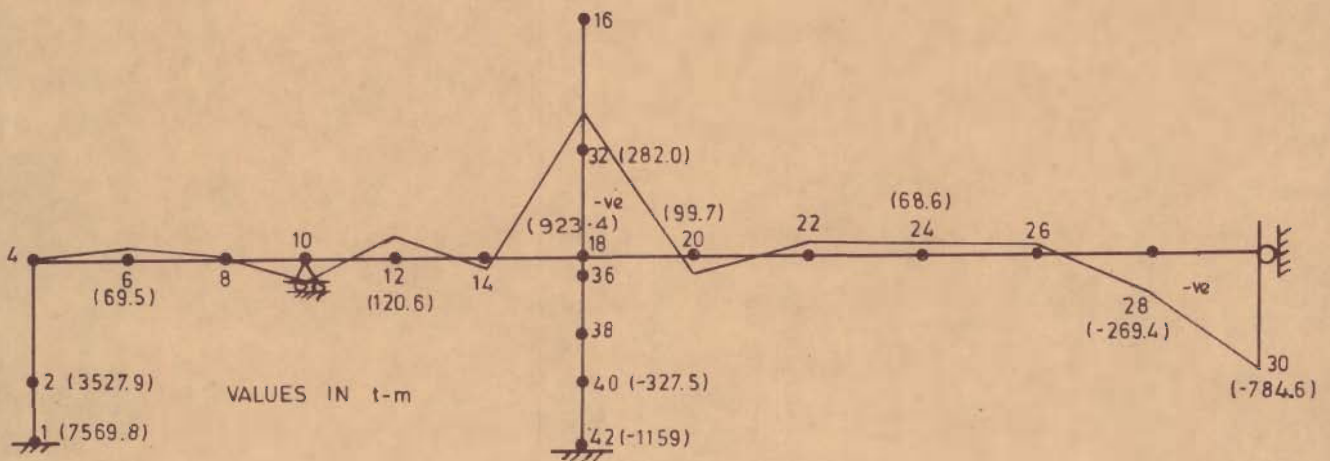
Distribution of deformations and forces of 5-span system (S8) under eccentric vertical loads (L5) is shown in fig. 7.2. On a comparison of behaviour of S1 presented in fig. 6.2 and S8 presented in fig. 7.2, it is observed that the general nature of deformations and forces of the loaded side of the bridge is the same in the two cases. The maximum vertical deflection at the centre of the main span of S8 is about 7% higher than that of S1. The maximum axial compression in deck element near the tower is about 26% higher, sagging moment at the centre of the main span is about 5% higher, maximum hogging moment in the deck is about 6% higher and the axial forces in cables, towers and substructure elements differ, in general, within 5% in respect of corresponding values in S1. However, there is a large reduction in the bending moments at the base of the substructure of S8 as compared to those of S1.



a - LONGITUDINAL AND VERTICAL DEFORMATIONS



b - AXIAL FORCES



c - MEMBER END MOMENTS

FIG. 7.2 - DISTRIBUTION OF DEFORMATIONS AND FORCES (LINEAR) IN 5-SPAN SYSTEM (S8) UNDER ECCENTRIC VERTICAL LOADS (L5)

The following specific observations are made from tables 7.5 to 7.10 about the space action of structure S8 under the effect of L5.

(i) On the unloaded side of the bridge, the maximum vertical deflection at the centre span is about 11% and the maximum longitudinal deflection at the top of the tower is about 14% of the corresponding value on loaded side.

(ii) Cable forces on the unloaded side are in general less than 10% of the forces on loaded side with a tendency of change in the nature of force in cables near the tower.

(iii) Axial forces on the unloaded side of the girder elements near tower are about 10 to 20% of those on the loaded side while they have equal and opposite values in the elements near centre of the main span due to horizontal bending of the main span.

(iv) Maximum twisting in the deck occurs near tower. The magnitude is about 25% of the maximum bending moment in longitudinal direction at the same location.

(v) Axial forces on the unloaded side of the tower legs are about 16% of those on the loaded side. The twisting moments and the bending moments in the longitudinal direction are almost equal.

(vi) Bending moments in tower legs, pier and well below tower are very high in the transverse direction. The ratio of maximum values of bending moments in the transverse

and the longitudinal directions is about 15.

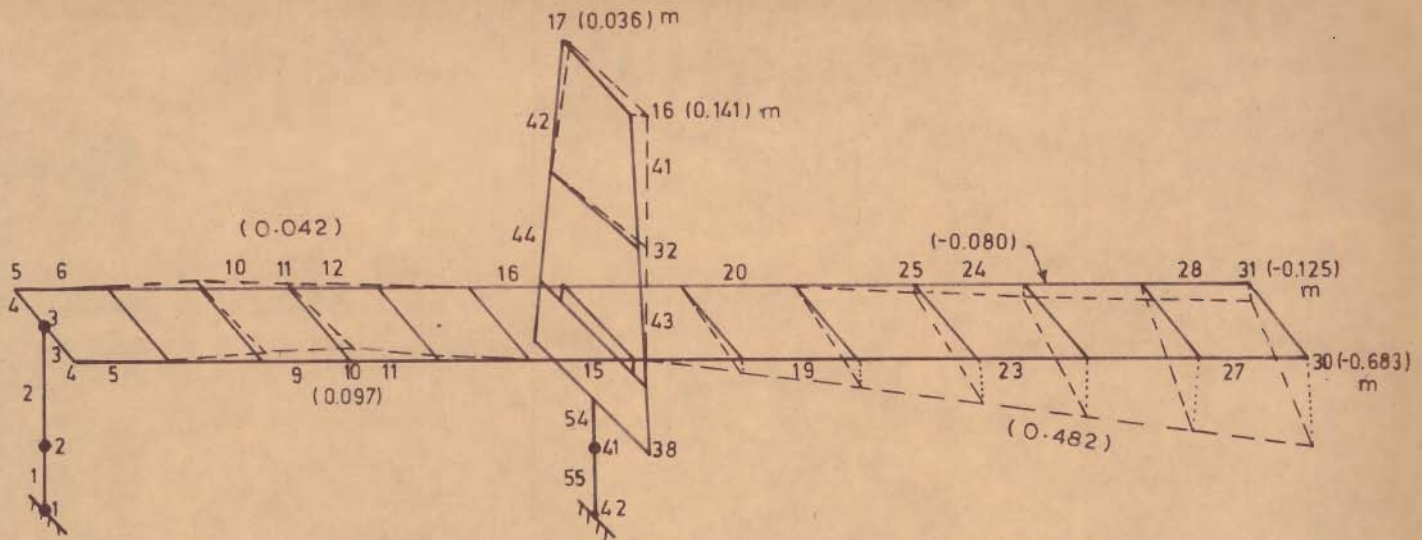
(b) 5-span System S9; Effect of Soil Structure Interaction:

The effect of soil-structure interaction is significant only on the behaviour of the substructure elements. The effects on the behaviour of the superstructure can be considered to be less than 10% in general.

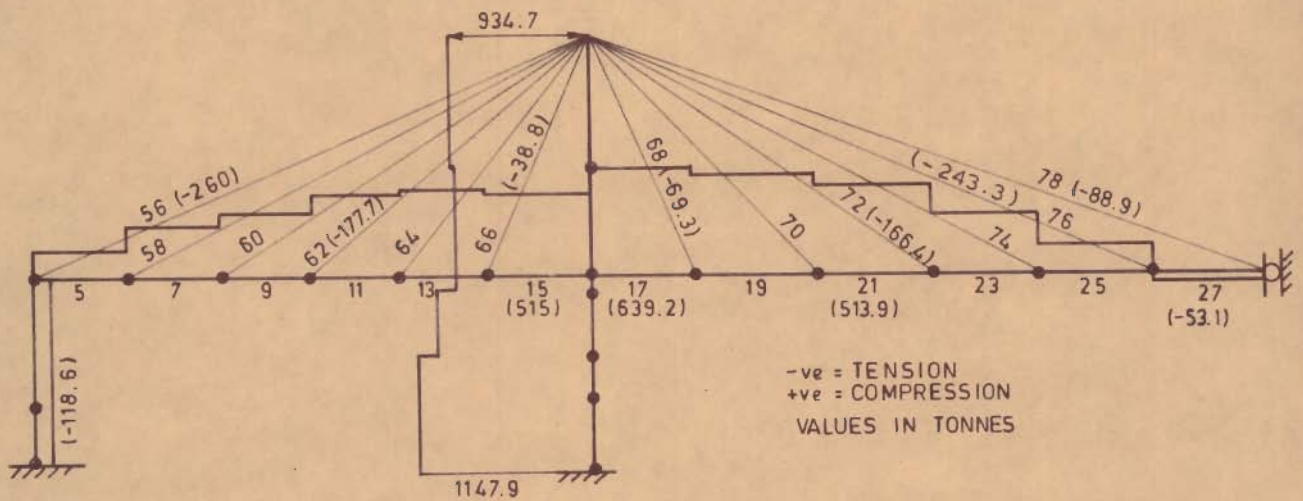
(c) 3-Span Systems (S10): Distribution of deformations and forces of the 3-span system (S10) under eccentric vertical loads (L5) is shown in fig. 7.3. On comparing the behaviour of S3 presented in fig. 6.3 and S10 presented in fig. 7.3, it is observed that the general nature of deformations and forces of the loaded sides of the bridge is the same in the two cases. The maximum vertical deflection at the centre of the main span of S10 is about 3% higher than that of S3. The maximum axial compression in the deck is about 42% higher, sagging moment at the centre of main span is about 2% lower and maximum hogging moment in the deck is about 5% higher in S10 than in S3. The difference in the maximum cable force, which occurs in the top cable of the end span, is about 15% whereas the general difference of axial forces in cables, towers and substructure elements is less than 5% as compared to S3. Bending moment at the base of the end well is about 50% and the one at the base of the well below the tower is more than doubled.

The observations made from table 7.5 to 7.10 about the space action of structure S8 under effect of L5 apply in

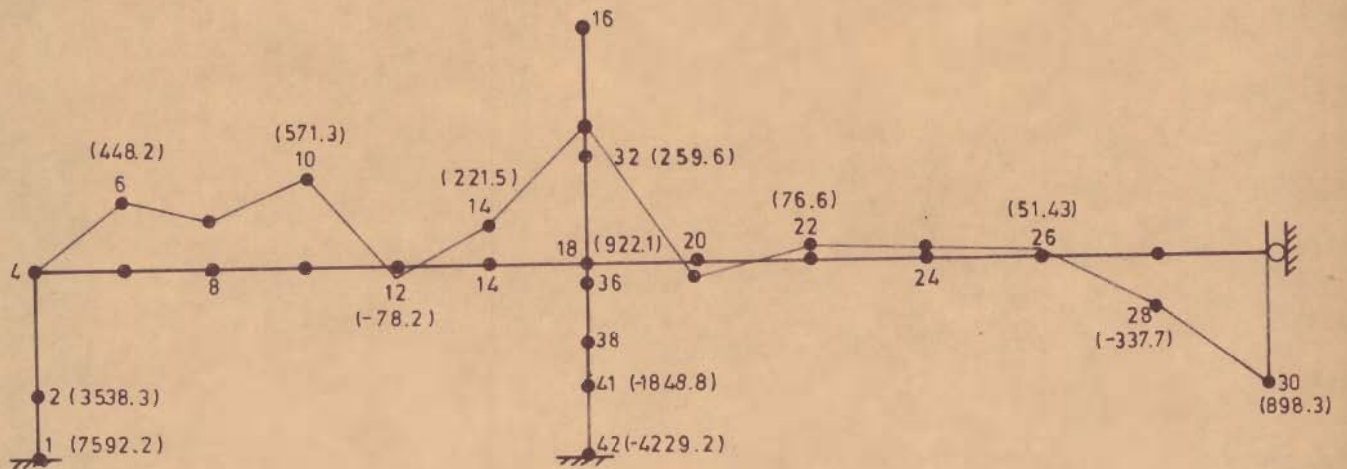




a - LONGITUDINAL AND VERTICAL DEFORMATIONS



b - AXIAL FORCES



c - MEMBER END MOMENTS

FIG. 7.3 - DISTRIBUTION OF DEFORMATIONS AND FORCES (LINEAR) IN 3-SPAN SYSTEM (S 10) UNDER ECCENTRIC VERTICAL LOADS (L 5)

general to S10 also with the following deviations:

(i) On the unloaded side of the bridges the maximum vertical deflection at the centre span is about 18% and the maximum longitudinal deflection at the top of tower is about 25% of the corresponding value on loaded side.

(ii) Top cable of the unloaded side of end span takes about 25% of the corresponding cable force of the loaded side. The cable forces on the unloaded side are, in general, about 10% of the corresponding cable forces on loaded side.

(d) 3-Span System (S11): The behaviour, under the effect of soil-structure interaction, of this 3-span structure is similar to that of S10.

#### 7.4.3 Maximum Values of Forces

A summary of maximum values of forces in different components of S8 to S11 under L5 is given in table 7.11. The following observations are made for 5-span system, S8, and similar observations are applicable for S9 to S11.

(i) The ratio of maximum value of principal bending moment to axial force in the deck as well as the tower leg is high. Axial-flexural interaction will depend on the level of axial force in the component with respect to its Euler buckling force, causing nonlinearity in the behaviour of the structure.

(ii) Maximum twisting in the deck is about 25% and the horizontal bending due to eccentric vertical loading is within 10% of the principal longitudinal bending.

(iii) Maximum twisting of the tower is about 30% and the secondary bending is about 45% of the principal bending.

(iv) Portals do not draw heavy axial forces but twisting moments and bending moments have comparable maximum values.

(v) Compared to the substructure below tower, the substructure at the end draws less axial force (also opposite in nature), less twisting moment (less than 3%) and less secondary bending effects. The principal moment at the base of substructure at the end is about seven times that at the base of substructure below tower.

#### 7.4.4 Discussion.

In general, the 5-span system exhibits greater overall stiffness to the action of eccentric vertical loads than the 3-span system. It is observed that the forces and deformations in the planar bridge elements under full symmetric loads and the elements of space structure under the action of half the vertical loads applied on the axis of one of the two main girders are more or less equal. Space action is observed to be more predominant in the 3-span system as compared to the 5 span system because the percentage of forces in the elements of unloaded side is higher in the

3-span system. The effect of soil-structure interaction is observed to be insignificant on the bridge substructure. The effect of soil flexibility has been studied by taking a practical value of the coefficient of subgrade reaction ( $n_H=130$  t/m<sup>2</sup>) for the case of loose sand. Yet the flexibility added to the system as a whole is not appreciable since the superstructure is already much more flexible. But the moments and deflections of the rigid substructures are appreciably altered by the soil flexibility. Stiffer soils would naturally provide greater elastic stiffness at the base and sides of the substructure, and therefore, will modify the values in the structure even smaller extent.

## 7.5 LATERAL LOAD ANALYSIS

### 7.5.1 Results

The results of analysis of S8 to S11 under lateral loading L6 are presented in tables 7.12 to 7.18. Actual values of deformations at salient locations and axial forces and bending moments in important elements of S8 have been tabulated and comparative values have been presented for S9 to S11 in terms of multiples of corresponding values of S8.

### 7.5.2 Interpretation.

The purpose of the analysis of S8 to S11 under the effect of lateral forces (L6) is to study and compare the behaviour of the 5-span and 3-span systems under space action and to study the effect of soil-structure interaction thereon.

Independent behaviour of 5-span and 3-span systems is first interpreted and then the two are compared in the following paragraphs.

TABLE 7.12 - DEFORMATIONS AT SALIENT LOCATIONS OF S8 TO S11 UNDER LATERAL FORCES (L6)

LOCATION	Node <sup>+</sup> No.	Actual Values		Values as multiple of corresponding value in S8			
		Along <sup>+</sup> axis of	in S8 <sup>+</sup> (m)	S8	S9	S10	S11
End span	4	X	-.001135	1	1.286	-1.576	-1.582
		Z	-.000272	1	7.522	-1.066	7.151
	8	Y	-.000663	1	1.062	17.00	14.96
		Z	-.001088	1	1.799	-13.36	-17.41
	12	Y	-.003112	1	0.897	2.88	2.44
		Z	+.009142	1	1.225	2.92	3.67
Tower top	16	X	-.002027	1	1.478	2.47	2.54
		Y	-.002671	1	0.492	1.148	0.559
		Z	+.116622	1	1.117	1.082	1.230
Centre span	24	Y	+.019525	1	1.154	1.149	1.234
		Z	+.183055	1	1.068	0.985	1.050
	30	Y	+.055651	1	1.076	1.086	1.115
		Z	+.261406	1	1.058	0.979	1.029

+See fig. 7.1

(a) 5-span System (S8): Distribution of deformations and forces of S8 under lateral loads (L6) is shown in fig. 7.4. The following specific points are observed from fig. 7.4 and tables 7.12 to 7.17.

(i) Maximum lateral deflection (0.261 m) at the centre of the main span (457.2 m) is about 1/1750 of the main span.

TABLE 7.13 - CABLE FORCES IN S8 TO S11 UNDER LATERAL FORCES (L6)

LOCATION	Memb. No.	Actual <sup>++</sup> values in S8 (t)	Values as multiple of corresponding value in S8			
			S8	S9	S10	S11
Top cables, end span	56	4.24	1	0.899	3.995	3.807
	57	1.13	1	0.956	-8.876	-9.655
	58	3.81	1	0.890	2.680	2.577
	59	-0.69	1	0.942	9.377	10.029
	60	5.01	1	0.920	0.599	0.587
Middle cables, end span	61	-3.88	1	1	0.588	0.603
	62	19.31	1	0.942	0.032	0.028
	63	-18.59	1	1.019	0.069	0.055
	64	6.89	1	0.946	-0.030	-0.067
	65	-6.44	1	0.989	0.043	-
Cables near tower	66	2.74	1	1.004	0.263	0.215
	67	-3.30	1	0.967	0.494	0.418
	68	-0.96	1	1.385	0.677	1.010
	69	1.69	1	1.160	0.882	1.03
	70	-2.31	1	1.121	0.952	1.065
Middle cables centre span	71	2.23	1	1.139	0.960	1.085
	72	-2.03	1	1.020	0.98	0.99
	73	1.91	1	1.073	0.99	1.042
	74	4.90	1	1.014	0.924	0.922
	75	-4.22	1	1.031	0.903	0.929
Top cables, centre span	76	23.78	1	1.001	0.931	0.925
	77	-21.08	1	1.040	0.925	0.956
	78	-19.72	1	0.996	0.920	0.913
	79	-18.18	1	1.041	0.920	0.951

+ See fig 7.1

++ -ve = Tension

TABLE 7.14 - AXIAL FORCES IN GIRDER, TOWER, PIER AND WELL ELEMENTS OF S8 TO S11 UNDER LATERAL FORCES (L6)

LOCATION	Memb. No.	Actual values in S8 (t)	++ Values as multiple of corresponding values in S8				
			S8	S9	S10	S11	
Well, pier, end span	1,2	4.3	1	0.837	1.209	0.907	
T       	End members	5	8.3	1	0.446	0.843	0.506
		6	127.4	1	1.122	-0.033	-0.095
		7	-103.2	1	1.237	-0.194	-0.200
		8	304.2	1	1.121	0.143	0.109
		9	-283.8	1	1.160	0.087	0.075
D	Central members end span	10	543.8	1	1.106	0.290	0.268
		11	-534.1	1	1.122	0.258	0.248
		12	581.2	1	1.046	0.575	0.550
		13	-562.0	1	1.060	0.557	0.544
		14	667.9	1	0.991	0.861	0.836
E	Members near tower	15	-645.9	1	1.002	0.858	0.843
		16	814.9	1	0.955	1.073	1.050
		17	-940.0	1	0.993	1.043	1.046
		18	491.1	1	0.935	1.080	1.038
		19	-403.1	1	0.985	1.102	1.111
C		20	35.7	1	0.112	2.095	1.507
		21	50.9	1	1.120	0.200	0.126
		22	-313.9	1	1.100	0.875	0.942
		23	400.3	1	1.015	0.898	0.889
		24	-564.1	1	1.055	0.931	0.967
K     	Members at centre of main span	25	656.2	1	1.009	0.937	0.932
		26	-718.6	1	1.044	0.945	0.974
		27	828.7	1	1.007	0.948	0.944
		28	-789.0	1	1.040	0.948	0.975
	Tower legs	41	-105.4	1	0.978	0.888	0.873
		42	89.4	1	1.101	0.982	0.980
		43	-246.2	1	0.986	0.974	0.964
		44	239.1	1	0.995	0.979	0.974
		45	-272.3	1	0.726	1.015	0.701
		46	266.1	1	0.728	1.019	0.703
Portals		47	- 0.2	-	-	-	-
		48	- 0.6	-	-	-	-
		49	-37.3	1	1.150	0.220	0.309
Well, Pier below tower	54,55	- 6.4	1	0.672	0.813	0.609	

+ See fig. 7.1

++ -ve = Tension

TABLE 7.15- TWISTING MOMENTS IN GIRDER, TOWER, PIER AND WELL ELEMENTS OF S8 TO S11 UNDER LATERAL FORCES (L6)

LOCATION	Memb. <sup>+</sup> No.	Actual values in S8 (t-m)	Values as multiple of corresponding value in S1				
			S8	S9	S10	S11	
D	Well, pier, end span	1,2	11.3	1	1.619	6.982	8.168
		5,6	2.5	1	0.40	17.44	16.88
		7,8	2.8	1	1.393	8.25	7.714
E	End span	9,10	0.2	1	5.00	13,5	7.50
C		11,12	25.2	1	1.143	0.377	0.413
		13,14	8.3	1	0.663	1.928	1.976
K	Member near tower	15,16	29	1	2.621	4.552	0.862
		17,18	38.8	1	1.356	1.131	1.477
		19,20	33.8	1	1.071	1.124	1.148
	Centre span	21,22	23.4	1	1.077	1.214	1.235
		23,24	20.2	1	1.064	1.213	1.223
		25,26	41.6	1	1.038	1.048	1.058
		27,28	45.5	1	1.029	0.987	0.998
Tower legs		41,42	90.2	1	1.106	1.106	1.125
		43,44	129.7	1	1.012	0.736	0.744
		45-46	162.8	1	0.964	0.780	0.752
Portals		47	58.5	1	1.101	1.003	1.036
		48	32.6	1	1.110	1.055	1.086
		49	103.4	1	1.069	0.846	0.879
	Well, pier below tower	54,55	5921.1	1	1.036	0.871	0.872

+See fig. 7.1



TABLE 7.16 - BENDING MOMENTS (M-Y) IN GIRDER, TOWER,  
PIER AND WELL ELEMENTS OF S8 TO S11  
UNDER LATERAL FORCES (L6)

LOCATION	Memb. No. +	Actual values in S8 (t-n)	Values as multiple of corresponding values in S8				
			S8	S9	S10	S11	
Pier, well, end span	1	2616.4	1	1.410	1.336	1.385	
	2	1452.0	1	1.342	0.872	0.914	
T	5	38.8	1	0.997	3.041	3.601	
	6	69.7	1	1.050	1.585	1.904	
	7	5.8	1	1.379	10.759	12.397	
	8	16.8	1	1.119	3.720	4.304	
	9	8.7	1	1.146	9.072	0.091	
	D Central members end span	10	68.7	1	1.194	0.084	0.111
		11	84.2	1	1.154	0.252	0.239
		12	65.3	1	1.208	0.213	0.202
		13	28.1	1	1.157	0.601	0.562
14		47.7	1	1.027	0.805	0.799	
E Members near tower	15	95.1	1	0.781	1.512	1.410	
	16	61.8	1	0.812	1.672	1.633	
	17	228.5	1	1.011	1.078	1.098	
	18	253.2	1	0.988	1.055	1.049	
	19	5.9	1	1.186	0.424	0.542	
C	20	16.1	1	1.037	0.988	1	
	21	38.6	1	1.034	0.930	0.948	
	22	39.4	1	1.030	0.924	0.947	
	23	52.9	1	1.028	0.945	0.960	
K	24	52.7	1	1.028	0.945	0.960	
	25	65.2	1	1.015	0.956	0.960	
	26	64.8	1	1.015	0.955	0.960	
	Members at centre of main span	27	63.3	1	1.028	0.954	0.972
		28	63.0	1	1.014	0.952	0.956
Tower legs	41	105.9	1	1.307	0.885	1.070	
	42	282.2	1	1.004	0.947	0.923	
	43	752.8	1	1.139	0.885	0.959	
	44	1097.7	1	1.039	0.916	0.920	
	45	1849.8	1	1.198	0.827	0.969	
	46	3018.8	1	0.997	0.895	0.861	
Portals (Moments about vertical axis)	47	92.7	1	1.107	1.104	1.123	
	48	211.9	1	1.062	0.884	0.907	
	49	363.0	1	1.053	0.914	0.926	
Well, pier below tower	54	45445.8	1	0.978	1.137	1.129	
	55	76474.9	1	1.016	1.150	1.194	

+See fig. 7.1

TABLE 7.17- BENDING MOMENTS (M-Z) IN GIRDER, TOWER, PIER AND WELL ELEMENTS OF S8 TO S11 ABOUT AXES PARALLEL TO TRANSVERSE AXIS OF BRIDGE UNDER LATERAL FORCES (L6)

LOCATION	Memb <sup>+</sup> No.	Actual values in S8 (t-m)	Values as multiple of corresponding values in S8						
			S8	S9	S10	S11			
D	Pier, well, end	1	1771.0	1	0.70	0.958	0.667		
	span	2	824.5	1	0.70	0.959	0.667		
			5	28.0	1	0.882	2.486	2.332	
			6	0.1	1	7.00	309.0	352.0	
			7	28.0	1	0.882	2.486	2.330	
			8	2.5	1	1.32	12.36	14.08	
			9	82.8	1	0.937	0.547	0.512	
		E	Central members,	10	63.4	1	0.992	0.298	0.341
			end span	11	82.8	1	0.937	0.219	0.199
	12		63.4	1	0.992	0.243	0.232		
	13		45.1	1	1.151	0.286	0.459		
	14		47.5	1	1.08	0.440	0.598		
C	Members near tower	15	45.1	1	1.151	0.286	0.521		
		16	44.0	1	1.166	0.552	0.857		
		17	60.2	1	0.877	0.831	0.651		
		18	66.4	1	0.818	0.904	0.682		
		19	14.5	1	1.359	1.159	1.60		
			20	21.6	1	1.074	0.926	0.986	
			21	12.2	1	1.041	0.844	0.861	
			22	21.6	1	1.074	0.926	0.981	
			23	39.5	1	0.985	0.911	0.891	
			24	33.1	1	1.057	0.903	0.949	
K	Members at centre of main span	25	56.5	1	0.982	0.874	0.864		
		26	62.5	1	1.045	0.902	0.936		
		27	260.2	1	1.011	0.978	0.972		
		28	203.2	1	1.047	0.967	0.999		
	Tower legs		41	872.7	1	0.998	1.027	1.026	
			42	874.2	1	0.998	1.026	1.024	
			43	1802.8	1	0.988	1.048	1.039	
			44	1792.0	1	0.987	1.053	1.043	
Portals**		45	9696.7	1	1.034	1.174	1.236		
		46	9754.3	1	1.034	1.169	1.230		
		47	874.2	1	0.998	1.026	1.024		
		48	2131.9	1	0.992	1.039	1.033		
		49	361.2	1	1.098	1.261	1.072		
Pier, well below tower	54	1907.0	1	1.137	1.006	1.135			
	55	3229.9	1	1.506	1.009	1.495			

+ See fig. 7.1

\*\* Moments about axes parallel to longitudinal axis of bridge.

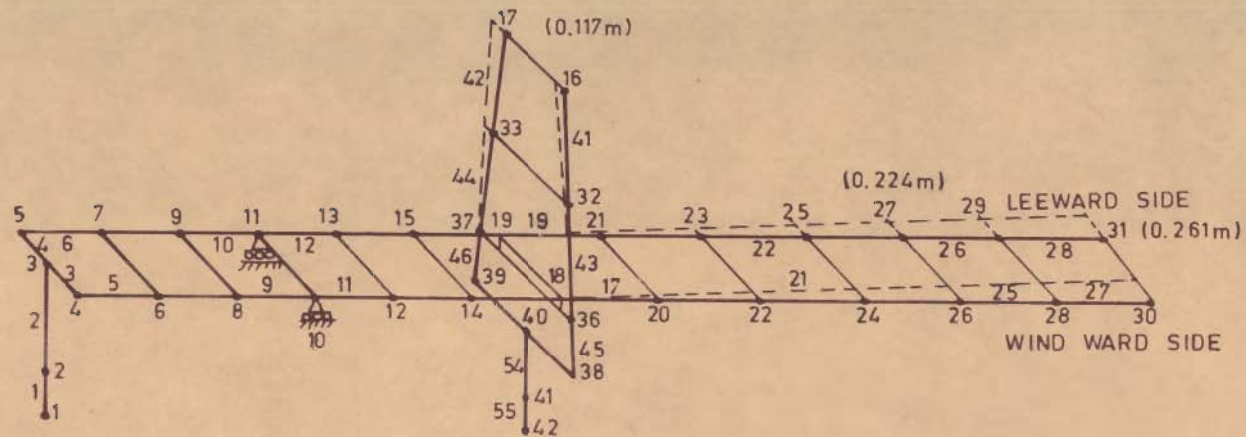
TABLE 7.18 - SUMMARY OF MAXIMUM VALUES OF FORCES IN S8 TO S11 UNDER LATERAL FORCES (L6)

DESCRIPTION	S8	S9	S10	S11
AXIAL FORCES (t)+				
Cables	+23.78	+23.80	+22.13	+21.99
Deck	+828.7	+834.6	+874.1	+856.0
Tower leg	-940.0	-933.5	-980.1	-983.4
Portal	+266.1	+237.9	+271.2	+233.0
End pier/well	-272.3	-242.7	-276.3	-237.4
Pier/well below tower	- 37.3	- 42.9	- 8.2	- 11.3
	+ 4.3	+ 3.6	+ 5.2	+ 3.9
	- 6.4	- 4.3	- 5.2	- 3.9
TWISTING MOMENT (t-m)				
Deck <sup>x</sup>	45.5	52.6	44.9	57.3
Tower leg	162.8	156.9	130.2	122.5
Portal	103.4	110.5	87.5	90.9
End pier/well	11.3	18.3	78.9	92.9
Pier/Well below tower	5921.1	6135.4	5156.8	5160.8
M-Y (t-m) <sup>++</sup>				
Deck	253.2	250.1	267.2	265.7
Tower leg	3018.8	3009.1	2701.4	2598.2
portal	363.0	382.2	331.7	336.2
End pier/well	2614.6	3686.8	3491.8	3620.1
Pier/well below tower	76474.9	77665.0	87915.3	91344.0
M-Z (t-m) <sup>++</sup>				
Deck	260.2	263.0	254.5	252.8
Tower leg	9754.3	10088.2	11401.4	12001.7
Portal	874.2	872.3	896.6	895.6
End pier/well	1771.0	1239.0	1696.9	1180.5
Pier/well below tower	3229.9	4865.6	3258.6	4829.6

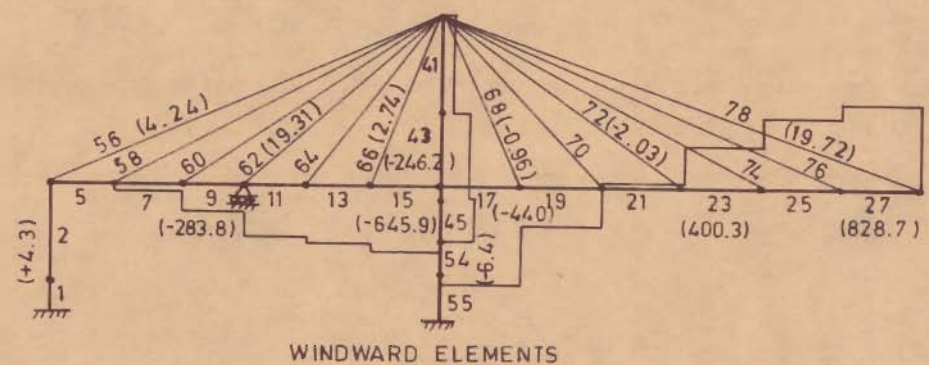
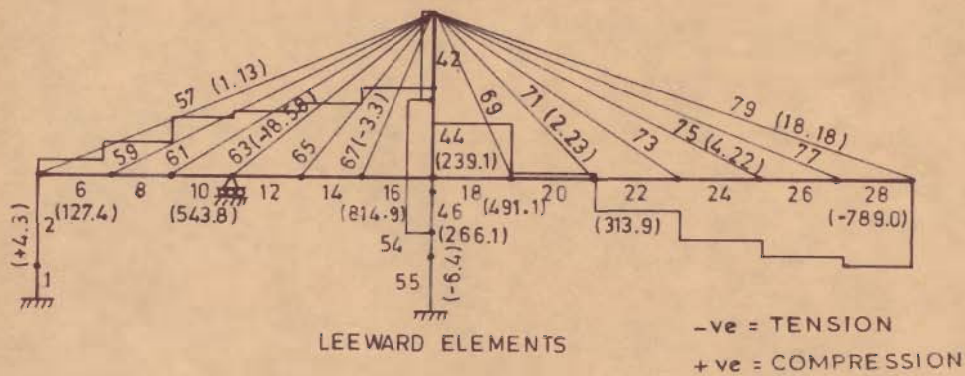
+ (+)ve = compression

x Location of maximum value has changed

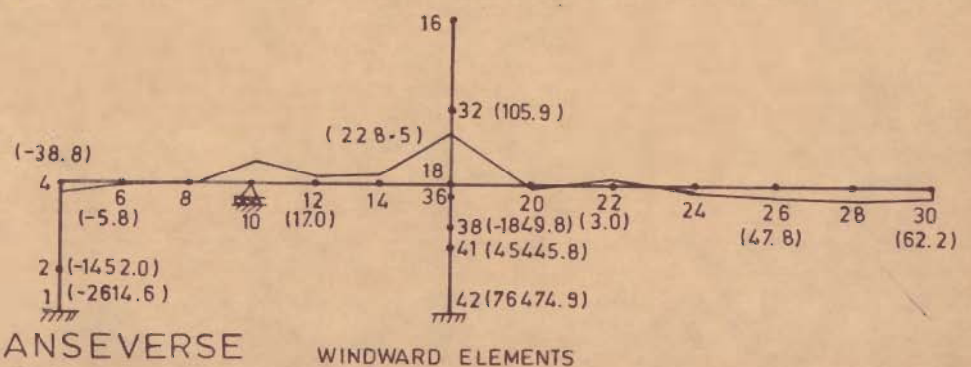
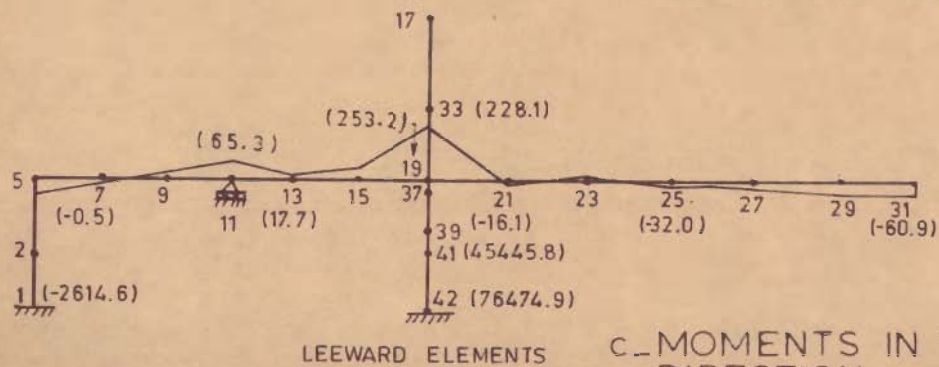
++ Refer to member axes defined in sec. 3.4



a- LATERAL DEFORMATIONS IN DECK AND TOWER



b- AXIAL FORCES



c- MOMENTS IN TRANSVERSE DIRECTION

FIG. 7.4 DEFORMATIONS AND FORCES IN S 8 UNDER L 6

(ii) Maximum lateral deflection (0.117m) at the top of the tower (103.59 m) is about 1/890 of the tower height.

(iii) Cables are subjected to small axial forces. The maximum cable force is only about 3% of the maximum axial force in a girder element.

(iv) Windward cables get, in general, compressive forces, except a few cables near the centre of the main span, which get tensile force. The forces in cables of leeward side are, in general, of opposite nature.

(v) Maximum axial forces in the girder elements occur near the tower. Windward girder elements of the end span and a few elements of the centre span near the tower are in tension while the elements near the centre of main span are in compression. The nature of forces in the leeward elements is reverse.

(vi) Bending moments in the transverse direction are very low in the superstructure as compared to the substructure. Heaviest bending moments occur at the base of well below tower and its magnitude is about 30 times the value at the base of end well.

(vii) Maximum twisting of deck elements is observed near centre of main span and the variation in other elements of main span is small.

(viii) Axial forces in tower elements of windward and leeward sides are of opposite nature and the axial forces in the substructure are negligible.

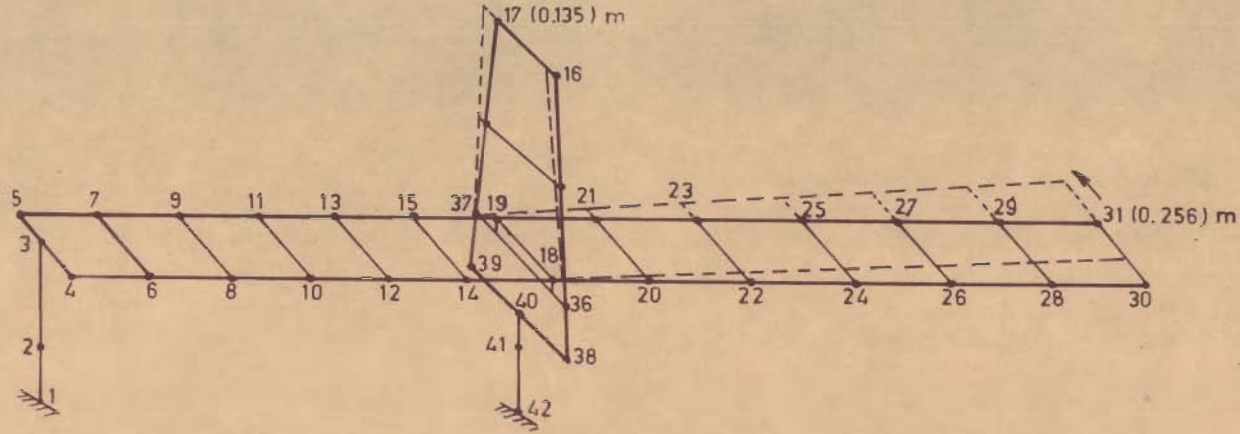
(ix) Maximum bending and twisting in the tower occurs at its foot.

(b) 5-Span System S9; Effect of Soil - Structure Interaction:

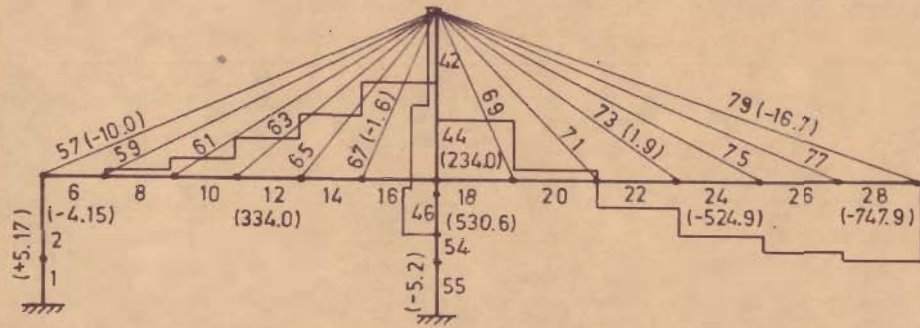
Behaviour of S8 and S9 is observed to be similar. The effect of soil-structure interaction is to increase the maximum lateral deflection at centre of main span by about 6% and at the top of tower by about 12%. Cable forces are, in general, changed by less than 5%. Maximum axial force in the deck element is changed by less than 5% and a similar effect is observed on axial forces of other elements of the bridge. The effects of soil-structure interaction on forces in superstructure elements is, in general, less than, 5% while it is significant on the forces and deformations in elements of substructure.

(c) 3- span System S10:

Distribution of deformations and forces of S10 under lateral forces L6 is shown in fig. 7.5. It is observed from fig. 7.5 and tables 7.12 to 7.17 that the main features of the behaviours of S8 and S10 are, in general, similar and as described in (a).

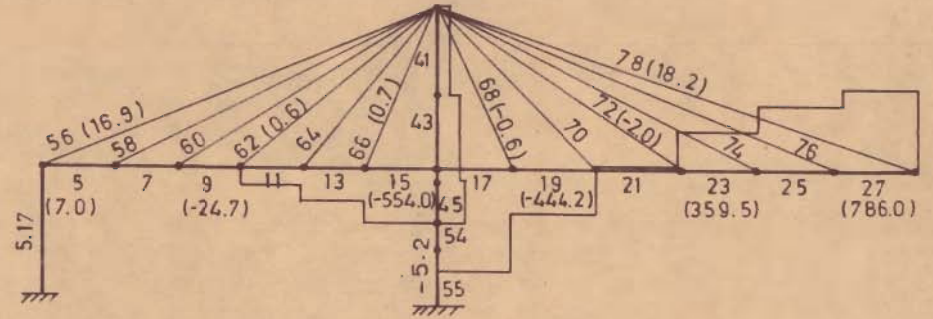


a\_ LATERAL DEFORMATIONS IN DECK AND TOWER



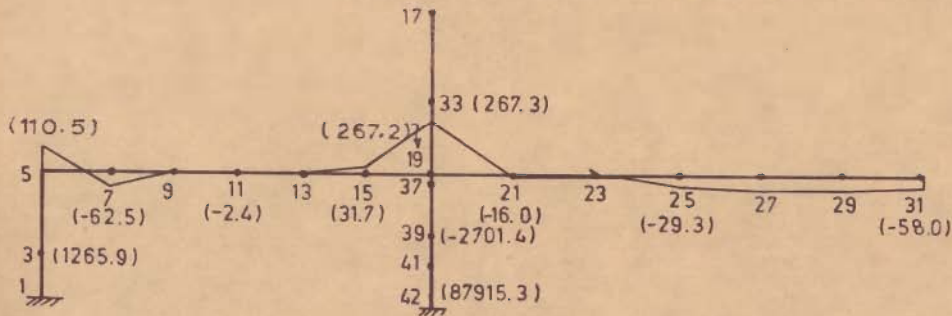
LEEWARD ELEMENTS

-ve = TENSION  
+ve = COMPRESSION

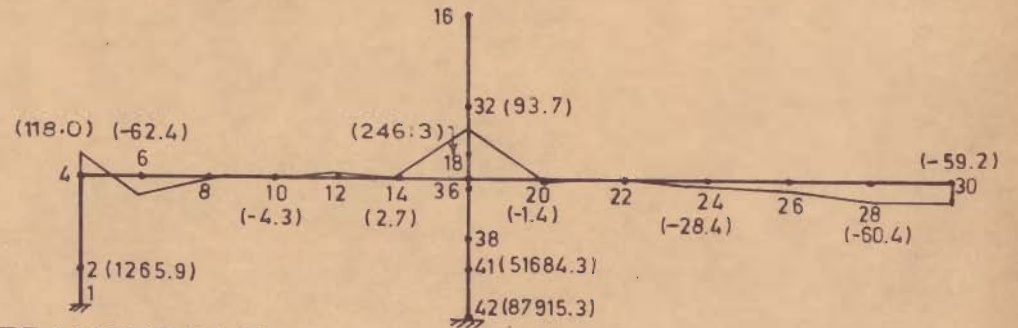


WINDWARD ELEMENTS

b\_ AXIAL FORCES



LEEWARD ELEMENTS



WINDWARD ELEMENTS

c\_ MOMENTS IN TRANSVERSE DIRECTION

FIG. 7.5\_ DEFORMATIONS AND FORCES IN S10 UNDER L6

(d) 3-Span System S11; Effect of Soil-Structure Interaction:

Behaviour of S10 and S11 is observed to be similar. Pronounced effects of soil-structure interaction are observed in the distribution of forces and deformations of the elements of substructure while the effect is not very significant on the behaviour of the superstructure.

7.5.3 Maximum Values of Forces

A summary of maximum values of forces in different components of S8 to S11 under L6 is given in table 7.18. The following observations are made for the 5-span system S8 and similar observations are applicable to S9 to S11.

(i) Maximum axial force in cables, portals, piers and wells is less than 5%, whereas in the tower leg it is less than one-third, of the maximum axial force in the deck elements.

(ii) Twisting moments in various elements of the structure are small as compared to their bending moments. The ratio of maximum twisting moment to the maximum bending moment in a girder element is about 1/6 and in the substructure below tower it is about 1/15. The ratio is even lesser for other elements of the structure.

(iii) The ratios of maximum values of M-Z and M-Y (referred to member axes) for various components of the bridge are as follows:



Element		Mz/My
deck	=	1.03
tower leg	=	3.23
portal	=	2.41
end pier/well	=	0.68
pier/well below tower	=	0.04

Under the effect of lateral forces, deck elements are subjected to high value of axial forces and low bending moments. The bending moments about both the axes of deck cross-section are almost equal.

#### 7.5.4 Discussion

The results show that the deck of the bridge behaves as if it were a continuous beam in the transverse direction carrying the lateral forces. The participation of cables, when they lie in vertical planes, is only secondary in the lateral force resistance of the bridge. Heavy axial forces are caused in the girder elements due to the horizontal bending of the deck whereas the substructure below tower is subjected to heavy moments. Because of the increased rigidity of the end spans of the 5-span system, the maximum deflection at the centre of the main span of the 5-span system is little more while the lateral deflection at the top of the tower is less than that of the 3-span system. The influence of soil-structure interaction is not significant on the behaviour of the deck whereas it may be considered significant on the lateral stiffness of the substructure.

7.6 EXPERIMENTAL VERIFICATION OF RESULTS

TABLE 7.19 - COMPARISON OF ANALYTICAL AND EXPERIMENTAL VALUES OF MAXIMUM DEFLECTIONS IN S12 UNDER L7 TO L10

Type of Loading	Deformations (mm)		% Variation
	Analytical	Experimental	
Eccentric Vertical Loads			
End span and centre span loaded (L7)	A	1.5915	9.3
	B	0.2557	12.0
Centre span loaded (L8)	A	2.2735	3.0
	B	0.5293	12.2
Lateral Forces			
End span and centre span loaded (L9)	A	0.2651	5.6
	B	0.1558	2.7
Centre span loaded (L10)	A	0.2952	3.3
	B	0.0991	11

A - Maximum vertical/lateral deflection of deck

B - Maximum longitudinal/lateral deflection of tower

Analytical and experimental results of aluminium model structure, S12, under eccentric vertical loads (L7, L8) and lateral forces (L9, L10) are given in table 7.19. Percentage variation of experimental values with respect to analytical values is also shown in the table. It is observed that the maximum percentage of variation is 12.2 and the comparison of analytical and experimental values is excellent.

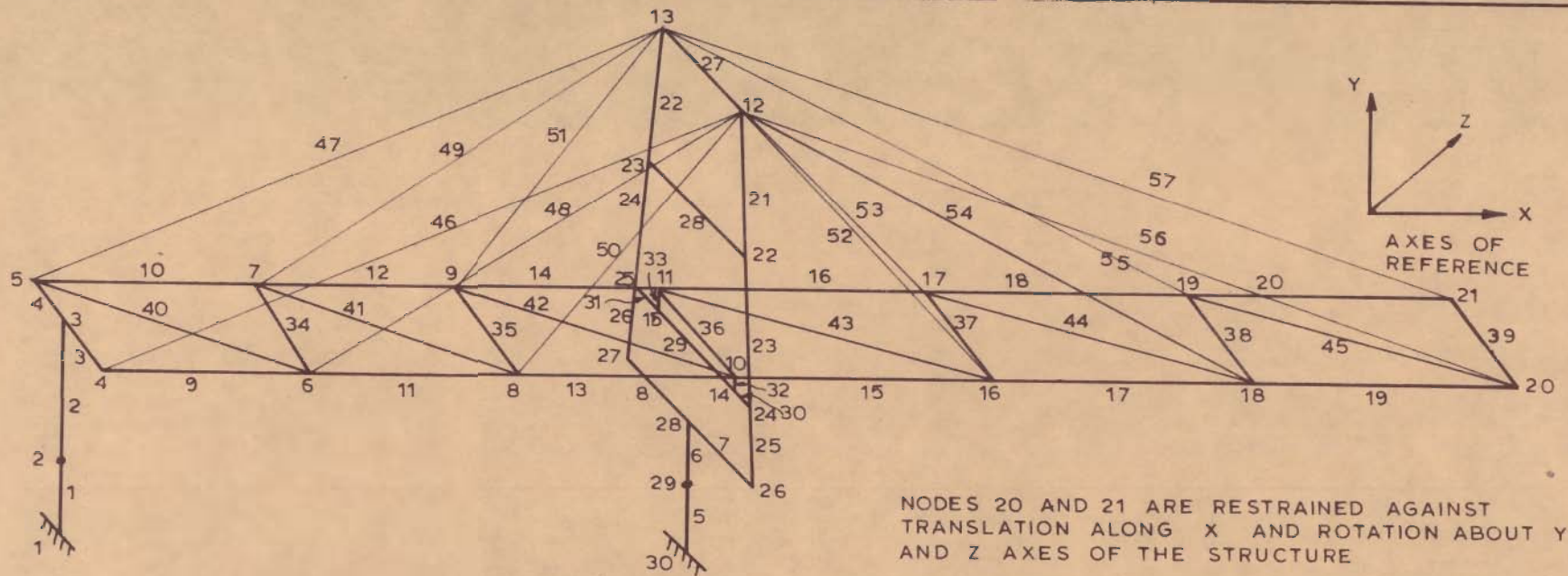
## 7.7 PARAMETRIC STUDY UNDER LATERAL FORCES

Behaviour of radiating type 3-span cable-stayed bridge with its substructure fixed at the base has been investigated under the effect of following parametric variations:

- (i) Ratio of side span to centre span ( $\alpha$ )
- (ii) Ratio of tower height to centre span ( $\beta$ )
- (iii) Ratio of width of deck to centre span ( $\nu$ )
- (iv) Ratio of cable area to girder torsional rigidity ( $\gamma$ ).

Nondimensional values of  $\alpha$ ,  $\beta$ ,  $\nu$  and  $\gamma$  are given in fig. 7.6.

The planar and space frame investigations reported in the present thesis relate to radiating 6-cable systems. To reduce the volume of results and to save in the computational time, the bridge structures chosen for the parametric studies are equivalent 3-cable systems (fig. 7.6). The equivalence with 6-cable system such as S10 is established by lumping the areas of two consecutive cables of the 6-cable system at one node, thus reducing the number of cables from six to three. Since this results in increasing the panel length of the deck between cable points, the stiffness of fictitious diagonal braces 40-45 (fig. 7.6) of the equivalent 3-cable system have been derived afresh in accordance with the criterion described in appendix-C to represent the lateral stiffness of the deck plate properly.



NODES 20 AND 21 ARE RESTRAINED AGAINST TRANSLATION ALONG X AND ROTATION ABOUT Y AND Z AXES OF THE STRUCTURE

STRUCTURE DESIGNATION	$\alpha = \frac{\text{SIDE SPAN}}{\text{CENTRE SPAN}}$	$\beta = \frac{\text{TOWER HEIGHT}}{\text{CENTRE SPAN}}$	$\nu = \frac{\text{WIDTH OF DECK}}{\text{CENTRE SPAN}}$	$\eta = \frac{W \cdot A_X}{G \cdot I_X}$	STRUCTURE DESIGNATION	$\alpha = \frac{\text{SIDE SPAN}}{\text{CENTRE SPAN}}$	$\beta = \frac{\text{TOWER HEIGHT}}{\text{CENTRE SPAN}}$	$\nu = \frac{\text{WIDTH OF DECK}}{\text{CENTRE SPAN}}$	$\eta = \frac{W \cdot A_X}{G \cdot I_X}$
S 13	0.40	0.17	0.06015	$6.159 \times 10^{-6}$	S 19	0.40	0.30	0.06015	$6.159 \times 10^{-6}$
S 14	0.35	0.17	0.06015	$6.159 \times 10^{-6}$	S 20	0.40	0.17	0.04921	$6.159 \times 10^{-6}$
S 15	0.45	0.17	0.06015	$6.159 \times 10^{-6}$	S 21	0.40	0.17	0.07108	$6.159 \times 10^{-6}$
S 16	0.50	0.17	0.06015	$6.159 \times 10^{-6}$	S 22	0.40	0.17	0.06015	$5.543 \times 10^{-6}$
S 17	0.40	0.12	0.06015	$6.159 \times 10^{-6}$	S 23	0.40	0.17	0.06015	$6.929 \times 10^{-6}$
S 18	0.40	0.22	0.06015	$6.159 \times 10^{-6}$					

W = TOTAL LATERAL FORCE ON THE STRUCTURE,  $A_X$  = AREA OF CABLE,  
 G = ELASTIC MODULUS OF RIGIDITY,  $I_X$  = TORSIONAL RIGIDITY OF GIRDER CROSS-SECTION

FIG. 7.6 \_MATHEMATICAL MODEL OF STRUCTURES S13 TO S23

To compare the lateral deformations of the 6-cable system and equivalent 3-cable system the results of a test problem are given in table 7.20. It may be observed that the values in the main span for 6-cable system and equivalent 3-cable system are quite close. Therefore the parametric results of 3-cable systems can be used for the interpretation of behaviour of corresponding 6-cable systems.

TABLE 7.20 - COMPARISON OF LATERAL DEFORMATIONS OF 6-CABLE SYSTEM AND EQUIVALENT 3-CABLE SYSTEM

Node <sup>+</sup> No.	Lateral Deflections (m)		% Variation	Node <sup>+</sup> No.	Lateral Deflections (m)		% Variation
	6-cable system	3-cable system			6-cable system	3-cable system	
8	0.0145	0.0114	27	26	0.2190	0.2225	2
9	0.0141	0.0114	24	27	0.2194	0.2226	1
12	0.0267	0.020	34	30	0.2559	0.2585	1
13	0.0257	0.0195	32	31	0.2559	0.2585	1
16	0.1262	0.1103	14	32	0.0991	0.0831	19
17	0.1262	0.1103	14	33	0.0991	0.0831	19
18	0.0468	0.0356	31	34	0.0469	0.0357	31
19	0.0468	0.0356	31	35	0.0469	0.0357	31
22	0.1342	0.1330	1	36	0.0464	0.0354	31
23	0.1351	0.1334	1	37	0.0465	0.0354	31

+ Refer fig. 7.1

### 7.7.1 Details of Structures S13 to S23

The idealized mathematical model for structures S13 to S23 is shown in fig. 7.6. Geometrical properties of elements of S13 are given in table 7.21. Suitable changes in the data of S13 were done to obtain parametric variation for S14 to S23 tabulated in fig. 7.6.

The behaviour at nodes 4,5, 14, 15, 20 and 21 of 3-cable system shown in Fig. 7.6 would represent the behaviour at nodes 4, 5, 34, 35, 30 and 31 respectively for the structure in fig. 7.1. Likewise, the behaviour of members 3,4, 7, 8, 32 and 33 of fig. 7.6 would represent the behaviour of members 3, 4, 52, 53, 50 and 51 respectively of fig. 7.1.

### 7.7.2 Loadings L11 to L17

Lateral forces applied on S13 to S23 for parametric study are given in tables 7.22 to 7.28. The basis of calculation of these forces is the same as that used for loading L6.

### 7.7.3 Results

The results of parametric study are presented in figures 7.7 to 7.21. From the study of behaviour of S13 under the action of lateral forces (L11) it is observed that the force in top cables is two to three times greater than the force in other cables while the maximum force in a cable is only about 5% of the maximum axial force in a girder element. Girder elements near the tower and at the centre

TABLE 7.21 - GEOMETRICAL PROPERTIES OF MEMBERS OF S13

Member No. (fig. 7.6)	Length (m)	Area (m <sup>2</sup> )	Inertia-x (m <sup>4</sup> )	Inertia-Y (m <sup>4</sup> )	Inertia-Z (m <sup>4</sup> )
1	28.956	12.087	588.90	603.82	311.95
2	25.247	3.095	0.984	181.18	6.058
3,4	13.75	152.95	49.215	9059.1	302.89
5	21.945	32.311	3721.3	4284.8	1564.0
6	12.391	13.733	304.43	2195.9	105.3
7,8	18.00	686.65	15222.0	1.46x10 <sup>5</sup>	5265.1
9-14	61.009				
15-20	76.215	0.35	0.30	0.30	0.50
21,22	40.104	0.475	1.189	1.181	0.818
23,24	38.302	0.569	1.655	1.432	1.195
25,26	25.271	0.689	2.173	1.774	1.605
27	27.5	0.199	0.301	0.154	0.584
28	30.78				
29	27.5	0.236	0.435	0.189	1.176
30,31	3.21				
32,33	0.44	0.219	0.435	0.254	1.176
34,35	27.5	0.584	0.15x10 <sup>-3</sup>	0.018	0.503
36-39	27.5	0.73	0.20x10 <sup>-3</sup>	0.022	0.629
40-42	66.92	0.577	0	0	0
43-45	81.03	0.563	0	0	0
46,47	201.76	0.04	0	0	0
48,49	147.37	0.04	0	0	0
50,51	100.85	0.04	0	0	0
52,53	107.89	0.04	0	0	0
54,55	169.79	0.04	0	0	0
56,57	240.08	0.04	0	0	0

TABLE 7.22 - LATERAL FORCES (L11) APPLIED TO S13,  
S20 TO S23

Node no. (fig.7.6)	Lateral Force (t)	Node No. (fig.7.6)	Lateral Force (t)	Node No. (fig.7.6)	Lateral Force (t)
2	15.95	13	34.22	24	31.14
4	45.09	16	145.69	25	31.14
6	116.56	18	145.69	26	20.87
8	116.56	20	72.85	27	20.87
10	131.12	22	60.77	29	13.30
12	34.22	23	60.77		

TABLE 7.23 - LATERAL FORCES (L12) APPLIED TO S14

Node no. (fig.7.6)	Lateral Force (t)	Node no. (fig.7.6)	Lateral Force (t)	Node no. (fig.7.6)	Lateral Force (t)
2	15.95	13	34.22	24	31.14
4	40.67	16	154.53	25	31.14
6	107.72	18	154.53	26	20.87
8	107.72	20	77.27	27	20.87
10	131.12	22	60.77	29	13.30
12	34.22	23	60.77		



TABLE 7.24- LATERAL FORCES (L13) APPLIED TO S15

Node No. (fig.7.6)	Lateral Force (t)	Node No. (fig.7.6)	Lateral Force (t)	Node No. (fig.7.6)	Lateral Force (t)
2	15.95	13	34.22	24	31.14
4	48.92	16	138.03	25	31.14
6	124.22	18	138.03	26	20.87
8	124.22	20	69.01	27	20.87
10	131.12	22	60.77	29	13.30
12	34.22	23	60.77		

TABLE 7.25 - LATERAL FORCES (L14) APPLIED TO S16

Node No. (fig.7.6)	Lateral Force (t)	Node No. (fig.7.6)	Lateral Force (t)	Node No. (fig.7.6)	Lateral Force (t)
2	15.95	13	34.22	24	31.14
4	52.37	16	131.13	25	31.14
6	131.13	18	131.13	26	20.87
8	131.13	20	65.56	27	20.87
10	131.13	22	60.77	29	13.30
12	34.22	23	60.77		

TABLE 7.26 - LATERAL FORCES (L15) APPLIED TO S17

Node <sup>+</sup> no.	Lateral Force (t)	Node <sup>+</sup> No.	Lateral Force (t)	Node <sup>+</sup> No.	Lateral Force (t)
2	15.95	13	22.81	24	31.08
4	45.09	16	145.69	25	31.08
6	116.56	18	145.69	26	20.87
8	116.56	20	72.85	27	20.87
10	131.12	22	40.54	29	13.30
12	22.81	23	40.54		

+ Refer fig. 7.6

TABLE 7.27 - LATERAL FORCES (L16) APPLIED TO S18

Node <sup>+</sup> No.	Lateral Force (t)	Node <sup>+</sup> no.	Lateral Force (t)	Node <sup>+</sup> No.	Lateral Force (t)
2	15.95	13	44.78	28	46.91
4	45.09	16	145.69	25	46.91
6	116.56	18	145.69	26	20.87
8	116.56	20	72.85	27	20.87
10	131.12	22	80.39	29	13.30
12	44.78	23	80.39		

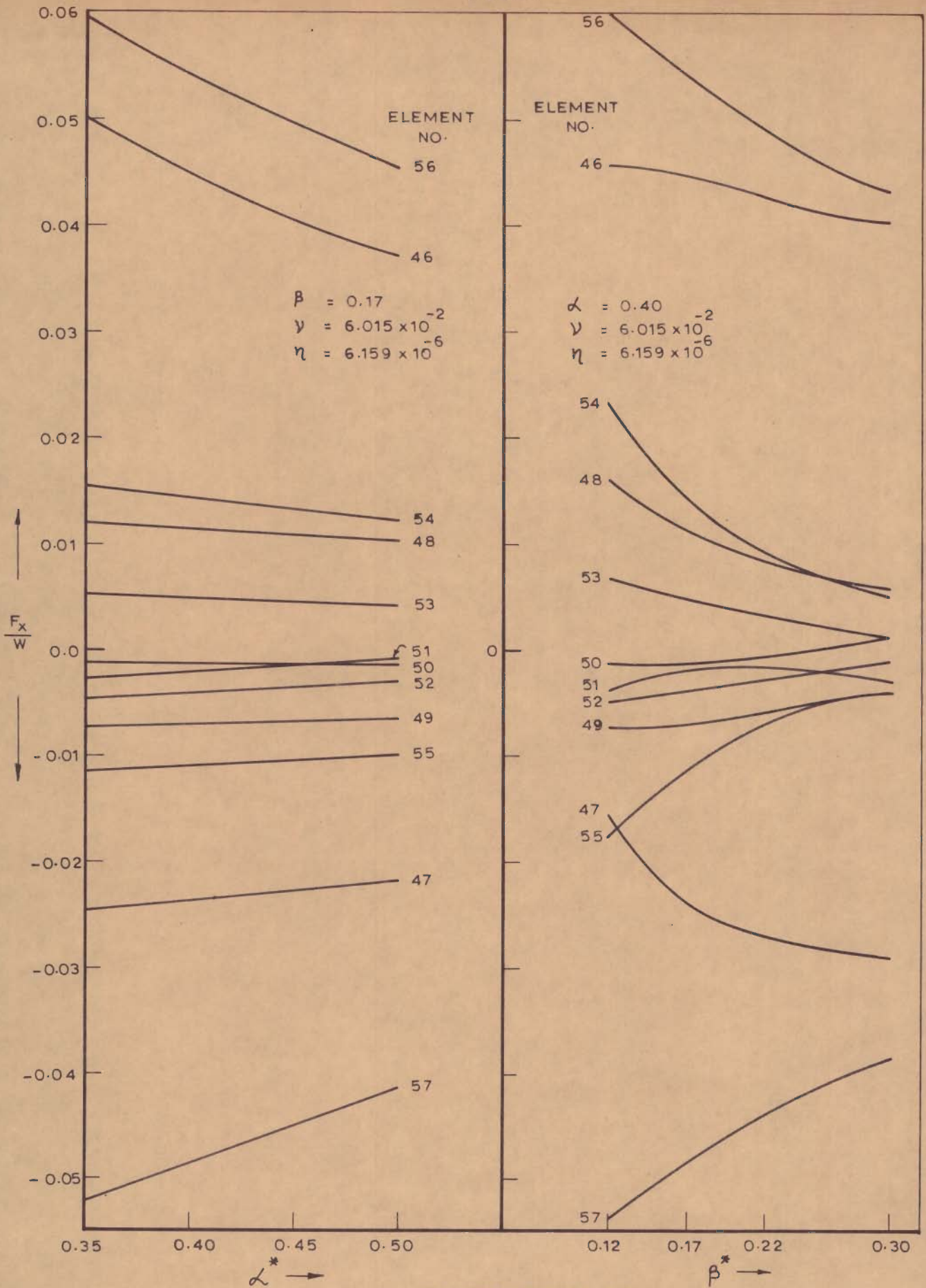
+ Refer fig. 7.6

TABLE 7.28 - LATERAL FORCES (L17) APPLIED TO S19

Node <sup>+</sup> No.	Lateral Force (t)	Node <sup>+</sup> No.	Lateral Force (t)	Node <sup>+</sup> No.	Lateral Force (t)
2	15.95	13	62.25	24	60.10
4	45.09	16	145.69	25	60.10
6	116.56	18	145.69	26	20.87
8	116.56	20	72.85	27	20.87
10	131.12	22	114.23	29	13.30
12	62.25	23	114.23		

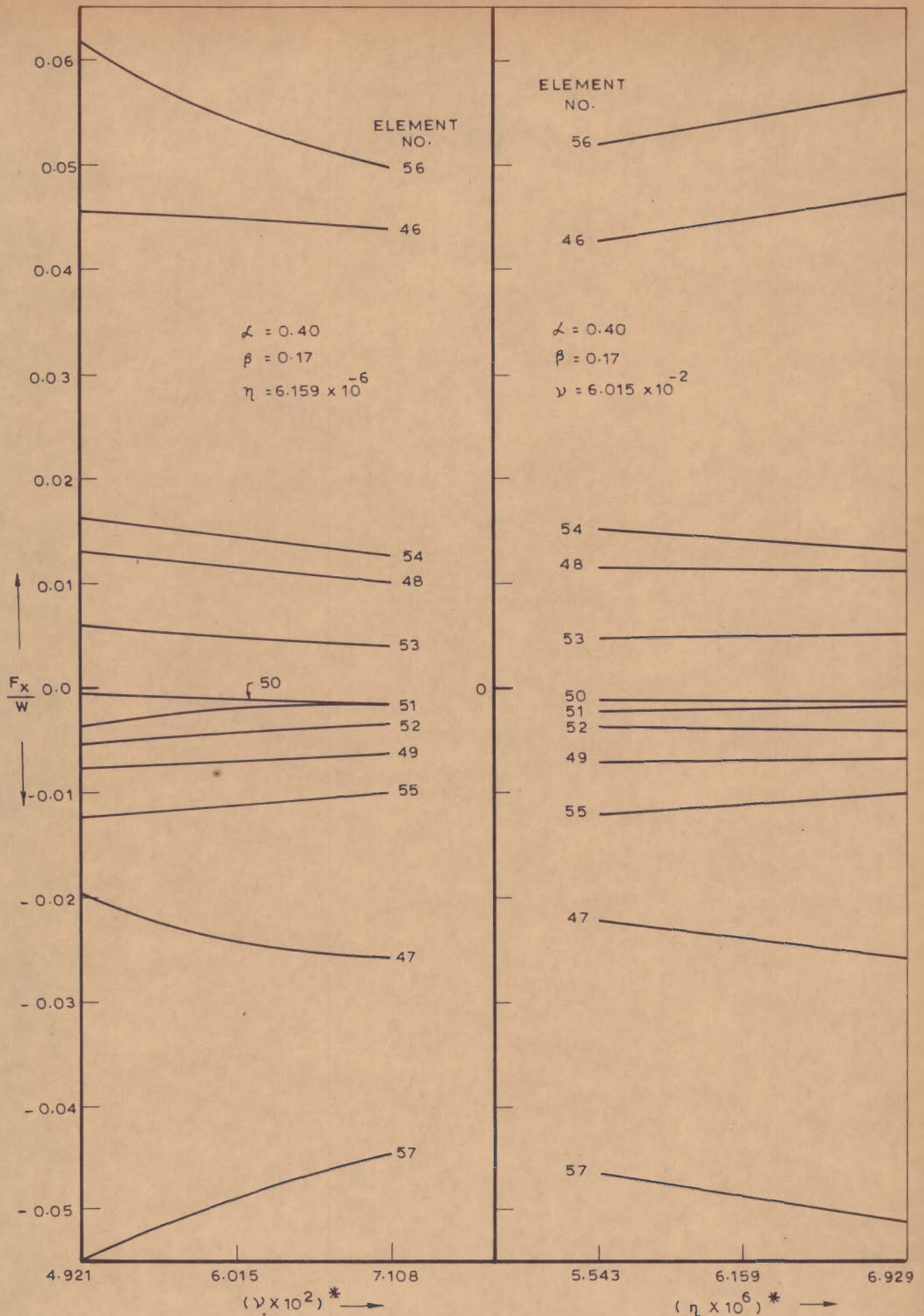
+Refer fig. 7.6

of the main span carry axial forces which are three times higher than the axial forces in other girder elements. Girder shears are less than 1% of the maximum girder axial force and the maximum girder moment about a vertical axis is about six times the maximum torsional moment in the girder and twice the maximum girder moment about horizontal axis of the girder cross-section. Maximum axial force and maximum shear in a tower leg is about two-thirds of the maximum axial force in a girder element. Maximum moment in a tower leg about an axis parallel to the transverse axis of the bridge is three times the maximum moment about an axis parallel to longitudinal axis of the bridge and about twenty times the maximum twisting moment of the tower leg. Following further observations, can be made with regard to effect of various



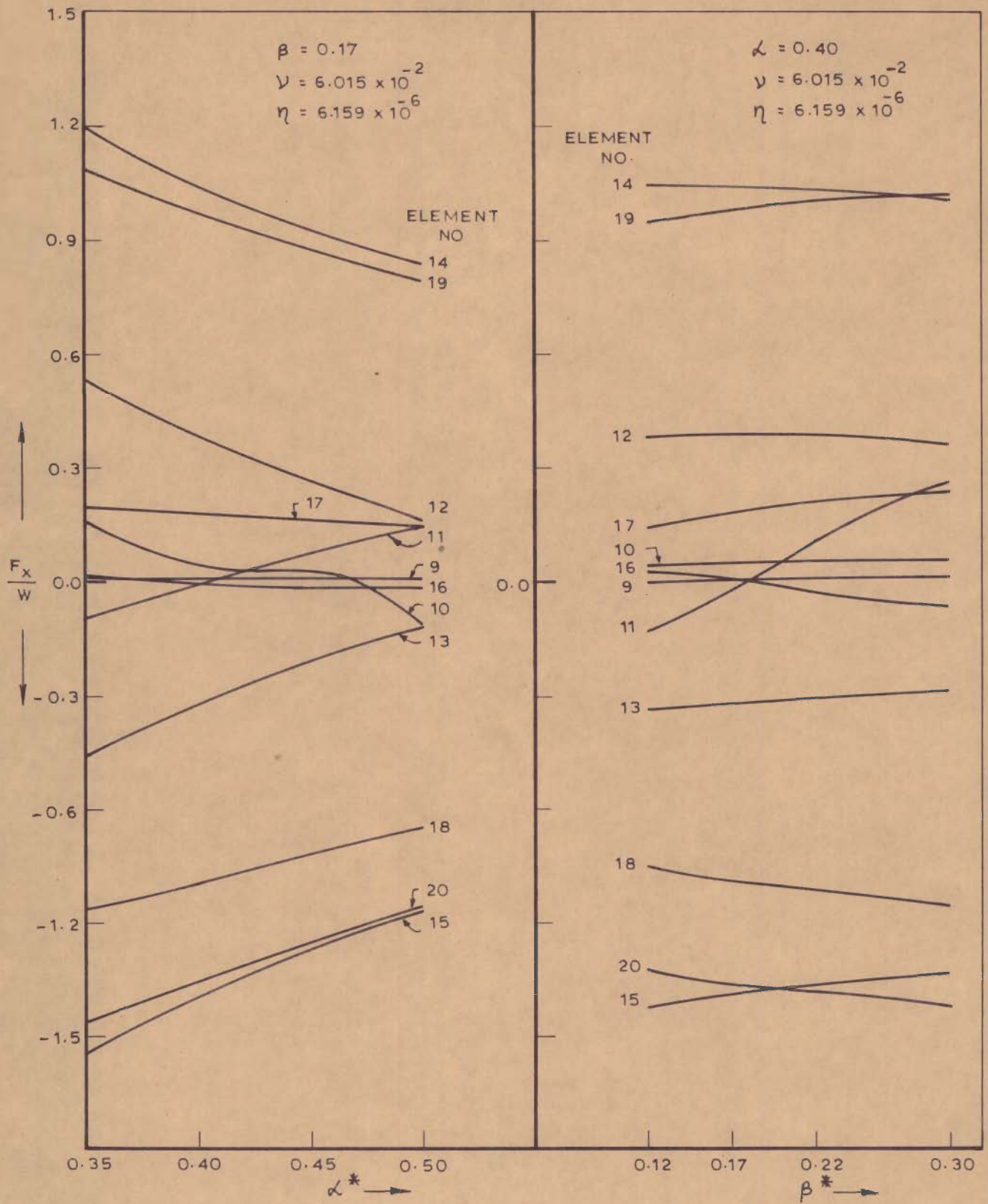
\* -REFERRED TO FIG. 7.6

FIG. 7.7 - VARIATION OF CABLE FORCES WITH  $\alpha, \beta$  UNDER UNIFORM WIND LOAD



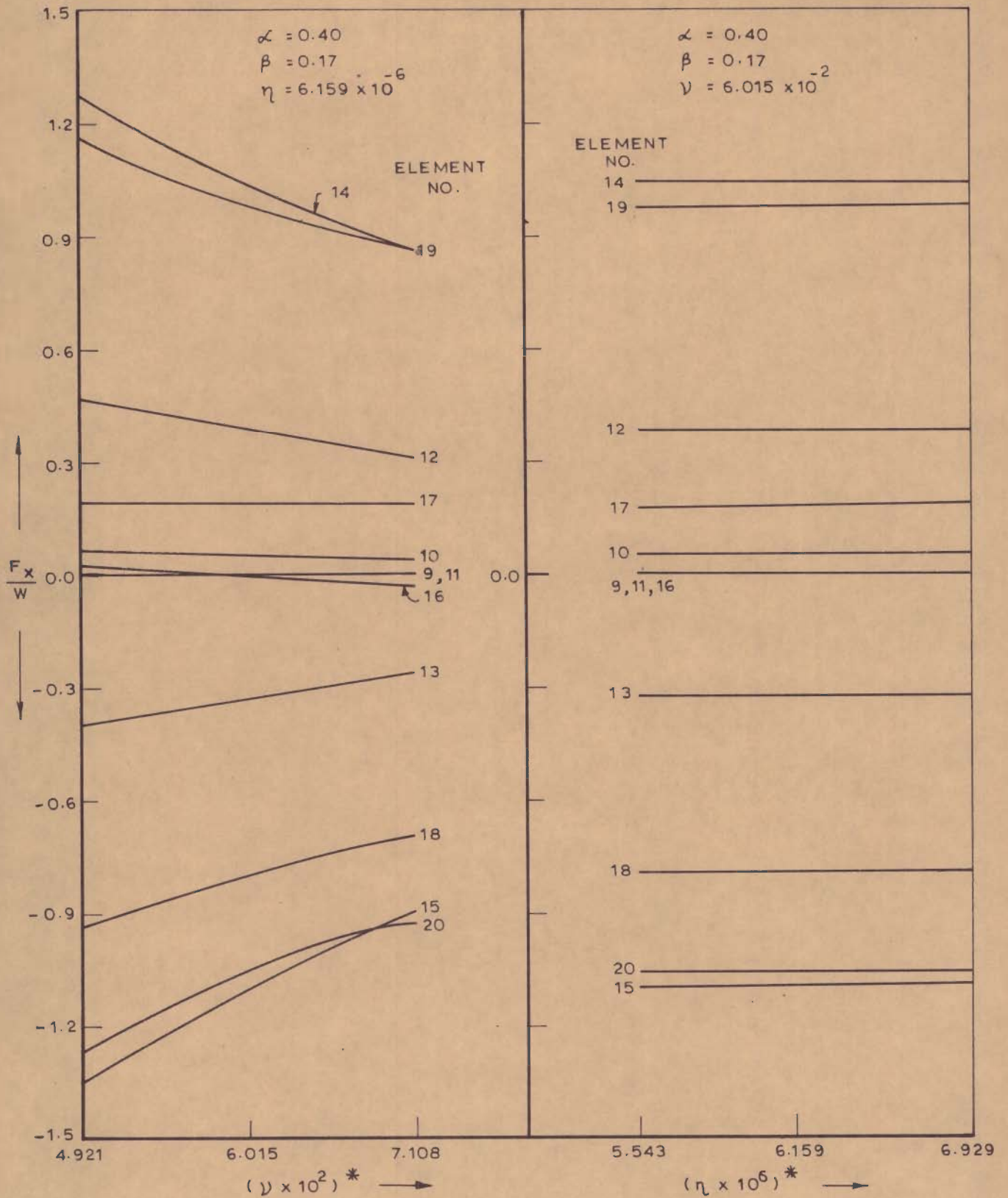
\* - REFERRED TO FIG. 7.6

FIG. 7.8 - VARIATION OF CABLE FORCES WITH  $\gamma, \eta$  UNDER UNIFORM WIND LOAD



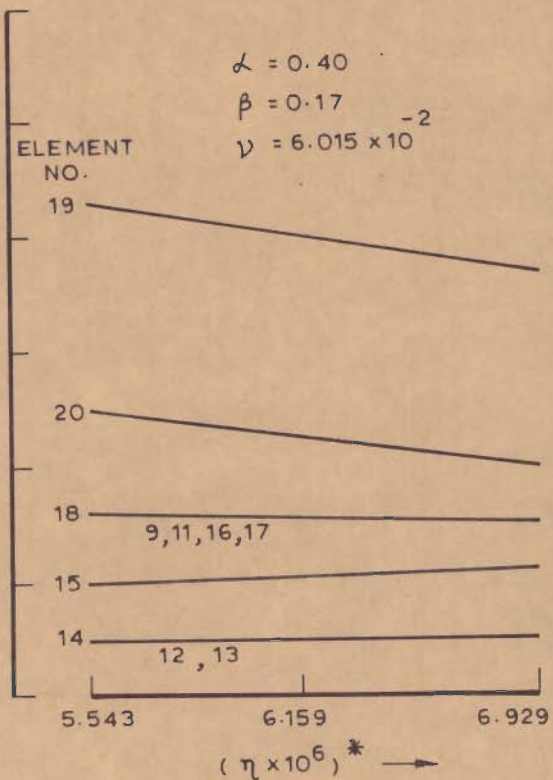
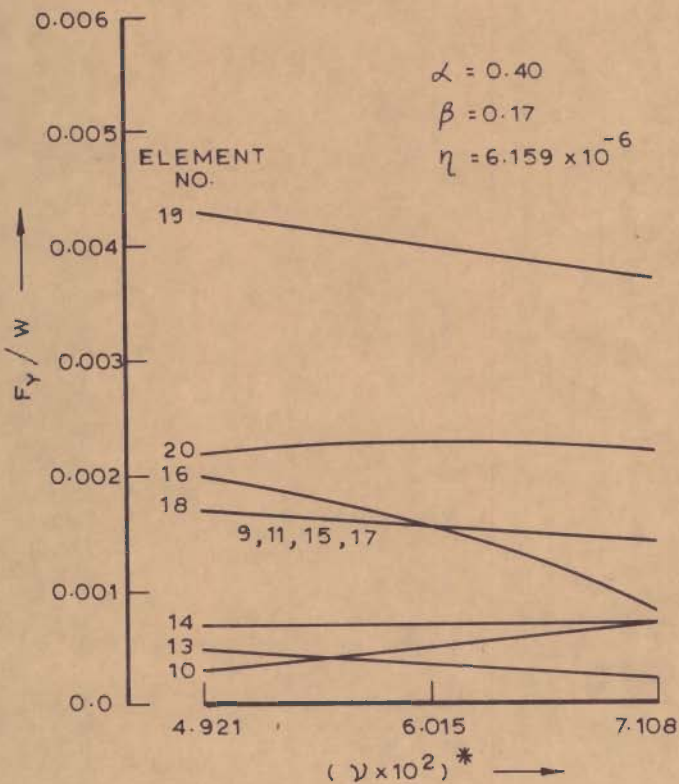
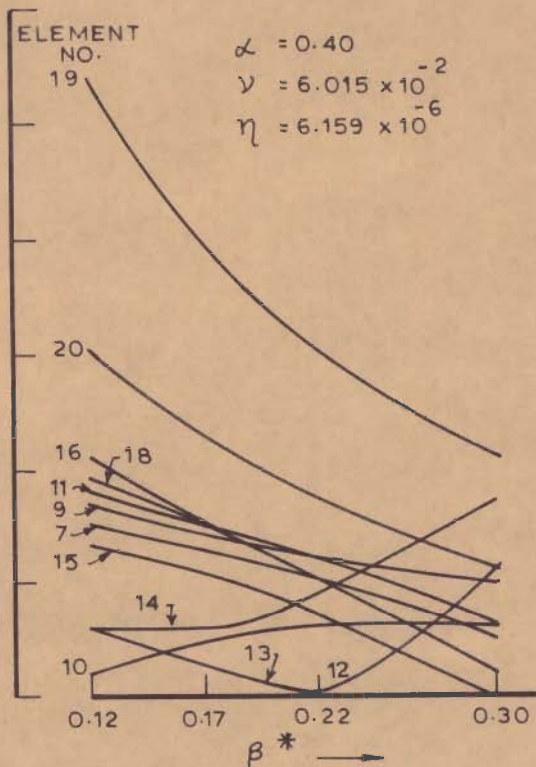
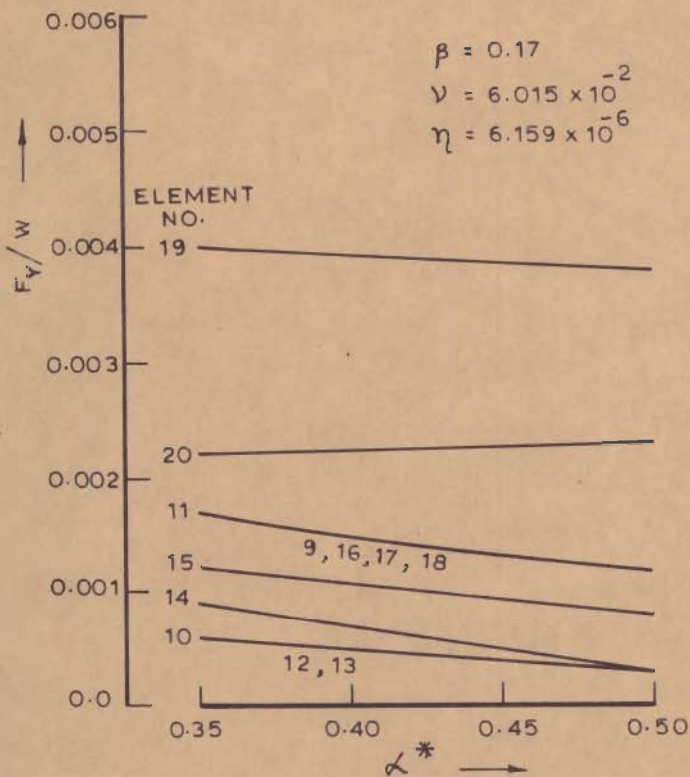
\* - REFERRED TO FIG. 7.6

FIG. 7.9 - VARIATION OF AXIAL FORCES IN MAIN GIRDER ELEMENTS WITH  $\alpha, \beta$  UNDER UNIFORM WIND LOAD



\* - REFERRED TO FIG. 7.6

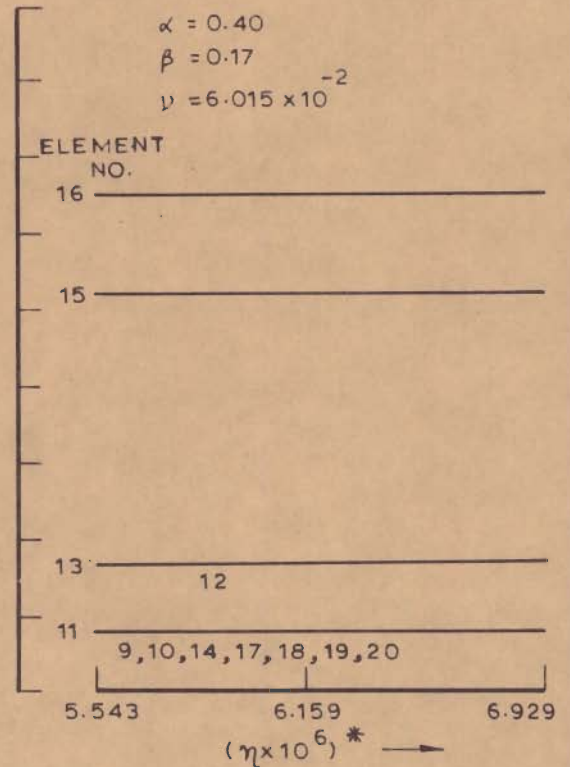
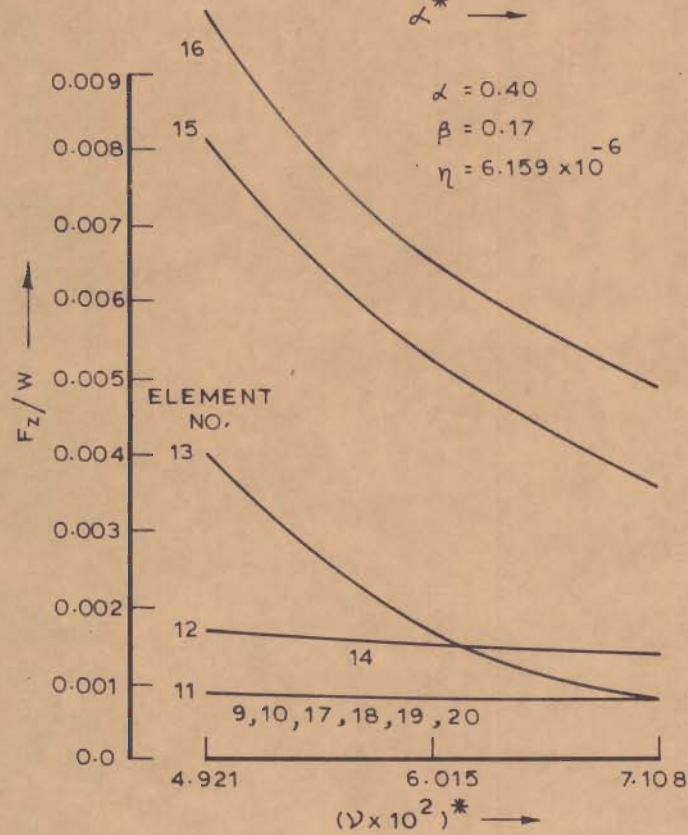
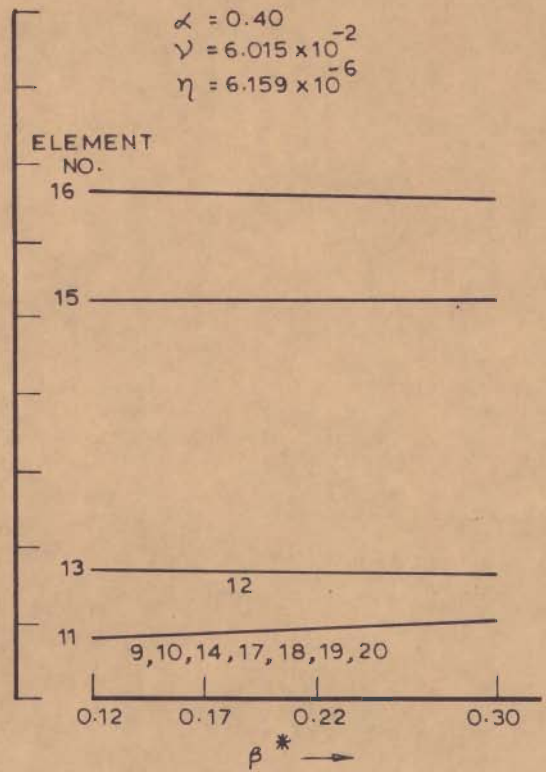
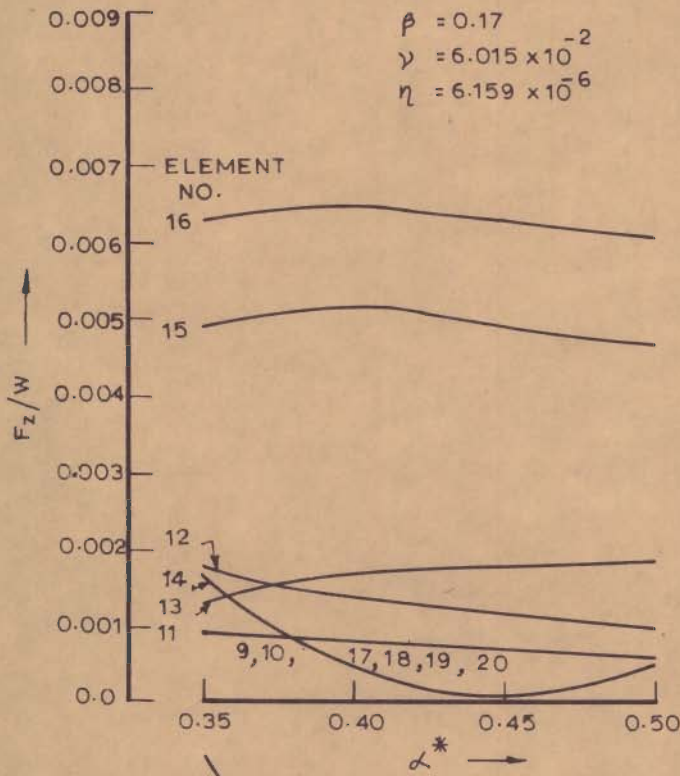
FIG. 7.10 VARIATION OF AXIAL FORCES IN MAIN GIRDER ELEMENTS WITH  $\nu, \eta$  UNDER UNIFORM WIND LOAD



\* - REFERRED TO FIG. 7.6

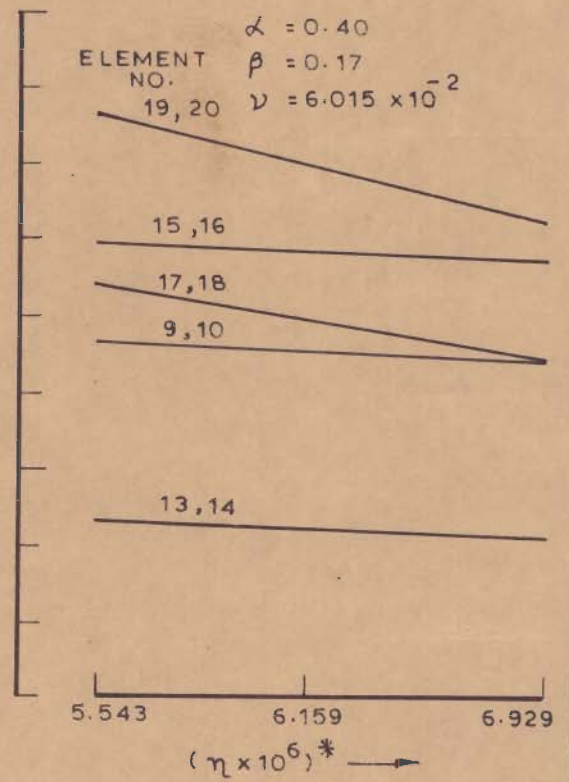
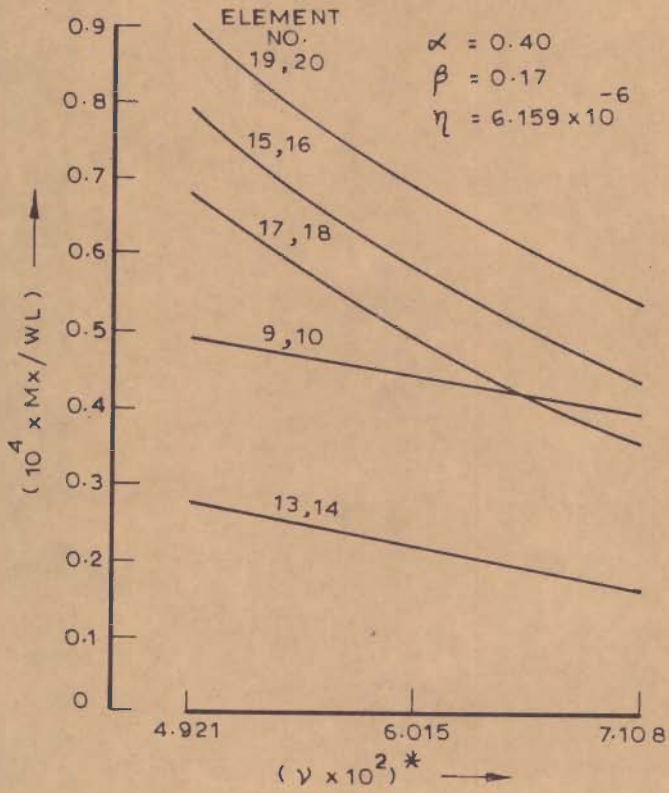
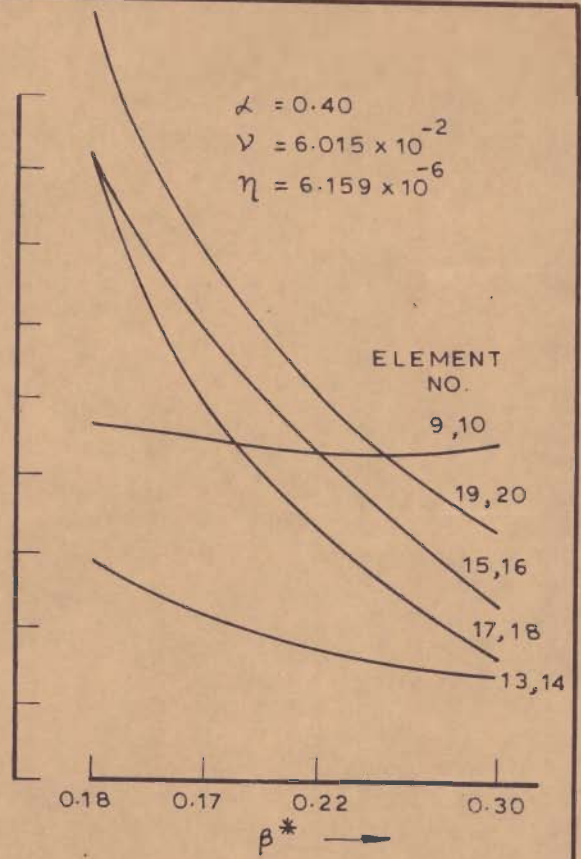
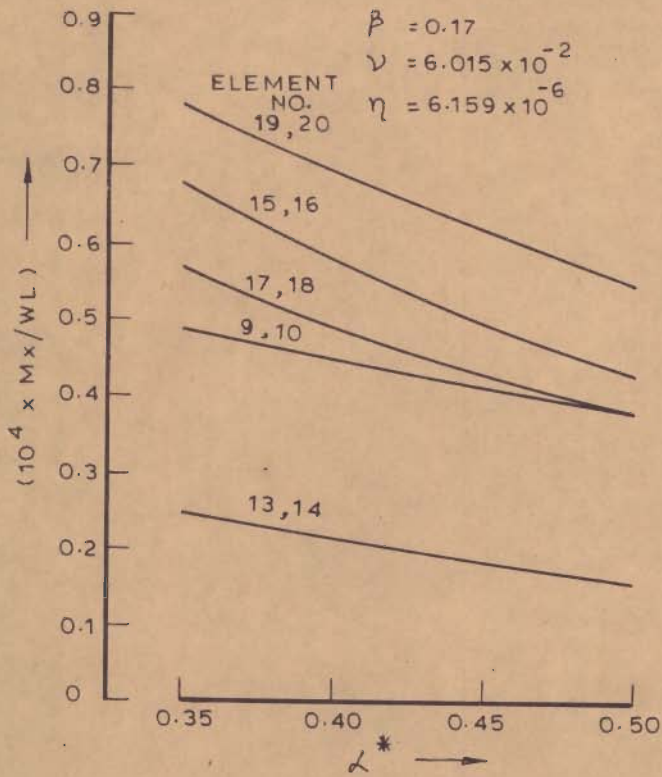
FIG. 7.11 - VARIATION OF VERTICAL SHEARS IN MAIN GIRDER ELEMENTS UNDER UNIFORM WIND LOAD





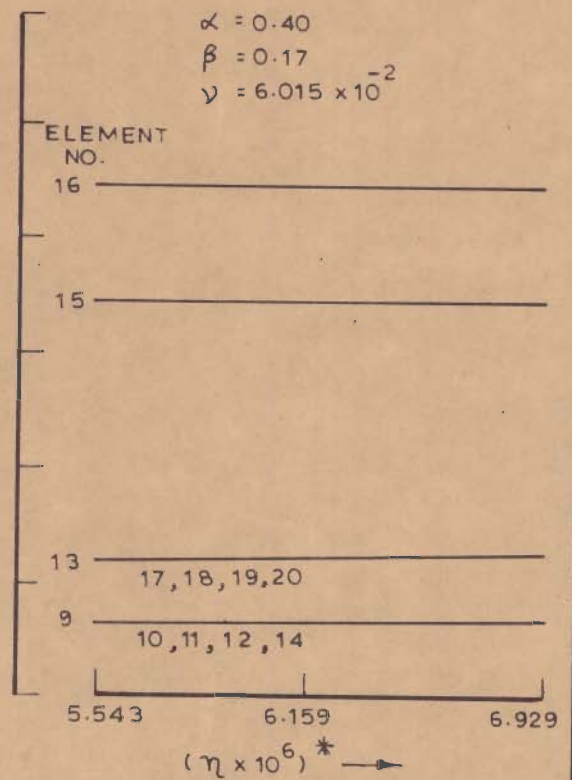
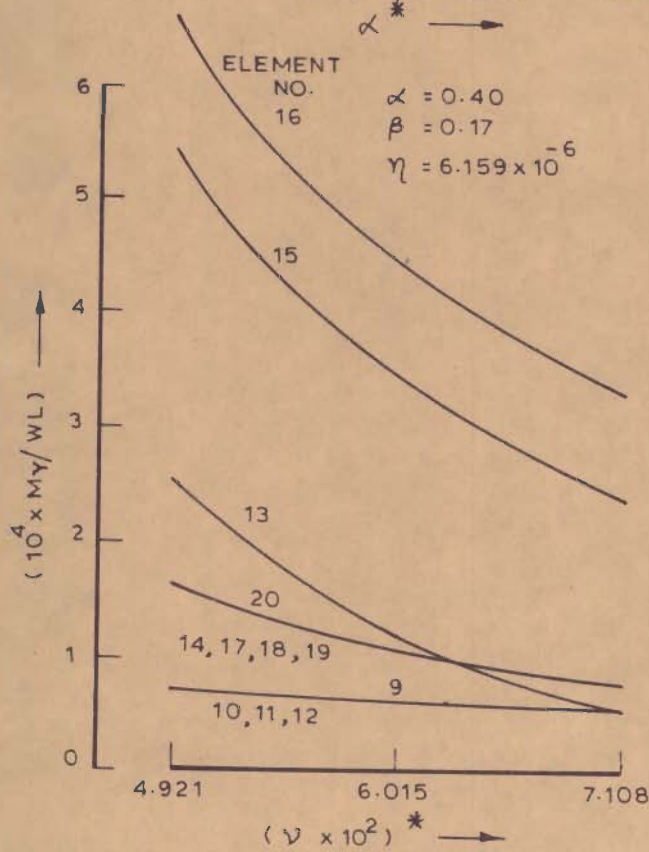
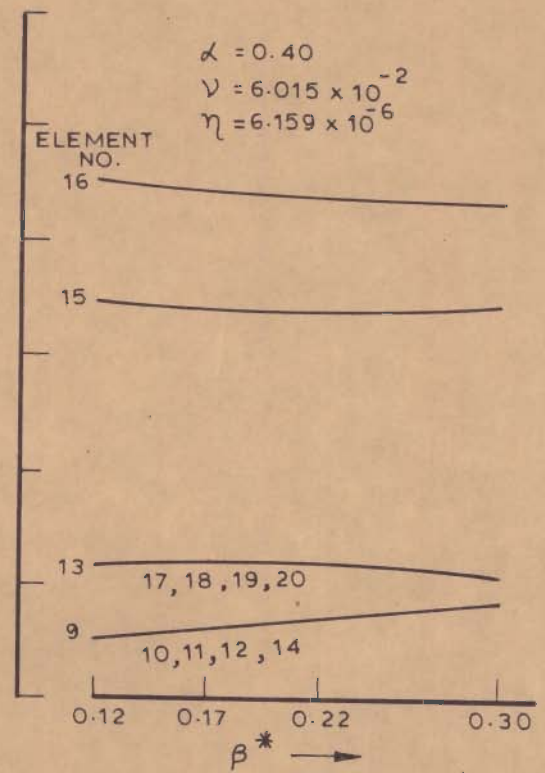
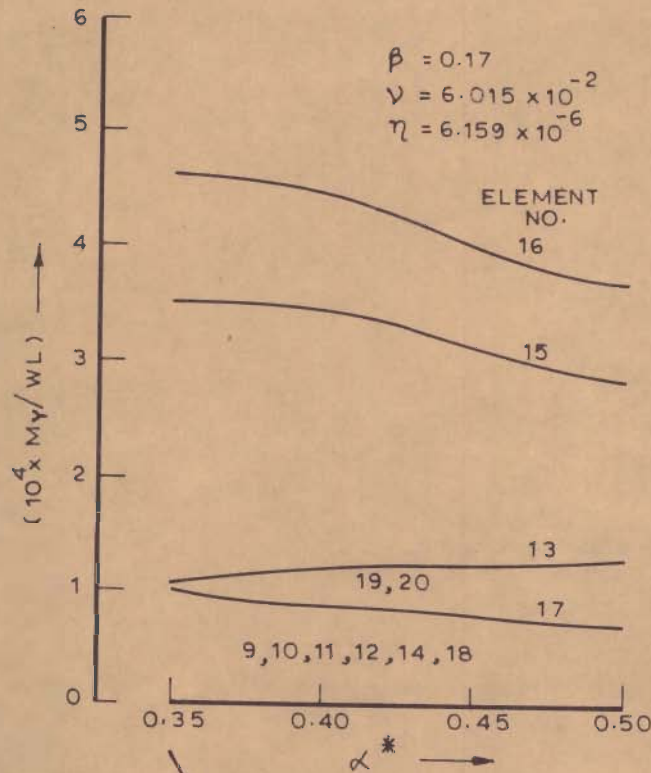
\* - REFERRED TO FIG. 7.6

FIG. 7.12 - VARIATION OF HORIZONTAL SHEARS IN MAIN GIRDER ELEMENTS UNDER UNIFORM WIND LOAD



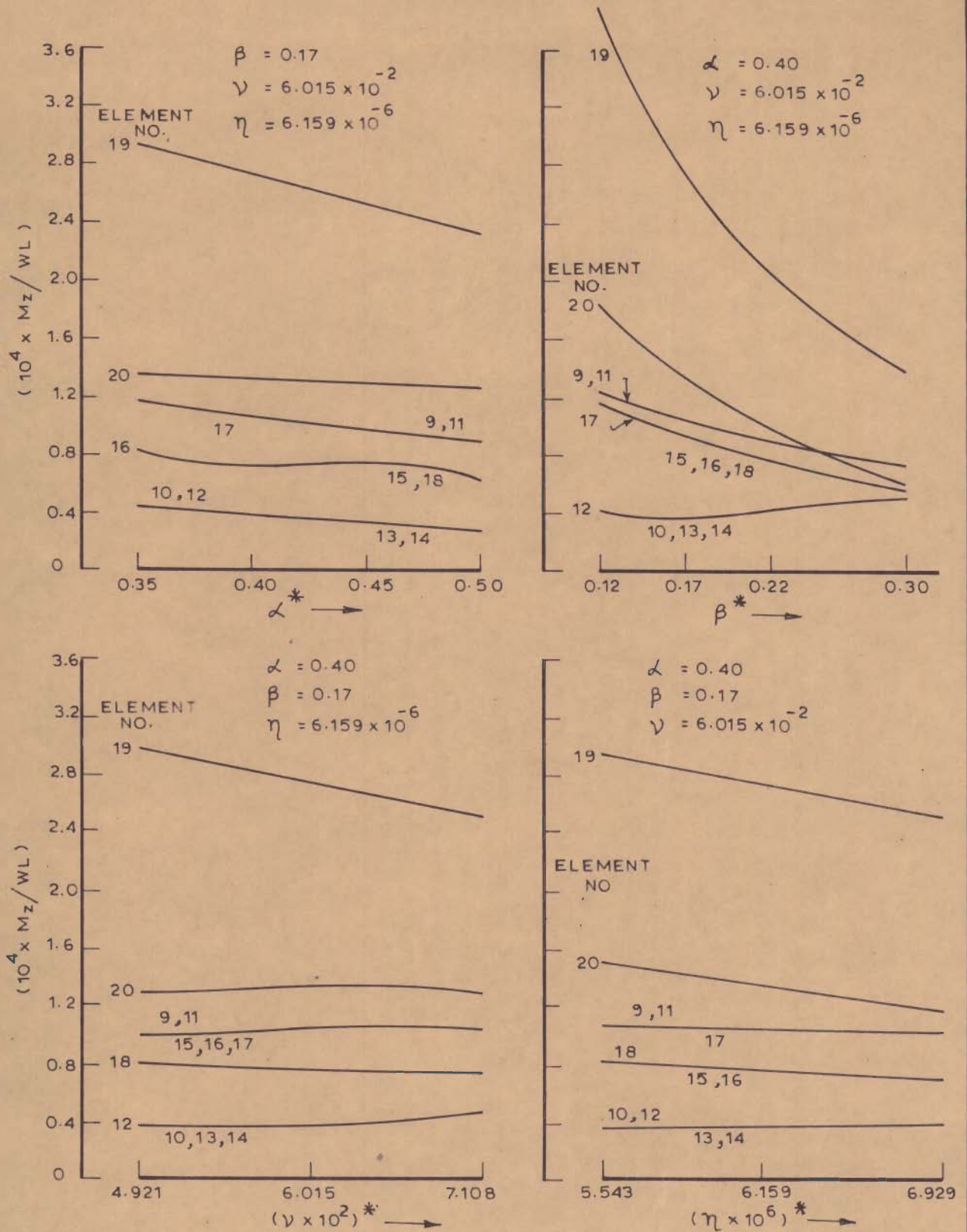
\* - REFERRED TO FIG. 7.6

FIG. 7.13 - VARIATION OF TWISTING MOMENTS IN MAIN GIRDER ELEMENTS UNDER UNIFORM WIND LOAD



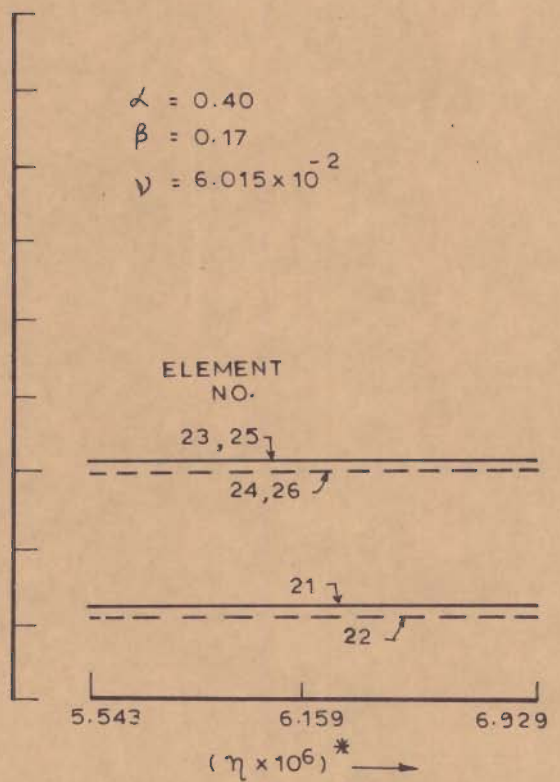
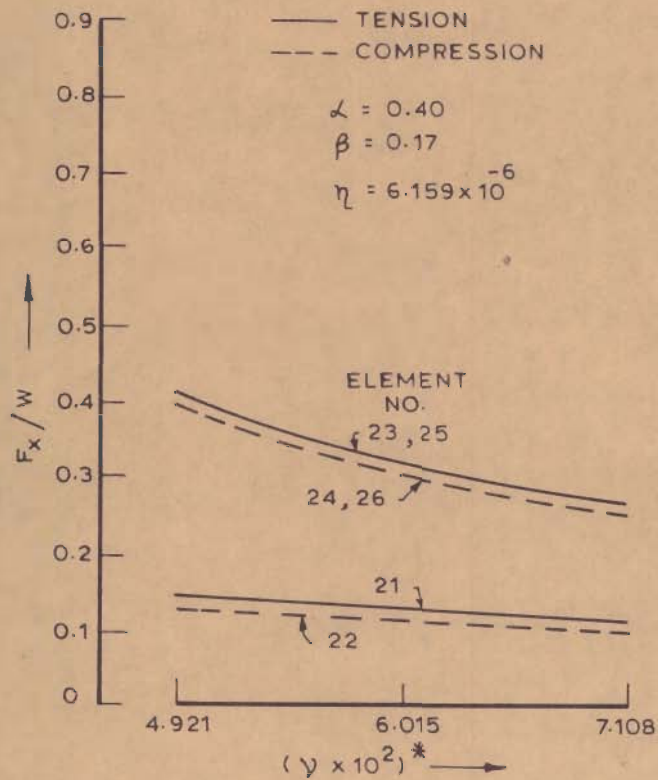
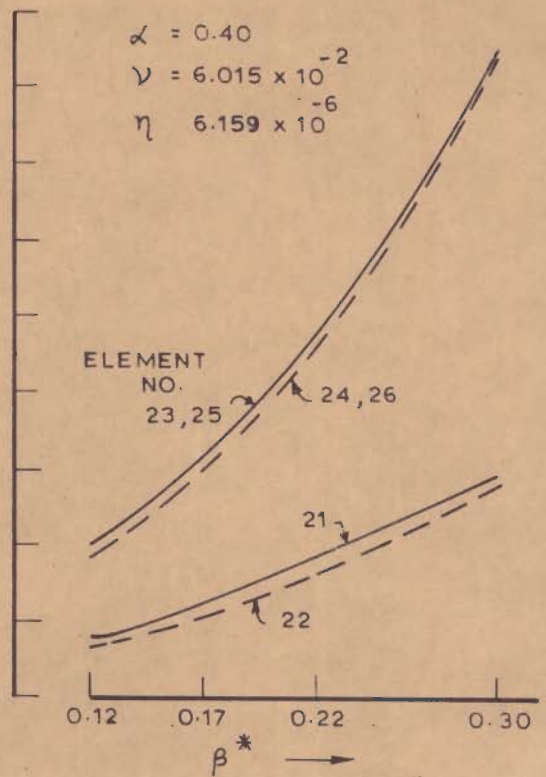
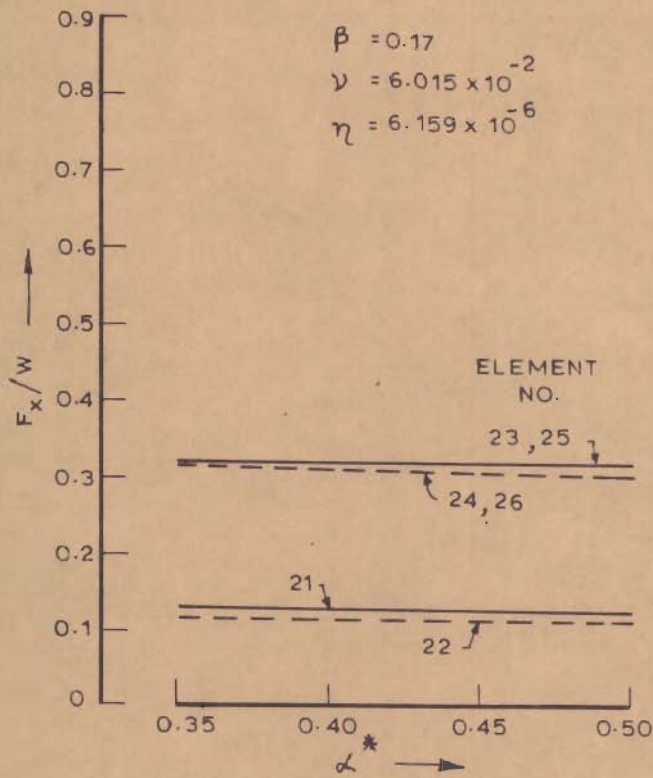
\* REFERRED TO FIG. 7.6

FIG. 7.14\_VARIATION OF MOMENTS ABOUT VERTICAL AXIS IN GIRDER ELEMENTS UNDER UNIFORM WIND LOAD



\* - REFERRED TO FIG. 7.6

FIG. 7.15 - VARIATION OF MOMENTS ABOUT HORIZONTAL AXIS IN GIRDER ELEMENTS UNDER UNIFORM WIND LOAD



\* - REFERRED TO FIG. 7.6

FIG. 7.16\_VARIATION OF AXIAL FORCES IN TOWER LEGS UNDER UNIFORM WIND LOADS

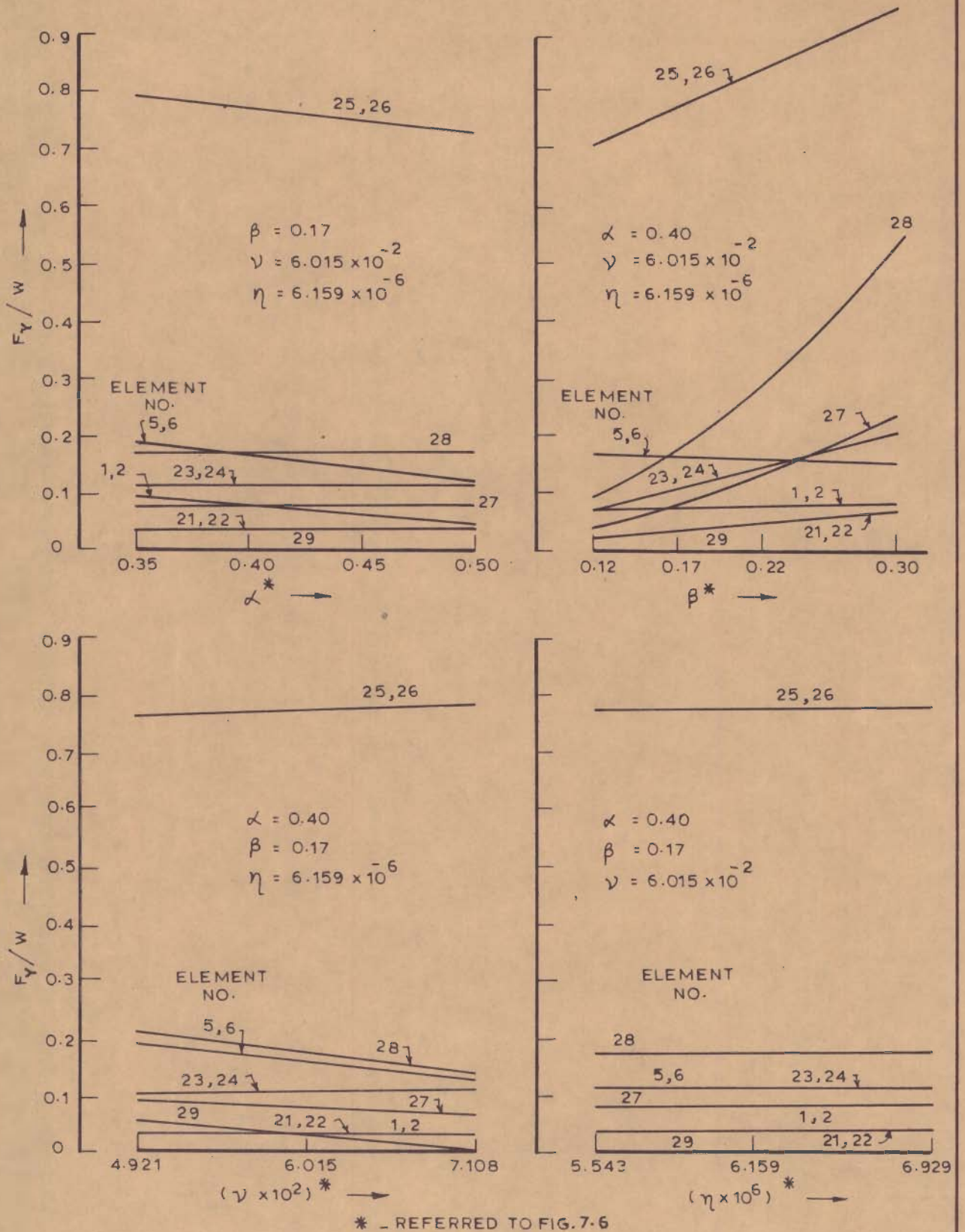
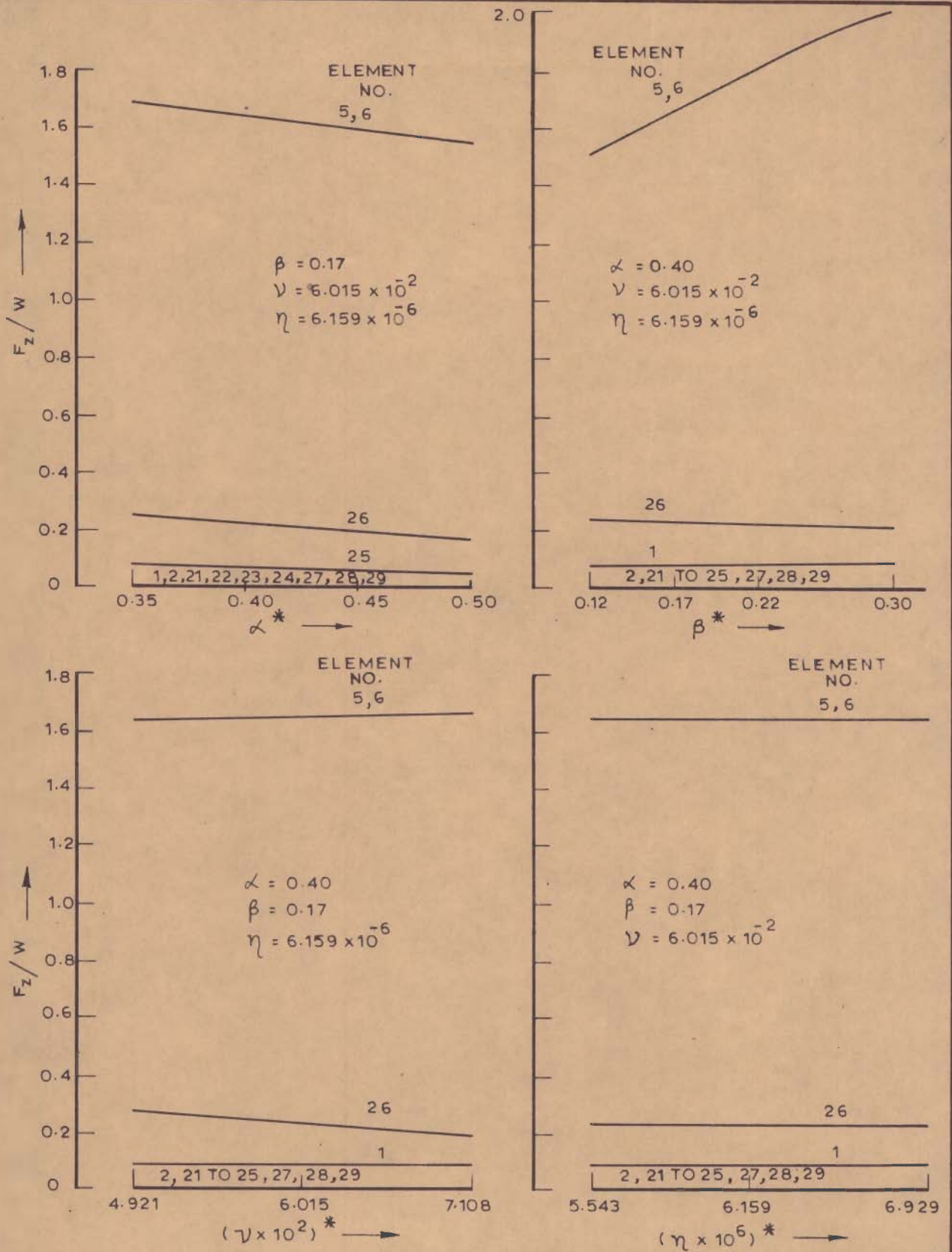
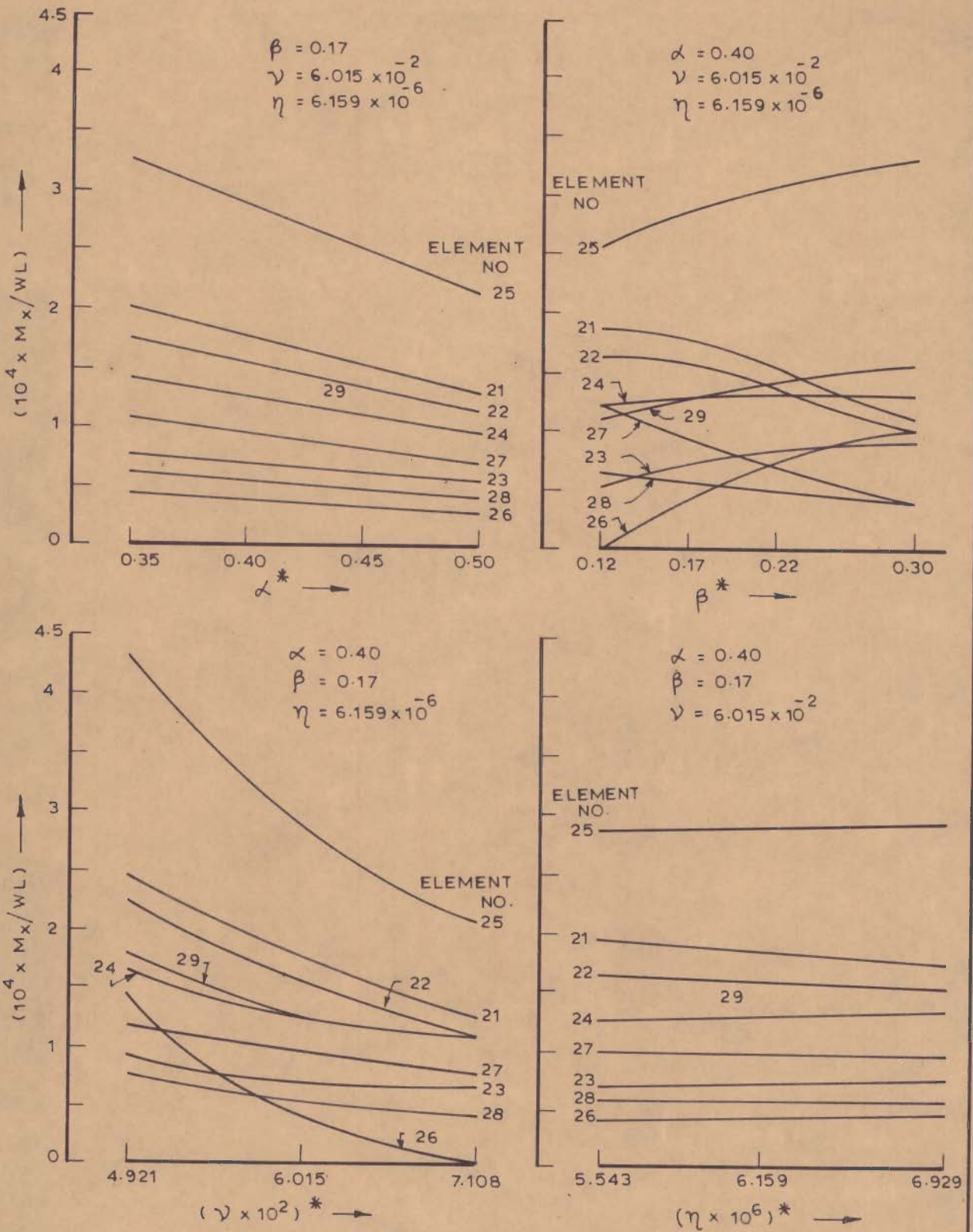


FIG. 7.17 - VARIATION OF SHEARS F-Y (MEMBER AXES) IN TOWER LEGS, PORTALS, PIERS & WELLS UNDER UNIFORM WIND LOAD



\* - REFERRED TO FIG 7.6

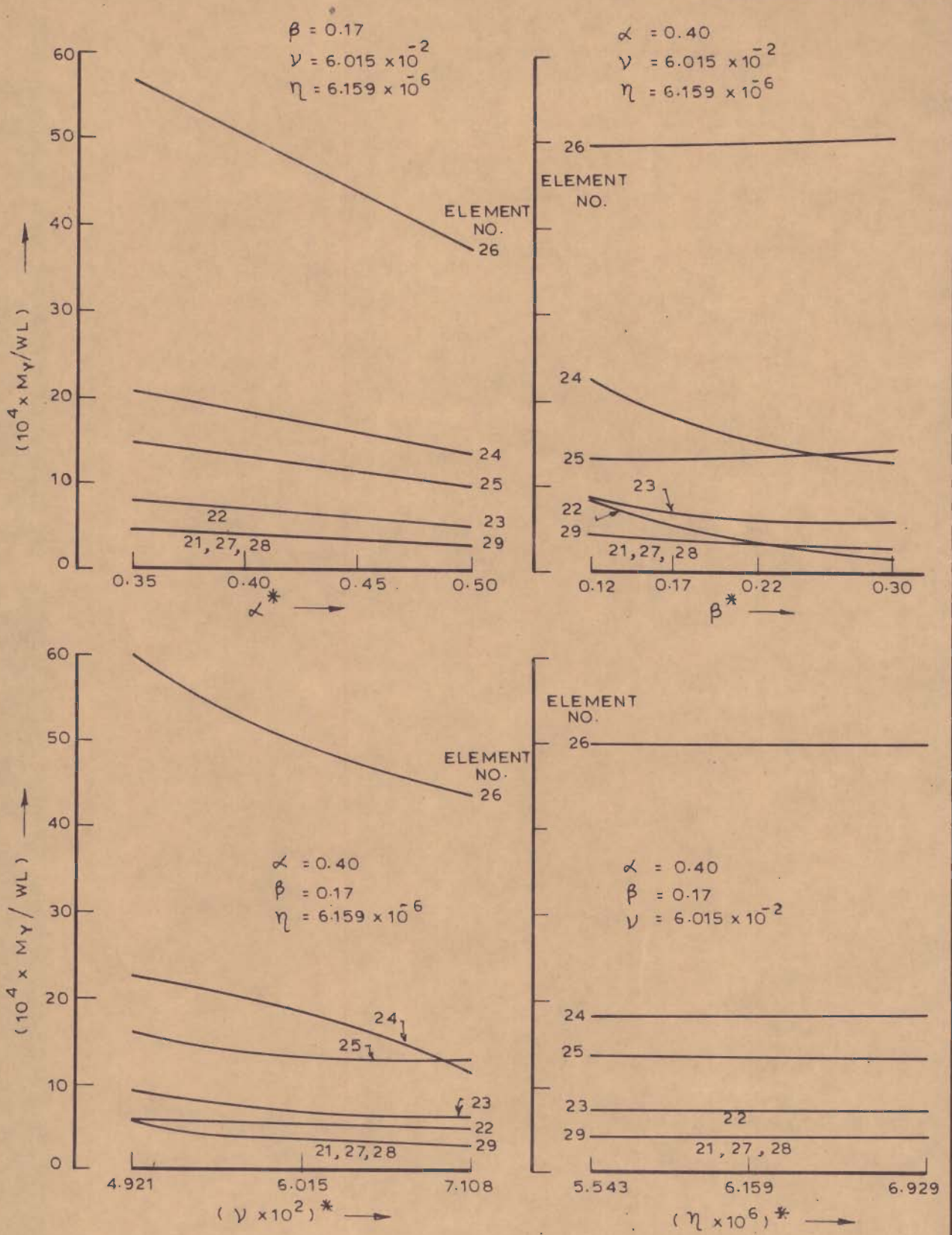
FIG. 7.18 - VARIATION OF SHEARS  $F_z$  (MEMBER AXES) IN TOWER LEGS, PORTALS, PIERS & WELLS UNDER UNIFORM WIND LOAD



\* - REFERRED TO FIG. 7.6

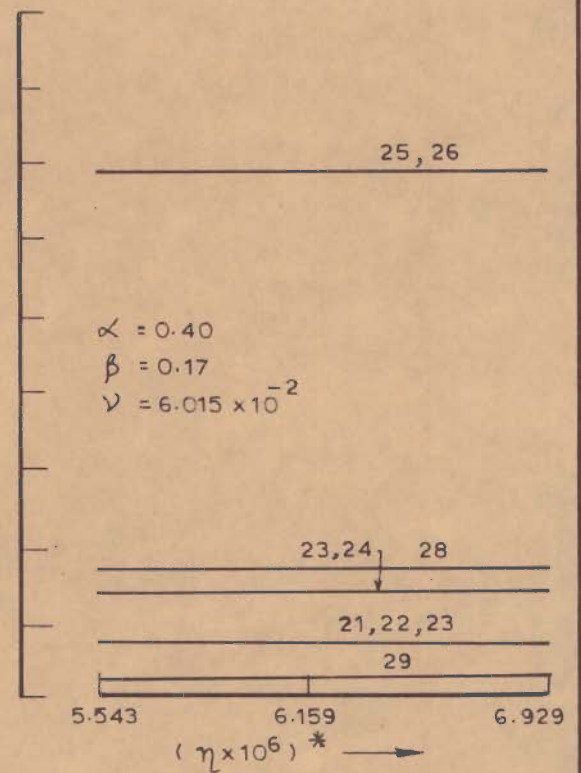
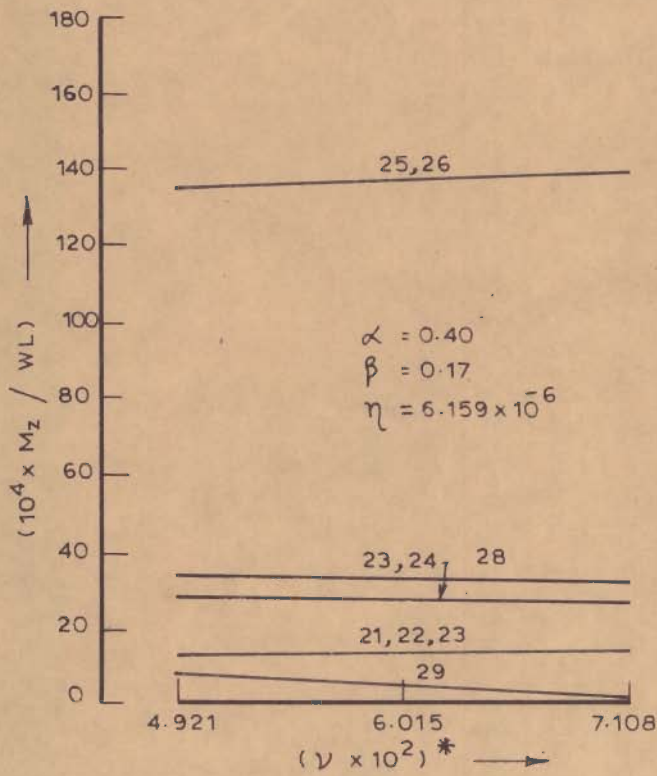
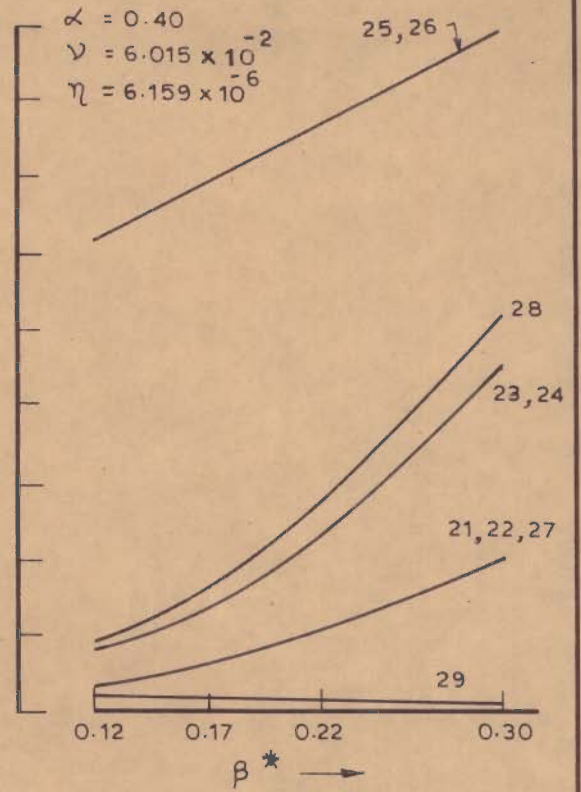
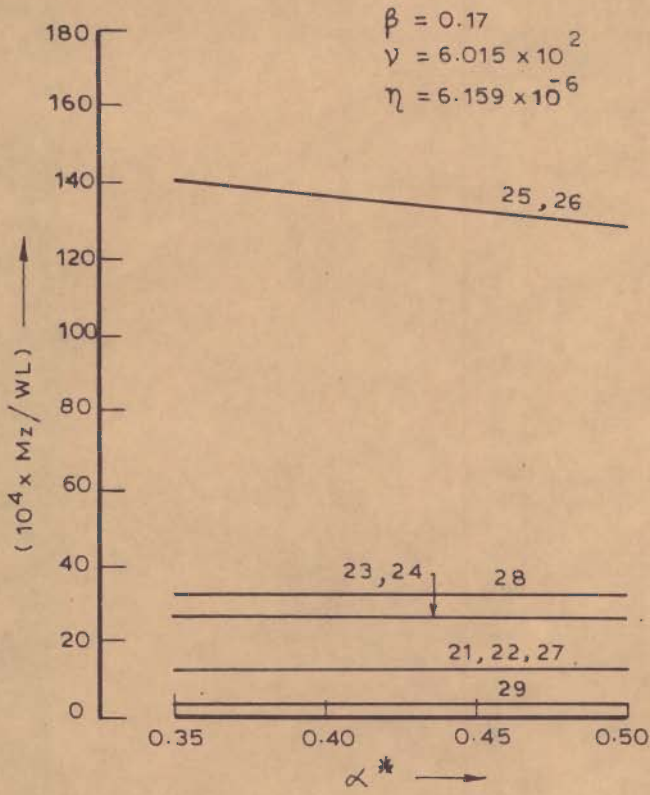
FIG. 7.19 - VARIATION OF TWISTING MOMENTS IN TOWER LEGS & PORTALS UNDER UNIFORM WIND LOAD





\* - REFERRED TO FIG.7.6

FIG.7.20 - VARIATION OF MOMENTS M-Y (MEMBER AXES) IN TOWER LEGS & PORTALS UNDER UNIFORM WIND LOAD



\* - REFERRED TO FIG. 7.6

FIG. 7. 21 - VARIATION OF MOMENTS M-Z (MEMBER AXES) IN TOWER LEGS, PORTALS UNDER UNIFORM WIND LOADS

parameters on the behaviour of the bridge under lateral forces.

(i) Axial forces in cables, axial forces, shears and moments in girder elements and shears and moments in tower legs decrease with the increase of the ratio of side span to centre span while the axial forces in tower legs increase.

(ii) Axial forces in cables and shears and moments in girder elements decrease while axial forces, shears and moments in tower legs and axial forces in girder elements increase with the increase in the ratio of tower height to centre span.

(iii) As the ratio of deck width to main span increases, the axial forces in cables, axial forces, shears and moments in girder elements and axial forces, twisting moment and moment about the axis of the tower legs parallel to the longitudinal axis of the bridge decrease whereas shears and moments about the axis of the tower legs parallel to transverse axis of the bridge increase.

(iv) As the total cable area increases in relation to torsional rigidity of girder elements, cable forces tend to increase but shears, twisting moment and the moment about axis parallel to transverse axis of the bridge in the cross-section of the girder element decrease. Other forces in the girder elements and tower legs remain unchanged due to change in this ratio.

## 7.8 SUMMARY

The results of the analysis of radiating type cable-stayed bridges as space frames, under the action of eccentric vertical live loads and lateral wind forces as interpreted and discussed in this chapter are summarized below.

### A. Behaviour Under Eccentric Vertical Loads

(i) The pattern of forces and deformations of the bridge obtained from plane frame analysis under the action of full live loads and that obtained from space frame analysis (loaded side of the bridge considered) under the action of half the live loads applied on the axis of one of the two main girders is more or less similar.

(ii) The space action, by way of transfer of loads on the unloaded side, is observed to be activated more in 3-span system than in the 5-span system. This may be attributed to the greater longitudinal flexibility of the 3-span system relative to the 5-span system.

(iii) Axial forces on the unloaded side of the girder elements near tower are about 10 to 20 percent of these on the loaded side while they have equal and opposite values in the elements near centre of the main span due to horizontal bending of the main span. Other forces and deformations in the elements of unloaded side also vary, in general, from 10 to 25 percent of the corresponding value on loaded side.

(iv) Effect of soil-structure interaction may be considered significant on the behaviour of substructure of the bridge but the effects are insignificant on the behaviour of the superstructure.

#### B. Behaviour Under Lateral Forces

(i) Cables (in vertical plane) as well as the elements of substructure are subjected to negligible axial forces.

(ii) Nature of axial forces is reverse, in general, in the windward and leeward elements of the bridge.

(iii) Bending moments in transverse direction of the bridge are low in the superstructure as compared to substructure. Heavy bending moments are induced at the base of the well below tower. Bending moment at the base of well at the end support is about  $1/30$  of the value at the base of well below tower.

(iv) Effect of soil-structure interaction is significant on the behaviour of the substructure of the bridge but the effects are insignificant on the deformation and forces in the superstructure.

(v) Figures 7.7 to 7.21 present the summary of the effects of various parameters on the forces in various elements of radiating type cable-stayed bridges under the action of lateral wind forces.

## C H A P T E R 8

### DYNAMIC INVESTIGATIONS

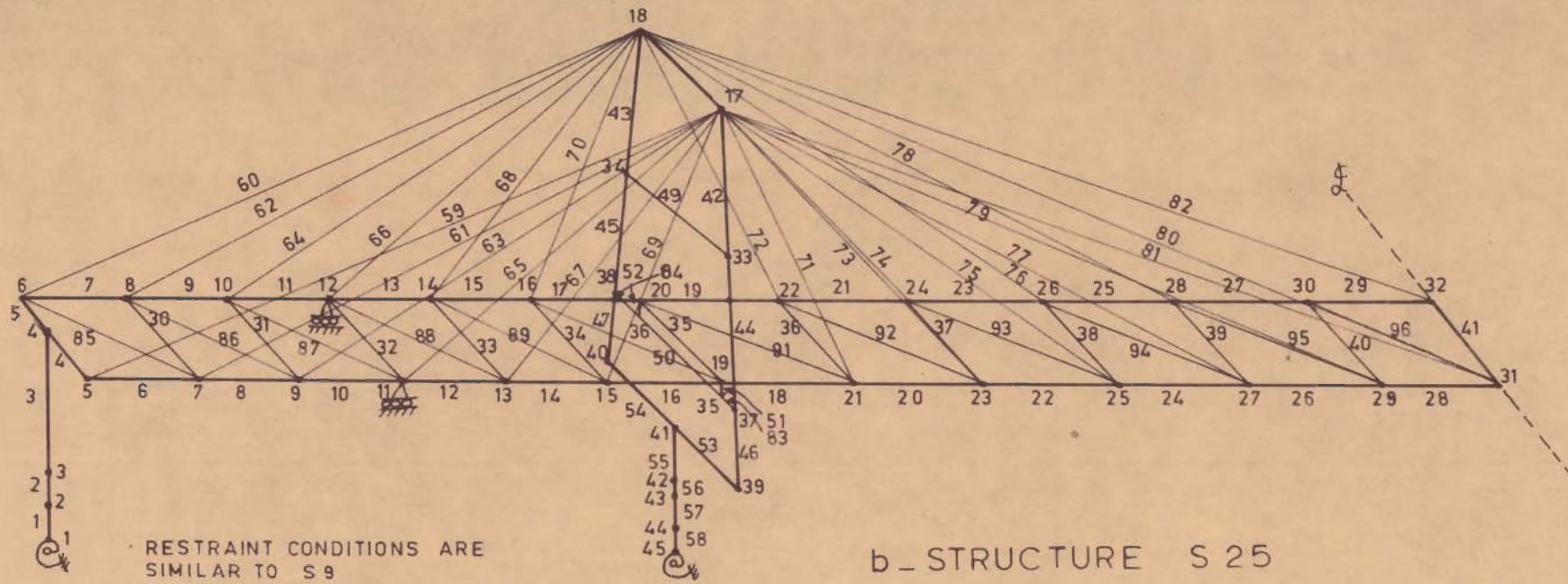
#### 8.1 INTRODUCTION

Free vibration analysis is presented here for a 5-span cable-stayed bridge in vertical, longitudinal and lateral directions. Experimental and analytical values of free vibration frequencies in the principal directions of the model bridge have been compared and experimental observations of the forced vibration tests have been discussed. Also, the response of the bridge is computed for earthquake motion in the traffic direction represented by an acceleration spectrum (37).

#### 8.2 STRUCTURES FOR DYNAMIC ANALYSIS

##### (a) Structure S24 :

A 5-span planar structure with a cambered profile (fig. 8.1a). The camber in the end span is 1 in 25 and that in the centre span is 1 in 50. The nodal coordinates and weights lumped at different nodes of this structure are given in table 8.1. The base of the substructures of S24 is assumed to be supported on elastic springs. The stiffnesses of elastic springs are same as those used for S3 (Chapter 6). The member properties of S24 represent the properties at the longitudinal line of symmetry of the structure. These have been appropriately taken from table 6.2 with due modifications. Weights of full structure have been appropriately lumped at the nodes. Free vibration and response analyses of S24 are presented later.



- 245 -

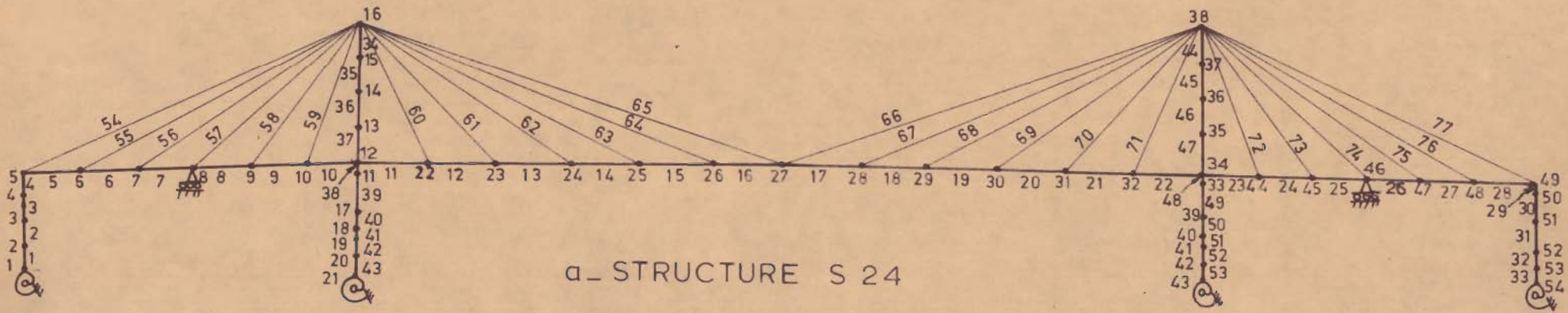


FIG. 8.1 - MATHEMATICAL MODELS OF STRUCTURES USED FOR DYNAMIC ANALYSIS

TABLE 8.1- NODAL COORDINATES AND WEIGHTS LUMPED AT DIFFERENT NODES OF S24

Node No.	COORDINATES		Weight lumped (t)	Node No.	COORDINATES		Weight lumped (t)
	X (m)	Y (m)			X (m)	Y (m)	
1	0	0	5249.0	28	449.58	65.35	992.0
2	0	14.48	10403.0	29	487.68	64.59	974.0
3	0	28.96	6549.0	30	525.78	63.83	962.0
4	0	41.59	1240.0	31	563.88	63.07	940.7
5	0	54.23	1405.0	32	601.98	62.31	970.0
6	30.48	55.45	933.0	33	640.08	61.11	285.0
7	60.96	56.67	957.0	34	640.08	61.55	994.0
8	91.44	57.89	874.0	35	640.08	80.25	171.0
9	121.92	59.11	699.0	36	640.08	99.25	208.5
10	152.40	60.33	764.0	37	640.08	119.42	149.5
11	182.88	61.11	285.0	38	640.08	139.45	478.6
12	182.88	61.55	994.0	39	640.08	35.86	5217.0
13	182.88	80.25	171.0	40	640.08	23.47	17533.0
14	182.88	99.38	208.5	41	640.08	19.81	16725.0
15	182.88	119.42	149.5	42	640.08	10.67	18861.0
16	182.88	139.45	478.6	43	640.08	1.52	9430.0
17	182.88	35.86	5217.0	44	670.56	60.33	764.0
18	182.88	23.47	17533.0	45	701.04	59.11	699.0
19	182.88	19.81	16725.0	46	731.52	57.89	874.0
20	182.88	10.67	18861.0	47	762.00	56.67	957.0
21	182.88	1.52	9430.0	48	792.48	55.45	933.0
22	220.98	62.31	970.0	49	822.96	54.23	410.0
23	259.08	63.07	960.0	50	822.96	53.79	1000.0
24	297.18	63.83	962.0	51	822.96	41.37	1240.0
25	335.28	64.59	974.0	52	822.96	28.96	6549.0
26	373.38	65.35	992.0	53	822.96	14.48	10403.0
27	411.48	66.11	1014.0	54	822.96	0	5249.0



(b) Structure S25:

A 5-span space frame structure with base supported on elastic supports (fig. 8.1b). The structure is the same as S9 with the exception of a few additional nodes in the substructure. The data has been appropriately taken from table 7.2. This structure has been analysed to obtain the lateral torsional and flexural modes of free vibrations.

(c) A Note on the Analysis of S25:

If the procedure of free vibration analysis outlined in Chapter 4 is directly used and if the rotational degrees of freedom at each node of the structure are eliminated from the overall stiffness matrix used for the free vibration analysis, a matrix of the order of 135 x 135 has to be inverted to obtain the flexibility matrix. The operational cost and time for the above on the digital computer available for use would have been prohibitive. Therefore, a selective inversion technique, described hereunder, was adopted to obtain a flexibility matrix of the order of 56 x 56.

To obtain the torsional and lateral modes of free vibration, only antisymmetric loading conditions of the bridge have been used for getting the flexibility coefficients. Antisymmetric unit loads were applied, one set at a time, corresponding to a particular degree of freedom at the two nodes (such as nodes 7 and 8 of fig. 8.1) which are symmetrically located from the longitudinal axis of the bridge and flexibility coefficients at various nodes of the structure were

computed by the stiffness matrix method described earlier in Chapter 3. Translational degrees of freedom considered are:

(i) The longitudinal and lateral directions for nodes 2 to 4 and 41 to 44 (fig. 8.1b) of the substructure.

(ii) The vertical and lateral directions for the nodes of the deck.

(iii) All the three directions for the nodes of the tower.

The selection of these degrees of freedom was considered to yield a flexibility matrix which could be used to obtain torsional and lateral flexural modes of free vibration of the bridge.

A condensed flexibility matrix of order 56 was, thus, obtained for selected degrees of freedom and then used for determining frequencies and modes as explained earlier in Chapter 4.

For the dynamic analysis of S25, the direction of the translational degree of freedom considered at a particular node and the weight lumped at that node (in the direction of the degree of freedom considered) is given in table 8.2.

### 8.3 VIBRATIONS IN VERTICAL PLANE

#### 8.3.1 Periods and Modes

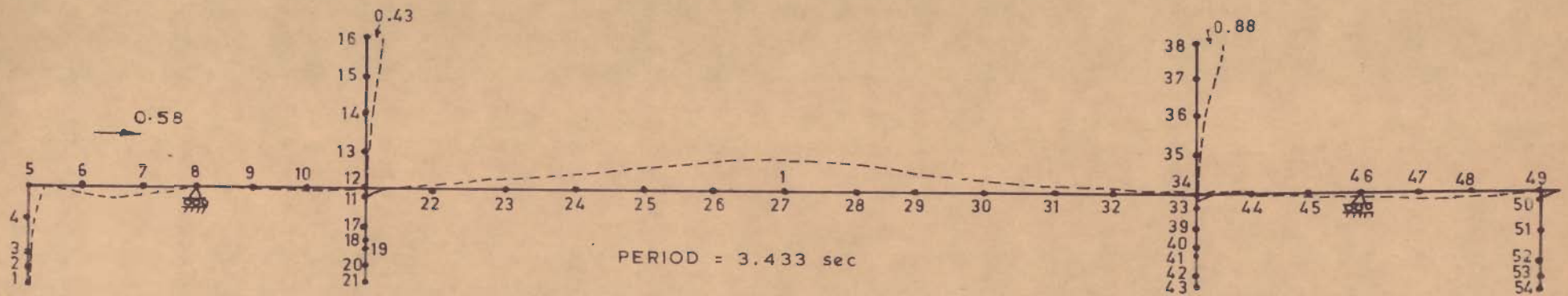
The first six time periods of the structure S24 in the vertical plane and the associated modeshapes are shown in

TABLE 8.2 - DEGREES OF FREEDOM CONSIDERED AND LUMPING OF WEIGHTS FOR DYNAMIC ANALYSIS OF S25

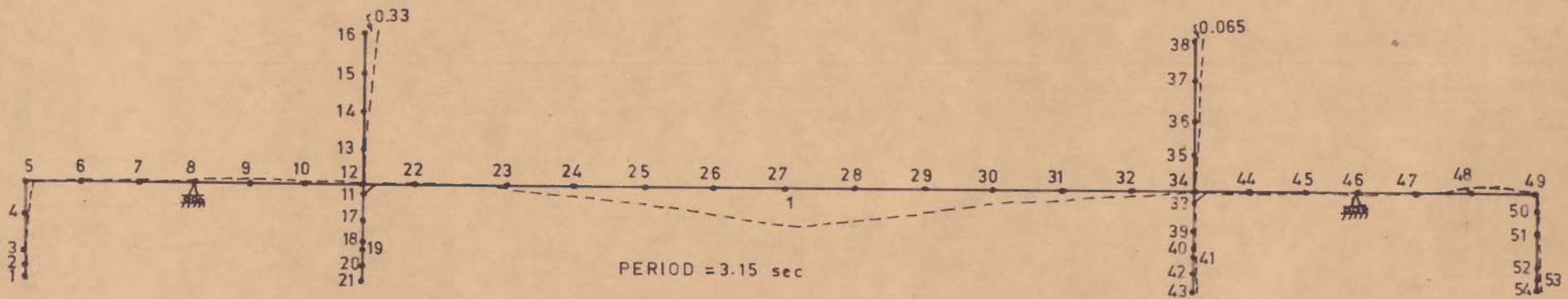
Node No	Directions in which translational degree of freedom is considered	Weight lumped (t)
2	x, z	11403.0
3	x, z	7169.0
4	x, z	1240.0
5	x, y, z	392.5
7	y, z	466.5
9	y, z	478.5
11	y, z	437.0
13	y, z	349.5
15	y, z	382.0
17	x, y, z	314.0
19	y, z	497.0
21	y, z	485.0
23	y, z	480.0
25	y, z	481.0
27	y, z	487.0
29	y, z	496.0
31	y, z	253.0
33	x, y, z	184.4
35	x, y, z	131.5
37	x, y, z	153.8
39	x, y, z	55.65
41	x, z	5161.4
42	x, z	17533.0
43	x, z	16725.0
44	x, z	18861.0

figures 8.2 and 8.3. From these, it is observed that the first mode is a longitudinal deflection mode in the towers and the substructures. Normally the deck could be expected to undergo rigid body translations in such an antisymmetric mode of vibration but it is observed that, in this case, the main span of the deck is also set to its vertical vibrations, and incidentally, the maximum modal deflection occurs in the deck itself. The first mode is, therefore, a combination of the flexibilities of substructures, towers as well as the deck. Looking at the performance of the structure in higher modes, in which the longitudinal displacements are either small or negligible, the first mode can be considered an antisymmetric mode causing dominant longitudinal translations.

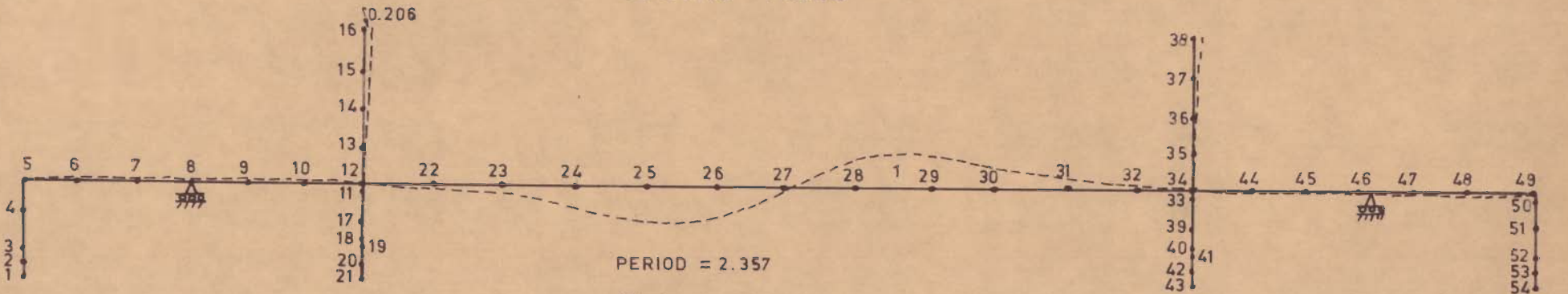
The dominance of the vertical deflections of the deck in the main span is clearly observed in the second, third and the fourth modes. These modes can be compared to the first three modes of a swinging string. The longitudinal deflections of the towers are seen to be gradually reducing and the deck deflections in the end spans are negligible. The study indicates that the main span of the bridge vibrates as if it is simply supported at the locations of the towers with small restraint provided by the presence of end spans. The second mode is a symmetric vertical mode, the third mode is an antisymmetric vertical and the fourth mode is a symmetric vertical mode.



First Mode

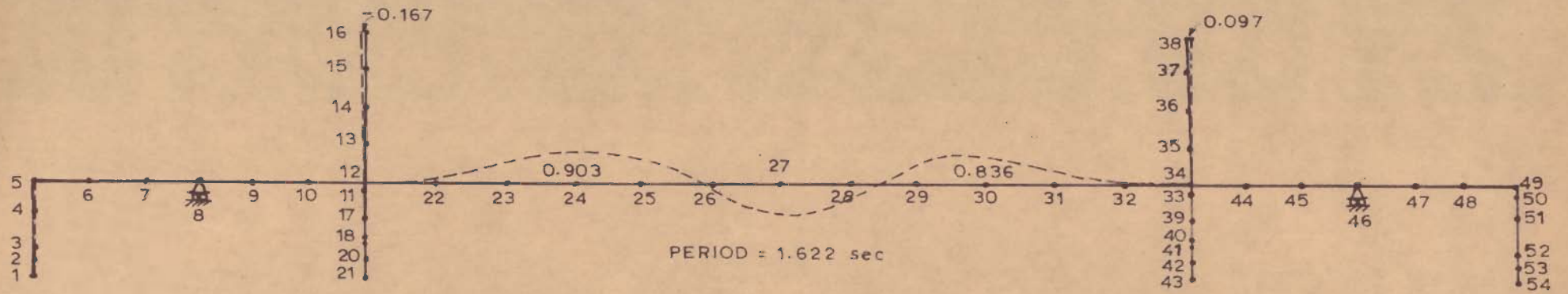


Second Mode

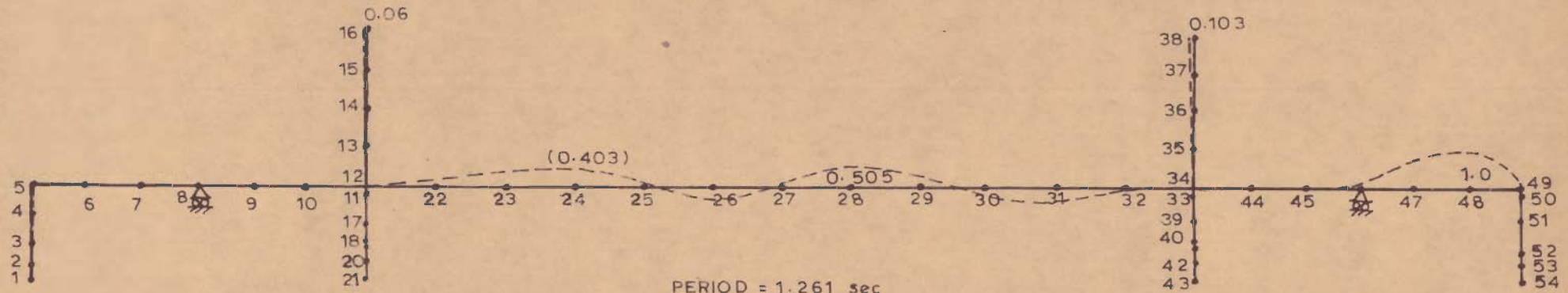


Third Mode

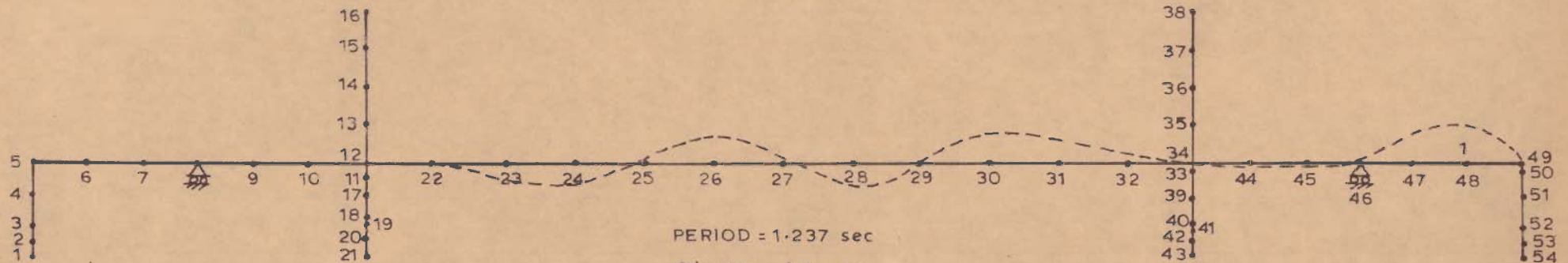
FIG. 8.2 - FREE VIBRATION MODES I TO III OF STRUCTURE S24



Fourth Mode



Fifth Mode



Sixth Mode

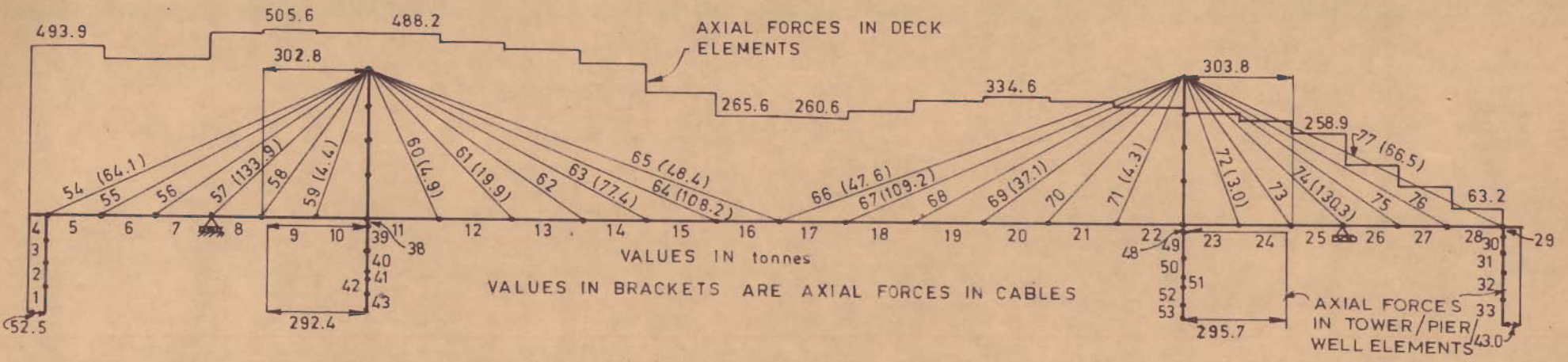
FIG. 8.3 \_FREE VIBRATION MODES IV TO VI OF STRUCTURE S 24

The fifth mode, which is antisymmetric vertical mode, can be considered in continuation of the modes discussed above. The maximum intensity of vertical deflection in this mode occurs in the end span which is connected to the substructure through a link. The number of computational iterations exceeded the specified limit (20) in this mode before the specified convergence (0.1 %) was achieved. The magnitudes of deflections of this mode can, therefore, in slight error.

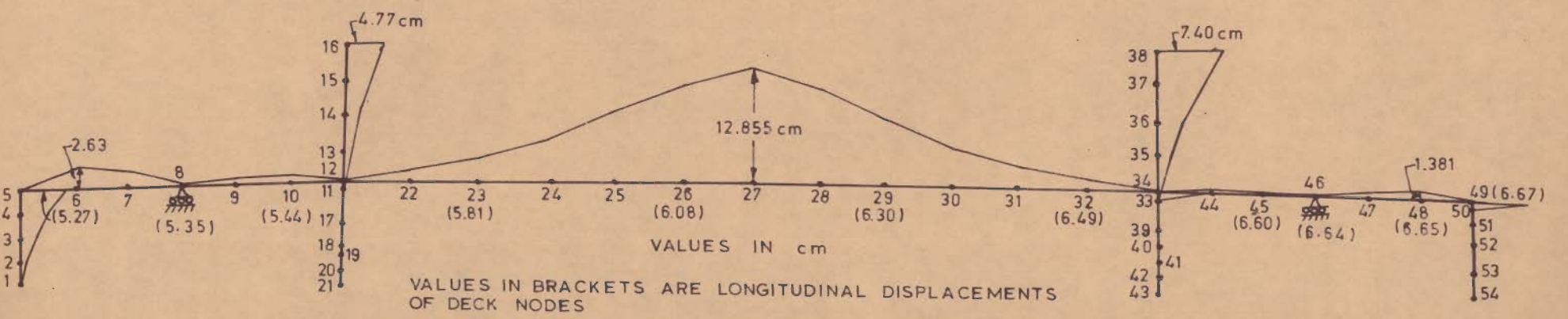
### 8.3.2 Seismic Response

The spectral accelerations due to horizontal ground motion for 10% damping (38) which have been used to carry out the response analysis of structure S24 are given in table 8.3. The probable maximum values of displacements at various nodes and axial forces in various members are shown in fig. 8.4. These values were obtained by taking the squareroot of the sum of squares of the modal values. This method of combination is henceforth referred to as SRSS. Similarly, fig. 8.5 shows SRSS values of shears and moments. Contribution of first four modes has been considered in the evaluation of the above responses.

From a study of the values in figures 8.4 and 8.5, it is observed that the vertical deck deflections in the main span of the bridge are predominant. The longitudinal deflections of the tower near the hinged end of the deck are lower than those of the other tower. Longitudinal deformations in the substructure at the hinged end of the deck are considerably



a - AXIAL FORCES



b - LONGITUDINAL AND VERTICAL DISPLACEMENTS

FIG. 8.4 - SRSS VALUES OF DISPLACEMENTS AND AXIAL FORCES FOR STRUCTURE S24



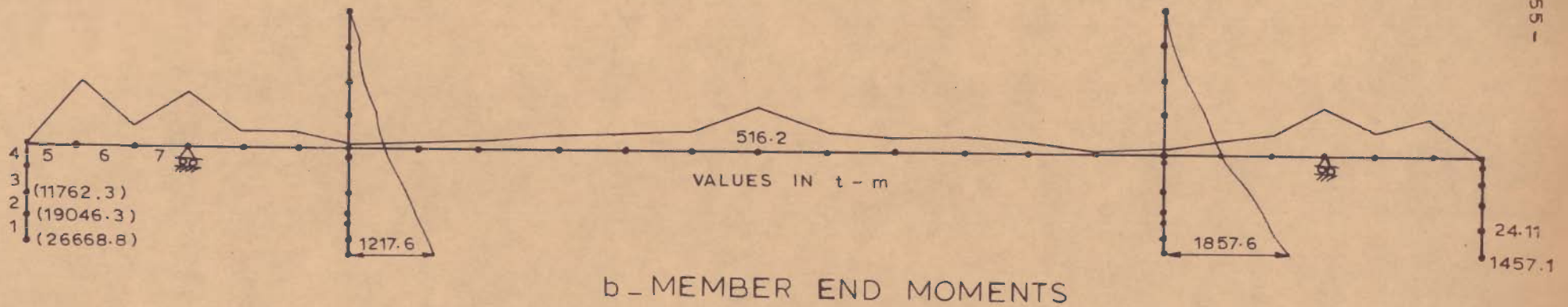
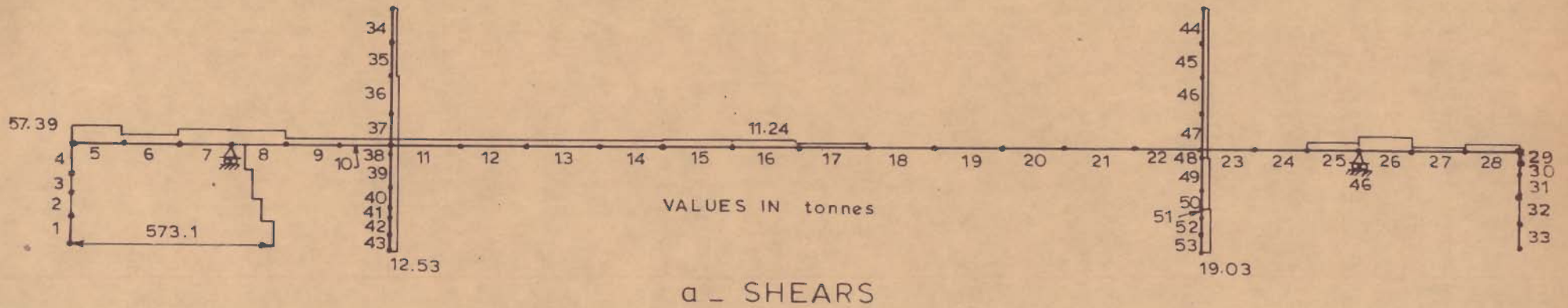


FIG.8.5 - SRSS VALUES OF SHEARS AND MOMENTS FOR STRUCTURE S 24

TABLE 8.3 - SPECTRAL ACCELERATIONS DUE TO HORIZONTAL  
GROUND MOTION FOR 10% DAMPING (Ref. 38)

Period Sec.	Horizontal ground motion Sahr/g	Period Sec.	Horizontal ground motion Sahr/g
0.15	0.07125	1.60	0.04875
0.18	0.09	1.70	0.045
0.20	0.10725	1.80	0.04125
0.30	0.12375	1.90	0.0375
0.40	0.12375	2.00	0.03375
0.50	0.12375	2.1	0.031875
0.60	0.12375	2.2	0.03
0.70	0.12375	2.3	0.03
0.80	0.11625	2.4	0.03
0.90	0.10725	2.5	0.03
1.00	0.0975	2.6	0.03
1.10	0.08625	2.8	0.03
1.20	0.075	3.0	0.03
1.30	0.0675	3.5	0.0225
1.40	0.05625	3.75	0.01875
1.50	0.04875	4.00	0.01875

high. The deformations in the substructures at other locations are negligible due to the presence of links or rollers under the deck. Heavy axial forces occur in girder elements near the hinged end. Thus considerable nonlinear axial-flexural

interaction should be expected in the overall behaviour of the bridge structure under dynamic loads. Cables connected to the intermediate supports of the end spans draw maximum tensile forces. The substructures at the ends are subjected to small axial forces while the axial forces in full length of towers and the substructures below them are almost constant. The shears in whole of the structure are very small except in the elements of the substructure at the hinged end of the deck. This behaviour is expected because the cables reduce the shears of the deck while the links at various locations of the deck do not allow transfer of horizontal forces to the substructure below towers and at the roller end of the deck. Bending moments are also very high in the substructure at the hinged end as compared to the values in substructures at other locations. Moments in the end spans are more than the moment at the centre of main span.

#### 8.4 VIBRATIONS IN THE TRANSVERSE DIRECTION OF THE BRIDGE

The time periods of the structure S25 in first six modes of free vibrations and their associated modeshapes are shown in figures 8.6 and 8.7. From the study of these figures it is observed that the first mode is a transverse mode (period = 2.41 sec.) and the second mode is a torsional mode (period = 1.91 sec.) in the main span of the deck. The deformations of the substructures, tower and the end span are not significant in these modes. The third mode is a lateral mode in the tower with small lateral deflections in the main span

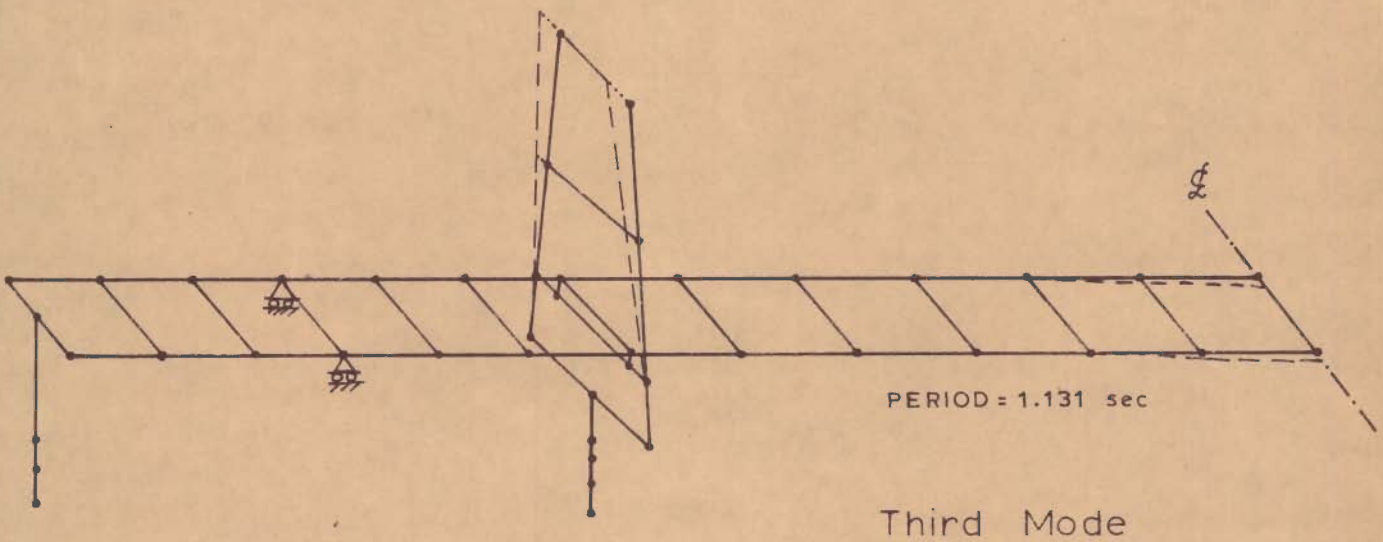
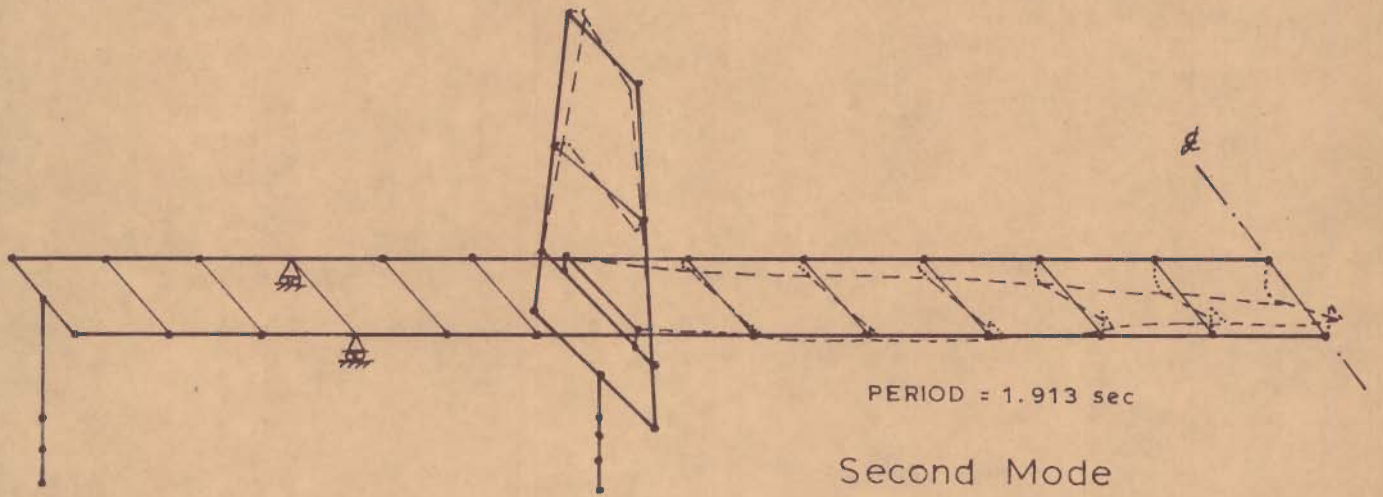
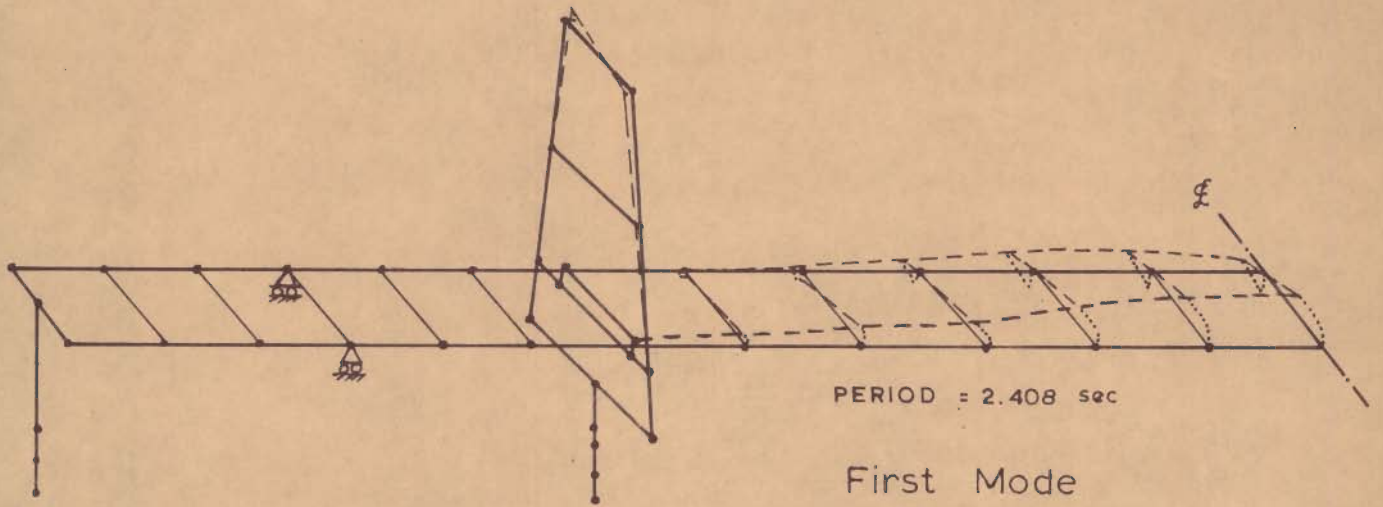


FIG. 8.6 - TORSIONAL FLEXURAL MODES I TO III OF STRUCTURE S25

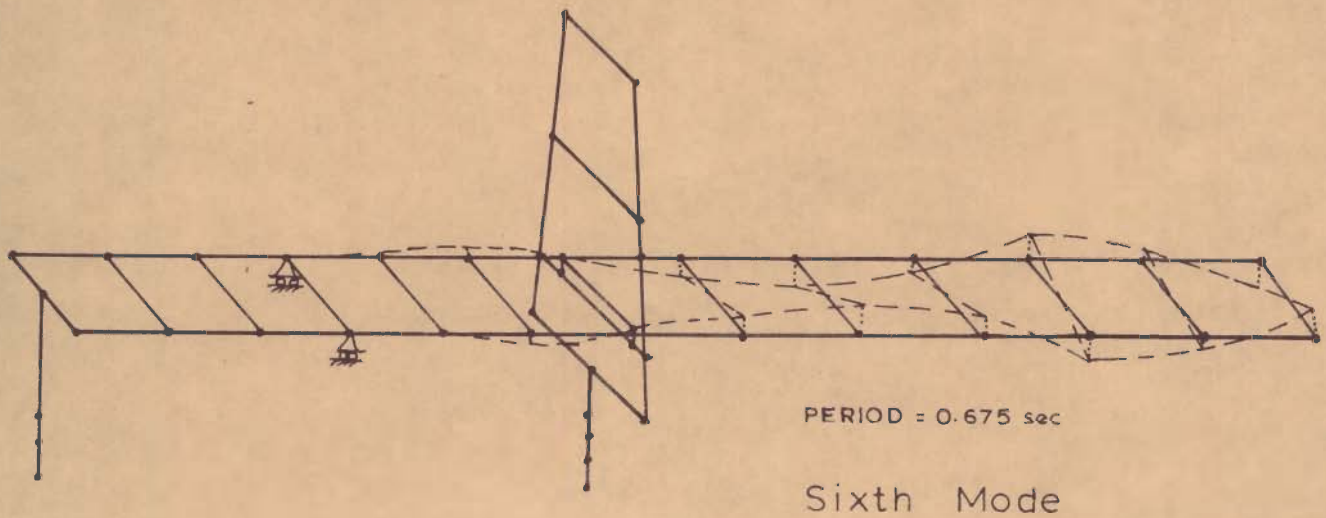
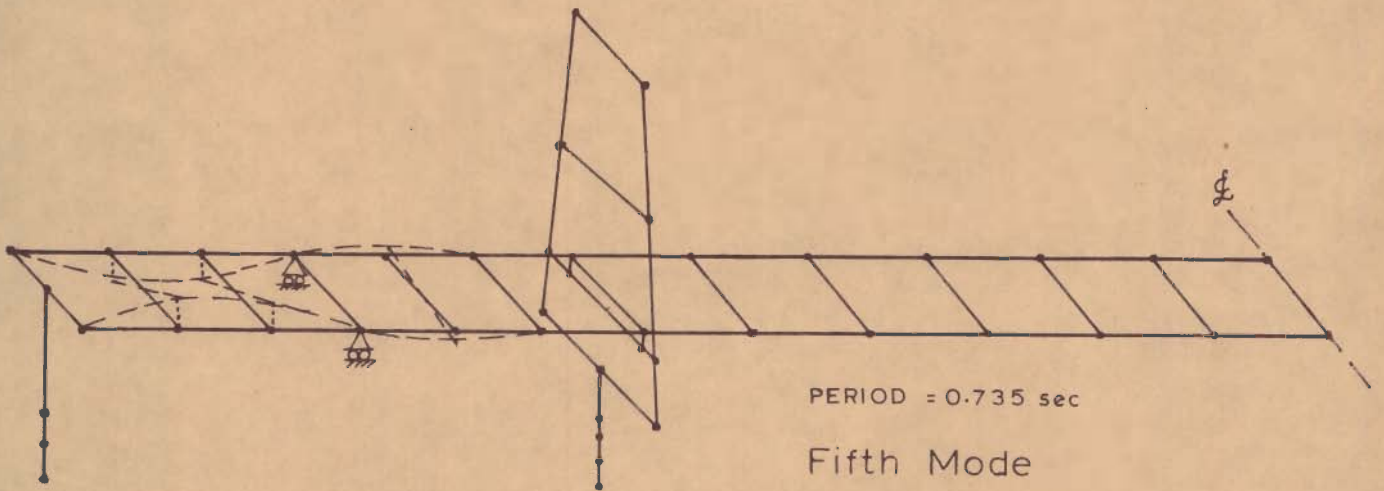
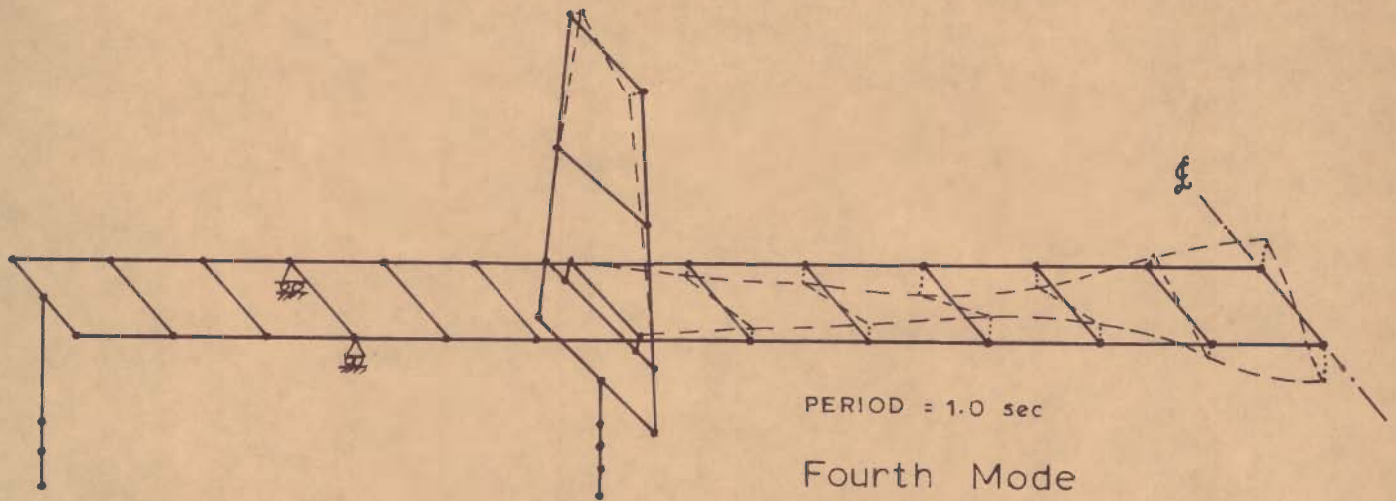


FIG.8.7 \_ TORSIONAL FLEXURAL MODES IV TO VI  
OF STRUCTURE S25

of the deck while the deformations in the end spans and the substructures are negligible. The fourth (period = 1.0 sec.), fifth (period = 0.735 sec.) and sixth (period = 0.675 sec.) modes are the torsional modes of the deck with negligible deformations in the tower and the substructures. The fourth mode causes torsional deformations only in the main span of the deck while the fifth mode causes torsional deformations only in the end spans of the deck. It is observed that in the first five modes, the main span of the deck does not significantly interact with the side spans and its dynamic behaviour is, as if the deck is simply supported between the towers. The sixth mode has predominant torsional deformations of the main span which are transmitted, to some extent, to the end spans also.

The time periods obtained for torsional and transverse flexural modes are seen to be well separated, a fact that helps in numerical analysis.

#### 8.5 DISCUSSION OF OVERALL DYNAMIC BEHAVIOUR OF 5- SPAN SYSTEM

Structures S24 and S25 chosen for the dynamic analysis, represent a single structure in space whose symmetric and antisymmetric modes of free vibrations in the longitudinal and vertical directions have been obtained by the planar structure S24 and the torsional and lateral modes of free vibrations have been obtained by getting a condensed flexibility matrix for the dynamic analysis of space frame structure S25.

A combined study of the dynamic behaviour of S24 and S25 can be summarised in the following:

(i) The 5-span system of the cable-stayed bridge, under study, has the fundamental mode (period = 3.43 sec) which is mixed in nature causing longitudinal vibrations in the tower and the substructures while the deck vibrates in symmetric vertical mode.

(ii) A purely antisymmetric mode in the longitudinal direction of the bridge is not excited in the structure.

(iii) The second mode (period = 3.15 sec) is a symmetric vertical mode. Vertical deck deflections are observed primarily in the main span of the deck.

(iv) The third mode (period = 2.41 sec) is a lateral mode. Lateral deflections are observed primarily in the main span of the deck.

(v) The fourth mode (period = 2.36 sec) is an antisymmetric vertical mode with predominant vertical deflections of the main span of the deck.

(vi) The fifth mode (period = 1.913 sec) is a torsional mode with predominant deformations of the main span of the deck.

(vii) The sixth mode (period = 1.622 sec) is a symmetric vertical mode with predominant vertical deflections in the main span of the deck.

Other modes of free vibration can not be placed in an order because of slight numerical inaccuracy that could be

present due to incomplete iterations in the fifth and sixth modes of structure S24 obtained by plane frame analysis. However, it is clearly observed that the transverse mode that causes predominant flexural deformations of the tower has a place after the sixth mode. Further torsional modes of the deck follow this lateral mode.

### 8.6 EXPERIMENTAL VERIFICATION OF RESULTS

Dynamic analyses of structures S7 (Chapter 6) and S12 (Chapter 7) were performed on lines similar to those adopted for structures S24 and S25 respectively for the experimental verification of the analytical results. The comparison of analytical and experimental frequencies is given in table 8.4.

TABLE 8.4 - COMPARISON OF ANALYTICAL AND EXPERIMENTAL VALUES OF NATURAL FREQUENCIES IN LONGITUDINAL, VERTICAL AND LATERAL DIRECTIONS

Direction of bridge	Natural frequency in cycles/sec		% Variation
	Analytical	Experimental	
Longitudinal	22.5	25	10
Vertical	51.4	55	6.5
Transverse	49.3	30.0	39.2

It is observed from table 8.4 that the analytical and experimental values of natural frequencies are close in the longitudinal and vertical directions of the bridge whereas the difference is large in the transverse direction. This



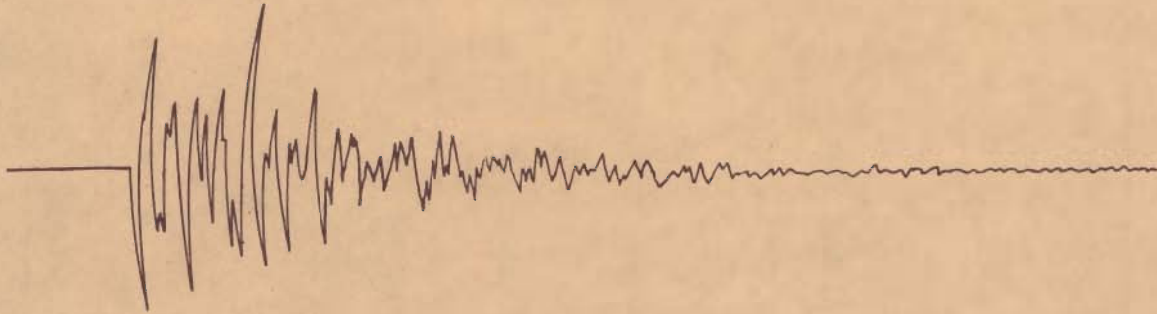
difference is after accounting for the actual rotational and torsional stiffnesses at the base of the substructure and the actual tensile stiffnesses of cable wires.

Steady state vibrations in the transverse direction of the bridge model produced a peak in the amplitudes of acceleration records at a frequency of 30 cycles per second. This corroborates with the free vibration test value of 30 cycles per second stated before.

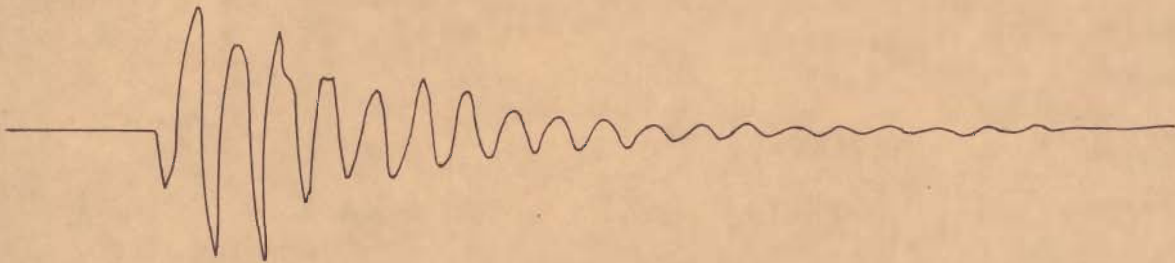
A study of the effect of using a condensed flexibility matrix of the space frame structure on the frequency in transverse direction could not be attempted in the present investigation. Therefore, the reasons of the large difference seen in analytical and experimental values remain unexplained. Hence, the quantitative implications of the results of analysis of structure S25, discussed earlier in section 8-5, have to be viewed with some caution.

Some more observations of the experimental study of the bridge model are given hereunder.

(i) Due to the presence of cables, the mixing of higher modes was significant in the acceleration records of longitudinal and vertical directions taken at the locations of the superstructure. The records taken at the points of the substructure gave a clearer picture of the lowest frequency of vibration in all the three directions. Fig. 8.8 shows two typical records of acceleration in the vertical



a\_ For a location in superstructure



b\_ For a location in substructure

FIG. 8.8 \_ TYPICAL ACCELERATION RECORDS OF  
FREE VIBRATION IN VERTICAL DIRECTION

direction, due to free vibration, taken at locations of the superstructure and the substructure.

(ii) Steady state vibrations in the longitudinal direction of the bridge, at frequency equal to the lowest natural frequency of longitudinal vibration, did not induce appreciable peaks in the values of accelerations at the locations of the superstructure. This may again be attributed to the presence of cables which tend to retard the dynamic amplifications.

#### 8.7 SUMMARY

The results of analytical and experimental investigations of the dynamic behaviour of the cable-stayed bridges under study can be summarised as follows:

(i) A purely antisymmetric fundamental mode in the longitudinal direction of the bridge is not excited in the structure.

(ii) Main span of the deck undergoes predominant deformations in most of the lower modes of free vibration. The deformations of the end spans, towers and the substructures are either small or negligible.

(iii) The response of the structure to static and dynamic loading conditions is similar.

(iv) Experimental and analytical values of fundamental frequencies are close in the longitudinal and the

vertical directions. However the difference in the two results in transverse direction is quite large and could not be fully explained.

(v) It is difficult to induce a pure mode in the superstructure due to the presence of cables.

## C H A P T E R 9

### SUMMARY AND CONCLUSIONS

#### 9.1 STUDIES CARRIED OUT

The following static and dynamic studies of the cable-stayed bridges have been presented in the earlier chapters.

(a) Study of the bridge considered as a plane frame system subjected to the action of vertical loads and analysed as a linear system; determination of the extent of axial-flexural interaction and the effect of initial prestressing on the consequent nonlinearity; and, the effect of soil-structure interaction.

(b) Study of the bridge, considered as a space frame under the action of eccentric vertical as well as lateral loads, analysed as a linear system, and determination of the effect of soil-structure interaction; study of the effect of various parameters on the behaviour of the bridge under lateral forces.

(c) Study of periods and modes of free vibration in the principal directions of the bridge and determination of its response to a ground motion acceleration spectrum.

(d) Experimental verification of static and dynamic results of the analysis of a small scale aluminium model.

## 9.2 SIGNIFICANT RESULTS

The following significant results have been obtained as reported in earlier chapters.

### A. Behaviour Under Symmetric Vertical Loads

1. Pattern of distribution of forces in cables of the end spans changes with the introduction of additional anchor piers at intermediate nodes of the end span but this does not significantly change the distribution of cable forces in the main span.

2. Maximum axial compression in the deck elements occurs near the towers. This, for the example chosen, is of the order of 40% of the maximum axial compression of the tower leg and the substructure below it. Axial-flexural interaction increases the axial forces in the deck elements by 20 to 60% or more but there is practically no change in the tower or substructure forces.

3. Some elements of the deck, near the end supports and the centre of the main span, which are found to be in tension from the linear analysis, show compression when axial-flexural interaction is considered.

4. A three span system, in general, is more flexible than the five span system obtained by inserting anchor piers. The effect of axial-flexural interaction was to increase the flexibility of a 5-span system by about 10%.

5. A camber in the deck is seen to impart a small degree of extra stiffness to the system and nonlinear effects due to axial-flexural interaction are reduced by about 2% on this account.

6. The effect of the end support condition, that is, one end hinged and the other on rollers in an otherwise symmetrical bridge under vertical symmetrical loads was to introduce small amount of unsymmetry in the forces in two halves of the bridge. The variation of forces is seen to be about 10% in the corresponding elements.

#### B. Behaviour Under Eccentric Vertical Loads

7. When the bridge is treated as a space frame, its behaviour on the loaded side under half deck load, is nearly the same as that obtained from a plane frame analysis of the bridge under full deck live load.

8. The space action, by way of sharing of loads by the unloaded girder, is activated more in the 3-span system than in the 5-span system due to the greater longitudinal flexibility of the 3-span system.

9. Axial force on the unloaded side of the girder elements near the tower are about 10 to 20% of those on the loaded side while they have equal and opposite values in the elements near the centre due to horizontal bending of the main span. Other forces and deformations in the elements of the unloaded side also vary, in general, from 10 to

25 percent of the corresponding value on the loaded side.

### C. Behaviour Under Lateral Forces

10. Under the action of lateral loads, cables as well as the elements of the substructure are subjected to negligible axial forces.

11. Nature of axial forces is generally opposite in the windward and leeward elements of the bridge, the deck acting like a horizontal girder.

12. Heavy bending moments are induced in the substructures, particularly at the base of the well below the tower.

### D. Parametric Study Under Lateral Forces

Figures 7.7 to 7.21 present the summary of the effects of various parameters on forces in various elements of the bridge. The broad conclusions are as follows:

13. Axial forces in cables; axial forces, shears and moments in girder elements and shears and moments in tower legs decrease with the increase of the ratio of side span to centre span while the axial forces in the tower legs increase.

14. Axial forces in cables; shears and moments in girder elements decrease while axial forces, shear and moments in tower legs and axial forces in girder elements increase with the increase in the ratio of tower height to centre span.



15. As the ratio of width of deck to main span increases, the axial forces in cables; axial forces, shears and moments in girder elements and axial forces, twisting moment and transverse moment in the tower legs decrease whereas longitudinal shears and moments in tower legs show increase.

16. Cable forces increase; shears, twisting and longitudinal moment in the girder element decrease; as the ratio of cable area to girder torsional rigidity increases. Other forces in the girder elements and tower legs remain unchanged due to this change.

17. Axial forces and moments in the main girder elements are significantly effected by the ratio of the side span to centre span. The ratio of tower height to centre span has significant effect on twisting and horizontal bending of the main girders and axial forces, shears and moments in the tower and the substructure, The ratio of cable stiffness to girder torsional stiffness effects horizontal bending and twisting of tower legs. The effects of increasing the width of deck is to decrease the horizontal bending of the deck.

#### E. Effect of Soil-Structure Interaction

18. The soil flexibility has the effect of increasing the flexibility of the bridge, but even for loose sand the effect on deflections is seen to be only about 2%. For

stiffer soils, the effects can be expected to be even smaller.

19. In the case of the substructure, the effect on shears and moments is, however, significant, although, it is small in the superstructure.

#### F. Dynamic Behaviour

20. A purely antisymmetric fundamental mode in the longitudinal direction of the bridge is not excited in the structure. The deflections of the main span, in fact, predominate in most of the lower modes. The deformations of the end spans, towers and the substructure are either small or negligible.

#### G. Comparison of Analytical and Experimental Results

21. The deflections of the model under static loading conditions are close to the actual values when the actual fixity conditions at the base of substructures and actual cable stiffnesses are duly accounted for.

22. Experimental and analytical values of fundamental frequencies are close in the longitudinal and vertical directions. However, the difference in the two results in transverse direction is quite large and could not be explained.

#### H. Experimental Observations

23. It does not appear possible to induce a pure vibration mode in the superstructure due to individual

vibration of cables.

### 9.3 CONCLUSIONS

The main conclusions arrived at from the study are the following:

1. The three span system is appreciably more flexible than the five span system. The effect of axial-flexural interaction is to increase the overall flexibility of the system. The increase is seen to be within 10% for the five span system, but the increase in the axial forces in main girder elements is seen to be significant. The prestressed cables are seen to reduce the nonlinear axial-flexural effect by about 2% in the 5-span system.

2. The mutual sharing of eccentric vertical loads by the main girders is moderate as seen from the study of the bridge under vertical loads applied to one of the main girders. The forces and deformations in the unloaded side lie generally between 10 to 25% of those on the loaded side. Other effects of eccentric loading are the horizontal bending and twisting of the deck near the centre of main span which must be considered in the design.

3. Under the action of lateral forces, the deck tends to act as a horizontal girder with cables carrying only negligible axial forces. Axial forces and moments in the main girder elements are significantly effected by the ratio of the side span to centre span. The ratio of tower

height to centre span has significant effect on twisting and horizontal bending of the main girders and axial forces, shears and moments in the tower and the substructure. The ratio of cable stiffness to girder torsional stiffness effects horizontal bending and twisting of tower legs. The effects of increasing the width of deck is to decrease the horizontal bending of the deck.

4. The effect of soil-structure interaction, even when soil is soft, is seen to be negligible on the superstructure forces but the substructure forces are significantly increased.

5. Most of the lower modes of free vibration are characterised by the deflections of the deck in the vertical plane. Experimentally, it does not appear possible to induce a pure mode in the superstructure due to cable vibrations.

6. Comparison of analytical and experimental results is generally good which proves the adequacy of the analyses adopted.

#### 9.4 SCOPE FOR FURTHER RESEARCH

Some points which appear to be of significance and will need further investigation are listed below:

(a) Nonlinearity in the behaviour of cable-stayed bridges could be caused due to axial-flexural interaction, change in geometry due to large deflections and material

nonlinearity beyond the yield point. The study presented in this thesis covers the nonlinear effect of axial-flexural interaction to some extent. The available literature also shows little attention to these effects. This is an important aspect of the cable-stayed bridge to be studied.

(b) Analytical procedures are also wanted, still, to determine the ultimate load carrying capacity of the bridge structure under combined vertical and horizontal loads and the mode in which such a bridge is likely to fail. This study is important so as to ascertain the reserve of strength in the structure beyond the working loads.

(c) A methodology, taking into account the various types of nonlinear effects is still to be developed for finding the true state of stress in various components of the bridge for different stages of erection. Optimization in the initial state of stress of the bridge under the action of dead loads and cable prestress may lead to economy in the construction of cable-stayed bridges.

(d) The study of soil-structure interaction has been carried out by assuming elastic behaviour of soil at the base and sides of the substructure. It is further assumed that full area of soil at the base of the substructure develops resistance while the soil resistance at the sides of the substructure is independent of the width of contact. This method of representing soil stiffness is believed to give greater flexibility to the springs than

may really be available. Information is not sufficient on the actual behaviour of well foundations. Although the effects due to this parameter on the superstructure are seen to be small, the substructure stability as well as forces are directly dependent on the soil stiffness and resistance. Studies are called for on this aspect.

BIBLIOGRAPHY

1. Ahmad, S., 'Influence of Horizontal Subgrade Reaction on Dynamic Behaviour of Cable-stayed Bridges', M.E. Thesis, SRTEE, Univ. of Roorkee, India, 1977.
2. Anonymous, 'An Original Foot Bridge in Germany', Civ. Engg. publ. Wks. Rev., 1111-1113, Sept; 1962.
3. Anonymous, 'The New Wye and Usk River Bridges', Building with Steel, J. Br. Constr. Steelwork Asc., 2(8) 16-18, Nov., 1963.
4. Anonymous, 'Pylons Support Welded Steel Span', Engng. News Rec., 42, 28 Nov., 1963.
5. Anonymous, 'Norderelbe' Bridge K6: A Welded Steel Motorway Bridge', Acier-Stahl-Steel, No.11, 499-500, 1963.
6. Anonymous, 'An Original Bridge in Germany', Civ. Engng. publ. Wks. Rev., 173, Feb., 1964.
7. Anonymous, 'Longest Span Proposed', Engng. News Rec., 16, 30 April, 1964.
8. Anonymous, 'The George Street Cable Cantilevered Bridge at Newport', Civ. Engng. publ. Wks. Rev., 575, May, 1964.
9. Anonymous, 'Montreal Hosts a Double Bridge Spectacular in the St Lawrence', Engng. News Rec., 24-27 and 31, 5 Aug., 1965.
10. Anonymous, 'Polcevera Difficult Site is Spur to Design', Engng. News Rec., 32-34, 26 Aug., 1965
11. Anonymous, 'Welded Steel Boxes Assembled on Site for Britain's Wye Bridge', Engng., News Rec., 26, 27 and 29, 21 July, 1966.

12. Anonymous, 'An Original Suspension Footbridge in Belgium', Civ. Engng. pub. Wks. Rev., 1365, Nov., 1966.
13. Anonymous, 'Great Belt Bridge Award Winners', Consult. Engr., St. Joseph, 31 (3), 63-69, March 1967.
14. Anonymous, 'Cable Stayed and Orthotropic Structures at Expo', Highw. publ. Wks, 24-25 and 27, April, 1967.
15. Anonymous, 'Another Cable-Stayed Bridge Conquers the Rhine', Engng. News Rec., 103, 25 May, 1967.
16. Anonymous, 'Leaning Tower Supports Stayed Truss Span', Engng News Rec., 24-25, 22 June, 1967.
17. Anonymous, 'Cable-Stayed Footbridge in Laminated Timber', Highw. pub. Wks., 31 Aug., 1967.
18. Anonymous, 'Neubau Kniebrücke, Teil 1', Strombrücke, Landeshauptstadt Düsseldorf, 1967.
19. Anonymous, 'Rheinbrücke Ress-Kalkar', Bundesminister für Verkehr, Bonn, 1967.
20. Anonymous, 'Batman Bridge Near Completion', Aust. Civ. Engng. Constr., 13-16, 5 April, 1968.
21. Anonymous, 'Le Pont Suspendu à Haubans de Saint - Florent-le-vieil (Maine et Loire)', Travaux, 765-766, July-Aug., 1968.
22. Anonymous, 'Superstructure Started for Erskine Bridge', Highw. publ. Wks, 34-35, Dec., 1968.
23. Anonymous, 'Die Sehragseilbrücke in Kiev', Bauingenieur, No. 11, 426-427, 1968.
24. Anonymous, 'Rheinbrücke Bonn Nord', Tiefbau, 29-40, 1968.



25. Anonymous, 'Rheinbrücke Duisburg-Neuen-kamp', Landschaftsverband Rheinland, 1968.
26. Anonymous, 'Inclined Tower Bridges', Consult. Engr., St. Joseph, 58-61, June 1969.
27. Anonymous, 'Record Span is Cable-Stayed', Engng. News Rec., 34, 20 Nov., 1969.
29. Anonymous, 'The Cable-Stayed Suspension Bridge at Saint Florent-le-Vieil, France', Acier-Stahl-Steel, No.2, 92, 1969.
29. Anonymous, 'New Oberkasseler Bridge, Dusseldorf', Highw. Traff. Engng., 27, 28 and 30 June, 1970.
30. Anonymous, 'Great Belt Crossing, Civ. Engng., Easton, Pa, 79, June, 1970.
31. Anonymous, 'Record All-Welded, Cable-Stayed Span Hangs from Pylons', Engng. News Rec., 20-21, 3 Sept., 1970.
32. Anonymous, 'The Paris-Massena Bridge. A Cable-Stayed Structure', Acier-Stahl-Steel, No.6, 278-284, 1970.
33. Anonymous, 'Erskine Bridge Near Completion', Highw. Traff. Engng., 46, April/May, 1971.
34. Anonymous, 'Erskine Road Bridge', Civ. Engng. publ, Wks. Rev., 505, 507, 509 and 510, May, 1971.
35. Anonymous, 'Longest Concrete Cable-Stayed Span Cantilevered over Tough Terrain', Engng. News Rec., 28-29, 15 July, 1971.
36. Arya, A.S. and Thakkar, S.K., 'Earthquake Response of a Tied Cantilever Bridge', Proc. of Third European Symp. on Earthquake Engng., Sofia, 343-353, Sept. 14-17, 1970.

37. Arya, A.S., Krishna, P., Srivastava, L.S., Thakkar, S.K., Rani, P., 'First Report of Seismic Investigations of Second Hooghly Bridge', EQ-74-6, A Report of SRTEE, Univ. of Roorkee, India, 1974.
38. Arya, A.S., Krishna, P., Thakkar, S.K., Rani, P. and Pandey, A.D., 'Second Report of Seismic Investigations of Second Hooghly Bridge', Earthquake Engng. Studies, EQ-75-17, SRTEE, Univ. of Roorkee, India, 1975.
39. Arya, A.S., Thakkar, S.K. and Rani, P., 'Approximate Vibration Analysis of a Cable-Stayed Bridge', Preprint, Sixth World Conf. on Earthquake Engng., New Delhi, 9/163, Jan. 10-14, 1977.
40. Ascheuberg, H. and Freudenberg., G., 'Die Brücke Über die Norderelbe im Zuge der Bundesautobahn südliche Umgehung Hamburg. Teil II : Konstruktion des Brückenerbaues', Stahlbau, No. 8, 240-248, Aug., 1963; Teil III: Statische Berechnung des Brückenerbaues', Stahlbau, No. 9, 281-287, Sept., 1963.
41. Bachelart, H., 'Pont de la Bourse Footbridge Over the Bassin du Commerce, Le Havre (France)', Acier-Stahl-Steel, No. 4, 167-168, 1970.
42. Baker, J.F., 'The Mechanical and Mathematical Stress Analysis of Steel Building Frames', Inst of Civ. Engrs., Selected Engng. Paper No. 131, 1932.
43. Balbachevski, G.N., 'Study Tour of the A.F.P.C.', Acier-Stahl-Steel, No.2, 73-74, 1969.
44. Baresford, F.D. and Lewis, R.E., 'Dynamic Studies of a Large-Model of a Prestressed Concrete Foot-bridge', Rilem International Symp. on Testing Methodology and Technique of Full-Scale or Model Structures Under Static and Dynamic Loads, Bucharest, pp. 1-22, 9-11 Sept., 1969.
45. Barken, D.D., 'Dynamics of Bases and Foundations', McGraw Hill Book Co., 1962.

46. Baron, F. and Linen, S.Y., 'Analytical Studies of the Southern Crossing Cable-Stayed Girder Bridge', Report No. VC-SESM 71-10, Vol.I and II, Dept. Civ. Engng., Univ. of Calif., Berkeley, California, June 1971.
47. Baron, F. and Lein S.Y., 'Analytical Studies of a Cable-Stayed Girder Bridge', Computers and Structures, Vol. 3, Pergamon Press, New York, 1973.
48. Bayer, E. and Tussing, F., 'Nordbrücke Dusseldorf', Stahlbau, Nos. 2,3 and 4, 1955.
49. Bayer, E., 'Nordbrücke Dusseldorf', Landes-hauptstadt, Dusseldorf, 1958.
50. Bayer, E. and Schmidt, H., 'Entwurfsbearbeitung und Modellversuche', Nordbrücke Dusseldorf, Landeshauptstadt Dusseldorf, pp. 28-36, 1958.
51. Bayer, E. and Ernst, H.J., 'Brücke Julicher Strasse in Dusseldorf', Bauingenieur, No.12, 469-477, Dec.1964.
52. Beggs, G.E., 'An Accurate Mechanical Solution of Statically Indeterminate Structures by the Use of Paper Models and Special Gauges', Proc. ACI, 18, 58, 1922.
53. Beggs, G.E., Timby, E.K. and Birdsall, B., 'Suspension Bridge Stresses Determined by Model', Engng. News Rec., 828-832, 9 June, 1932.
54. Benjamin, R.J., and Williams, H.A., 'The Behaviour of One Storey Reinforced Concrete Shear Walls', Jor. Struct. Div., ASCE, Vol. 83, No. ST.3, Proc. Paper 1254, May, 1957.
55. Biggs, J.M., 'Introduction to Structural Dynamics', McGraw-Hill Book Company, 1964.
56. Binkhorst, J., 'De Galecopperbrugte Utrecht', Ingenieur, No.16, B89-B96, 23 April, 1971.

57. Brown, C.D., 'Design and Construction of the George Street Bridge over the River Usk, at Newport, Monmouthshire', Proc. Instn. Civ. Engrs., No. 32, 31-52, Sept. 1965.
58. Clark, E., 'Britannia and Conway Tubular Bridges'(2 vols), Vol. 1, Day and Day, London, 1850.
59. Clive, T.H., 'Mr clives System of Constructing Suspension Bridges', Mechanics' Magazine, London, 39 (1050), 225-227, 23 September, 1843.
60. Connor, J.J. et al., 'Nonlinear Analysis of Elastic Framed Structures', Proc. ASCE, 94(ST6), 1525-1547, June, 1968.
61. Daniel, H., 'Die Bundesautobahnbrücke Über den Rhein bei Leverkusen, Planung, Wettbewerb und seine Ergebnisse', Stahlbau, No.2, 33-36; No.3, 83-86; No.4, 115-119; No.5, 153-158; No.12, 362-368, 1965.
62. Daniel, H. and Urban, J., 'Die Bundesautobahnbrücke Über den Rhein bei Leverkusen. Unterbauten der Strombrücke', Stahlbau, No.7, 193-196, July, 1966.
63. Daniel, H. and Schumaun, H., 'Die Bundesautobahnbrücke über den Rhein bei Leverkusen', Stahlbau, No. 8, 225-236, Aug., 1967.
64. Demers, J.G. and Marquis, P., 'Le Pont a Haubans, No. 231, 24-28, June, 1968.
65. Demers, T.G. and Simonsen, O.F., 'Montreal Boasts Cable-Stayed Bridge', Civ. Engng., Easton, Pa., 59-63, Aug., 1971.
66. de Nausouty, M., 'Road-Bridges over the Rhone at Lyons', Proc. Inst. Civ. Engrs., London, 108, 430-432, 1892.
67. Dischinger, F., 'Hängebrücken für schwerste Verkehrslasten', Bauingenieur, No.3, 65-75, 1949; No.4, 107-113, 1949.

68. Donnelly, J.A., 'Footbridge at Berlin (Germany); Acier-Stahl-Steel, No.6, 263-265, 1971.
69. Dove, R.C., Adams, P.H., 'Experimental Stress Analysis and Motion Measurement', Prentice Hall of India (Pvt.) Ltd., New Delhi, 1965.
70. Drewy, C.S., 'A memoir on Suspension Bridges', Longman, Orma, Brown, Green and Longman, London, p. 24-26, 1832.
71. Eney, W.J. 'New Deformeter Apparatus', Engng. News Rec., 221, 16 Feb., 1939.
72. Ernst, H.J., 'Erection of a Cable-Stayed Girder in the Construction of a Large Bridge', Stahlbau, No.5, 101, 1956 (In German).
73. Ernst, J.H., 'Der E-Modul Von Seilen unter Berücksichtigung des Durchhanges', Der Bauingenieur, Vol. 40, No. 2, pp. 52-55, Feb. 1965.
74. Falk, S., 'Die Berechnung des Beliebigen Gestützten Durchlaufträgers nach dem Reduktionsverfahren', Ing.-Arch., 24(2,3), 216-232, 1956.
75. Falk, S., 'Das Reduktionsverfahren der Baustatik unter besonderer Berücksichtigung der Programmierbarkeit für digitale Rechenautomaten,' Inaugural lecture, Technische Hochschule, Braunschweig, 1956-57.
76. Falk, S., 'Die Berechnung offener Rahmentragwerke nach dem Reduktionsverfahren, Ing.-Arch., 26(i), 61-80, 1958.
77. Falk, S., 'Die Berechnung geschlossener Rahmentragwerke nach dem Reduktionsverfahren', Ing.-Arch., 26(2) 96-109, 1958.
78. Farquharson, F.B., Vincent, G.S., et al., 'Aerodynamic Stability of Suspension Bridges with Special Reference to the Tacoma Narrows Bridge', Bul. No. 16, Univ. of Washington, Engng. Exptl. Stn., Parts I to V, 1949-54.

79. Faustus Verautius, 'Machinae novae Fausti Verautu, Venice, 1617.
80. Feige, A., 'The Evolution of German Cable-Stayed Bridges- An Overall Survey', AISC Engng. J., 118, July, 1967.
81. Finsterwalder, U., 'Free-Cantilever Construction of Prestressed Concrete Bridges and Mushroom-shaped Bridges', First International Symp., Concr. Bridge Design, ACI Publication SP-23, pp. 467-494, 1969.
82. Fischer, G., 'The Severin Bridge at Cologne (Germany)', Acier-Stahl-Steel, No. 3, 97-107, 1960.
83. Fox, L., 'An Introduction to Numerical Linear Algebra', Clarendon Press, Oxford, 1964.
84. Frazer, R.A. and Scruton, C., 'A summarized Account of the Severn Bridge Aerodynamic Investigation', Report NPL/Arro/222, HMSO, London, 1952.
85. Freudeuberg, G., 'Die Stahlhochstrasse uber den neuen Hauptbahnhof in Ludwigshafen/Rhein', Stahlbau, No.9, 257-267, Sept., 1970; No. 10, 306-314, Oct., 1970.
86. Fuchs, D., 'Der Fussgangersteg auf der Brusseler Wattausstellung 1958. Eine Seitentragerbrücke', Stahlbau, No. 4, 91-97, April, 1958.
87. Gee, A.F., 'Cable-Stayed Concrete Bridges', Developments in Bridge Design and Construction, Ed. Rockey, K.C.; Baunister, J.L. and Evans, H.R., Conf. Proc., Univ. College, Cardiff, Crosby Lockwood, London, pp. 462, 64-65, 70, 72, 74, 1971.
88. Gere, J.M. and Weaver, W.Jr., 'Analysis of Framed Structures', D. van Nostrand Co., INC., 1965.
89. Gilbert, R., 'Modern Development in Design and Construction of Long Span Bridges', Canadian Struct. Engng. Conf., Toronto, p. 2-19, 1968.

90. Gilbert, R., 'Severn River Suspension Bridge', Civ. Engng., 68-73, Aug., 1969.
91. Gimsing, U.J., 'Anchored and Partially Stayed Bridges', Proc. of the International Symp. on Suspension Bridges, Lisbon, Laboratorio Nacional De Engenharia Civil, p.475-84, 1966.
92. Gisclard, A.V., 'Note sur un nouveau type de pont suspendu rigide', Annl's Ponts Chauss, 1899-1900.
93. Golub, H., 'Cable-Stayed Bridges', Civ. Engng., Easton, Pa, 43, Aug. 1971.
94. Goschy, B., 'Dynamics of Cable-Stayed Pipe Bridges', Acier-Stahl-Steel (English version), No. 6, pp 277-82, June, 1961.
95. Gottschalk, O., 'Mechanical Calculation of Elastic Systems', J.Franklin Inst., 202, 61-87, July, 1926.
96. Hadley, H.M., 'Tied-Cantilever Bridge-Pioneer', Civ. Engng., Easton, Pa, 48-50, Jan., 1958.
97. Hass, B., 'Eine Ungewöhnliche Belastung der Brücke über die Norderelbe im Zuge der BAB Südliche Umgehung Hamburg', Bautechnik, No.5, 145-151, May, 1964.
98. Havemann, H.K., 'Die Seilverspannung der Autobahnbrücke über die Norderelbe-Bericht über Versuche zur Dauerfestigkeit der Drahtseile', Stahlbau, No.8, Aug. 1962.
99. Havemann, H.K., 'Die Brücke über die Norderelbe im Zuge der Bundesautobahn Südliche Umgehung Hamburg, Teil I: Ideen und Bauwettbewerb', Stahlbau, No.7, 193-198, July 1963.
100. Havemann, H.K., 'Die Brücke über die Norderelbe im Zuge der Bundesautobahn südliche Umgehung Hamburg. Teil IV: Bauausführung der Stahllernen Überbauten', Stahlbau, No. 10, 310-317, Oct., 1963.

101. Heeb, A., Gerold, w., and Dreher, W., 'Die Stahlkonstruktion der Neckarbrücke Untertürkheim', Stahlbau, No. 2, 33-38, Feb., 1967.
102. Hess, H., 'Die Severinsbrücke Köln, Entwurf und Fertigung der Strombrücke', Stahlbau, No.8, 225-261, 1960.
103. Holmes, M., 'Steel Frames with Brickwork and Concrete Infilling', Proc. Inst. of Civ. Engrs, Vol. 19, p. 473, 1961.
104. Homberg, H., 'Einflusslinien von Schrägeseilbrücken, Der Stahlbau, No. 2, Feb., 1955.
105. Homberg, H., 'Progress in German Steel Bridge Construction', Report on Steel Congress of the High Authority of the European Economic Committee, 1964.
106. Hopper, C.J., 'Eine neue Strassenhängebrücke über den Kleinen Belt' (A new suspension highway bridge over the Little Belt), Bauingenieur, 45, 226, 1950.
107. Kajita T. and Cheung, Y.K., 'Finite Element Analysis of Cable-Stayed Bridges', IABSE, Pub. 33-II, 1973.
108. I.R.C. Standard Specifications and Code of Practice for Road Bridges'; Section II; Loads and Stresses, Indian Roads Congress, 1966 edition.
109. Kardestuncer, H., 'Elementary Matrix Analysis of Structures', McGraw Hill Book Co., 1974.
110. Kavangh, T.C., Discussion of 'Historical Development of Cable-Stayed Bridges', by Podolny and Fleming, Jor. Struct. Div., ASCE, Vol. 99, No.ST.7, Proc. Paper 9826, July 1973.
111. Kersten, R., 'Das Reduktionsverfahren der Baustatik', Springer-Verlag, Berlin, p. 6-25, 46, 1962.
122. Kireenko, B.I., 'Reinforced Concrete, Cable-Stayed Bridge', Beton Zhelezo-beton, No.6, 5-10, 1965 (in Russian).



113. Kireenko, B.I., 'Cable-Stayed Bridges', Kiev, pp. 25-27 and 81-92 (in Russian), 1967.
114. Klingenberg, W., 'Ideenwettbewerb fur eine feste Verbindung uber den Großen Belt', Bauingenieur, No.11, 389-408, Nov. 1967.
115. Klingenberg, W. and Thul, H., 'Ideenwettbewerb fur einen Bruckenschlag uber den Großen Belt', Stahlbau, No.8, 225-236, Aug., 1968.
116. Kloppel, K. and Thiele, F., 'Modellversuch im Windkanal zur Bemessung von Bruckengegeßen die Gefahr winderregter Schwingungen', Stahlbau, 20 (12), 353-365, Dec., 1967.
117. Krishna, J., Arya, A.S. and Thakkar, S.K., 'Dynamic Analysis and Model Studies of Ganga Bridge at Allahabad for Earthquake Motions, A report of SRTEE, Univ. of Roorkee, India, Oct. 1969.
118. Krishna, J. and Chandrasekaran, A.R., 'Elements of Earthquake Engineering', Sarita Prakashan, Nauchandi, Meerut, India, 1976.
119. Landeshauptstadt Dusseldorf, Die neue Oberkasseler Rheinbrücke, 1968.
120. Landstrom, B., 'Sailing Ships', Doubleday, New York, 1969.
121. Lazar, B.E., 'Stiffness Analysis of Cable-Stayed Bridges', Jor. Struct. Div. ASCE, Vol. 98, No. ST.7, July, 1972.
122. Lazar, B.E., Troitsky, M.S. and Douglass, M. Mc C., 'Load Balancing Analysis of Cable-Stayed Bridges', Jor. of the Struct. Div., ASCE, Vol. 98, No. ST. 8, Aug. 1972.
123. Leckie, F. and Pastel, E., 'Transfer Matrix. Fundamentals', Int. J. Mech. Sci. 2(3), 137-167, 1960-61.
124. Leinekeigel le Cocq, G., 'Bonhomme Suspension Bridge over the Balvet', Proc. Inst. Civ. Engrs., 162(4), 436-437, 1905.

125. Leinekugel le Cocq, G. 'Ponts Suspendus, tomes 1 and 2', Octave Doin et Fils, Paris, 1911.
126. Lentze, K., 'Bemerkungen über die grossjern Brückenbauwerke in Frankreich, England Und Ireland, auf einer Reise im Winter 1844-1845 gesammelt, verh. d. ver.Z, Befordd. Gewerbefl', In Preussen, p. 88, 1846.
127. Leonhardt, F. and Andra, W., 'Fussgangersteg über die Schillerstrasse in Stuttgart', Bautechnik, No.4, 110-116, 1962.
128. Leonhardt, F., 'Zur Entwicklung aerodynamisch stabiler Hängebrücken', Bautechnik, 45(10), 325-326; (11), 372-380, 1968.
129. Leonhardt, F. and Zellner, W., 'Cable-Stayed Bridges-Report on Latest Developments', Canadian Struct. Engng. Conf., Toronto, Feb. 16-17, 1970.
130. Leonhardt, F. and Zellner, W., 'Vergleiche zwischen Hängebrücken und Schrägkabelbrücken für Spannweiten über 600 m', IABSE Vol. 32, 1972.
131. Lewenton, G., 'The Pavilions of the German Federal Republic at the Universal and International Exhibition, Brussels, 1958', Acier-Stahl-Steel, No.6, 243-248, June, 1958.
132. Lin, T.Y., 'A New Concept for Prestressed Concrete', Construction Review, Sydney, Australia, 1961.
133. Lipton, T.M. and Beresford, F.D., 'Static Load Testing of a Model of a Post Tensioned Concrete Footbridge', Federation Internationale de la Precontrainte, pp.1-12, Sixth Congress, Praha, 1970.
134. Livesley R.K., 'Matrix Methods of Structural Analysis', Pergamon Press, The MACMILLAN Co., New York, 1964.

135. Loscher, C.T., 'Angabe einer ganz besondern Hange-  
werksbrücke, die mit weniger und schwachem Holze,  
Ohne im Bogen geschlossen, sehrweit über einer Fluss-  
cann gespannt werden, die grossten Lasten trägt und  
fordern starksten Eisfahrten sicher ist', Leipzig, 1784.
136. Lustgarten, P., 'Brücke Über den See von Maracaibo',  
Bauingenieur, No. 10, 365-373, Oct., 1962.
137. Majid, K.I. 'Nonlinear Structures-Matrix Methods of  
Analysis and Design by Computers, Butterworths London,  
1972.
138. Mallick, D.V., 'Determination of Lateral Stiffness  
of Infilled Frames by the Finite Element Method',  
Third Symp. on Earthquake Engng., Nov. 1966, Univ.  
of Roorkee, India.
139. Mehrtens, G.C., 'Vorlesungen über Ingenieur-Wissen-  
schaften, Zweiter Teil-Eisenbrückenbau, Erster Band',  
W. Engelmann, Leipzig, 1908.
140. Merchant, W., and Brotton, D.M., 'A Generalized Method  
of Analysis of Elastic Plane Frames', IABSE Symp.,  
Rio de Janeiro, 1964.
141. Mignot and Gandil, 'Le Pont Massena a Paris (2<sup>e</sup>  
partie)', Travaux, 1-23, July-Aug., 1970.
142. Miller, M.A., Brotton, D.M. and Merchant, W., 'A  
computer Method for the Analysis of Nonlinear Elastic  
Plane Framework', International Symp. on Use of  
Computers in Struct. Engng., Dept. Civ. Engng., Univ.  
of Newcastle upon Tyne, England, 1966.
143. Morandi, R., 'The Bridge Spanning Lake Maracaibo',  
Bauingenieur, J. Prestr. Concr. Inst., 12-27, June,  
1961.
144. Morandi, R., 'Viaducto de la Magliana, Italia,  
Informes de la Construccion Revista de Information  
Technia, No. 208, Instituto Eduardo Torroja, Madrid,  
pp. 73-74, March, 1969.

145. Morandi, R., 'Some Types of Tied Bridges in Prestressed Concrete', Concrete Bridge Design, ACI Publication SP-23, American Concr. Inst., Detroit, Michigan, pp. 447-465, 1969.
146. Morandi, R., 'Past and Future Achievements in Reinforced Concrete', Concrete, 5(2), 41-46, 1971.
147. Morley, G.W., 'The Erskine Bridge over the River Clyde', Civ. Engng, publ. Wks. Rev., 440-443, May, 1969.
148. Morris, N.F., 'Analysis of Cable Stiffened Space Structures', Jor. Struct. Div., ASCE, ST.3, Vol.102, pp. 501-513, March, 1976.
149. Motley, T., 'On a Suspension Bridge over the Avon, Twerton', Mechanics', Magazine, London, 29 (790), 468, Sept., 1838.
150. Murphy, G., 'Similitude in Engineering', The Ronald Press Company, New York, 1950.
151. Navier, C.L., 'Report et Me'moire sur les Ponts Suspendus, de l'Imprimerie Royale, Paris, p. 8-10, 1823.
152. O'connor, C., 'Design of Bridge Superstructures', John Wiley & Sons, Inc., New York, 1971.
153. Paez, A., 'Our Fiftieth Anniversary', Concr. Constr. Engng., 187-188, Jan, 1956.
154. Payne, R.J., 'The Structural Requirements of Batman Bridge as They Affect Fabrication of the Steelwork', J. Instn. Engrs. Aust., 199-207, Dec. 1967.
155. Pestel, E.C. and Leckie, F.A., 'Matrix Methods in Elastomechanics, McGraw-Hill, New York, 1963.

156. Pippard, A.J.S. and Sparkes, S.R., 'Some Experimental Solutions of Certain Structural Problems', Proc. Inst. of Civ. Engrs., 4, 79, 1936-37.
157. Podolny, W., Jr., 'Static Analysis of Cable-Stayed Bridges', Ph.D. Thesis, Univ. of Pittsburgh, 1971.
158. Podolny W. Jr. and Fleming, J.F., 'Cable-Stayed Bridges A State of the Art', preprint 1346, ASCE National Water Resources Engng. Meeting, Phoenix, Arizona, p. 30, 11-15 Jan., 1971.
159. Podolny, W. Jr. and Fleming, J.F., 'Historical Developments of Cable-Stayed Bridges', Jor. Struct. Div., ASCE, Vol. 98, No. ST. 9, Sept, 1972.
160. Podolny, W. Jr. and Fleming, J.F., 'Cable-Stayed Bridges- Single Plane Static Analysis', Highway Focus, Vol. 5, No. 2, U.S. Dept. of Transp., Federal Highway Administration, Washington, D.C., Aug., 1973.
161. Podolny, W. Jr., 'Cable-Stayed Bridges', Engng. Jor., AISC, First Quarter, 1964.
162. Podolny W. Jr., and Scalzi, J.B., 'Construction and Design of Cable-Stayed Bridges', John Wiley & Sons, 1976.
163. Polyakov, S.V., 'An Investigation into the Strength and Stiffness of Masonry Infilling', Symp. on Tall Bldg., held at the Univ. of Southampton, 13-15, April, 1966.
164. Protte, W. and Tross, W., 'Simulation as Design Procedure for Cable-Stayed Bridges', Stahlbau, 35, 208-211, 1966.
165. Reimers, K., 'Fussganger brucke uber die Glaciers-chaussee in Hamburg fur die Internationale Gartenbau-Ausstellung 1963', Schweiss, Schnied., No.6, 262-264, 1963.

166. Reutter, K., 'Konstruktion und Fertigung der Seil Kammer für die Stahlhockstrasse Ludwigshafen', Schweiss Schneid., No. 9, 418-420, 1968.
167. Rooke, W.G., 'Papineau Bridge Steel Erected in Record Time', Heavy Const. News, 4, 5 and 8, 1 Sept., 1969.
168. Saafan, S.A., 'Nonlinear Behaviour of Structural Plane Frames', Proc. ASCE, 89 (ST4), 557-579, Aug., 1963.
169. Samuel, P., 'The Design of Freeway Bridges for the Narrows Interchange in Perth', Constr. Rev., Aust., 19-30, April, 1968.
170. Sawhney, P.S., 'Influence Lines for Cable-Stayed Bridges, M.E. Thesis, Department of Civil Engng. Univ. of Roorkee, India, 1972.
171. Scarborough, J.B., 'Numerical Mathematical Analysis', Oxford Book Co., 1964.
172. Scheer, J., 'Benützung Programmgesteuerter Rechenautomaten für statische Aufgaben, erläutert in Beispiel der Durchlaufträgerberechnung', Stahlbau, 27 (9), 225; (10), 275, 1958.
173. Schmitz, H. and Jetter, R., 'Planung und Bauausführung der Schiffahrtsoffnungen der Maracaibobrücke in Venezuela', Bauingenieur, No. 8, 283-302, Aug., 1963.
174. Schottgen, J. and Wintergerst, L., 'Die Strassenbrücke über den Rhein bei Maxau', Stahlbau, No. 1; 1-9, Jan., 1968; No. 2, 50-57, Feb., 1968.
175. Schussler, K., 'Wettbewerb 1954 zum Bau einer Rheinbrücke oder eines Tunnels in Köln im Zuge Klappergasse Gotenring', Stahlbau, No. 8, 205, 253, 294 and 326, 1957.

176. Scruton, C., 'An Experimental Investigation of the Aerodynamic Stability of Suspension Bridges with Special Reference to the Proposed Severn Bridge', Proc., Inst. Civ. Engrs., No. 1, 189-222, March, 1952
177. Seim, C., Larsen, S. and Daug, A., 'Design of the Southern Crossing Cable Stayed Girder', Preprint paper 1352, ASCE, National Water Resources Engng. Meeting, Phoenix, Arizona, Jan. 11-15, 1971.
178. Seim, C., Larsen, S. and Dang, A., 'Analysis of the Southern Crossing Cable Stayed Girder', Preprint paper 1402, ASCE National Struct. Engng. Meeting, Baltimore, Maryland, April 19-23, 1971.
179. Simons, H., Wind, H. and Moser, W.H., 'The Bridge Spanning Lake Maracaibo in Venezuela', Bauverlag, Wiesbaden-Berlin, 1963.
180. Simpson, C.V.J., 'Modern Long Span Steel Bridge Construction in Western Europe', Proc. Inst. Civil Engrs., London, Suppl. II, 1970.
181. Smith, B.S., 'Lateral Stiffness of Infilled Frames', Proc. ASCE, Vol. 88, No. ST.6, P. 183-99, 1962.
182. Smith B.S., 'Behaviour of Square Infilled Frames', Proc. ASCE, Vol. 92, No. ST.1, Feb., 1966.
183. Smith, B.S., 'The Single Plane Cable-Stayed Girder Bridge: A method of Analysis Suitable for Computer Use', Proc. Inst. Civ. Engrs, 37, 183-194, May, 1967.
184. Smith, B.S., 'A Linear Method of Analysis for Double Plane Cable-Stayed Girder Bridges', Proc. Inst. Civ. Engrs, Jan., 1968.
185. Sondh, Capt. B.S., 'Beam-Column Effect in Cable-Stayed Bridges', M.E. Thesis, Dept. of Civ. Engng., Univ. of Roorkee, India, 1977.
186. Stahlbau Taschenkalender, 'Norderelbebrücke, Autohahnbrücke, Baujahr 1960/61, Deutscher Stahlbau Verband, Kolu, Schweiss Schneid, 12(57), 189-194, 1960.

187. Steinman, D.B., 'Rope-Strand Cables Used in New Bridge at Portland, Oregon', Engng. News Rec., 272-277, 13, Feb, 1930.
188. Steinman, D.B., 'The Builders of the Bridge', Harcourt, New York, 1950.
189. Streletzkii, N.N., 'Reinforced Concrete Bridges', Moscow, pp. 119-127, 1965 (in Russian).
190. Tamms, F. and Bayer, E., 'Kniebrücke Dusseldorf', Beton-Verlag GmbH, Dusseldorf, 1969.
191. Tamms, F., and Beyer, E., 'Kniebrücke Dusseldorf', Beton-Verlag GmbH, Dusseldorf, 1970.
192. Tang, M.C., 'Analysis of Cable-Stayed Girder Bridges', Jor. Struct. Div., ASCE, Vol. 97, No. ST5, May, 1971.
193. Tang, M.C., 'Design of Cable-Stayed Girder Bridges', Jor. Struct. Div., ASCE, Vol. 98, No. ST8, Aug., 1972.
194. Tang, M.C., 'Buckling of Cable-Stayed Girder Bridges', Jor. Struct. Div., ASCE, pp. 1675-1684, Sept. 1976.
195. Terzaghi, K., 'Evaluation of Coefficient of Subgrade Reaction', Geotechnique, Vol. V, No. 4, pp. 297-326, Dec., 1955.
196. Tesar, A., 'Das Project der neuen Strassenbrücke über die Donau in Bratislava/CSS Proj. Bauingenieur, No.6, 189-198, June, 1968.
197. Thomass, S., 'Spannbeton-Kongress Paris 1966- Arbeitssitzung V. bemerkenswerte Bauwerke- Brücken', Beton Stahlbetonb, No. 12, 289-297, Dec., 1966.
198. Thul, H., 'Stahlerne Strassenbrücken in der Bundesrepublik', Bauingenieur, No.5, 169-189, May 1966.
199. Thul, H., 'Cable-Stayed Bridges in Germany', British Constructional Steelwork Association Conf. pp. 10, 1966.



200. Thul H., 'Cable-Stayed Bridges in Germany', Proc. Conf. on Struct. Steel work Asso. Ltd., p. 66-81, 1966.
201. Torroja, E., 'Philosophy of Structures', Univ. of Calif. Press, Berkeley and Los Angeles, pp. 128-129, 1962.
202. Troitsky, M.S., 'North Romaine River Bridge Mile 5.8', Report by the Foundation of Canada Engng. Corp. Ltd., Montreal, Feb. 1960.
203. Troitsky, M.S. and Lazar, B., 'Model Investigation of Cable Stayed Bridges', Report no. 1, Sir George Williams Univ., Montreal, Canada, 1969.
204. Troitsky M.S. and Lazar, B., 'Model Investigation of Cable Stayed Bridges- Influence Lines', Report No.2, Sir George Willains Univ., Faculty of Engng, Feb., 1970.
205. Troitsky, M.S. and Lazar, B., 'Model Investigation of Cable-Stayed Bridges. Structural Analysis of the Bridge Prototype', Report No. 3, Sir George Williams Univ., April, 1970.
206. Troitsky, M.S. and Lazar, B., 'Model Investigation of Cable-Stayed Bridges- Nonlinear Behaviour', Report no. 4, Sir George Williams Univ. Montreal, Canada, 1970.
207. Troitsky, M.S. and Lazar. B., 'Model Investigation of Cable-Stayed Bridges- Post-Tensioning of Cables', Report No. 5, Sir George Williams Univ., Montreal, Canada, 1970.
208. Troitsky, M.S. and Lazar, B.E., 'Model Analysis and Design of Cable-Stayed Bridges', Proc. Inst. Civ. Engrs, 439-464, March, 1971.
209. Troitsky, M.S., 'Cable-Stayed Bridges - Theory and Design', Crosby Lockwood Staples, London, p. 11, 1977.

210. Tung, D.H.H. and Kudder, R.J., 'Analysis of Cables as Equivalent Two-Force Members', Engng. Jor., American Inst. of Steel Const., pp. 12-19, Jan. 1968.
211. Tyrrel, H.G., 'History of Bridge Engineering', published by the author, Chicago, p. 230, 1911.
212. Valentin, Mignot and Gandil, 'Le Pont Massenaa Paris (1 re partie)', Travaux, No. 420, 157-175, March, 1970.
213. Van der Molen, J.I., 'Barwon River Footbridge, Geelong, Austrelia', Concr. Q., Lond., 33-35, July-Sept., 1969.
214. Van der Molen, J.I., 'Prestressed Concrete Stayed Girder Bridge', Constr. Rev. Aust., No. 1, 19-21, 1969.
215. Vogel, G., 'Die Montage des Stahluberbauesder Severinsbrucke Koln', Stahlbau, No. 9, 269-293, 1960.
216. Vogel, G., 'Erfahrungen mit geschweissten Montages-tassen beim Bau der Severinsbrucke in Koln', Schweiss Schneid, 12(5) 189-194, 1960.
217. Wagner, P., 'Die Bosphorus-Brucke bei Istanbul', (The Bosphorus Bridge, near Istanbul), Bauingenieur, 45, 371-372, 1970.
218. Webster, L.F., 'Papineau Cable-Stayed Bridge - Canadian First', Engng. Contract Rec., 68-69, Oct., 1969.
219. Wenk, H., 'Die Stromsundbrucke (the Stromsund Bridge)', Stahlbau, 23(4), 73-76, 1954.
220. Wenk, H., 'The Stromsund Bridge', Demag News, No. 136, Duiburg, 1954.

221. Wever, W.Jr., 'Computer Programs for Structural Analysis', D. van Nostrand Co. INC.
222. Wilkinson, J.H., 'The Algebraic Eigenvalue Problem', Clarendon Press, Oxford, 1965.
223. Woods, S.W., Discussion of 'Historical Development of Cable-Stayed Bridges', By Podolny and Fleming, Jor. Struct. Div., ASCE, Vol. 99, No.ST4, April, 1973.

APPENDIX A

CALCULATION OF ROTATIONAL STIFFNESS AT THE  
BASE OF SUBSTRUCTURE WELLS

Cross-sections of concrete wells, one at the end and the other below the tower, are shown in fig. A.1. Values of moments of inertia about principal axes are also given in the figure.

Rotational stiffness ( $K\theta_1$ ) at the base of a well is calculate by using eq. 2.11 given below.

$$K\theta_1 = 2n_H \cdot H \left( I + \frac{H^3}{24} \right) \quad \dots (2.11)$$

where

- $n_H$  = coefficient of horizontal subgrade reaction ( $t/m^3$ ),
- $H$  = depth of foundation below scour level (m),
- $I$  = moment of inertia at the base (active in the direction of rotation) ( $m^4$ ).

For the case of loose sand ( $n_H = 130 t/m^3$ ), the values of rotational stiffnesses calculated for sections shown in fig. A1 are given hereunder.

End Well:	t-m/rad.
Longitudinal direction	$0.6076 \times 10^8$
Transverse direction	$1.195 \times 10^8$
Well below tower:	
Longitudinal direction	$1.9352 \times 10^8$
Transverse direction	$7.2713 \times 10^8$

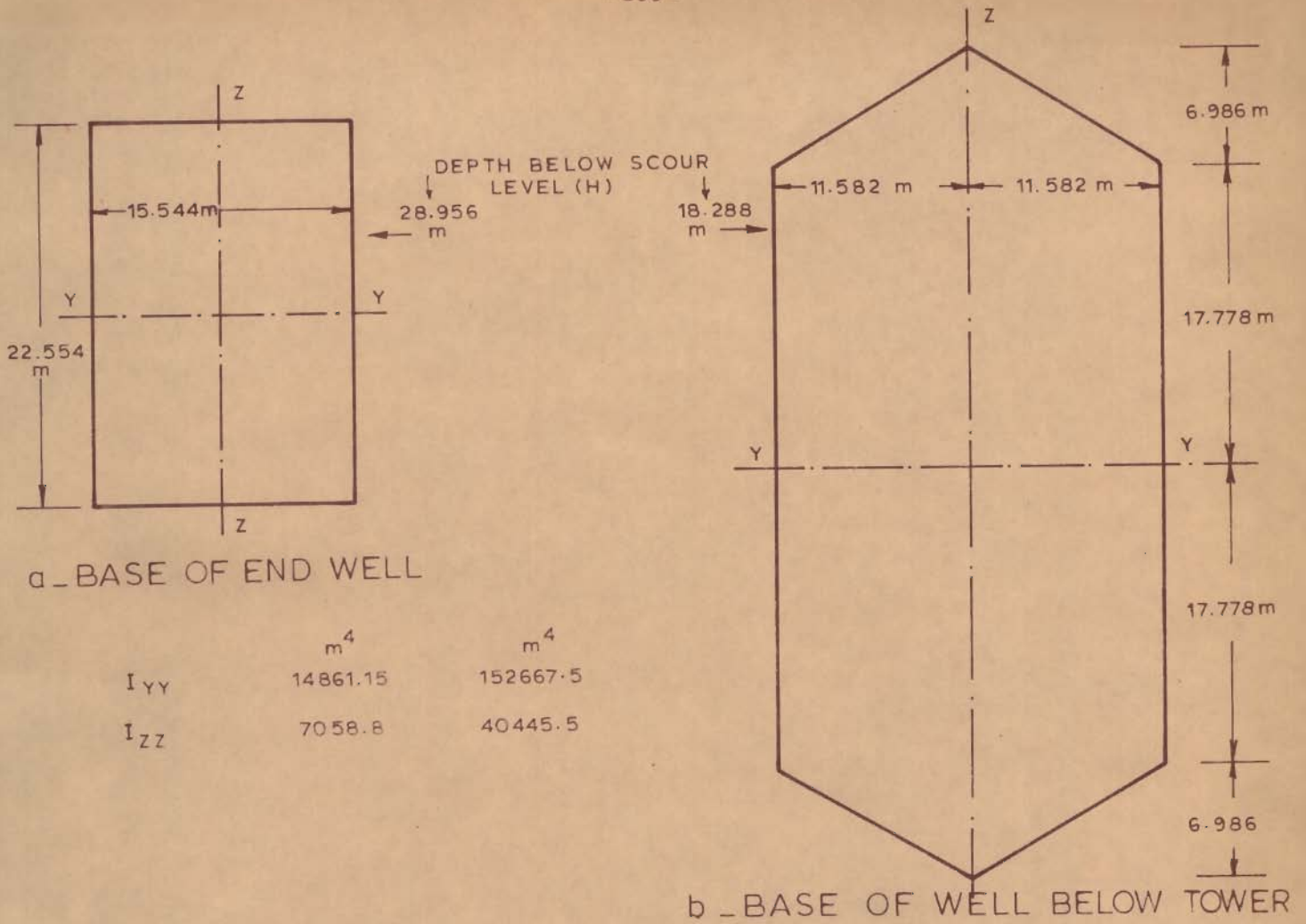


FIG. A1 \_SECTIONS AT THE BASE OF CONCRETE WELLS

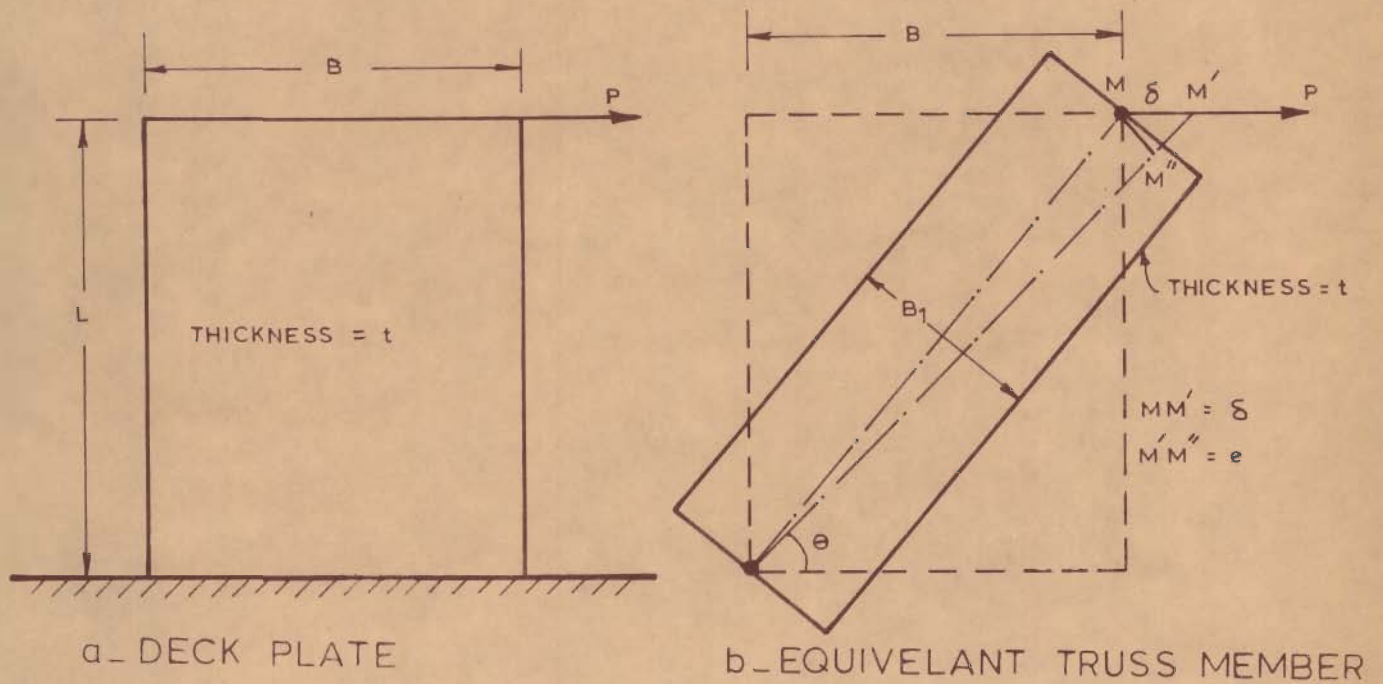


FIG. B1 \_REPRESENTATION OF DECK- PLATE STIFFNESS BY EQUIVALENT TRUSS MEMBER

APPENDIX - B

REPRESENTATION OF DECK-PLATE STIFFNESS BY EQUIVALENT TRUSS MEMBER

Figure B1 (a) shows a segment of deck plate; with length L, width B and thickness t; between two longitudinal stiffening girders and two cross-girders. An equivalent truss members of length equal to the length of diagonal with width Bl and thickness t is shown in fig. B1 (b).

Lateral deflection ( $\delta$ ) of the actual deck plate under a lateral force (P) is given by:

$$\delta = \frac{PL^3}{CE(tB^3/12)} + \frac{1.2 PL}{G.t.B} \quad \dots (B1)$$

where,

- C = a constant depending on the condition of rigidity due to continuity at the other end,  
= 12 for a fixed case,
- E = modulus of elasticity of material of plate,
- G = modulus of rigidity of material of plate,  
= 0.4 E.

Eq. B1 can be written in a simplified form as:

$$\delta = \frac{12PL^3}{CEtB^3} \left( 1 + \frac{CB^2}{4L^2} \right) \quad \dots (B2)$$

Elongation (e) of the equivalent truss member under lateral force (P) is given by:

$$e = \frac{P \sec \theta}{AE} (B^2 + L^2)^{1/2} \quad \dots (B3)$$

where;

A = area of cross-section of diagonal truss member

$\theta$  = angle of the diagonal member with the lateral force.

The corresponding movement ( $\delta'$ ) in the direction of lateral force is given by:

$$\delta' = \frac{e}{\cos \theta} = \frac{P}{AE} \sec^2 \theta (B^2 + L^2)^{1/2} \quad \dots (B4)$$

$$\text{we have, } \sec^2 \theta = \frac{B^2 + L^2}{B^2}$$

$$\delta' = \frac{P}{AE} \cdot \frac{(B^2 + L^2)^{3/2}}{B^2} \quad \dots (B5)$$

For equivalence of deformations  $\delta$  and  $\delta'$  in the direction of lateral force,

$$\frac{12PL^3}{CEtB^3} \left(1 + \frac{CB^2}{4L^2}\right) = \frac{P}{AE} \frac{(B^2 + L^2)^{3/2}}{B^2}$$

on simplification,

$$A = \frac{CB (B^2 + L^2)}{4L^3 \left(1 + \frac{CB^2}{4L^2}\right)} \cdot \frac{t(B^2 + L^2)^{1/2}}{3}$$

$$\text{or } A = K \cdot \frac{t(B^2 + L^2)^{1/2}}{3} \quad \dots (B6)$$

$$\text{where, } K = \frac{CB (B^2 + L^2)}{4L^3(1 + \frac{CB^2}{4L^2})} \quad \dots (B7)$$

In the case of square infills, it has been experimentally established (103) that the square infill can be replaced by equivalent diagonal truss member of width equal to one-third the length of diagonal and thickness equal to  $t$ . Thus, when  $B = L$  and  $K = 1$ , for a square infill, we get  $C = 4$  (by substituting values in Eq. B7).

Assuming the value of  $C = 4$ ; a constant to represent the condition of rigidity due to continuity at the other end; the value of  $K$  for a rectangular panel subjected to lateral forces is obtained from Eq. B7 as;

$$K = \frac{B}{L} \quad \text{and,}$$
$$A = \frac{B}{L} \cdot \frac{t (B^2 + L^2)^{1/2}}{3} \quad \dots (B8)$$

Thus, for the purpose of lateral load analysis, the continuous deck plate between the main stiffening girders of the bridge can be replaced by equivalent truss type diagonal braces connecting two diagonally opposite nodes of the stiffening girders and having width equal to one-third of the length of diagonal times the ratio of the two sides of the rectangle and thickness equal to the thickness of the deck plate.



APPENDIX - C

REPRESENTATION OF DECK PLATE STIFFNESS OF 6-CABLE SYSTEM IN EQUIVALENT 3-CABLE SYSTEM

Using suffix 1 for 6 cable system and suffix 2 for 3 cable system, area ( $A_1$ ) of equivalent truss member of 6-cable system is given by Eq. B8 as:

$$A_1 = \frac{B_1}{L_1} \cdot \frac{t(B_1^2 + L_1^2)^{1/2}}{3} \quad \dots (C1)$$

The stiffness ( $S_1$ ) of the diagonal truss member is given by,

$$S_1 = \frac{A_1 E}{(B_1^2 + L_1^2)^{1/2}} \quad \dots (C2)$$

For the stiffness of the diagonal truss member of 3-cable system to be equal to that of 6-cable system,

$$\frac{A_1 E}{(B_1^2 + L_1^2)^{1/2}} = \frac{A_2 E}{(B_2^2 + L_2^2)^{1/2}}$$

$$\text{or } A_2 = A_1 \cdot \frac{(B_2^2 + L_2^2)^{1/2}}{(B_1^2 + L_1^2)^{1/2}}$$

Using eq. C1. for calculation of value of  $A_1$ ,

$$A_2 = \frac{B_1 t}{3L_1} \cdot (B_2^2 + L_2^2)^{1/2} \quad \dots (C3)$$

Eq. C3 can be used to calculate the stiffness of diagonal truss member of equivalent 3-cable system.